A MULTIPLEX OF POLYBORATE BRØNSTED ACIDS EMPLOYED IN THE CATALYTIC ASYMMETRIC AZIRIDINATION REACTION

By

Wynter E. G. Osminski

A DISSERTATION

Submitted to
Michigan State University
in partial fulfillment of the requirements
for the degree of

Chemistry − Doctor of Philosophy

2013

ABSTRACT

A MULTIPLEX OF POLYBORATE BRØNSTED ACIDS EMPLOYED IN THE CATALYTIC ASYMMETRIC AZIRIDINATION REACTION

By

Wynter E. G. Osminski

A large family of chiral boroxinate catalysts derived from the VANOL and VAPOL ligands were synthesized using various protocols developed here. In order to study these chiral Brønsted acids, a modified procedure for the Wulff catalytic asymmetric aziridination reaction was developed, which is referred to as the 6-component AZ reaction throughout this dissertation. Electronics and sterics were both studied in the B3 catalyst system via altering the phenol or alcohol derivative incorporated into the boroxine ring of the B3 catalyst. It was realized that electron rich phenols and alcohols allowed for higher enantioselectivities to be obtained in the AZ reactions whereas electron deficient phenols decreased the enantioselectivities observed in the AZ reaction. Both proton and boron NMR studies were performed on the B3 catalyst system to better understand the non-covalent interactions between the imine and B3 catalyst.

A multi-component AZ reaction was developed, which eliminated the need for synthesizing the imine precursors for the AZ reaction. Using a one-pot protocol can be highly beneficial when synthesizing aliphatic aziridines due to side reactions occurring when attempting to synthesize and isolate the imine precursors. It was found with this specific protocol that benzoic acid was an important additive, which promoted full conversion of imines to aziridines.

Since the VANOL and VAPOL ligands are based on the linear BINOL ligand, a series of reactions were performed in order to generate various BINOL borate species. Attempts were made to synthesize B1, B2, and BLA BINOL species. Unfortunately, B1 proved to be very difficult to generate and was not produced here in any substantial amount. However, Kaufmann's propeller, B2 and BLA species were generated using various protocols.

To
My Family, Friends, and Professors
In Memory of
Sommer Lee Anthony Kellogg & James and Gladys Gilson

ACKNOWLEDGEMENTS

I would like to begin by expressing my appreciation to my research advisor, Professor William D. Wulff, who was the most influential person during my graduate career. A few of the many benefits of having Professor Wulff as a research advisor is that he has a plethora of knowledge in many areas of chemistry, he is concerned with the details of every group members work, and he promotes each student to solve his or her problem while simultaneously guiding them in the correct direction. This third quality is probably the most beneficial when obtaining your doctorate. Anyone can set up an organic reaction, but only an independent thinker can think outside the box when it comes to problem solving. This is the type of learning that Professor Wulff supports in his group and will benefit myself for the entirety of my life. As Professor Wulff taught me *"it is not the answer that is the issue, but the question."*

I am also grateful to Professor Babak Borhan, James Jackson, and James Geiger for being in my committee. Babak has been by far the best instructor that I have had throughout both my undergraduate and graduate career. I would also like to give a special thanks to Professor Jackson for all of his help in the area of physical organic chemistry. His advise was very beneficial in reference to my research and when writing my dissertation.

I would also like to thank Dr. Richard Staples at the Center for Crystallographic Research for obtaining my crystal structures and Ms. Chen Lijun and Dr. Daniel Jones at the Mass facility in biochemistry at Michigan State University for training me in HRMS. The retired technician Huang Rui is also appreciated for his help in CHN

analysis. I would like to give a special thanks to Dr. Daniel Holmes and other NMR staff members for all of the training I received for the NMR facility and interpretation of my NMR data. Dr. Holmes contributed many hours to help me learn a plethora of NMR techniques not typically taught during the first year training sessions such as boron NMR, cold NMR studies, and exchange studies. He also took extra time to help me install many programs on my personal computer.

I would also like to thank our former group members. In particular, I am very thankful to Dr. Anil K. Gupta, Dr. Munmun Mukherjee, and Dr. Dmytro Berbasov. When you spend five years in a small room with your lab mates, a friendship is created unlike any other. Anil was the light of our lab. When he was around, everyone would become happy instantaneously. His creative problem solving was a significant amount of help when I came across problems in my research. Walking into a chemistry lab with the Titanic soundtrack playing will be greatly missed. Munmun would be considered the Hope diamond of the chemistry department. She is a true angel who has an extensive amount of knowledge in organic chemistry. When anyone needs to figure out a mechanism or know the name of a reaction, they come to Munmun. Over the past five years, I have referred to her as “encyclopedia Munmun”. It is rare to find such a humble person who is as kind and knowledgeable as she. Dima was a great conversationalist who always gave unique insights to problems that would arise in my research.

Other current and previous group members that I would like to thank are Zhenjie Lu, Zhensheng Ding, Alex Predeus, Aman Desai, Li Huang, Yong Guan, Hong Ren, Victor Prutyanov, Mathew Vetticatt, WenJun Zhao, Xin Zhang, Yubai Zhou, Xiaopeng Yin, Yijing Dai, and Prakash Shee. A special thanks to Dr. Hong Ren and WenJun Zhao who

were great friends especially during my last year of graduate school when all of my lab mates had graduated and left MSU. Also, I would like to wish Prakash Shee and Yijing Dai good luck as they are just beginning their graduate careers in the Wulff group. I am very appreciative as well of our postdoc Dr. Mathew Vetticatt who did many theoretical calculations for my catalyst studies. He was very interactive during group meetings as well and showed an interest in everyone's research.

I am very thankful for the many friends outside of the Wulff lab as well. Mike Kuszpit was my hallway buddy who I would always have great conversations with. Gina Comiskey has been one of my closest friends throughout the past six years. She has always been there for me both academically and personally. I have had many wonderful girls' nights with Gina, Miriam, Katie, Nicole, and Olivia that I will always remember and cherish. There are so many other friends that I have made at MSU, and I am very blessed to have had their friendship over the past several years.

Lastly and most importantly, I would like to thank my family. I am so lucky to have all of my siblings, which includes Nolan, Joey, Nikki, Spring, Autum, Lee (Sommer) and Samantha. Among my many brothers and sisters, Spring and Autum are the two sisters who have had to put up with me day in and day out for my entire life. Autum has been and always will be there for me whenever I need her. The number one lesson I learned from her is never to end a sentence in a preposition, which I still sometimes do. Ever since I was a little girl, I wanted to be like my big sister Spring. In my eyes, Spring is the perfect sister. She is the main reason that I have gone so far in my life. Without her, I would not have gotten involved in sports, taken honors courses throughout high school

and college, and constantly strived to make the best grades possible. I am so thankful to have her as a sister and as a friend.

I would like to thank my father, Gary Gilson, who has always been supportive of every path that I have chosen throughout my life. He has been a great help to me, especially while I have been living in Michigan for graduate school. What I love best about him are his philosophical sayings that always make me feel better no matter how bad a situation may seem. I will never be able to thank my mother, Cindy Gilson, enough. She has basically given her entire life so that her children could be happy. She is what we kids call “super mom.” She worked full time while raising four children as a single mother. She would give her last dollar if she new it would make her children happy. She has been my inspiration in life and my best friend. She is also one of my favorite travel buddies. Lastly, I would like to thank my husband, Jake, for always being there for me. He is the one who had to put up with me whether I was happy, sad, angry, irritable, excited, or anxious. He has been my rock to lean on for the past four years, and I am so thankful to have him in my life.

"More powerful than the will to win is the courage to begin."

by Unknown

TABLE OF CONTENTS

LIST OF TABLES

LIST OF FIGURES

LIST OF SCHEMES

CHAPTER ONE

LINEAR AND VAULTED BRØNSTED ACIDS EMPLOYED IN THE SYNTHESIS OF CHIRAL AZIRIDINES AND AMINES

1.1 Introduction

Chiral aziridines are very important building blocks in the organic synthetic world today. They can be applied as or transformed into subunits of natural products,[1] anti-bacterial agents[2] such as florfenicol,[3] and various nitrogen containing compounds such as amino acid derivatives.[4] A key route to synthesizing chiral aziridines is starting from substituted imines. These aziridinations are primarily governed by the active catalyst, which is used to promote the reaction while generating asymmetric induction. Therefore, the catalyst plays an important role in aziridinations, as well as many other reactions. Catalysts are selected, synthesized, and modified with specific reactions and substrates in mind. Therefore, attempts to make large catalyst families are now at the forefront of asymmetric catalysis. Previously, there have been several Brønsted acids reported for asymmetric organocatalysis. Amongst these, the linear and vaulted biaryl ligands are of particular interest.

Discovered as a racemate in 1873 by von Richter[5] and later used as a pure enantiomer in 1926 by Pummerer,[6] the linear biaryl ligand BINOL **1** (1,1'-bi-2-naphthol) has been commonly used in asymmetric catalysis.[7] However, in 1993, the Wulff group created a new class of vaulted biaryl ligands, VANOL **2** (3,3'-diphenyl-[2,2'-binaphthalene]-1,1'-diol) and VAPOL **3** (2,2'-diphenyl-[3,3'-biphenanthrene]-4,4'-diol) (Figure 1.1).[8] These ligands have been used to generate induction in several different

reactions including but not limited to the Diels-Alder,[8] heteroatom Diels-Alder,[9] aza-Cope, [10] epoxidation, [11] imino-aldol, [12] Baeyer Villiger, [13] Petasis, [14] Ugi, [15] and aziridination reactions.[16]

1.2 Chiral ligands used in the synthesis of chiral aziridines and amines

The BINOL, VANOL, and VAPOL ligands have been used in the synthesis of chiral aziridines and amines for over a decade.[7,16k] The major differences between these two types of linear and vaulted ligands are their chiral pockets. In BINOL **1**, the major chiral pocket lies on the opposite side of the active binding site. Due to the unique vaulted backbone of VANOL **2** and VAPOL **3**, the major chiral pocket lies on the same side as the active binding site, which gives the VANOL and VAPOL ligands an advantage over the BINOL ligand (Figure 1.1).

Figure 1. 1 Major chiral pockets and active binding sites of BINOL, VANOL, and VAPOL

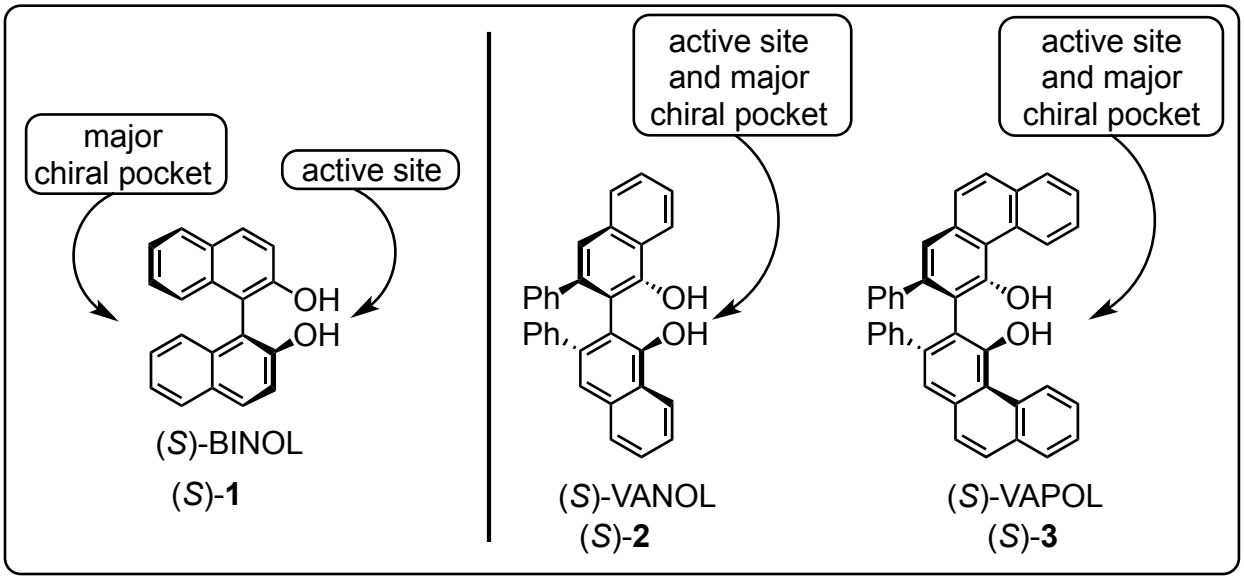

1.2.1 BINOL as a chiral Brønsted acid in organocatalysis

There are numerous examples in the literature today that reveal the versatility of BINOL **1** in asymmetric catalysis.[7] Several families of BINOL derivatives that have been discovered and employed as Brønsted acids in organocatalysis are the 3,3'-BINOL derivatives **4**, BINOL incorporated bifunctional organocatalysts, BINOL dicarboxylic acids **6**, BINOL phosphoric acids **5**, and BINAM **7** (Figure 1.2). Each of these Brønsted acids appearing in Figure 1.2 will be discussed in the ensuing sections. The majority of these families modify the substituents on the 3 and 3' positions of the naphthol moiety to achieve higher enantioselectivity in a variety of reactions, which will be exhibited in examples shown throughout this chapter.

Figure 1.2 Common Brønsted acids derived from the BINOL ligand employed in asymmetric catalysis

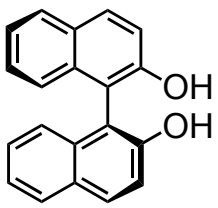

BINOL
(S)-**1**

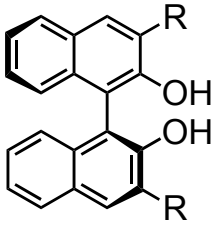

3,3'-substituted BINOL
(S)-**4**

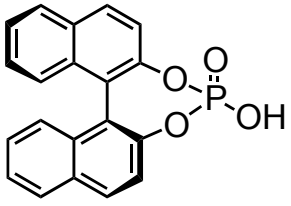

BINOL phosphoric acid
(S)-**5**

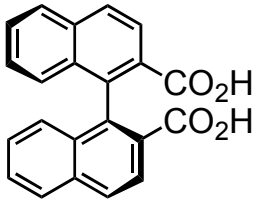

BINOL dicarboxylic acid
(S)-**6**

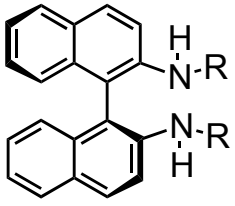

BINAM derivatives
(S)-**7**

1.2.1.1 Use of 3,3'-BINOL derivatives in asymmetric catalysis

The 3,3'-BINOL derivatives have been studied for their ability to substantially increase enantioselectivity of numerous classes of reactions as compared to its unaltered BINOL counterpart. In order to narrow the topic, the focus here will be specifically on reactions that use 3,3'-BINOL derivatives as Brønsted acids in enantioselective addition of nucleophiles to imines to generate either chiral amines or chiral aziridines.

In 2007, Wipf and Lyon generated cis-aziridines **10** from diphenylmethyl protected imines **8** and ethyl diazoacetate (EDA) **9** using bulky 3,3'-substituted BINOL ligands **4** (Scheme 1.1).[17]

Scheme 1.1 Reaction of imines with EDA to give cis-aziridines moderated by **4a**

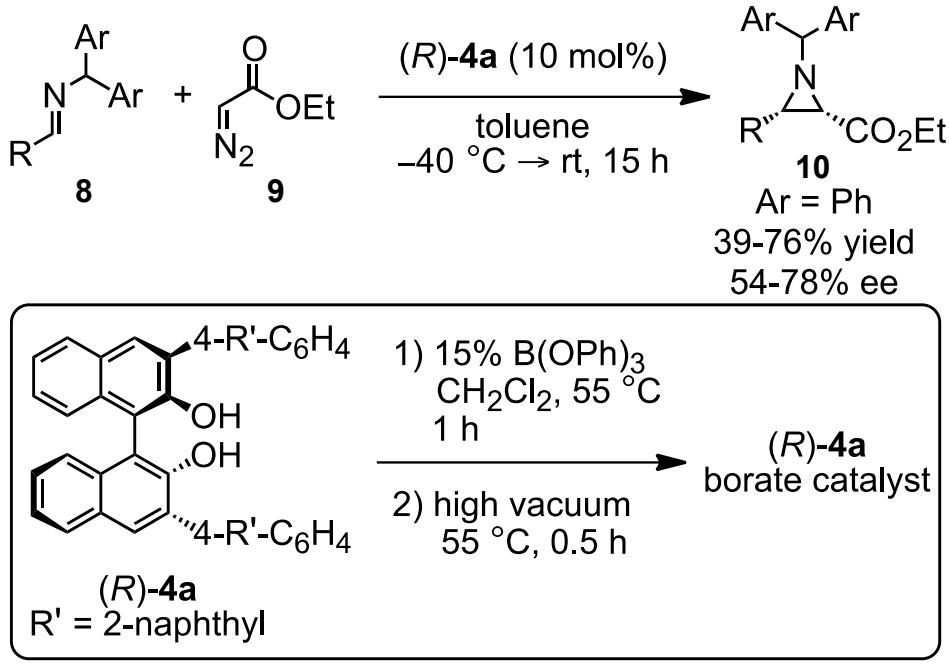

Wipf and Lyon designed six bulky ligands resulting in (*R*)-**4a** giving optimal enantioselectivity. Using this bulky BINOL ligand **4a** resulted in decent yields and

enantioselectivity. However, the substrate scope was limited to aromatic substituted imines.

BINOL derivatives have also been employed in nucleophilic additions to imines generating chiral amines. In 2005, Dixon and Tillman reported enantioselective addition reactions of methyleneaminopyrrolidine **11** to Boc (*tert*-butoxycarbonyl) protected imines **12** using their 3,3'-bismethanol-2,2'-binaphthol (BIMBOL) catalyst **4b** (Scheme 1.2).[18] These reactions resulted in chiral amines **13** in moderate to good yields and ee's.

Scheme 1.2 Imine additions moderated by the BIMBOL ligand **4b**

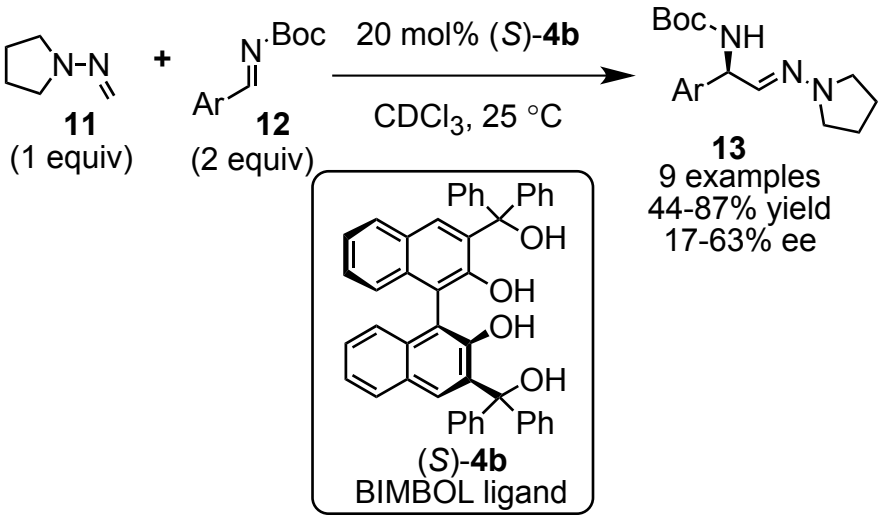

In these addition reactions, the protecting group of the imine proved to be very important. There must be the capability for the protecting group to perform hydrogen bonding, as with the N-Boc-imine **12** seen in Scheme 1.2, in order for the reaction to proceed. Performing the reaction using BINOL **1** with diphenylmethyl protected imine **8** resulted in 0% conversion. However, when using a protecting group capable of hydrogen bonding such as SO_2R or CO_2R in the presence of BINOL **1** resulted in

conversions of ≥ 66%. When BINOL was replaced with BIMBOL **4b**, the results increased to 87% yield and 63% enantioselectivity (Scheme 1.2).

1.2.1.2 Bifunctional organocatalyst incorporating both Lewis base and Brønsted acid moieties

Another interesting BINOL derivative is the bifunctional organocatalyst designed by Sasai et al. in 2005.[19] This bifunctional catalyst incorporates both Lewis base and Brønsted acid units (Figure 1.3), which aid in the aza-Morita-Baylis-Hillman (aza-MBH) reaction (Scheme 1.3).

Figure 1.3 General structure for the bifunctional organocatalyst

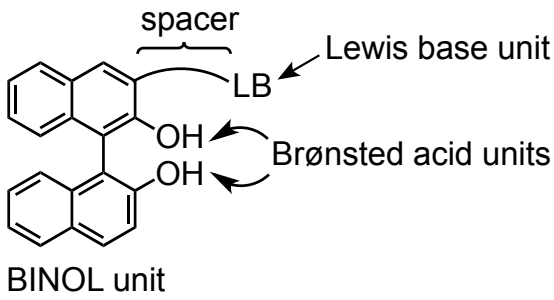

When the bifunctional organocatalyst is applied in the aza-MBH reaction, the Lewis base facilitates the Michael addition. Simultaneously, the Brønsted acid activates the α□β-unsaturated carbonyl. Following the Michael reaction, the Lewis base is eliminated via a retro-Michael reaction (Scheme 1.3).

This bifunctional organocatalyst proved to be very efficient in the enantioselective aza-Morita-Baylis-Hillman reaction. It resulted in both high to excellent yields and ee's (Scheme 1.4).

Scheme 1.3 Aza-Morita-Baylis-Hillman reaction using the bifunctional organocatalyst

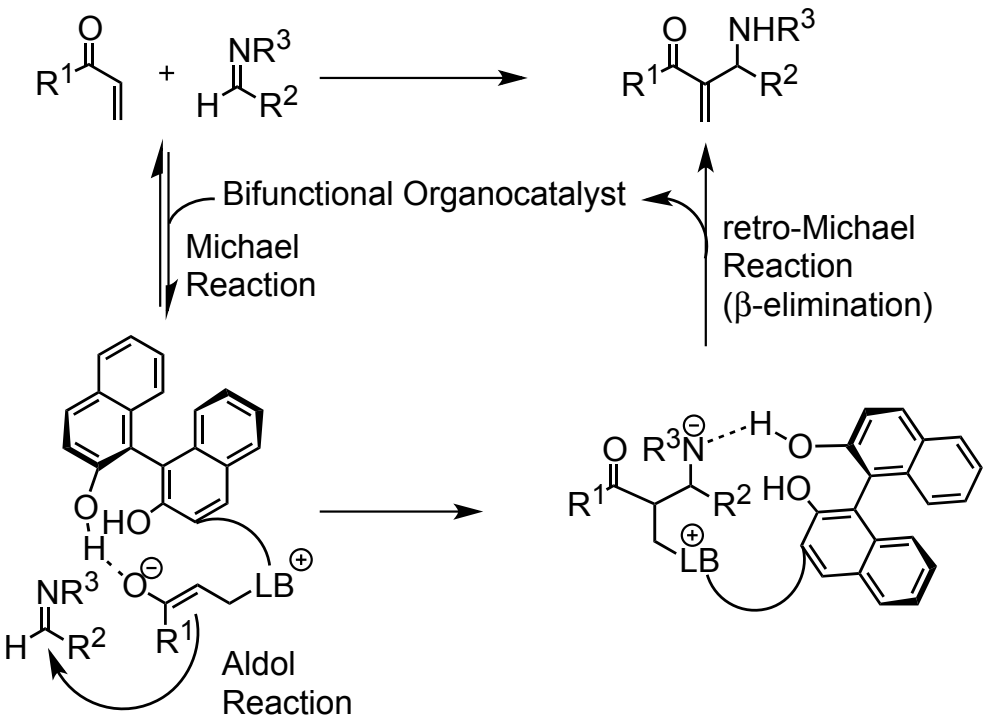

Scheme 1.4 Aza-Morita-Baylis-Hillman reaction using bifunctional organocatalyst **4c**

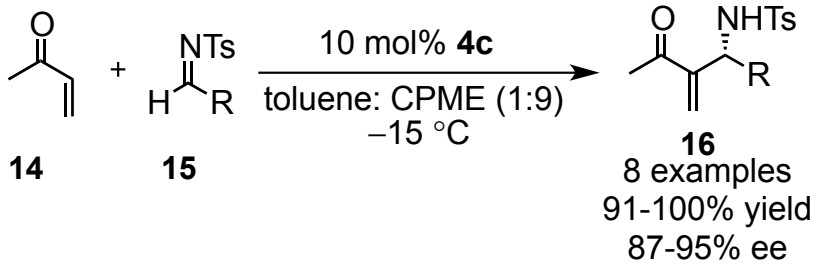

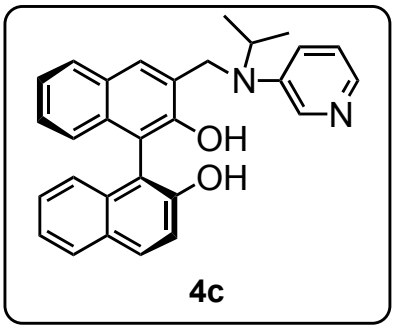

4c

There were three key pieces of the reaction that played an important role in yielding optimal results. Firstly, the optimal solvent found was a mixture of toluene and cyclopentyl methyl ether (CPME). Secondly, the best temperature was at -15 °C. Thirdly, and most importantly, the pyridine moiety attached to the aniline amine incorporated in **4c** must be connected at the meta position. If this position was switch to ortho or para, the reaction was either ineffective or resulted in decreased enantioselectivity. The only significant drawback to this system is the semi-high catalyst loading of 10 mol%.

1.2.2 BINOL dicarboxylic acids applied in asymmetric catalysis

Previously, a new family of chiral Brønsted acids has been explored branching from the BINOL family. Maruoka and Hashimoto first explored the BINOL dicarboxylic acid derivatives in 2007.[20] They presumed that prior neglect of carboxylic acids in hydrogen-bonding catalysis is due to the poor reactivity and difficulty constructing a chiral recognition site around the carboxylic acid. To remedy this concern, they proposed to combine carboxylic acids with the chiral binaphthyl moiety to give BINOL dicarboxylic acid derivatives.

This catalyst family was initially employed in the asymmetric Mannich reaction. Maruoka and Hashimoto performed asymmetric additions of diazoacetates **17** to N-Boc-imine **12** to give chiral amines **18** with moderate to high yields and high to excellent ee's (Scheme 1.5).

Scheme 1.5 Asymmetric Mannich reactions using a dicarboxylic acid BINOL derivative

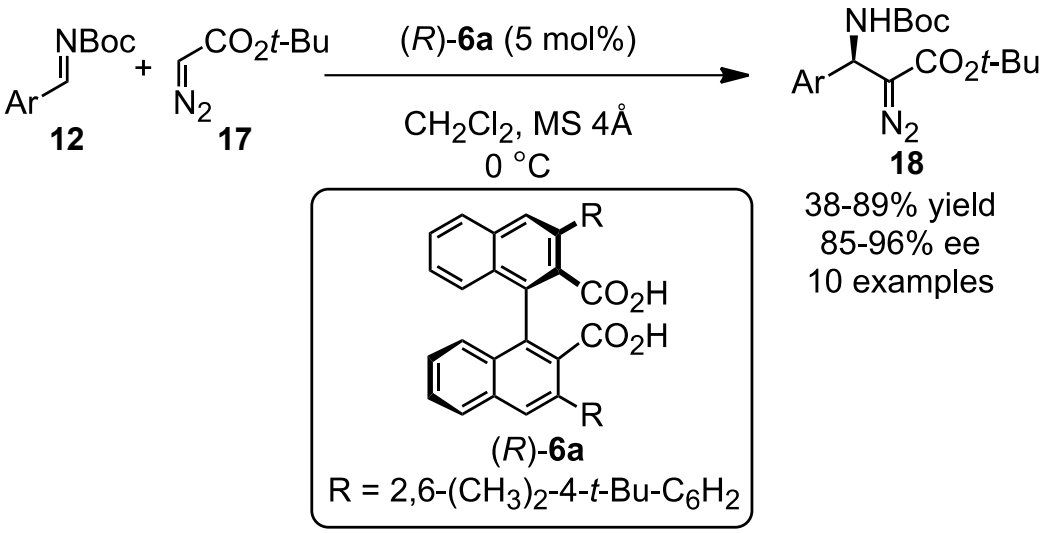

In 2008, Maruoka and coworkers applied their dicarboxylic acid BINOL derivatives to asymmetric aziridination reactions.[21] The reaction between diazoacetamides **19** and N-Boc-imine **12** resulted in trans-aziridines **20** in low to moderate yields, good to excellent ee's, and >20:1 trans/cis ratios (Scheme 1.6).

Scheme 1.6 Trans-aziridination reaction using a dicarboxylic acid BINOL derivative

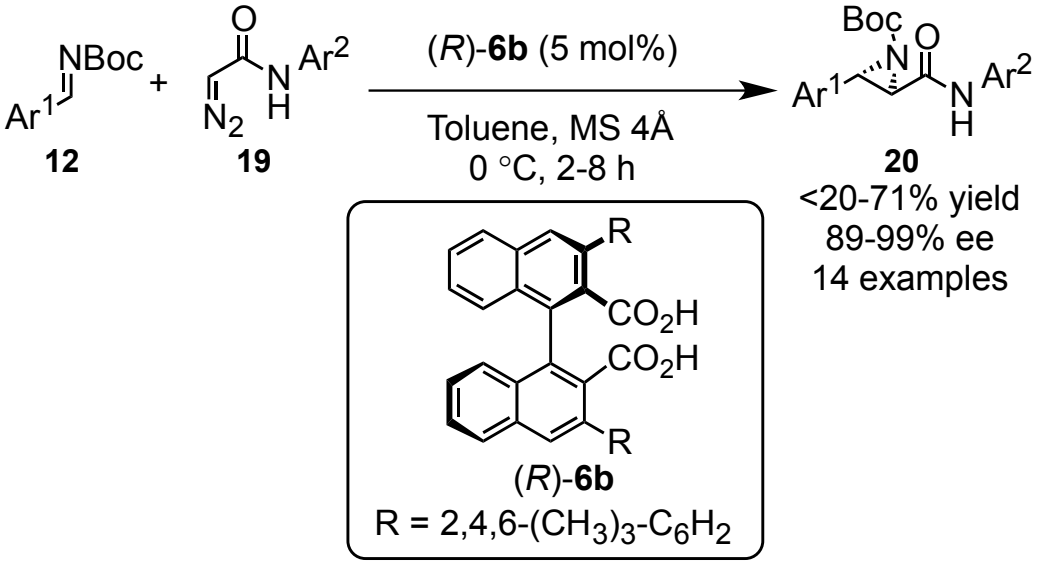

Both the asymmetric Mannich and aziridination reactions above performed by Maruoka et al. were carried out with molecular sieves to prevent hydrolysis of the imine and increase yields.

1.2.3 BINOL phosphoric acids applied in asymmetric catalysis

BINOL phosphoric acids, first pioneered by Akiyama et al. and Terada et al.,[22,23] have been used to induce chirality in a plethora of reactions in organic synthesis. Here the focus will lie with aziridination reactions catalyzed by 3,3'-BINOL substituted phosphoric acids.

In 2009, Akiyama et al. reported a one-pot aziridination reaction that synthesizes an aldimine in situ via phenyl glyoxal derivatives **21** and *p*-anisidine (PMP-NH_2) **22**, which then reacts with EDA **9** to form cis-aziridines **23** in excellent yields and ee's (Scheme 1.7).[24]

Scheme 1.7 Cis-aziridines via a one-pot protocol

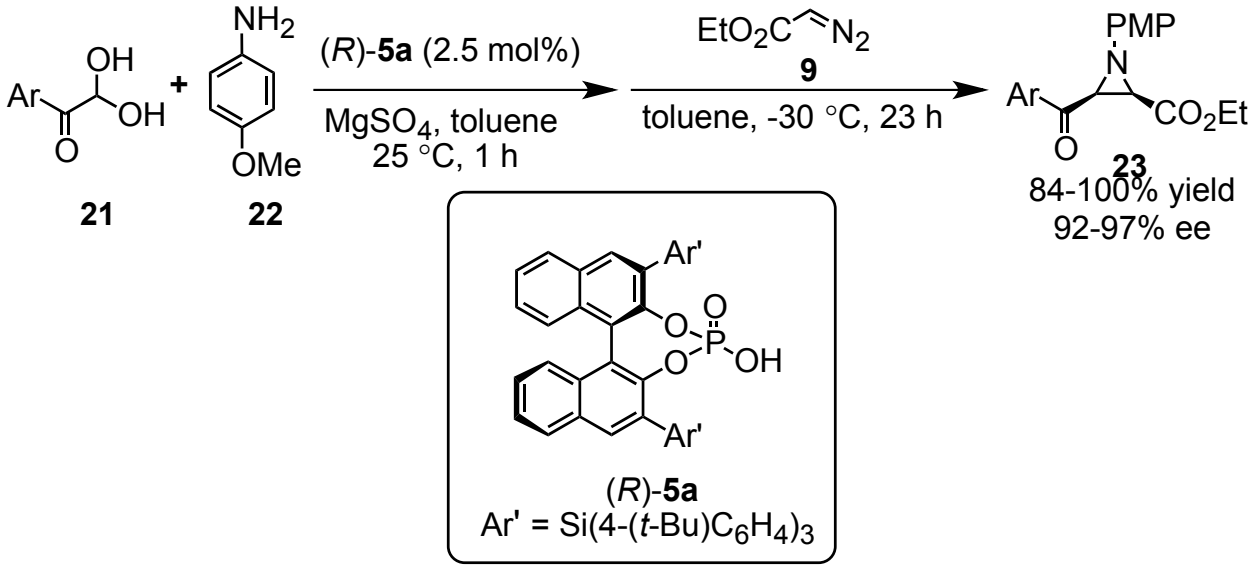

The BINOL phosphoric acid of choice consists of 3,3'-Si(4-(*t*-Bu)$C_6H_4)_3$ substituted BINOL phosphoric acid **5a**. It was found that the substituents placed on the silicon in the 3 and 3' positions were of extreme importance. When $SiPh_3$ was substituted in the 3 and 3' positions, the simpler reaction of aldimine to aziridination resulted in poor yield and enantioselectivity. Therefore, (*R*)-**5a** was used as the optimal catalyst. The substrate scope covered both electron deficient and enriched aromatic substrates, all resulting in excellent yields and ee's. However, the substrate scope lacked aliphatic substituted aziridines.

Also in 2009, Zhong et al. published a paper for trans-aziridination starting from N-Boc-imines **12** and diazoacetamides **19**.[25] These reactions were catalyzed by bulky 3,3'-BINOL substituted phosphoric acids **5b** to give trans-aziridines **20** in excellent yields and ee's (Scheme 1.8).

Scheme 1.8 Trans-aziridination of N-Boc imines and diazoacetamides

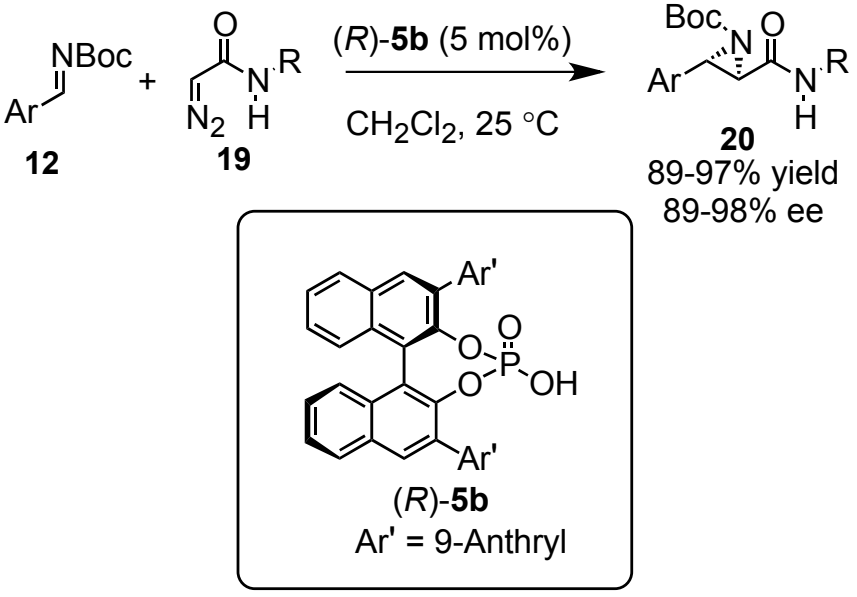

The substrate scope varied from electron deficient to electron rich aromatic imines. However, no aliphatic substituted imines were reported.

Another important example in the literature using BINOL phosphoric acids is the work done by Cahard et al. on the synthesis of trifluoromethyl substituted cis-aziridines.[26] Similar to the cis-aziridines reported by Akiyama et al. (Scheme 1.7), these reactions first generate aldimines in situ via phenyl glyoxal derivatives **21** and *p*-anisidine **22**. Furthermore, the trifluoromethyl substituted diazo reagents are also formed in situ, which then react with aldimines in the presence of 3,3′-bis(2,4,6-triisopropylphenyl)-1,1′-binaphthyl-2,2′-diyl hydrogenphosphate (TRIP) **5c** to give cis-aziridines **24** (Scheme 1.9).

Scheme 1.9 Synthesis of cis-aziridines containing a trifluoromethyl substituent

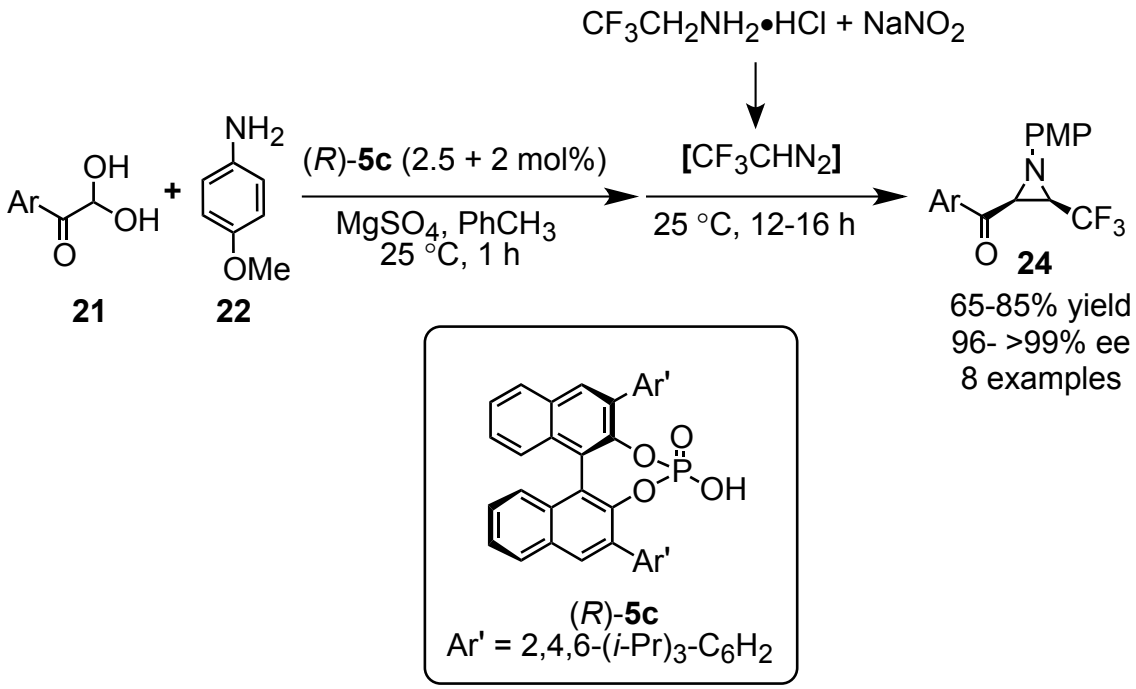

The main advantage to this system is its simplicity. All of the substrates are generated in situ and the reaction proceeds smoothly at room temperature to give high

yields and excellent ee's. The only non-simplistic aspect is that it involves two separate additions of the catalyst (2.5 mol% followed by 2 mol%). This is done in order to minimize the formation of byproducts.

1.2.3.1 BINOL phosphoric acid derivative used in the aziridination reaction

The previously discussed examples of BINOL phosphoric acids consisted of a hydrogen phosphate group as the Brønsted acid moiety. The following trans-aziridination published by Maruoka et al. uses the strongly acidic N-triflyl phosphoramide **5d** (Scheme 1.10).[27]

Scheme 1.10 Trans-aziridination of Boc protected ketimines and unsubstituted vs. substituted diazocarbonyls

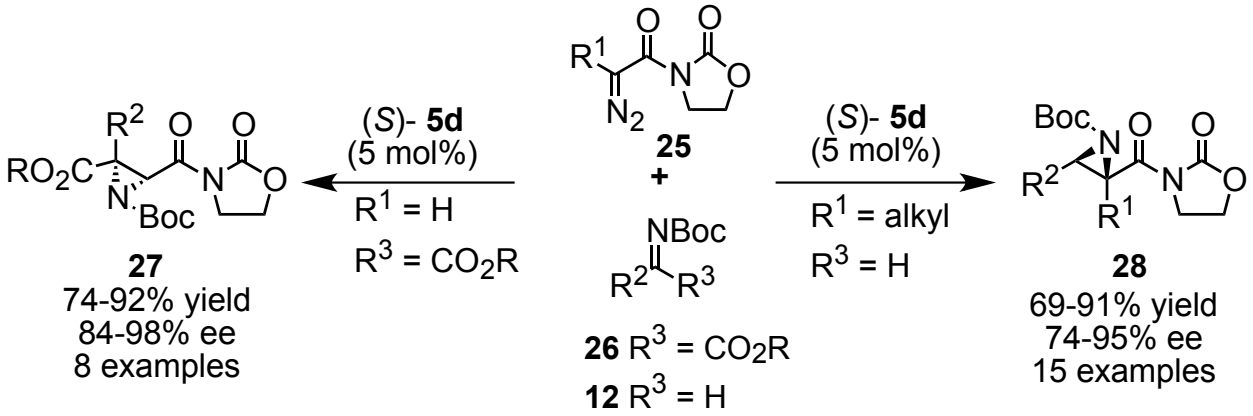

When using BINOL hydrogen phosphate **5**, the reaction resulted in 0% conversion. Therefore, the N-triflyl phosphoramide **5d** is crucial for this reaction. The reaction

between unsubstituted diazocarbonyls **25** (R^1 = H) and ketimines **26** resulted in high to excellent yields and ee's. When using substituted diazocarbonyls **25** with ketimines **12**, the reaction still proceed with only a slight decrease in enantioselectivity (Scheme 1.10).

1.2.4 BINAM ligand used in asymmetric catalysis

Another branch of BINOL derivatives is the 1,1'-binaphthalene-2,2'-diamine (BINAM) ligand **7** illustrated in Figure 1.2. The example shown here is known as either the aza-Henry or nitro-Mannich reaction.[28] Aromatic substituted N-Boc-imines **12** are reacted with nitro alkanes **29** to generate nitro incorporated chiral amines **30** in moderate to good yields and good to high ee's (Scheme 1.11). The active catalyst **7a** used here by Wulff et al. is a BINAM ligand that incorporates a bis-thiourea moiety. These thioureas promote hydrogen bonding with both the N-Boc-imines **12** and nitro substrates **29** to enhance enantioselectivity and increase conversion of starting materials to products.

Scheme 1.11 Chiral amines prepared using BINAM thiourea catalyst **7a**

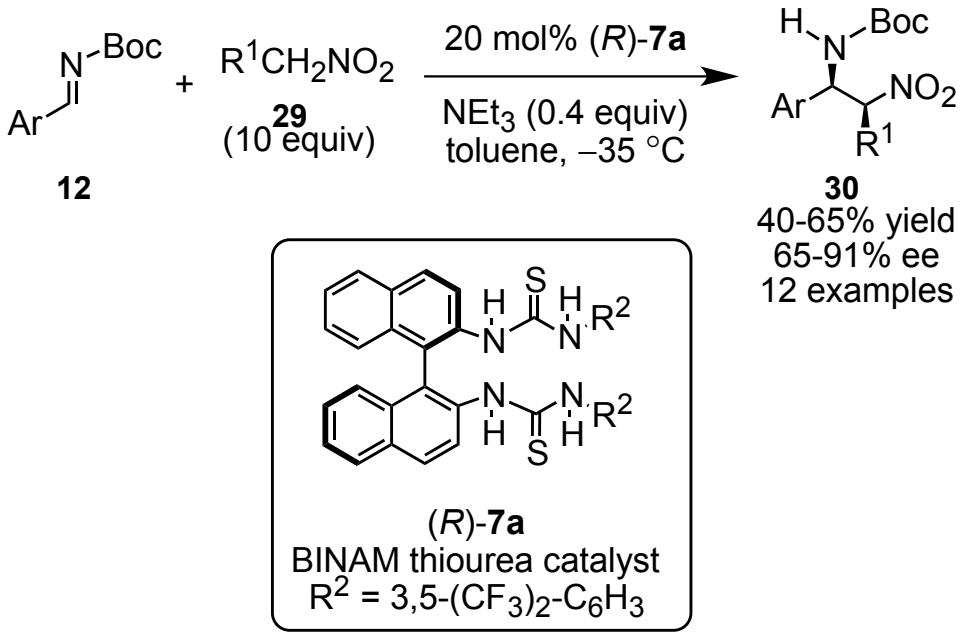

1.2.5 VANOL and VAPOL ligands applied in the synthesis of chiral aziridines and amines

The VANOL **2** and VAPOL **3** ligands were first synthesized in the Wulff group in 1993.[8] The concept for these ligands stemmed from the commonly used BINOL ligand and its many derivatives. As seen in Figure 1.1, VANOL and VAPOL have a distinct difference from BINOL in that the major chiral pockets for the VANOL and VAPOL ligands lie on the same side of the molecule as that of the active binding site, unlike that seen in BINOL. Ideally, this would allow for better binding to a substrate in asymmetric reactions. Furthermore, the Wulff group has made derivatives of VANOL and VAPOL similar to the BINOL derivatives that have been discussed throughout this chapter. These derivatives include but are not limited to VANOL/VAPOL phosphoric acids, *N*-TRIP-benzenesulfonyl VAPOL phosphoramide, *N*-nitrobenzenesulfonyl VAPOL phosphor-amide, and N-triflyl VANOL/ VAPOL phosphoramide.[29]

These ligands have been applied to a variety of reactions such as the Ugi,[15] Diels-Alder,[8] heteroatom Diels-Alder,[9] aza-Cope,[10] Petasis,[14] and Baeyer Villiger[13] reactions. However, one of the most important reactions that were born from the many studies with VANOL and VAPOL is the Wulff catalytic asymmetric aziridination reaction.[16] This reaction has shown its usefulness in the synthesis of florfenicol, an antibacterial active compound, which was synthesized by Chen et al. in 45% overall yield in 7 steps using a modified procedure of the Wulff catalytic asymmetric aziridination reaction.[3]

1.2.5.1 The Wulff catalytic asymmetric aziridination reaction

The Wulff catalytic asymmetric aziridination (AZ) reaction was first discovered in the Wulff research lab in 1999[16a] to synthesize cis-aziridines. In 2010, we advanced our system to include trans-aziridines,[30] making it a very robust method (Scheme 1.12). The AZ reaction uses the vaulted biaryl ligands VANOL **2** and VAPOL **3** to self assemble a chiral Brønsted acid in the presence of an imine or base. This chiral acid is then used to moderate the reaction between imines **8** and diazo compounds **9** or **19a** to their corresponding cis- or trans-aziridines **10** or **32** (Scheme 1.12).

Scheme 1.12 The Wulff catalytic asymmetric aziridination reaction

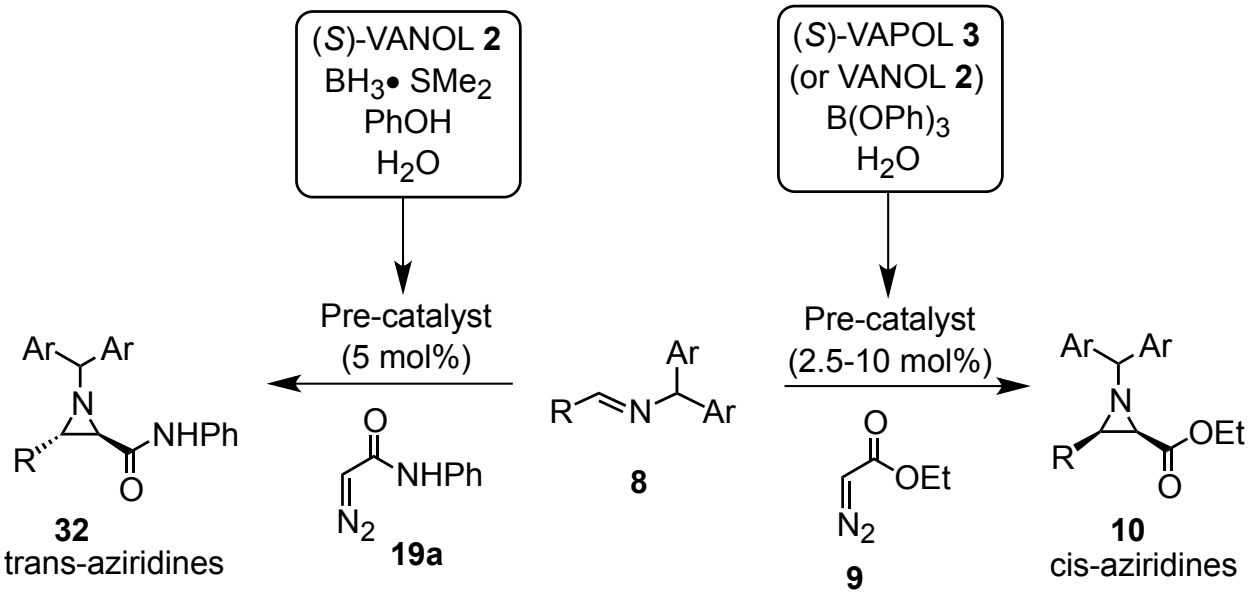

1.2.5.2 Cis-aziridines generated via the AZ reaction

The first catalytic asymmetric cis-aziridination protocol was published in 1999 resulting in good enantioselectivity and yields.[16a] An improved protocol reported the following year had the pre-catalyst generated by combining either VANOL **2** or VAPOL

3 with $B(OPh)_3$ and water.[16b] This pre-catalyst is composed of two species, B1 and B2, which are given their name according to the number of borons each species contains (Scheme 1.13). Mixing this pre-catalyst (B1 and B2) with a protected imine **8** and ethyl diazoacetate **9** results in the formation of cis-aziridines **10** in good yields and ee's (Scheme 1.12).[16a]

Scheme 1.13 Pre-catalyst species B1 and B2 generated from VANOL **2** or VAPOL **3**

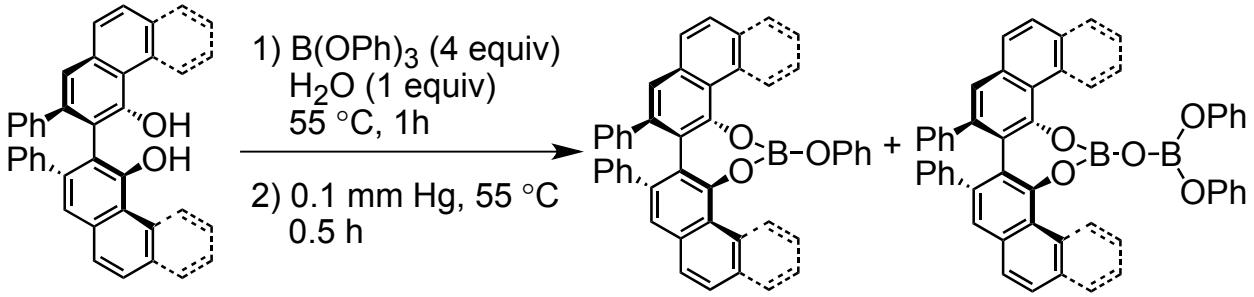

(*S*)-VANOL **2** or
(*S*)-VAPOL **3**

B1

B2

The protecting group (PG) located on the imine has been shown to substantially affect the outcome of the enantioselectivity of the aziridination reaction (Scheme 1.14). We began our aziridinations using commercially available diphenylmethyl (benzhydryl) as our protecting group. However, the induction capabilities of this reaction had room for further improvements. Therefore, our group synthesized and employed several alternate imine protecting groups, with three examples being shown here, in order to enhance the enantioselectivity in the aziridination reaction. These imine protecting groups used for the cis-aziridination in the Wulff group are Bh (benzhydryl), DAM (N-dianisylmethyl), MEDAM (3,5-dimethyldianisylmethyl), and BUDAM (3,5-di-*tert*-butyldianisylmethyl). The synthesized protecting groups (DAM, MEDAM, and BUDAM) showed significant

improvements in our ee's of our AZ reactions with MEDAM and BUDAM proving to be the best imine protecting groups for cis-aziridines (Scheme 1.14).[16i]

Scheme 1.14 Effects of imine protecting groups on enantioselectivity of aziridines

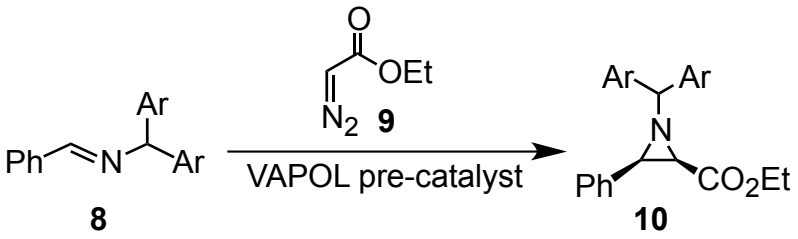

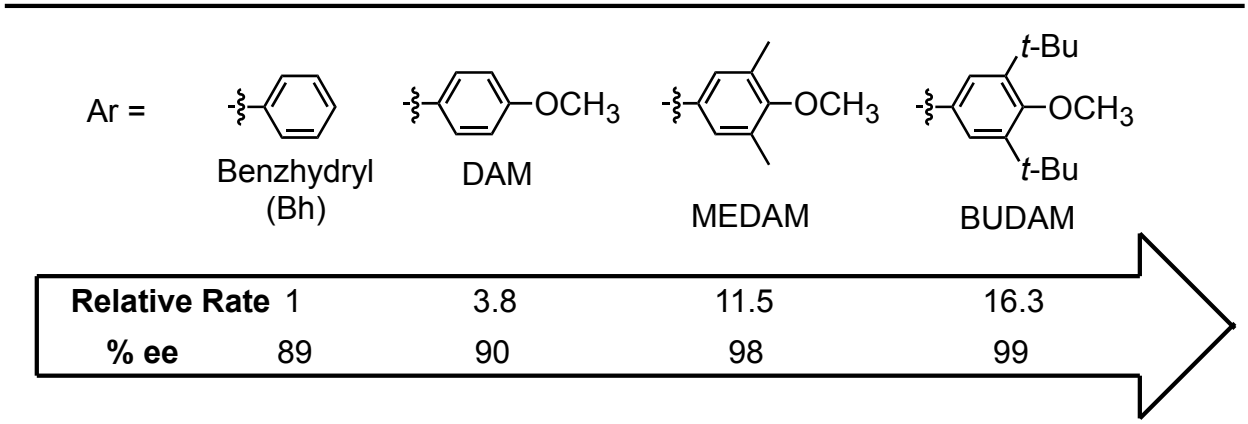

1.2.5.3 Assembly of chiral boroxinate catalyst and its role in the aziridination reaction

As previously mentioned, the AZ reaction is mediated by a chiral Brønsted acid, which incorporates either the VANOL **2** or VAPOL **3** ligand. This chiral acid is self assembled when mixing either VANOL **2** or VAPOL **3**, $B(OPh)_3$, water, and a base (typically imine) (Scheme 1.15).[31] This boroxinate catalyst, also represented as B3, can similarly be assembled starting from B1 and B2 pre-catalysts and adding a base or imine. We designate this boroxinate catalyst as B3 due to its core being composed of 3 borons.

Scheme 1.15 Chiral boroxinate catalyst, B3, acting as the Brønsted acid in the AZ reaction

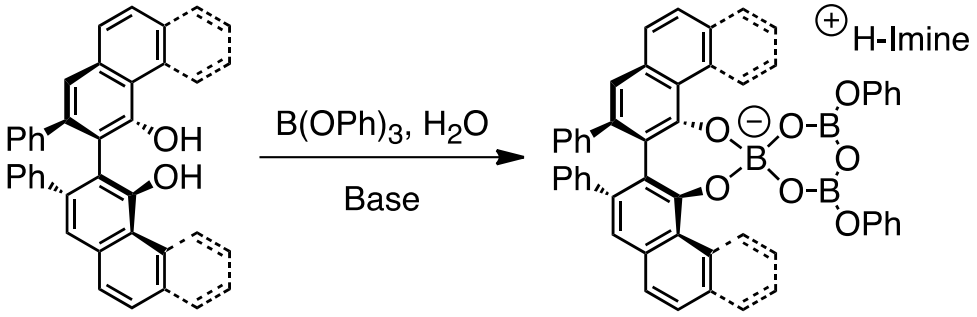

(*S*)-VANOL **2** / VAPOL **3**

Boroxinate Catayst (B3)

1.2.5.4 Proposed mechanism for the Wulff catalytic asymmetric aziridination reaction

Over the years, the Wulff group has gathered evidence to support the proposed mechanism of the Wulff catalytic asymmetric aziridination reaction. Once the crystal structure of our active boroxinate catalyst (B3) was elucidated, it was discovered that it was not a Lewis acid but rather a Brønsted acid.[31] With this in mind, we have proposed a catalytic cycle and mechanism for our AZ reaction incorporating B3 as our active catalyst, which is supported by studies of the transition states and rate limiting step in the aziridination reaction (Schemes 1.16 and 1.17).[32] The knowledge acquired about the structure of the boroxinate catalyst (B3) and the proposed catalytic cycle will be used to acquire further understanding of the Wulff AZ reaction in the following chapters of this thesis.

Scheme 1.16 Proposed catalytic cycle for the Wulff catalytic asymmetric aziridination reaction

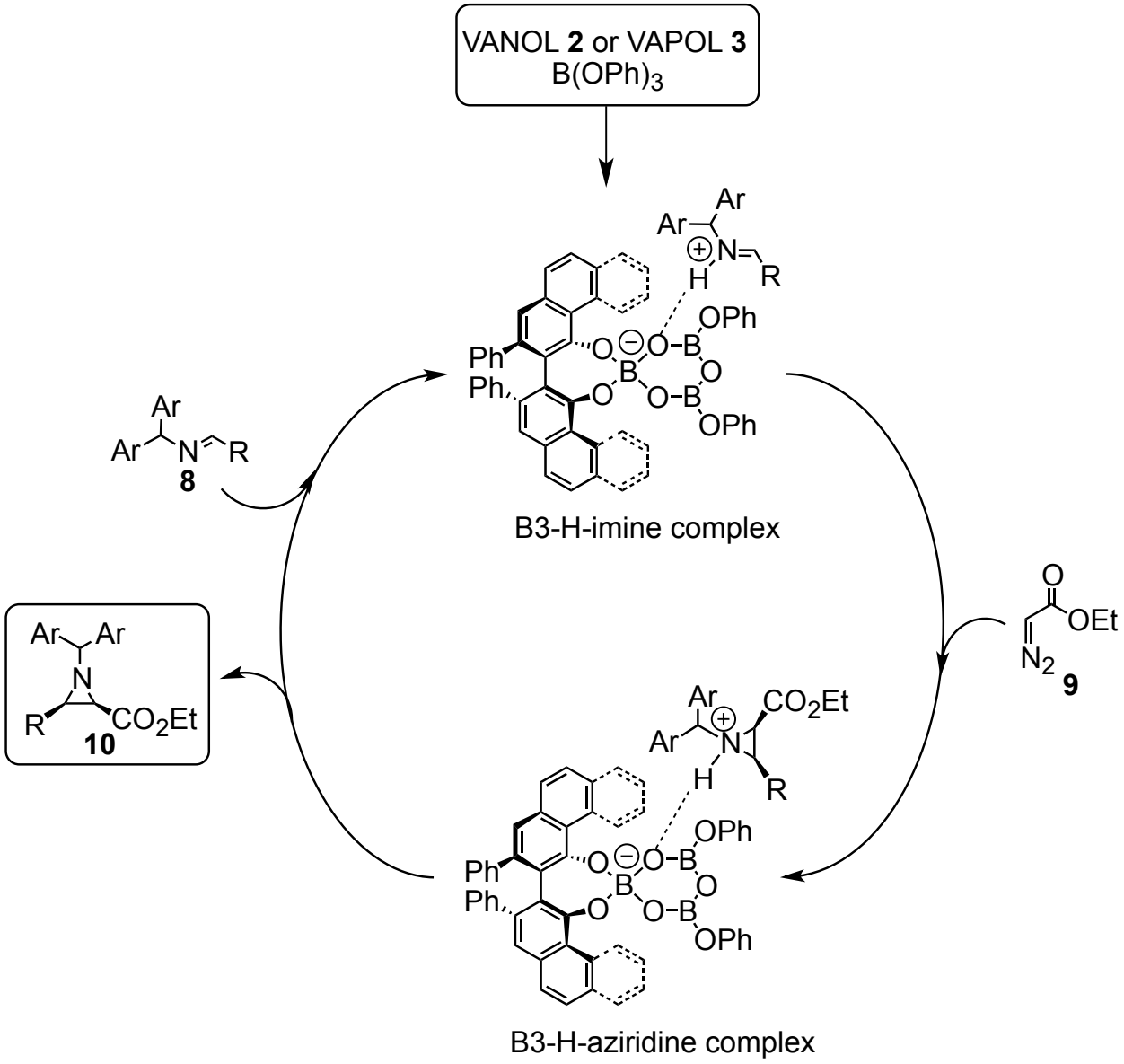

Scheme 1.17 Proposed mechanism for the Wulff AZ reaction

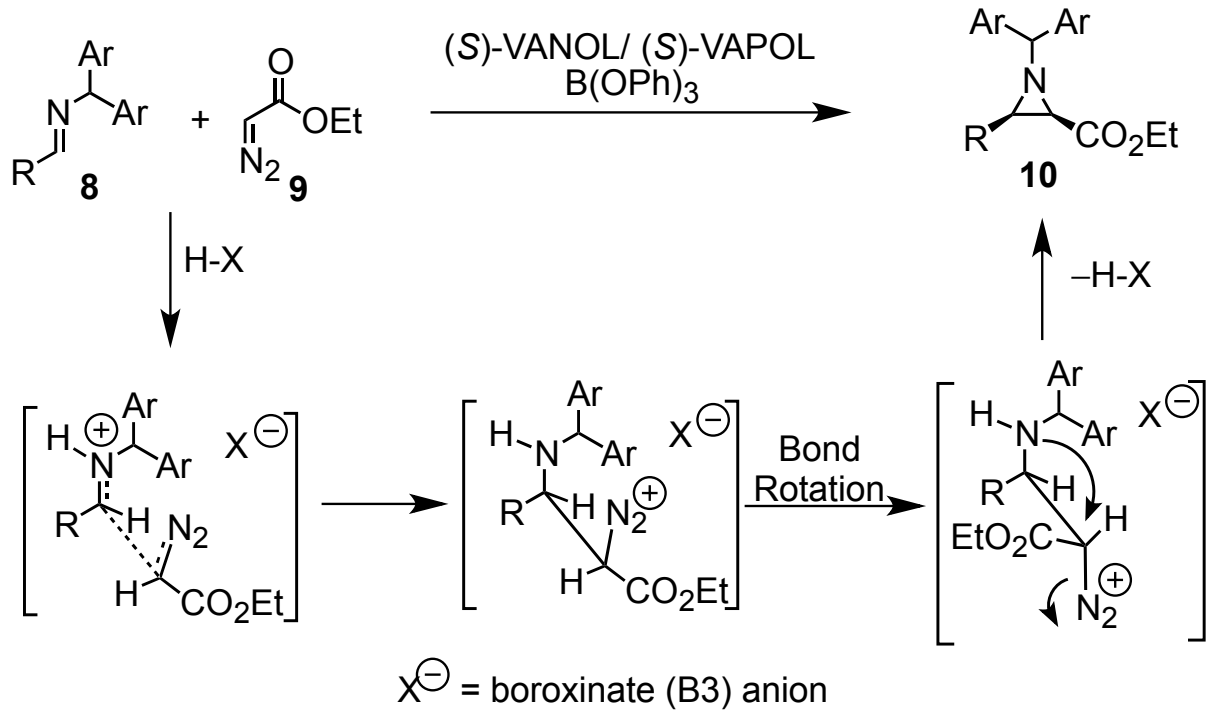

1.3 Conclusion

In summary, there are a variety of vaulted biaryl ligands that act or assist in Brønsted acid asymmetric catalysis. Our concept of creating the VANOL and VAPOL ligands stemmed from the commonly used BINOL ligand family. However, unlike the BINOL ligands, when creating our ligand family, we placed the major chiral pocket on the side of the ligand that is responsible for binding to the substrate. Furthermore, we have employed our ligands in many diverse reactions, especially the Wulff catalytic asymmetric aziridination reaction. This AZ reaction is the basis of the work to be described herein. Using the aziridination reaction as a template, we have gained insight into the active boroxinate catalyst (B3) and its mechanistic role as a chiral Brønsted acid, which will be discussed throughout this dissertation.

CHAPTER TWO

SUBSTRATE INDUCED ASSEMBLY OF A MULTIPLEX OF CHIRAL POLYBORATE BRØNSTED ACIDS WITH DIVERSITY IN THE BOROXINE RING

2.1 Introduction

An extended study is described here on exploring catalyst diversity in the catalytic asymmetric aziridination reaction of imines with ethyl diazoacetate mediated by catalysts prepared from either the VANOL or VAPOL ligand, borane dimethyl sulfide and an alcohol or phenol. This boroxinate catalyst acts as a Brønsted acid to promote the reaction between imine **8** and ethyl diazoacetate (EDA) **9** to generate cis-aziridines **10**. A general aziridination protocol that has been previously developed by the Wulff group gives either cis- or trans-aziridines in moderate to high yields and ee's, which will be referred to as the Wulff catalytic asymmetric aziridination (AZ) reaction.[16, 30] Within this chapter, the methodologies discussed will focus on cis-aziridination reactions only. This prior methodology established to generate cis-aziridines requires four components for the preparation of the boroxinate catalyst, which are the (1) VANOL or VAPOL ligand, (2) triphenyl borate, which contains a small amount of (3) water, and an (4) imine (or base). The first three components (ligand, $B(OPh)_3$, and water) generate the pre-catalyst, which is a mixture of B1 and B2 (Scheme 2.2). Upon the addition of an imine or base, self-assembly of the active boroxinate catalyst (B3) occurs in-situ (Scheme 1.15). When EDA **9** reacts with a protected imine **8** in the presence of the boroxinate catalyst (B3), cis-aziridines **10** are produced (Scheme 2.1).

One of the flaws in this method (Scheme 2.1) is the lack of diversity in the catalyst's structure.

Scheme 2.1 Wulff catalytic asymmetric aziridination reaction yielding cis-aziridines **10**

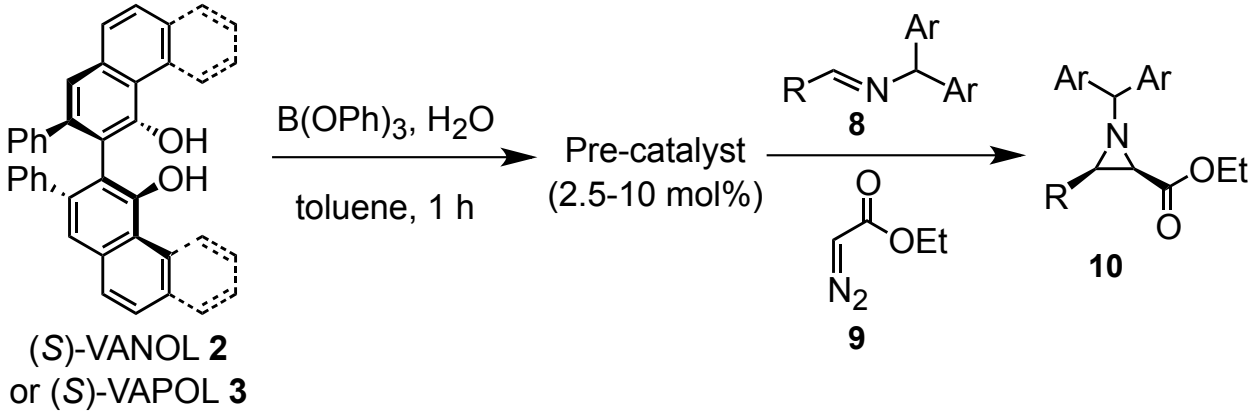

There are two areas in which the catalyst structure can be varied. First, the ligand could be altered to provide a variety of catalyst structures. However, to synthesize each ligand separately would be extremely time consuming. The alternative is to look at the other variable component in the B3 system, $B(OPh)_3$. The shortcoming to using triphenyl borate is that it allows for only one alcohol, phenol, to be present in the active B3 catalyst. By removing the triphenyl borate and making this species in situ using borane and various alcohols or phenols, we would be capable of diversifying the system by controlling the alcohol used to generate the B3 catalyst (Schemes 2.2 and 2.3). An extensive family of B3 catalysts can then be synthesized by using this new methodology. This new procedure to generate a large diverse catalyst family in situ will be employed in the AZ reaction and discussed in the ensuing sections.

Hitherto, it has been discovered from spectral analysis that we form two species by mixing the VANOL or VAPOL ligand, $B(OPh)_3$ and water. The first species involves one ligand molecule and one boron atom (B1). The second species involves one ligand molecule and two boron atoms (B2). Previously, the number of equivalents that were used was that which would optimize the formation of B1 and B2, which was

accomplished by mixing 1 equivalent of ligand, 2 equivalents of BH_3•SMe_2, 3 equivalents of phenol and 1 equivalent of H_2O (Scheme 2.2).[16h]

Scheme 2.2 Previous methodology used to prepare the B1 and B2 species

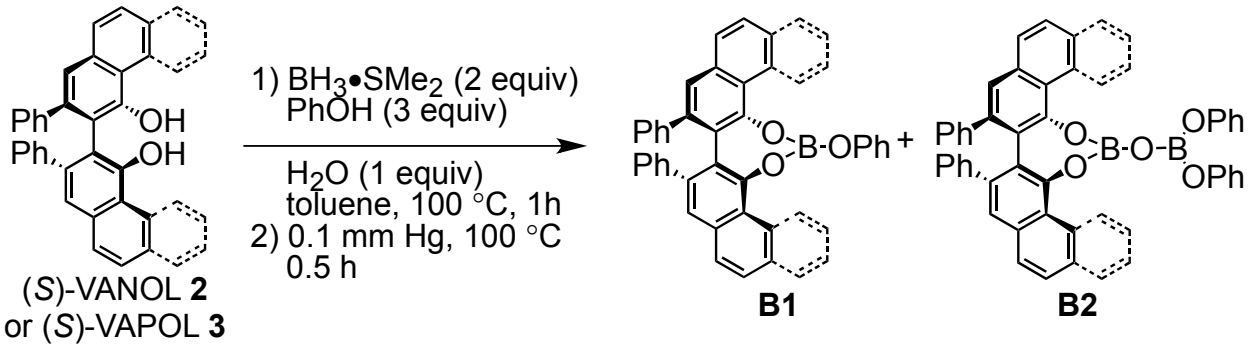

However, once we obtained the crystal structure and identified B3 as the active catalyst, it was clear that a new choice of stoichiometry would be required to better satisfy the formation of B3. The ideal proportions of reagents to generate the active boroxinate catalyst would require 3 equivalents borane dimethyl sulfide, 2 equivalents alcohol and 3 equivalents water in the presence of a base (Scheme 2.3).

Scheme 2.3 Equivalents used to generate the B3 complex using various alcohols. For interpretation of the references to color in this and all other figures, the reader is referred to the electronic version of this dissertation.

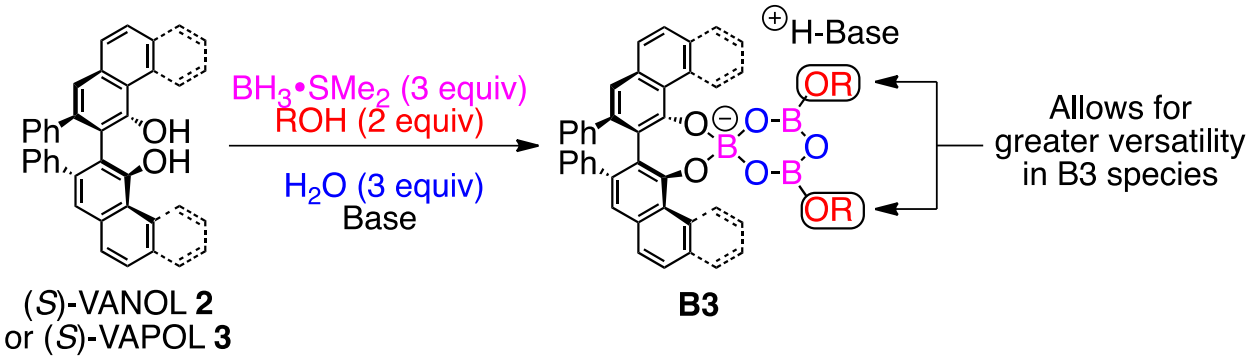

Furthermore, this large family of catalysts could be used not only for the Wulff catalytic asymmetric aziridination reaction but also for other reactions involving a Brønsted acid catalyst. Therefore, creating a method that allows for the alteration of the B3 catalyst presents a critical advantage when tweaking the system for a specific reaction.

2.2 Discovering the optimal protocol for the 6-component AZ reaction

2.2.1 Benzhydryl employed as the imine protecting group

Previously, the protecting groups on the imine used to synthesize the cis-aziridines have been optimized to give high yields and ee's. A range of protecting groups, which can be seen in Figure 2.1, have been synthesized and employed in the Wulff group for the AZ reaction.[16i]

Figure 2.1 Common protecting groups of imines used in the AZ reaction

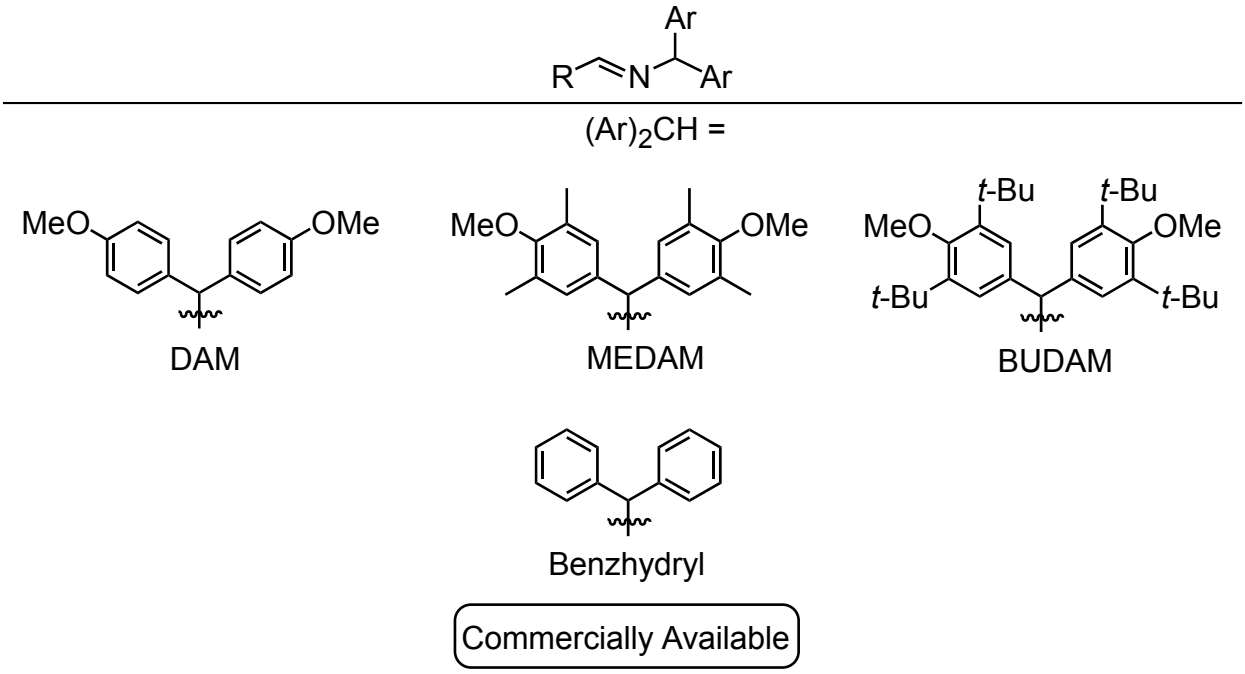

However, these protecting group precursors (in the form of amines) can be costly and time consuming to synthesize. Therefore, the commercially available protecting group

precursor, benzhydryl amine, will be seen most often in the ensuing research. However, there is a disadvantage to using benzhydryl protected imines in that they decrease the enantioselectivity in the aziridination reaction compared to that obtained with the other imine protecting groups such as MEDAM.

Overall, we will accomplish two goals with this new protocol. Firstly, diversification of our catalyst will be accomplished by generating a procedure that allows for various alcohols to be incorporated into the boroxinate catalyst. Secondly, optimization of the aziridination reaction will be investigated using the commercially available protecting group benzhydryl.

2.2.2 Exploration of procedures used in the formation of the VANOL/VAPOL boroxinate catalysts

The current protocol discussed here is termed the 6-component AZ reaction based upon the six reagents needed to generate cis-aziridines: 1) ligand, 2) borane dimethyl sulfide, 3) alcohol or phenol, 4) water, 5) imine, and 6) EDA. Four variables in the 6-component AZ reaction were evaluated in order to optimize B3 formation to establish an optimized procedure to generate cis-aziridines: 1) equivalents of reagents, 2) temperature, 3) mol% of ligand and 4) the presence of vacuum (Table 2.1). All of these variables could have a substantial impact in the results. Phenol was used as the standard alcohol when determining the optimized procedure. This was chosen based upon the previously employed protocol, which was optimized using triphenyl borate as the donator for the phenol portion of the B3 catalyst. With respect to solvent choice, toluene has been demonstrated in the past to be most advantageous for the AZ

reaction.[16h] Therefore, toluene was used as the solvent in the optimization of the 6-component AZ reactions seen in Table 2.1.

As observed in Table 2.1, temperature and the presence or absence of vacuum were the two variables that resulted in the most substantial impact on the reactions.

Table 2.1 Various methods employed in the 6-component AZ reaction [a]

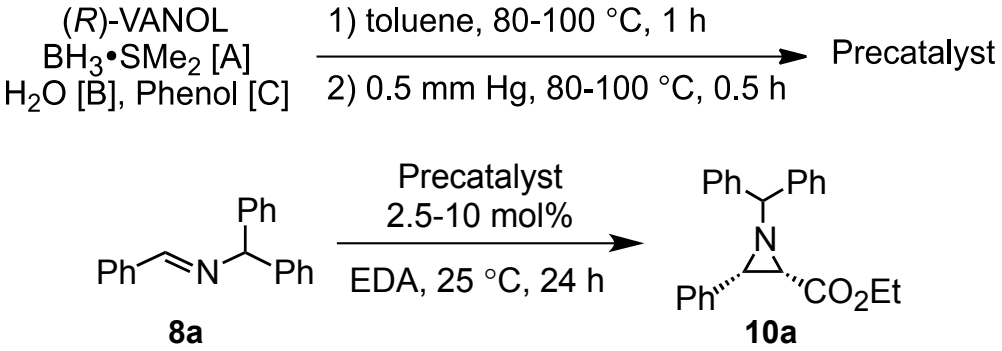

8a **10a**

entry	catalyst method [b]	equiv [A]:[B]:[C] [c]	mol % catalyst [d]	temp (°C)	vacuum	yield **10a** (%) [e]	ee **10a** (%) [f]
1	I	2:1:3	10	100	yes	93	92
2	II	3:3:2	5	100	yes	91	88
3	I	2:1:3	10	80	yes	91	91
4	II	3:3:2	5	80	yes	91	91
5	II	3:3:2	10	100	yes	92	91
6	II	3:3:2	2.5	80	yes	90	85
7	III	3:3:2	10	80	no	11 conv [h]	ND
8	III	3:3:2	10	100	no	57 [i]	88
9 [g]	III	3:3:2	10	100	no	80	95
10	IV	3:3:2	10	100	no	88	92
11	V	3:3:2	10	80	yes	25 conv [h]	ND

[a] Ligand, borane, water, and phenol were stirred in 0.1 M in ligand in toluene at the specified temperature for 1 h. Unless otherwise stated, the reaction was then exposed

to vacuum for 0.5 h. To the flask containing 2.5-10 mol% catalyst (with respect to imine) was added imine **8a** (1.00 equiv) and ethyl diazoacetate **9** (1.20 equiv) in a 0.5 M in imine in toluene solution. The reaction was stirred at 25 °C for 24 h. ND represents Not Determined. Unless otherwise stated, all reactions proceeded to 100% conversion and resulted in >50:1 cis/trans ratio. [b] Method I: A 1:2:1:3 ratio of ligand, borane, water, and phenol was used to generate the catalyst. Method II: A 1:3:3:2 ratio of ligand, borane, water, and phenol was used to generate the catalyst. Method III: A 1:3:3:2 ratio of ligand (0.10 equiv), borane (0.30 equiv), water (0.30 equiv), and phenol (0.20 equiv) were mixed with benzhydryl amine (1.00 equiv) and stirred at a specified temperature without the presence of vacuum for 1 h in order to generate the catalyst. Following the catalyst formation, 4Å powder molecular sieves, benzaldehyde (1.05 equiv), and EDA **9** (1.20 equiv) were added to a 1 M in imine in toluene solution containing the catalyst and stirred at 25 °C for 24 h. Method IV: A 1:3:3:2 ratio of ligand (0.10 equiv), borane (0.30 equiv), water (0.30 equiv), and phenol (0.20 equiv) was stirred at 100 °C for 1 h to generate the catalyst. After the catalyst formation, imine **8a** (1.00 equiv) was added to the catalyst and stirred at 25 °C for 1 h followed by the addition of EDA **9** (1.20 equiv). The reaction was then stirred at 25 °C for 24 h. Method V: A 1:3:3:2 ratio of ligand (0.10 equiv), borane (0.30 equiv), water (0.30 equiv), and phenol (0.20 equiv) was stirred in the presence of imine **8a** (1.00 equiv) at 80 °C followed by vacuum at 80 °C for 0.5 h. EDA **9** (1.20 equiv) was added to the mixture and stirred in 1 M in imine in toluene at 25 °C for 24 h. [c] Equivalents of borane [A], water [B], and phenol [C] are with respect to the ligand. [d] Mol% of ligand is in respect to imine (0.5 mmol). [e] Isolated yield after

column chromatography on silica gel. [f] Determined by chiral HPLC analysis. [g] (*S*)-VAPOL used as ligand. [h] Conversion based upon an internal standard ($CHPh_3$). [i] Reaction went to 68% conversion.

Applying both vacuum and heat during catalyst preparation with various ratios of reagents used to generate the pre-catalyst gave both high yields and enantioselectivities (Methods I/ II: entries 1-6, Table 2.1). Increasing the ligand loading from 5 mol% to 10 mol% resulted in a slight increase in enantioselectivity from 88% to 91% (entries 2 and 5). When decreasing the catalyst loading to 2.5 mol% and reducing the temperature to 80 °C, the enantioselectivity dropped to 85% (entry 6). When the addition sequence of the reagents and starting materials were changed, there were drastic consequences. When the imine was formed in situ, benzhydrylamine was added during the catalyst formation. Once the catalyst formation was complete, benzaldehyde (1.05 equiv) and molecular sieves were added just prior to EDA addition and stirred at 25 °C for 24 h (Method III). When VANOL was used to generate the catalyst and the vacuum was not applied during catalyst formation, both the enantioselectivity and yields dropped drastically (Method III: entries 7 and 8). A larger decrease was seen in entry 7 and this may be due to a decrease in temperature during catalyst formation. However, the VAPOL ligand was superior to the VANOL ligand in the absence of vacuum (entries 8 and 9). When the reaction was performed at 100 °C without applying vacuum and when the imine is added to the pre-catalyst and stirred for one hour at 25 °C prior to the addition of EDA, the yield was satisfactory with high enantioselectivity (Method IV: entry 10). Although this procedure did not give the optimal results, it would guarantee that no compounds were removed by vacuum allowing for knowledge of all species that are

present within the reaction. Furthermore, when compared to the previously used protocols, we have experimentally simplified the reaction by removing the need for vacuum. The final entry was to determine if the reaction would progress when imine was present during the catalyst formation step. This resulted in only 25% conversion (Method V, entry 11).

2.3 Phenols and alcohols used in the B3 catalyst formation for the 6-component AZ reaction

When exploring many alcohol and phenol derivatives that could be used to generate the boroxinate catalyst, sterically bulky phenols, electron deficient and electron rich phenols, and aliphatic alcohols were considered.

Figure 2.2 Interactions between VAPOL-B3 and MEDAM protected phenyl substituted imine as revealed by X-ray analysis [16j]

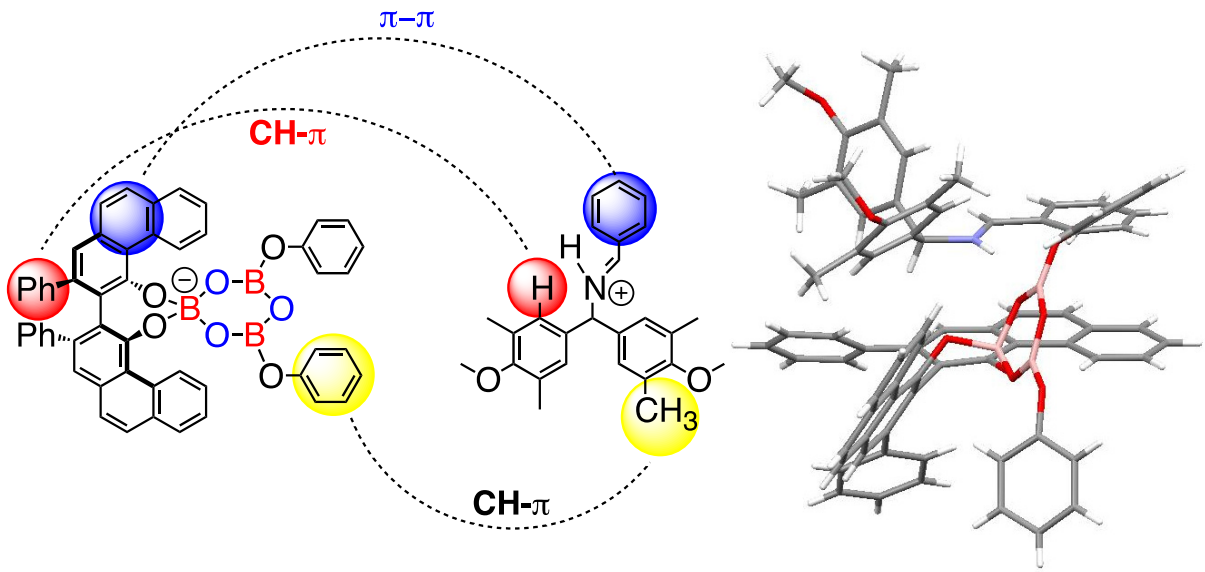

As previously seen in the Wulff group, aromatic substituted aziridines equipped with the MEDAM or BUDAM protecting group were formed in higher yields and

enantioselectivity than those aziridines having an aliphatic substituent equipped with the benzhydryl protecting group.[16] This can be explained by the π–π stacking and CH-π interactions between the imine and the catalyst (Figure 2.2).[16j] Therefore, both aromatic and aliphatic substituted aziridines (specifically phenyl and cyclohexyl) were looked at in this 6-component AZ reaction while studying the effects of various alcohols and phenols on the B3 system. This may give a greater insight on how to alter the catalyst to accommodate not only the 6-component AZ reaction but also any other reaction that may require a chiral Brønsted acid catalyst.

2.3.1 Aromatic substituted phenols used in the formation of the B3 catalyst

We began our investigation with aromatic substituted phenol derivatives in the B3 system to see how they would affect the yields and enantioselectivity of the AZ reaction. The phenol derivatives to be explored containing aromatic substituents include 1-naphthol, 2-phenylphenol, and 4-phenylphenol. These phenol derivatives gave similar results to the standard phenol (Table 2.2). The results were compared to that of the standard phenol. We employed a similar procedure to method IV given in Table 2.1.

This current procedure will be denoted as Method A. This method is similar to method IV but requires less reaction time when generating the B3 catalyst (entry 10, Table 2.1). When employing Method A, the catalyst is prepared by mixing a 1:3:3:2 ratio of ligand, borane dimethyl sulfide, water, and alcohol in toluene at 100 °C for 1 h followed by the addition of imine **8** at room temperature. This reaction mixture is then stirred at room temperature for 0.5 h to allow for the B3 catalyst to form followed by the addition of EDA **9**, which was stirred at room temperature for 24 h to give the cis-aziridine **10**. Vacuum is not applied during any portion of this method.

Table 2.2 Effects of phenyl substituted phenols employed in the B3 catalyst system [a]

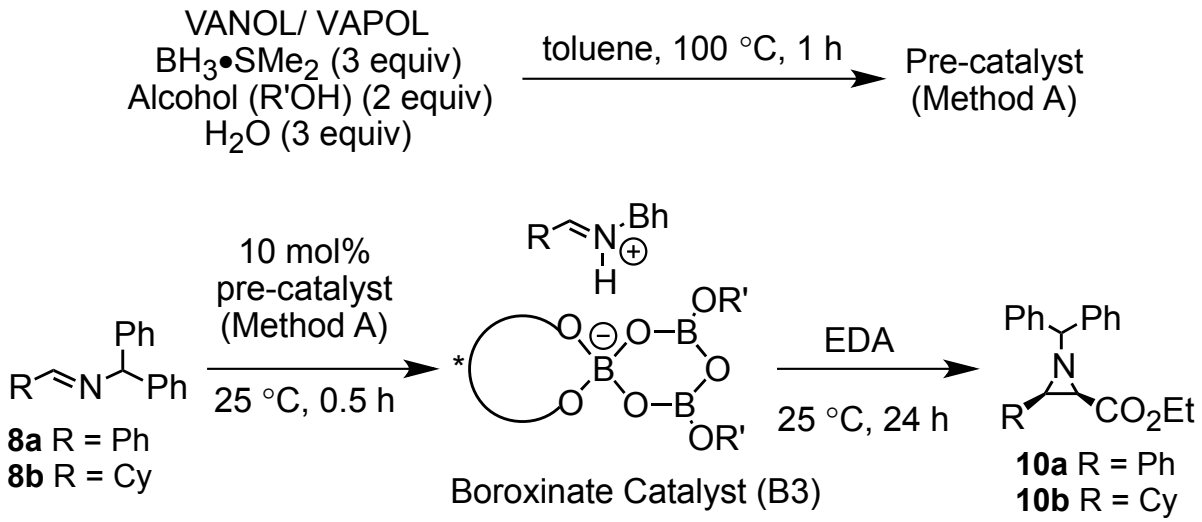

entry	alcohol (R'OH)	Imine	ligand	Catalyst (B3)	yield **10** (%) [b]	ee **10** (%) [c]	*cis/trans* [d]
1	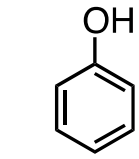	**8a**	(*S*)-VAPOL	**33a**	89	92	>100:1
2		**8a**	(*R*)-VANOL	**33b**	83	89	100:1
3		**8b**	(*S*)-VAPOL	**33a**	65	74	33:1
4		**8b**	(*R*)-VANOL	**33b**	78	79	50:1
5	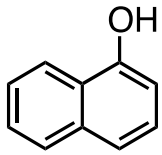	**8a**	(*S*)-VAPOL	**34a**	75	92	33:1
6		**8a**	(*R*)-VANOL	**34b**	92	86	33:1
7		**8b**	(*S*)-VAPOL	**34a**	71	79	33:1
8		**8b**	(*R*)-VANOL	**34b**	91	83	100:1
9	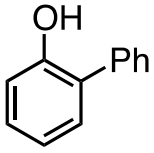	**8a**	(*S*)-VAPOL	**35a**	89	90	100:1
10		**8a**	(*R*)-VANOL	**35b**	93	87	100:1
11		**8b**	(*S*)-VAPOL	**35a**	84	71	25:1
12		**8b**	(*R*)-VANOL	**35b**	76	79	33:1
13	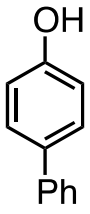	**8a**	(*S*)-VAPOL	**36a**	87	92	33:1
14		**8a**	(*R*)-VANOL	**36b**	86	87	100:1
15		**8b**	(*S*)-VAPOL	**36a**	81	79	25:1
16		**8b**	(*R*)-VANOL	**36b**	76	74	20:1

[a] Unless otherwise stated, reactions were run at 0.5 M in imine **8** (1.00 equiv) with EDA **9** (1.20 equiv) in the presence of 10 mol% catalyst in toluene at 25 °C for 24 h and went to 100% converison. The catalyst was prepared using 0.10 equiv ligand, 0.30 equiv borane, 0.30 equiv water, 0.20 equiv alcohol in 0.1 M in ligand in toluene at 100 °C for 1 h according to the general procedure (Method A). The enantiomer shown is the product for (*S*)-VAPOL. (*R*)-VANOL results in the opposite enantiomer. [b] Isolated yield after column chromatography on silica gel. [c] Analyzed using HPLC on a Chiralcel-OD-H column. [d] Determined from the ^{1}H NMR spectrum of the crude reaction mixture.

Phenol was used to generate the catalysts **33a/33b** in order to act as a standard for the remaining alcohols used in the B3 formation study. When synthesizing aziridine **10a**, the enantioselectivity for catalyst **33a** and **33b** was 92% and 89% respectively (entries 1 and 2, Table 2.2). When synthesizing aziridine **10b**, the yield decreased significantly and the enantioselectivity dropped to 74% for catalyst **33a** and 79% for catalyst **33b** (entries 3 and 4). This decrease in both enantioselectivity and yield is expected with the cyclohexyl substituent compared to its aromatic opponent, phenyl (see Figure 2.2).[16h]

1-Naphthol was used to generate catalysts **34a/34b**, which showed enantioselectivity similar to that of phenol catalysts **33a/33b** in the formation of aziridine **10a** (entries 5 and 6 vs 1 and 2). However, a slight increase in both yield and enantioselectivity was seen for aziridine **10b** with 1-naphthol catalysts **34a/34b** as compared to the phenol catalysts **33a/33b** (entries 7 and 8 vs entries 3 and 4).

Lastly, the 2-phenylphenol cataysts **35a/35b** showed similar results as 4-phenylphenol catalysts **36a/36b** when synthesizing aziridine **10a** (entries 9, 10, 13, and

14). However, in the case of VAPOL, **36a** gave higher enantioselectivity than **35a** in the synthesis of aziridine **10b** (entries 11 and 15). Where as, in the case of VANOL, catalyst **35b** gave higher enantioselectivity than **36b** in the synthesis of aziridine **10b** (entries 12 and 16).

2.3.2 Electronic and steric effects of phenol derivatives on the B3 catalyst

Since both electronic and steric effects play a large role in many organic reactions and catalysts, we speculated that the B3 catalyst would respond differently depending on the sterics and electronics of the phenol derivative used in its formation. The result of such effects could be experimentally tested using the AZ reaction.

2.3.2.1 Steric effects of phenol derivatives on the B3 catalyst

To investigate steric effects, phenol derivatives containing substituents on the 2,6, and/or 4 positions were examined (Table 2.3). It was discovered that a small amount of sterics in catalyst **37** varied in results depending on the ligand employed in the B3 catalyst (**37a** versus **37b**). When using catalyst **37a** to synthesize aziridine **10a**, a decrease in enantioselectivity was observed compared to that seen with the standard phenol catalyst **33a**. However, when using catalyst **37b**, the enantioselectivity of **10a** increased to 93% (entries 1 and 2, Table 2.3 versus entries 1 and 2, Table 2.2).

When placing the bulkier t-butyl group on the para position in catalysts **40a/40b** the enantioselectivity increased for aziridine **10a** to 94% and 90%. This is an improvement compared to that of the standard phenol catalysts **33a/33b** (entries 1,2,13, and 14, Table 2.3 versus entries 1 and 2, Table 2.2).

Table 2.3 Steric effects in the B3 catalyst using aliphatic substituted phenols [a]

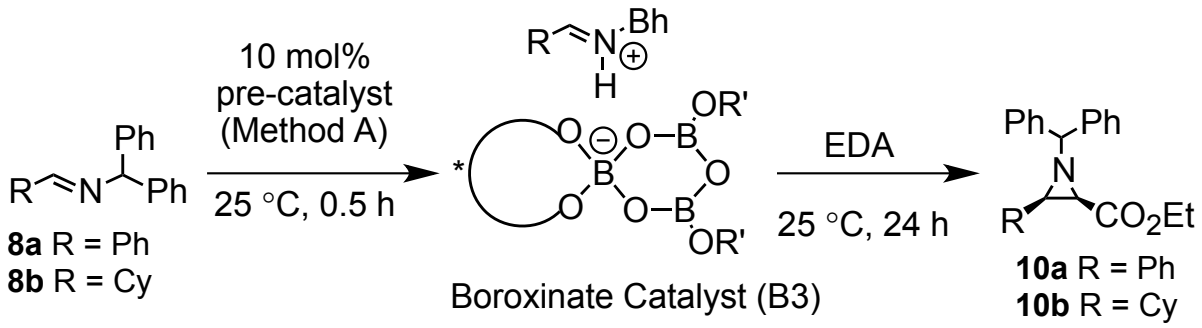

entry	alcohol	Imine	ligand	Catalyst (B3)	yield **10** (%) [b]	ee **10** (%) [c]	*cis/trans* [d]
1	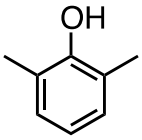	**8a**	(*S*)-VAPOL	**37a**	85	90	33:1
2		**8a**	(*R*)-VANOL	**37b**	95	93	>100:1
3		**8b**	(*S*)-VAPOL	**37a**	74	75	14:1
4		**8b**	(*R*)-VANOL	**37b**	80	79	100:1
5	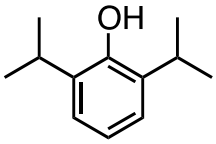	**8a**	(*S*)-VAPOL	**38a**	86	87	33:1
6		**8a**	(*R*)-VANOL	**38b**	93	86	100:1
7		**8b**	(*S*)-VAPOL	**38a**	68	76	>100:1
8		**8b**	(*R*)-VANOL	**38b**	86	77	>100:1
9	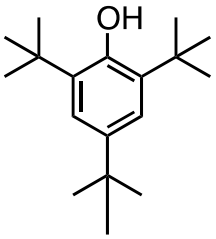	**8a**	(*S*)-VAPOL	**39a**	84	85	14:1
10		**8a**	(*R*)-VANOL	**39b**	90	85	50:1
11		**8b**	(*S*)-VAPOL	**39a**	81	68	25:1
12		**8b**	(*R*)-VANOL	**39b**	79	77	33:1
13	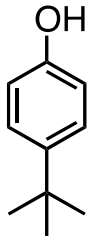	**8a**	(*S*)-VAPOL	**40a**	80	94	50:1
14		**8a**	(*R*)-VANOL	**40b**	81	90	100:1
15		**8b**	(*S*)-VAPOL	**40a**	77	80	100:1
16		**8b**	(*R*)-VANOL	**40b**	84	82	100:1

[a] Unless otherwise stated, all reactions were run at 0.5 M in imine **8** (1.00 equiv) with EDA **9** (1.20 equiv) in the presence of 10 mol% catalyst in toluene at 25 °C for 24 h and went to 100% conversion. The catalyst was prepared using 0.10 equiv ligand, 0.30 equiv borane, 0.30 equiv water, 0.20 equiv phenol derivative in 0.1 M in ligand in toluene at 100 °C for 1 h according to the general procedure (Method A, Table 2.2). The enantiomer shown is the product for (*S*)-VAPOL. (*R*)-VANOL results in the opposite enantiomer. [b] Isolated yield after column chromatography on silica gel. [c] Analyzed using HPLC on a Chiralcel-OD-H column. [d] Determined from the ^{1}H NMR spectrum of the crude reaction mixture.

However, when using too sterically bulky phenols such as 2,6-diisopropyl phenol and 2,4,6-tri-*tert*-butyl phenol to make the catalysts **38a/38b** and **39a/39b** resulted in a decrease in enantioselectivity (entries 5-12, Table 2.3). When synthesizing aziridine **10b**, catalysts **37, 38,** and **39** gave similar results with ee's ranging from 75-79% (entries 3,4,7,8, and 12), with the exception of 2,4,6-tri-*tert*-butylphenol catalyst **39a** giving a decrease in enantioselectivity of 68% (entry 11).

Conversely, when using the para t-butyl phenol catalyst **40a/40b** to generate aziridine **10b**, the enantioselectivity was increased to 80% and 82% ee respectively (entries 15 and 16).

Therefore, in the case of the alkyl substituted aziridines, when compared to the standard phenol, sterics placed on the ortho and para positions of the phenol derivative does have a slight effect on the enantioselectivity of aziridines **10** with 4-tert-butyl

phenol being the optimal phenol thus far in the B3 system (entries 13-16, Table 2.3 versus entries 1-4, Table 2.2).

2.3.2.2 Electronic effects of phenol derivatives on the B3 system

In addition to examining the steric effects, electronic effects of the B3 catalyst were examined as well (Table 2.4). This study incorporated both electron rich and electron deficient phenol derivatives. It was theorized that electron rich phenols would increase electron density on the B3 catalyst core while the electron deficient phenol derivatives would decrease it. Therefore, the hydrogen bonding capabilities of the catalyst would change according to the phenol derivative that was used to generate it.

When attempting the AZ reaction using catalysts incorporating nitrogen-substituted phenols, such as dimethyl aminophenol[33] or 8-hydroxyquinoline, the reaction resulted in very low conversions of <25%. A possible reason for this is that the electron pair of the amino group is interfering with our Brønsted acid system.[34] Therefore, this inhibits the catalyst turnover and ceases our reaction. However, as seen in catalysts **41a/41b**, if we use methoxy as our electron-donating group on the phenol derivative, we see moderate to high yields and ee's (entries 1-4, Table 2.4).

Table 2.4 Electronic effects in the B3 catalyst using electron deficient and electron rich phenol derivatives

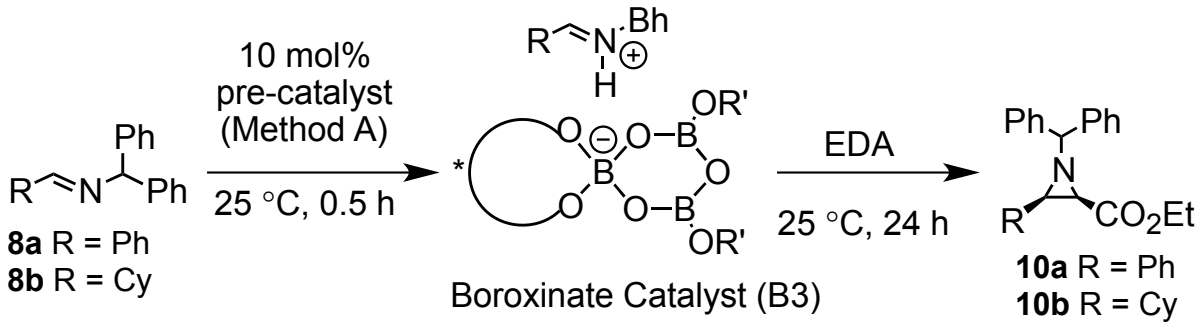

Table 2.4 (Cont'd)

entry	alcohol	Imine	ligand	Catalyst (B3)	yield **10** (%) [b]	ee **10** (%) [c]	*cis/ trans* [d]
1	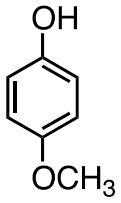	**8a**	(*S*)-VAPOL	**41a**	86	93	33:1
2		**8a**	(*R*)-VANOL	**41b**	90	90	50:1
3		**8b**	(*S*)-VAPOL	**41a**	68	77	20:1
4		**8b**	(*R*)-VANOL	**41b**	90	81	33:1
5	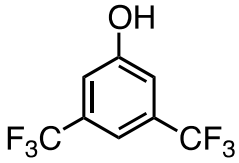	**8a**	(*S*)-VAPOL	**42a**	84	82	25:1
6		**8a**	(*R*)-VANOL	**42b**	96	80	100:1
7		**8b**	(*S*)-VAPOL	**42a**	81	68	25:1
8		**8b**	(*R*)-VANOL	**42b**	68	72	50:1
9	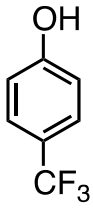	**8a**	(*S*)-VAPOL	**43a**	77	86	20:1
10		**8a**	(*R*)-VANOL	**43b**	82	81	100:1
11		**8b**	(*S*)-VAPOL	**43a**	77	73	25:1
12		**8b**	(*R*)-VANOL	**43b**	76	73	33:1
13	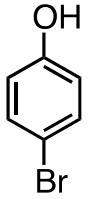	**8a**	(*S*)-VAPOL	**44a**	81	90	25:1
14		**8a**	(*R*)-VANOL	**44b**	84	86	>100:1
15		**8b**	(*S*)-VAPOL	**44a**	73	76	100:1
16		**8b**	(*R*)-VANOL	**44b**	83	80	100:1
17	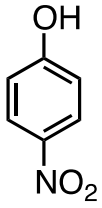	**8a**	(*S*)-VAPOL	**45a**	69	67	13:1
18		**8a**	(*R*)-VANOL	**45b**	85	68	33:1
19		**8b**	(*S*)-VAPOL	**45a**	88	47	33:1
20		**8b**	(*R*)-VANOL	**45b**	69	64	100:1

[a] Unless otherwise stated, all reactions were run at 0.5 M in imine **8** (1.00 equiv) with EDA **9** (1.20 equiv) in the presence of 10 mol% catalyst in toluene at 25 °C for 24 h and

went to 100% conversion. The catalyst was prepared using 0.10 equiv ligand, 0.30 equiv borane, 0.30 equiv water, 0.20 equiv alcohol in 0.1 M in ligand in toluene at 100 °C for 1 h according to the general procedure (Method A, Table 2.2). The enantiomer shown is the product for (*S*)-VAPOL. (*R*)-VANOL results in the opposite enantiomer. [b] Isolated yield after column chromatography on silica gel. [c] Analyzed using HPLC on a Chiralcel-OD-H column. [d] Determined from the ^{1}H NMR spectrum of the crude reaction mixture.

When electron deficient phenol derivatives are used in the B3 catalyst, we see a drastic decline in our results. With the moderate electron-withdrawing group CF_3 in catalysts **42a/42b** and **43a/43b**, the reaction proceeds but with a significant decrease in yields and enantioselectivites. (entries 5-12). When using 4-bromophenol in catalysts **44a/44b**, the results are similar to that of the trifluoromethyl substituted phenol catalysts **42** and **43** in that the overall yield and enantioselectivity decreased but to a slighter extent (entries 13-16). Furthermore, *para*-nitrophenol catalysts **45a/45b** incorporates a stronger electron-withdrawing group on the *para* position. This results in drastically decreasing the yields and ee's as low as 47% ee for aziridine **10b** in the presence of catalyst **45a** (entries 17-20).

This confirms that electronics has a clear and demonstrable effect on the B3 system. When decreasing the electron density on the phenol, this in turn could decrease the electron density on the core of the catalyst, which would inhibit the hydrogen bonding capabilities of the catalyst and therefore lowering the enantioselectivity. This assumption will be investigated further later in this chapter (Section 2.4.2).

2.3.3 Aliphatic alcohols used in the B3 catalyst formation

Once a number of phenol derivatives had been examined, we turned our sights to aliphatic alcohols. To study the steric effects, we needed to branch the alcohols close to the hydroxyl group. This would ensure that any significant steric effects on the catalyst would be observed. Therefore, we experimented with primary, secondary and tertiary alcohols, namely *n*-butanol, cyclohexanol, and *tert*-butanol (Table 2.5).

We first saw promising results with *n*-butanol catalysts **46a/46b** with yields in the 80's and *ee*'s up to 94% for aziridine **10a** and moderate yields and *ee*'s for aziridine **10b** (entries 1-4, Table 2.5). When we moved to a secondary alcohol, cyclohexanol, we saw yet further improvement.

Cyclohexanol catalysts **47a/47b** gave the best results of all the alcohol and phenol derived B3 catalysts previously studied with excellent yields and enantioselectivity in the mid 90's for aziridine **10a** and good yields and enantioselectivity for aziridine **10b** (entries 5-8).

Therefore, we hoped that the results would keep improving when moving on to a tertiary alcohol.

Table 2.5 Aliphatic alcohols employed in the B3 catalyst [a]

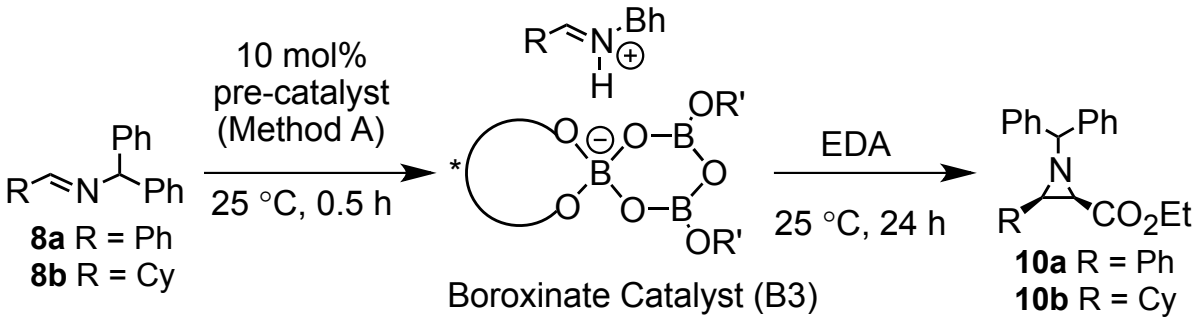

Table 2.5 (Cont'd)

entry	alcohol	Imine	ligand	Catalyst (B3)	yield **10** (%)[b]	ee **10** (%)[c]	*cis/trans*[d]
1	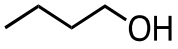	**8a**	(*S*)-VAPOL	**46a**	85	94	25:1
2		**8a**	(*R*)-VANOL	**46b**	86	92	>100:1
3		**8b**	(*S*)-VAPOL	**46a**	62	76	100:1
4		**8b**	(*R*)-VANOL	**46b**	71	83	50:1
5	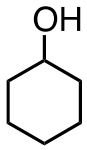	**8a**	(*S*)-VAPOL	**47a**	90	95	50:1
6		**8a**	(*R*)-VANOL	**47b**	88	94	100:1
7		**8b**	(*S*)-VAPOL	**47a**	67	79	100:1
8		**8b**	(*R*)-VANOL	**47b**	75	87	100:1
9	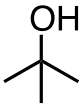	**8a**	(*S*)-VAPOL	**48a**	82	89	25:1
10		**8a**	(*R*)-VANOL	**48b**	65	74	100:1
11		**8b**	(*S*)-VAPOL	**48a**	76	73	50:1
12		**8b**	(*R*)-VANOL	**48b**	79	83	50:1
13	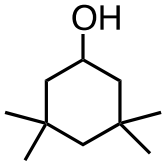	**8a**	(*S*)-VAPOL	**49a**	87	95	33:1
14		**8a**	(*R*)-VANOL	**49b**	81	93	100:1
15		**8b**	(*S*)-VAPOL	**49a**	77	83	100:1
16		**8b**	(*R*)-VANOL	**49b**	67	86	100:1
17	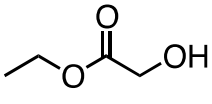	**8a**	(*S*)-VAPOL	**50a**	83	82	100:1
18		**8a**	(*R*)-VANOL	**50b**	86	89	50:1
19		**8b**	(*S*)-VAPOL	**50a**	83	72	33:1
20		**8b**	(*R*)-VANOL	**50b**	87	84	100:1

[a] Unless otherwise stated, all reactions were run at 0.5 M in imine **8** (1.00 equiv) with EDA **9** (1.20 equiv) in the presence of 10 mol% catalyst in toluene at 25 °C for 24 h and went to 100% conversion. The catalyst was prepared using 0.10 equiv ligand, 0.30

equiv borane, 0.30 equiv water, 0.20 equiv alcohol in 0.1 M in ligand in toluene at 100 °C for 1 h according to the general procedure (Method A, Table 2.2). The enantiomer shown is the product for (*S*)-VAPOL. (*R*)-VANOL results in the opposite enantiomer. [b] Isolated yield after column chromatography on silica gel. [c] Analyzed using HPLC on a Chiralcel-OD-H column. [d] Determined from the ^{1}H NMR spectrum of the crude reaction mixture.

Unfortunately, with *tert*-butanol catalysts **48a/48b**, the results dropped lower than that of the primary and secondary alcohol catalysts **46** and **47** (entries 9-12). The aliphatic alcohol ethyl-2-hydroxyacetate, which incorporates an electron-withdrawing group was also experimented with in catalysts **50a/50b**. This resulted in moderate yields and ee's but did not surpass the results seen with cyclohexanol catalysts **47a/47b** (entries 17-20).

Based on cyclohexanol catalyst **47** giving the optimal results thus far, 3,3,5,5-tetramethyl cyclohexanol **52** was synthesized to determine if sterically bulky groups being placed farther away from the binding oxygen would result in increased enantioselectivity. Catalysts **49a/49b** gave slightly better results than that of cyclohexanol catalyst **47** (entries 13-16), but taking into consideration that cyclohexanol is commercially available unlike 3,3,5,5-tetramethyl cyclohexanol **52**, it was determined that cyclohexanol would be the alcohol of choice.

3,3,5,5-Tetramethyl cyclohexanol **52** was synthesized via the reduction of 3,3,5,5-tetramethyl cyclohexanone **51** using sodium borohydride (Table 2.6). When attempting to reduce the carbonyl at room temperature with sodium borohydride alone, no product

was observed (entry 1). However, when following a modified procedure using SiO_2 and heating the reaction to 40 °C, the reaction was capable of being pushed to 95% conversion giving 88% yield of **52** (entries 2 and 3).[35] Since the reaction was performed following a modified literature procedure, the original entry ran in the absence of SiO_2 was not attempted at 40 °C.

Table 2.6 Synthesis of 3,3,5,5-tetramethyl cyclohexanol [a]

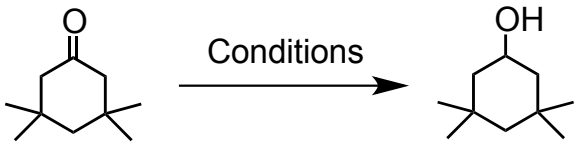

51 **52**

Entry	Conditions	Conversion (%) [b]	Yield (%) [c]
1	$NaBH_4$ (2 equiv), EtOH (2 drops), ether, 25 °C, 12 h	0	-
2	$NaBH_4$ (1.5 equiv), SiO_2, hexanes, 40 °C, 5 h	50	-
3	$NaBH_4$ (1.5 equiv), SiO_2, hexanes, 40 °C, 10 h	98	88

[a] The reactions were carried out in 0.1 M solutions. In the case of SiO_2, 3 grams were used for a 2 mmol scale reaction. [b] Conversions were calculated by crude ^1H NMR using an internal standard ($CHPh_3$). [c] Isolated yield after sublimation.

2.4 Correlation between electron density of the B3 catalyst and enantioselectivity of aziridines observed in the 6-componenet AZ reaction

2.4.1 Correlation amongst sigma para negative Hammett values of phenols in the boroxinate catalyst and enantioselectivity of aziridine formation

During the previous study where different alcohols and phenols were used to generate the B3 catalyst, we observed a trend between electronic effects of the phenols employed in the B3 system and the enantioselectivity of the aziridine product (Tables 2.2, 2.3, and 2.4). Therefore, in order to better understand these results, Hammett sigma values of para substituted phenols were taken into consideration.[36] Typically these values are used to determine rates of reactions. However, we have decided to use these values, which are dependent on the electronic features of the particular phenol, to correlate the electronically rich and deficient phenols employed in the B3 catalyst with the enantioselectivity seen in the 6-component AZ reaction. In order to keep the substitution pattern the same, we focused on the para substituted phenols only (Figure 2.3).

Figure 2.3 σ_p^- values for para substituted phenols

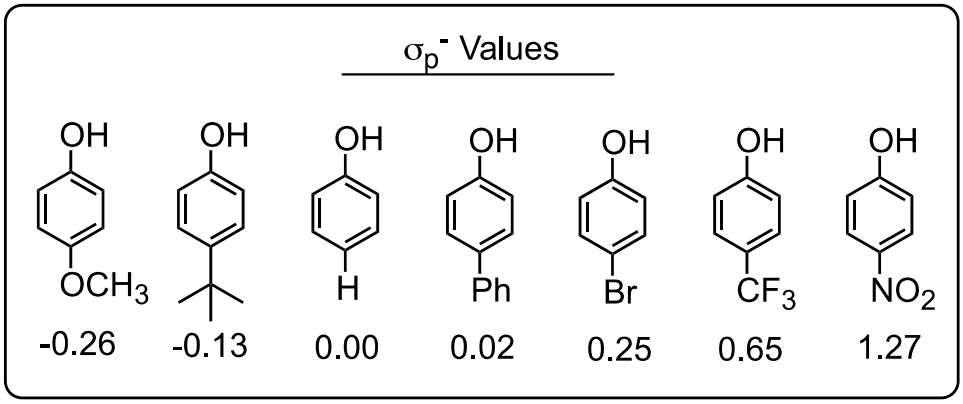

When plotting the sigma para negative values against the log of the enantiomeric ratios (enantiomeric ratios derived from ee's given in Tables 2.2, 2.3 and 2.4), a linear correlation appeared (Figures 2.4, 2.5, 2.6, and 2.7).

Figure 2.4 Correlations between enantioselectivity of aziridine **10a** and electronic effects of VANOL-B3 catalyst

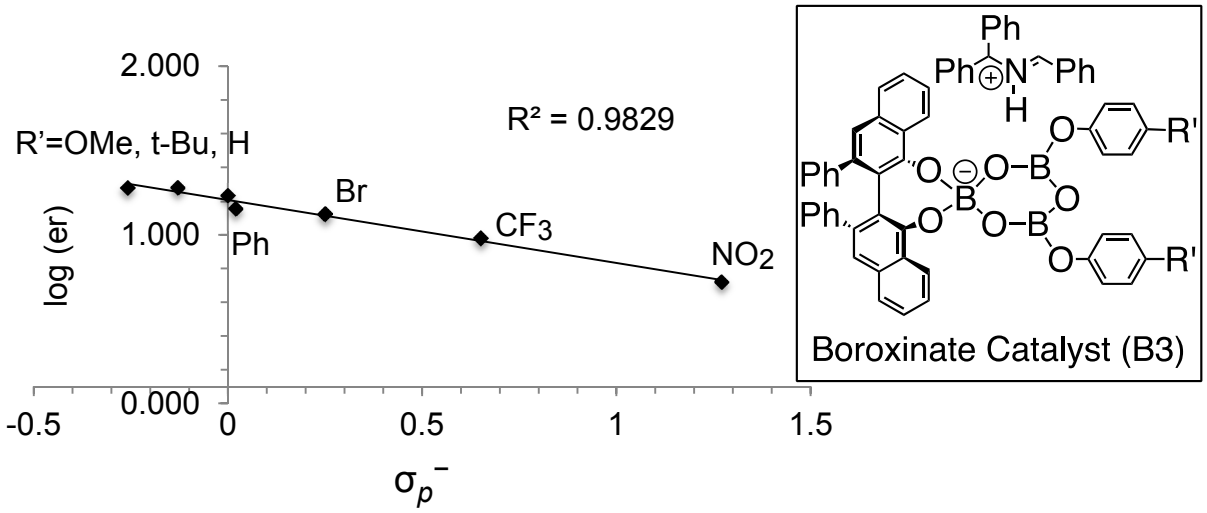

Figure 2.5 Correlations between enantioselectivity of aziridine **10a** and electronic effects of VAPOL-B3 catalyst

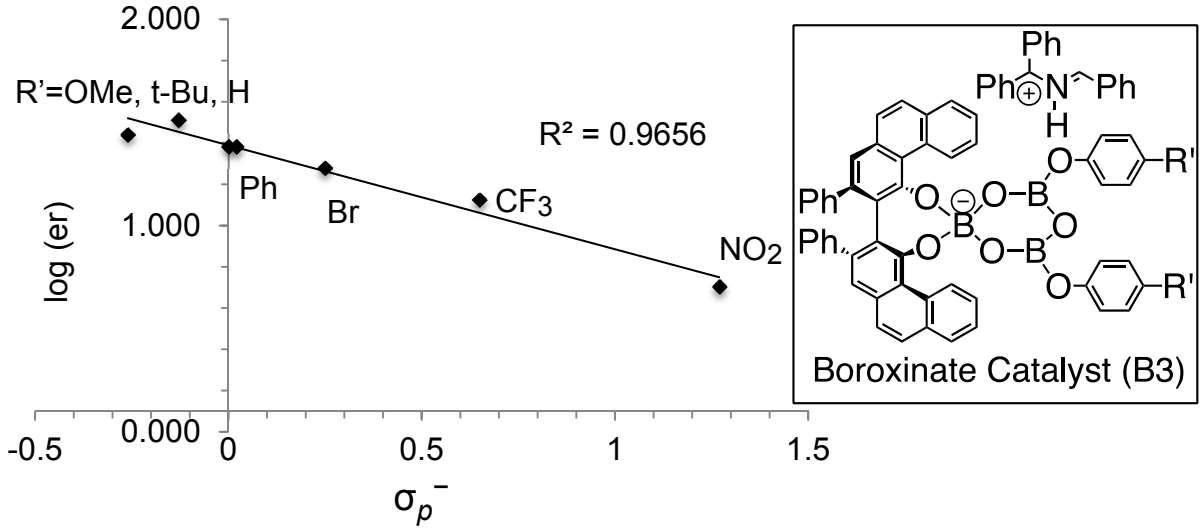

Figure 2.6 Correlations between enantioselectivity of aziridine **10b** and electronic effects of VANOL-B3 catalyst

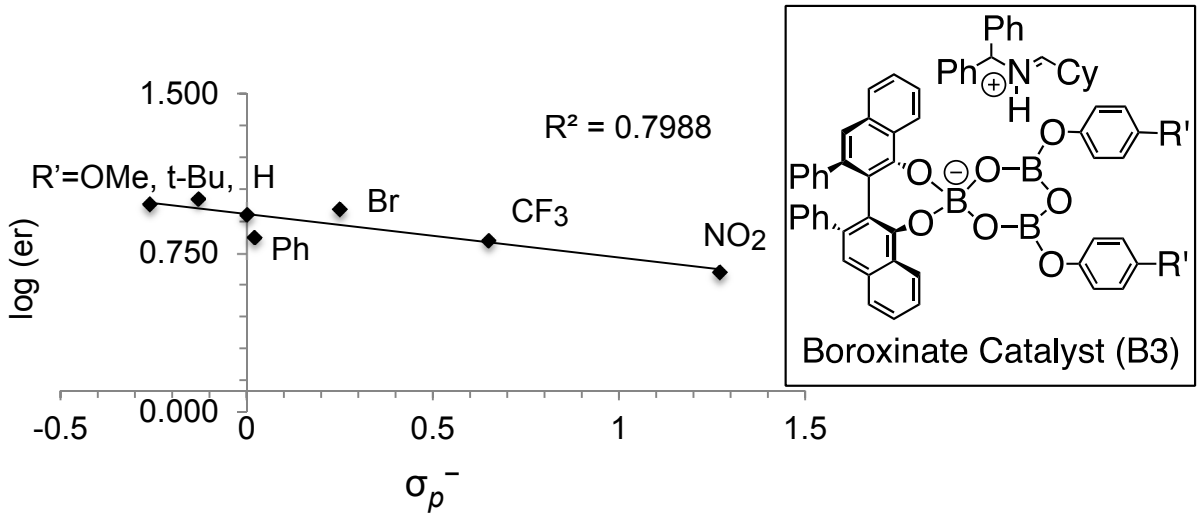

Figure 2.7 Correlations between enantioselectivity of aziridine **10b** and electronic effects of VAPOL-B3 catalyst

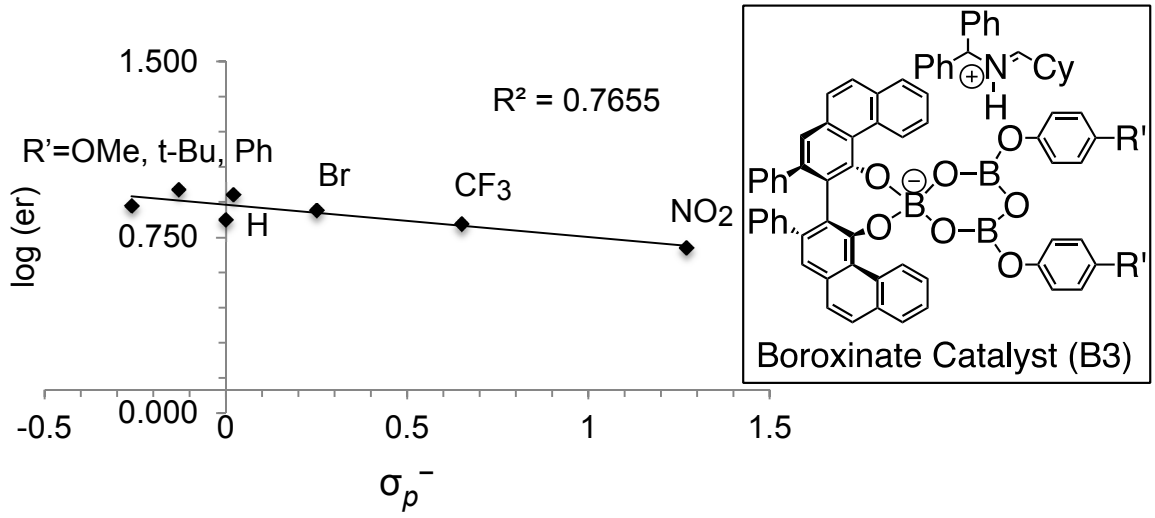

When comparing VANOL-B3 catalysts derived from phenols seen in Figure 2.3 with the enantioselectivity of aziridine **10a**, a good linear correlation occurred giving an R^2 value of 0.983 (Figure 2.4). When considering VAPOL incorporated catalysts to generate the phenyl substituted aziridine **10a**, the resulting R^2 value was 0.966 (Figure 2.5).

When considering the cyclohexyl substituted aziridine **10b**, the resulting R^2 value was 0.799 for VANOL (Figure 2.6) and 0.765 for VAPOL (Figure 2.7). When considering both cyclohexyl and phenyl substituted aziridines (**10a** and **10b**), a clear correlation between electronics and enantioselectivity was seen with aziridine **10a** and a slight correlation with aziridine **10b** (Figure 2.8).

Figure 2.8 Correlation between enantiomeric ratios of **10a/10b** and electronic density of the B3 catalysts

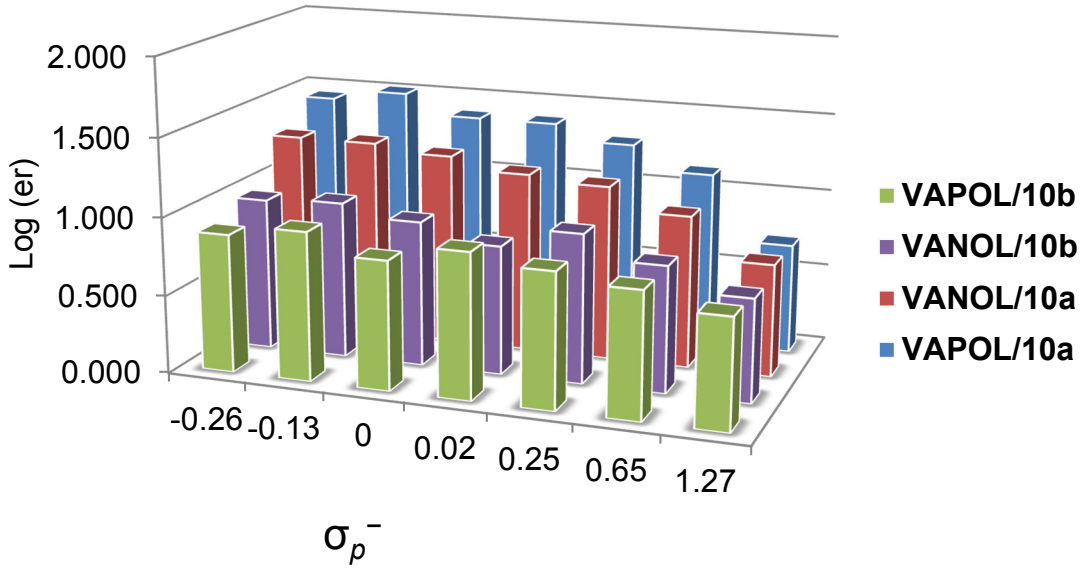

With these results, it was concluded that the electronics on the phenol were indeed having a direct correlation with the enantioselectivity seen in the 6-component catalytic asymmetric aziridination reaction.

2.4.2 Evaluation of electronic charges and bond distances between the B3 catalysts and imines 8a/8b

It has been demonstrated that electronics of the B3 catalyst plays an important role in the enantioselectivity of the 6-component AZ reaction. The previous section (Section 2.4.1) exhibited the correlation between electron densities of the phenols with the asymmetric induction seen in the AZ reaction. Looking at the hydrogen bonding occurring between the active boroxinate catalyst and imine **8** can further support these results. Therefore, calculations performed by Dr. Mathew Vetticatt (post doctoral group member) established these distances using hybrid ONIOM(B3LYP/6-31G*:AM1) method as executed in Gaussian 09 (Table 2.7).

Table 2.7 H-bonding distances between VANOL-B3 catalysts and imine **8** [a]

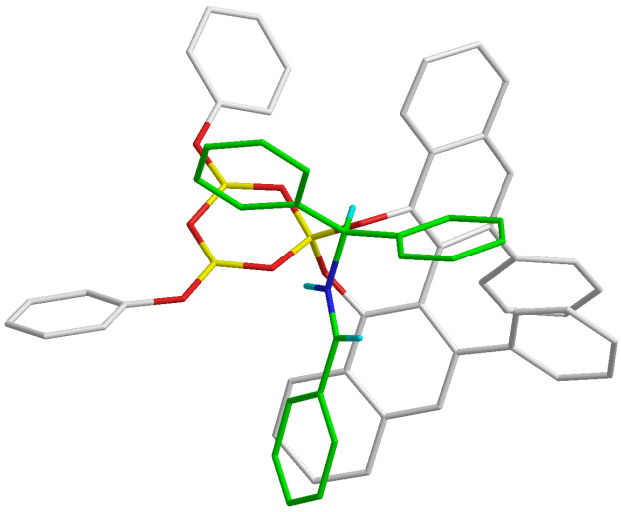

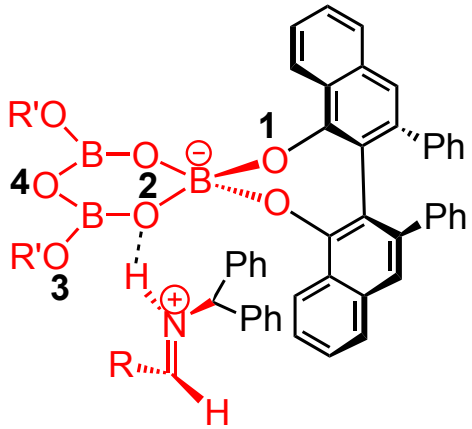

B3-H-Imine Complex

Table 2.7 (Cont'd)

Entry	Alcohol	Catalyst	Imine	H-Bond Distance (Å) Imine-H−O2
1	CyOH	**47b**	**8a**	1.72
2	CyOH	**47b**	**8b**	1.67
3	OMe-Phenol	**41b**	**8a**	1.75
4	OMe-Phenol	**41b**	**8b**	1.70
5	Phenol	**33b**	**8a**	1.76
6	Phenol	**33b**	**8b**	1.69
7	NO_2-Phenol	**45b**	**8a**	1.83 (O1) / 2.65 (O2)
8	NO_2-Phenol	**45b**	**8b**	1.70 (O1) / 2.59 (O2)

[a] The catalyst-imine complex bond distances were calculated using the hybrid ONIOM(B3LYP/6-31G*:AM1) method as executed in Gaussian 09. The atoms shown in red were calculated using the DFT method (B3LYP) while the portions in black were calculated using the semi-emperical (AM1) method.

Table 2.8 Electron densities based on NBO analysis of the boroxinate anion (B3) [a]

Entry	Alcohol	Catalyst	O1	O2	O3	O4
1	Cyclohexanol	**47b**	−0.772	−0.977	−0.763	−0.923
2	OMe-Phenol	**41b**	−0.773	−0.973	−0.725	−0.922
3	Phenol	**33b**	−0.773	−0.972	−0.723	−0.920
4	NO_2-Phenol	**45b**	−0.79	−0.949	−0.702	−0.924

[a] The natural bond orbital (NBO) analysis was calculated from a single point energy calculation performed at the B3LYP/6-31G* method on the ONIOM optimized geometry.

Furthermore, the electron densities situated on the oxygen atoms of the active B3 catalysts were also calculated using NBO analysis (Table 2.8). A decrease in electron density on O2 and an increase in electron density on 01 was seen when generating the boroxinate anion using the strongly electron withdrawing 4-nitrophenol (entry 4, Table 2.8). It is still uncertain why imine **8** prefers to H-bond to O1 in the case of catalyst **45b**.

The theoretical data supports the experimental results in that as the bond distance between the imine and catalyst shorten, the enantioselectivity increases (Table 2.7). Table 2.7 reveals that as the electron density in the phenol increases, the bond distance between O2 and the imine proton becomes shorter. It was also seen that the optimal alcohol, cyclohexanol, gave the shortest bond distances, which explains the high enantioselectivity of catalyst **47b** (entries 1 and 2, Table 2.7).

2.5 Variation of the ligand and protecting group in the AZ reaction

2.5.1 Use of tert-butyl VANOL ligand in the AZ reaction

It has recently been discovered in the Wulff group that the best ligand for the cis-aziridination is *tert*-butyl VANOL, which contains the bulky *t*-butyl group in the 7 and 7' positions of the VANOL ligand (Figure 2.9).[37]

The bulky *t*-butyl group alters the chiral pocket, which then increases the enantioselectivity seen in the AZ reaction. In the alcohol/phenol B3 study presented in this chapter, it was found that cyclohexanol gave the optimal results for the cis-aziridination reaction (Table 2.5). Therefore, the next logical step would be to combine the best alcohol (cyclohexanol) with the best ligand (t-butyl VANOL) to see the outcome of such a match (Table 2.9).

Figure 2.9 *tert*-butyl VANOL ligand

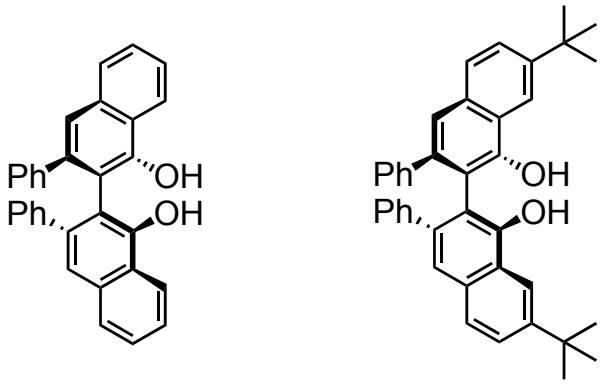

VANOL *tert*-butyl VANOL

Table 2.9 The 6-component AZ reaction employing t-butyl VANOL as the chiral ligand [a]

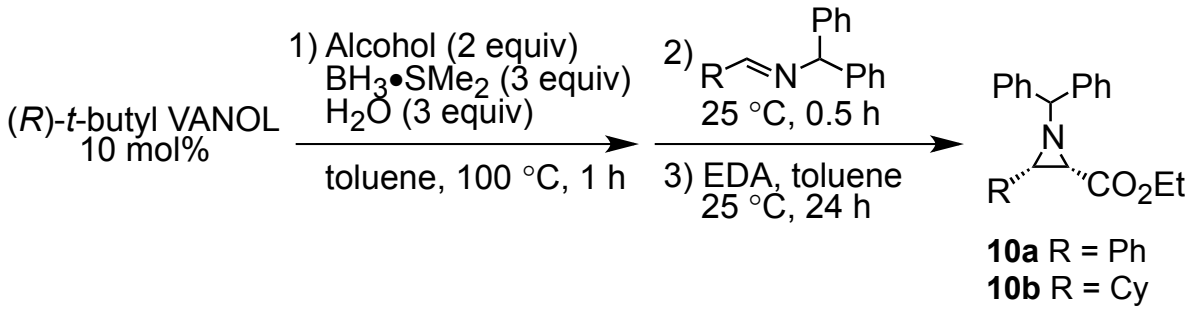

entry	alcohol	Aziridine	yield (%)[b]	ee (%)[c]	*cis/trans*[d]
1	Phenol	**10a**	95	98	>100:1
2	Phenol	**10b**	91	93	>100:1
3	Cyclohexanol	**10a**	96	98	>100:1
4	Cyclohexanol	**10b**	92	94	100:1

[a] Unless otherwise stated, all reactions were run at 0.5 M in imine **8** (1.00 equiv) with EDA **9** (1.20 equiv) in the presence of 10 mol% catalyst in toluene at 25 °C for 24 h and went to 100% conversion. The catalyst was prepared using 0.10 equiv ligand, 0.30 equiv borane, 0.30 equiv water, 0.20 equiv alcohol in 0.1 M in ligand in toluene at 100 °C for 1 h according to the general procedure (Method

A, Table 2.2). [b] Isolated yield after column chromatography on silica gel. [c] Analyzed using HPLC on a Chiralcel-OD-H column. [d] Determined from the ^1H NMR spectrum of the crude reaction mixture.

When using phenol as the standard alcohol with the *t*-butyl VANOL ligand, the results were better than VANOL or VAPOL with both the phenyl and cyclohexyl aziridines giving 98% and 93% ee respectively (entries 1 and 2, Table 2.9 versus entries 1-4, Table 2.2). When the optimal alcohol (cyclohexanol) was used in conjunction with the new ligand, *t*-butyl VANOL, the results were excellent. With the phenyl substituted aziridine **10a**, 96% yield and 98% ee was obtained (entry 3, Table 2.9). With the cyclohexyl substituted aziridine **10b**, 92% yield and 94% ee was obtained (entry 4). The results revealed that t-butyl VANOL is the best ligand giving excellent ee's (Table 2.9). Unfortunately, cyclohexanol does not have any major advantage over phenol when using the t-butyl VANOL ligand (entries 1 and 2 vs entries 3 and 4, Table 2. 9) as was seen in the earlier case when using VANOL and VAPOL ligands.

2.5.2 Use of MEDAM protected imine in the AZ reaction

As previously discussed, benzhydryl was employed as the nitrogen protecting group for the 6-component AZ reaction because of its commercial availability. It has been established that with the optimal alcohol, cyclohexanol, and the optimal ligand, tert-butyl VANOL, the enantioselectivty can reach 98% with aromatic aziridines and 94% with aliphatic aziridines (Table 2.9). The final test was to switch the protecting group from benzhydryl to MEDAM, which has more interactions with the catalyst therefore enhancing the enantioselectivity. When reacting MEDAM protected alkyl substituted imine **53** with EDA in the presence of cyclohexanol-B3 catalysts **47a** and **47b**, the 6-

component aziridination reaction gave enantioselectivities in the low 90's for aziridine **54** (Table 2.10). The AZ reactions using the MEDAM protected imine **53** resulted in high yields and ee (entries 1 and 2). When using phenol to generate catalysts **33a/33b**, the inductions for aziridine **54** have been observed to be 91% ee, which is the same as the when using catalysts **47a/47b**. However, for catalysts **33a/33b**, a different procedure was followed to generate the catalyst.[38]

Table 2.10 MEDAM imine **53** employed in the 6-component AZ reaction [a]

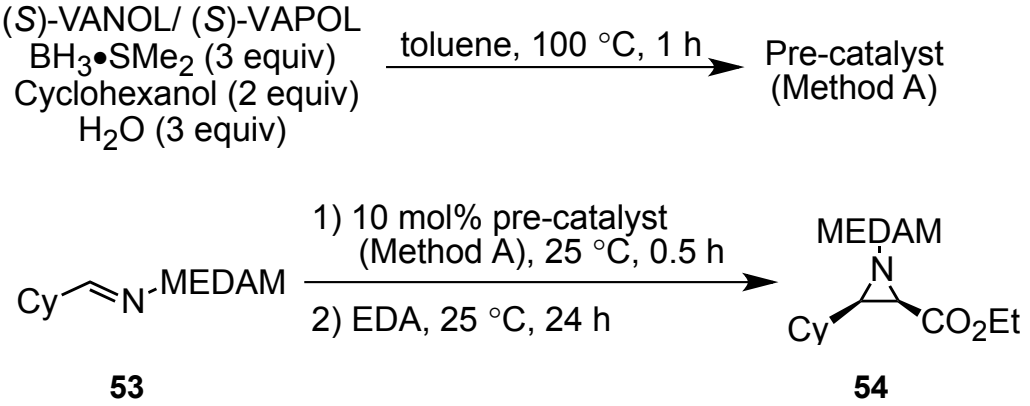

53 **54**

Entry	ligand	B3 catalyst	yield **54** (%) [b]	ee **54** (%) [c]	cis/trans [d]
1	(*S*)-VAPOL	**47a**	96	92	>100:1
2	(*S*)-VANOL	**47b**	93	91	>100:1
3 [e]	(*S*)-VAPOL	**33a**	98	91	>50:1
4 [e]	(*R*)-VANOL	**33b**	95	−91	>50:1

[a] Unless otherwise stated, all reactions were run at 0.5 M in imine **53** (1.00 equiv) with EDA **9** (1.20 equiv) in the presence of 10 mol% catalyst in toluene at 25 °C for 24 h and went to 100% conversion. The catalyst was prepared using 0.10 equiv ligand, 0.30 equiv borane, 0.30 equiv water, 0.20 equiv cyclohexanol in 0.1 M in ligand in toluene at 100 °C for 1 h according to the general procedure

(Method A, Table 2.2). [b] Isolated yield after column chromatography on silica gel. [c] Analyzed using HPLC on a Chiralcel-OD-H column. [d] Determined from the ^1H NMR spectrum of the crude reaction mixture. [e] 3 mol% catalyst was used here to generate cis-aziridine **54**. Catalyst was prepared from $B(OPh)_3$ using a different procedure as reported in the literature.[38]

However, the downfall to using imine **53** is that the synthesis of MEDAM amine can be time consuming and costly (Scheme 2.4).

Scheme 2.4 General synthesis for MEDAM amine **59**

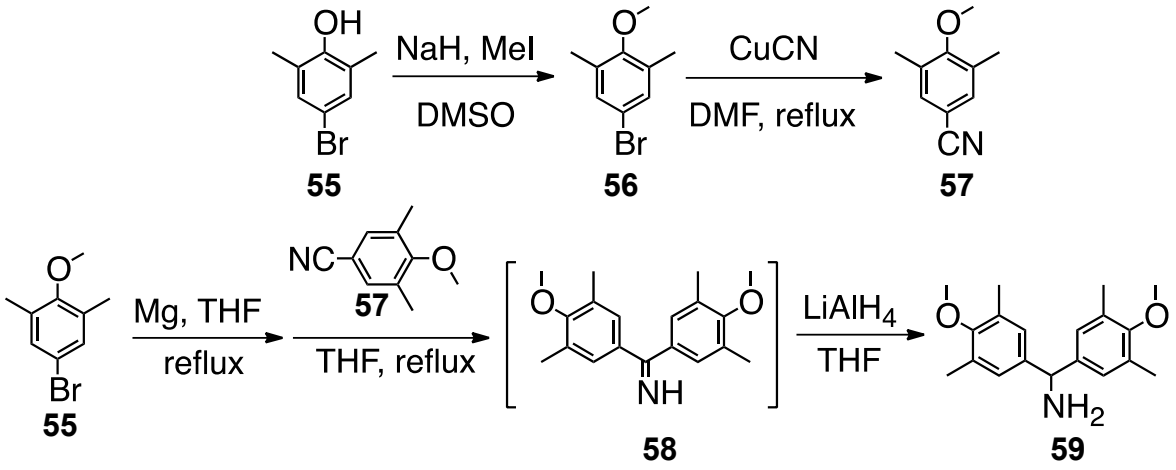

2.6 Confirmation of the absolute configuration of cyclohexyl substituted aziridine 10b

The cyclohexyl substituted benzhydryl protected aziridine's absolute configuration was determined by synthesizing the methyl benzyl amide substituted aziridine **60** from the original ester substituted aziridine **10b** (Scheme 2.5). With the methyl benzyl amide substituted aziridine, there is one previously established chiral carbon. This allows for the absolute configuration to be determined by x-ray crystallography. Once the aziridine

was transformed into its amide derivative **60**, a crystal structure was obtained to verify the stereochemistry of the aziridine ring (Figure 2.10).

Scheme 2.5 Synthesis of aziridine **60** from aziridine **10b**

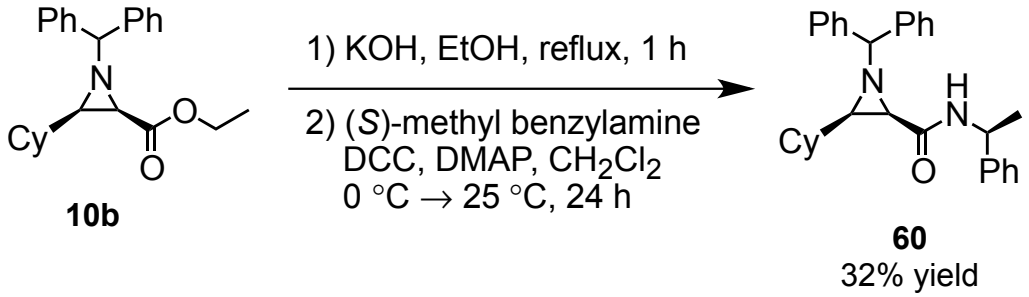

Until now, we have assumed the absolute configuration of aziridine **10b** based upon those previously reported aromatic aziridines generated from the B3 catalyst **33a**.[16k] Therefore, it is for the first time confirmed that synthesizing aziridine **10b** from (*S*)-VAPOL derived catalysts gives the (*R,R*)-aziridine **10b**.

Figure 2.10 Crystal structure of cyclohexyl substituted aziridine **60**

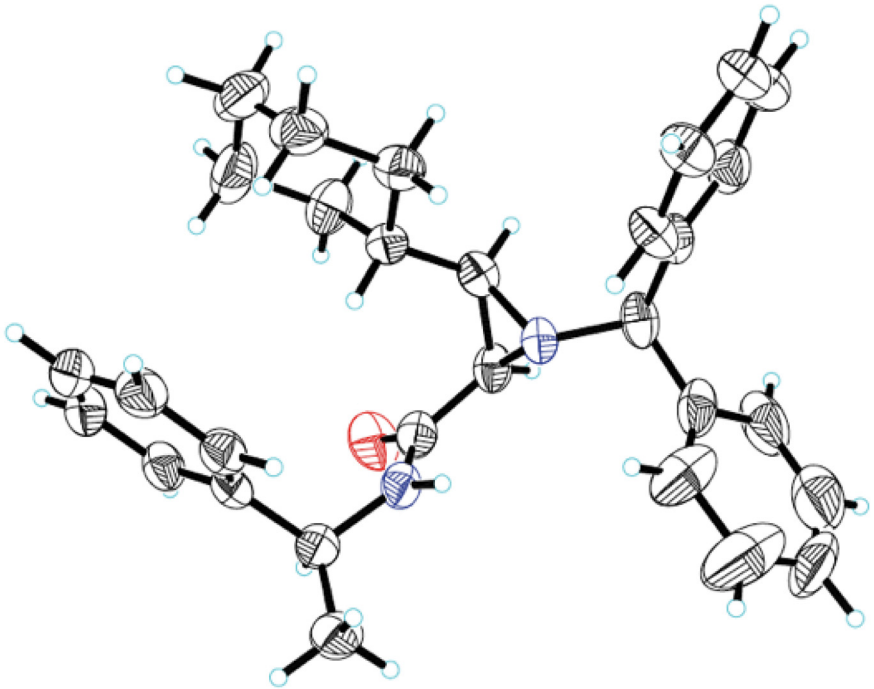

2.7 NMR analysis of various boroxinate catalysts

2.7.1 NMR analysis of cyclohexanol boroxinate catalyst

Once cyclohexanol was established as the optimal alcohol to use in the 6-component catalytic asymmetric aziridination reaction, further studies were performed on this system to gain evidence that the B3 boroxinate was indeed formed with cyclohexanol. Proton and boron NMR studies were performed on the VAPOL B3 system using cyclohexanol to generate the boroxinate catalyst **47a** complexed with imine **8a**. Surprisingly, there were no B3 bay protons (H's labeled in red in Figure 2.11) identified in the ^{1}H NMR at room temperature (entry 2, Figure 2.11). However, there was evidence of a tetra-coordinate boron species in the ^{11}B NMR, which would suggest some formation of the boroxinate catalyst (entry 2, Figure 2.12). Further studies indicated that when heating the NMR tube to 40 °C and then acquiring the spectra, a large broad peak appeared at 10.8 ppm (entry 1, Figure 2.11; spectra in red).

Figure 2.11 ^{1}H NMR for cyclohexanol incorporated boroxinate catalyst **47a**-imine **8a** complex

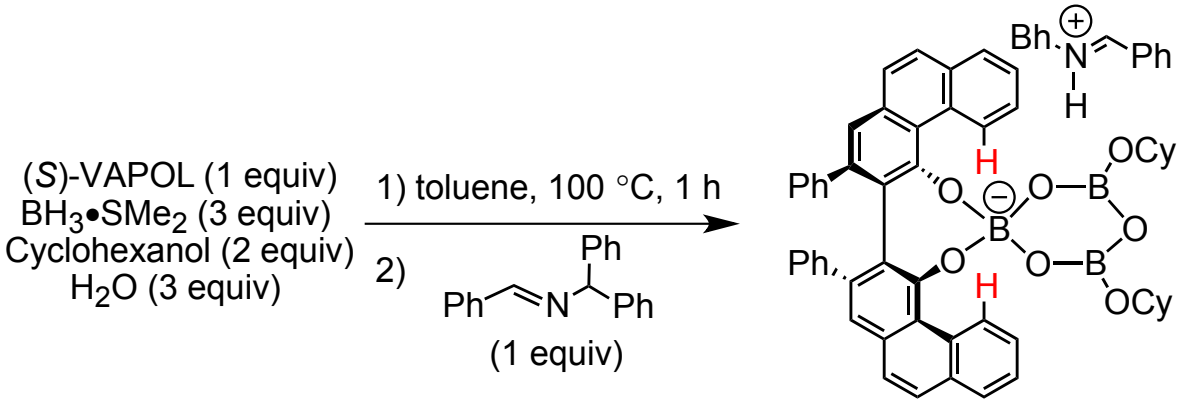

47a-8a B3 complex

Figure 2.11 (Cont'd)

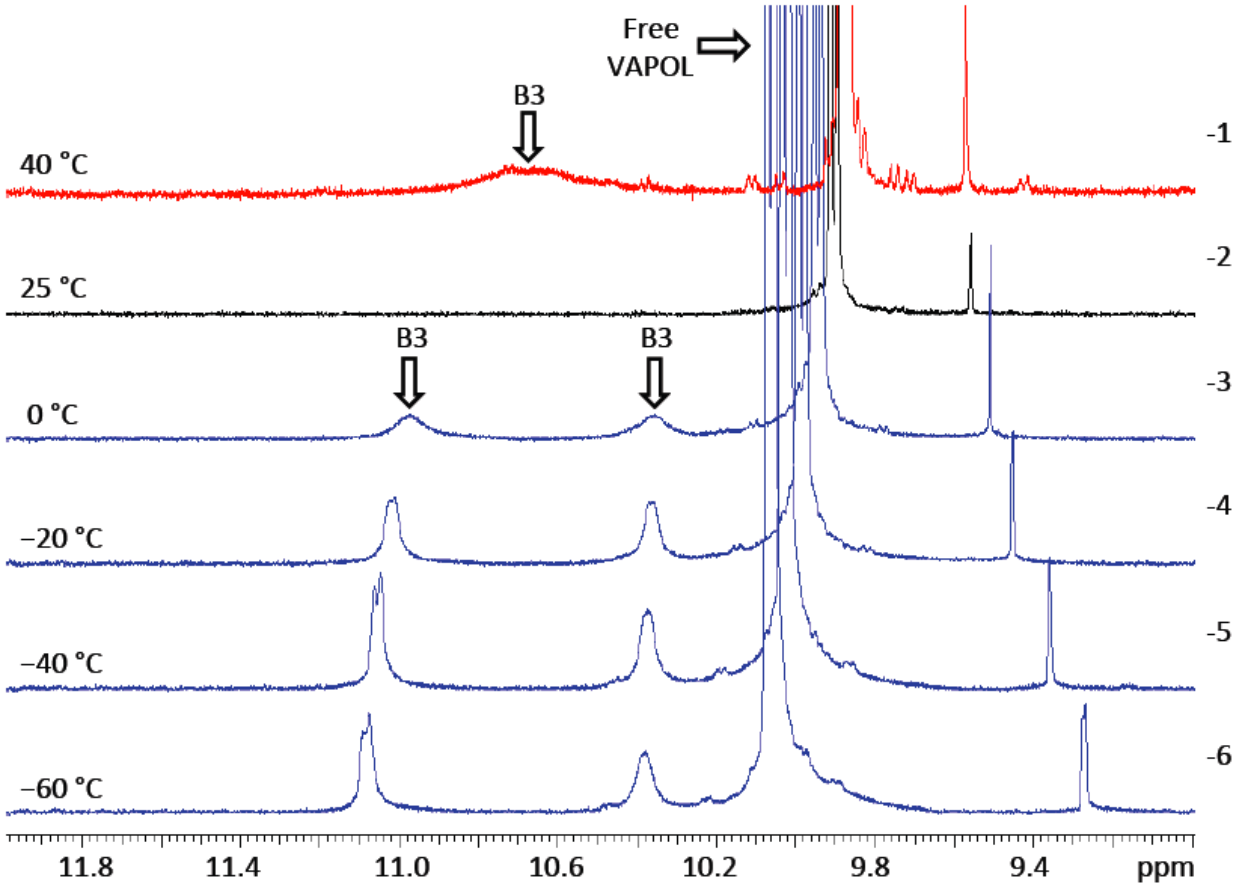

If the temperature is increased higher, the B3 begins to disassemble and the peak at 10.8 begins to decrease. This suggests that the B3 complex is unstable at high temperatures. Consequently, the mixture was cooled below room temperature to see if the B3 bay protons would appear. The proton NMR revealed peaks at 10.4 and 11.1 ppm at 0, −20, −40, and −60 °C, which would support formation of the B3 complex (entries 3-6, Figure 2.11; all spectra in blue). At 0 °C, the peaks appear broad and give a yield of 7% (11.1 ppm) and 6% (10.4 ppm) B3 when integrated against an internal standard (triphenylmethane). The yield of B3 changes when the temperature is dropped

to −20, −40, and −60 °C, yielding approximately 14% B3 at all three temperatures. This may be due to more accurate integration at low temperatures.

This data implies that when the B3 complex is cooled, the bay protons are exchanging at a rate slower than the NMR time scale. This in turn causes each bay proton, which lies in different environments, to appear as two separate signals. However, when heating the solution, a broad peak was observed, which indicates that the B3 bay protons are exchanging at a rate faster than the NMR time scale causing the peaks to coalesce. At room temperature, there was no peak observed for the B3 complex. This was due to intermediate exchange, which causes the peak to broaden to the point of becoming unobservable.

Verification of B3 existing at room temperature is established based on the boron NMR (Figure 2.12). Prior to imine addition, there is no B3 (tetra-coordinated boron species) seen in the ^{11}B NMR (entry 1, Figure 2.12). Once imine **8a** is added, the B3 catalyst **47a** self assembles and is observed at all temperatures in the boron NMR as a singlet at approximately 5 ppm (entries 2-6, Table 2.12).

Figure 2.12 ^{11}B NMR for cyclohexanol boroxinate catalyst **47a**-imine **8a** complex

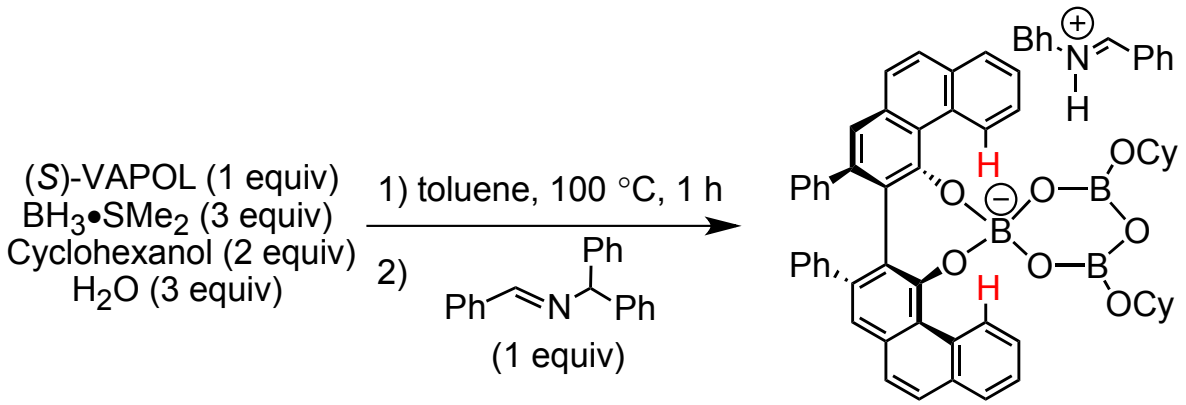

47a-8a B3 complex

Figure 2.12 (Cont'd)

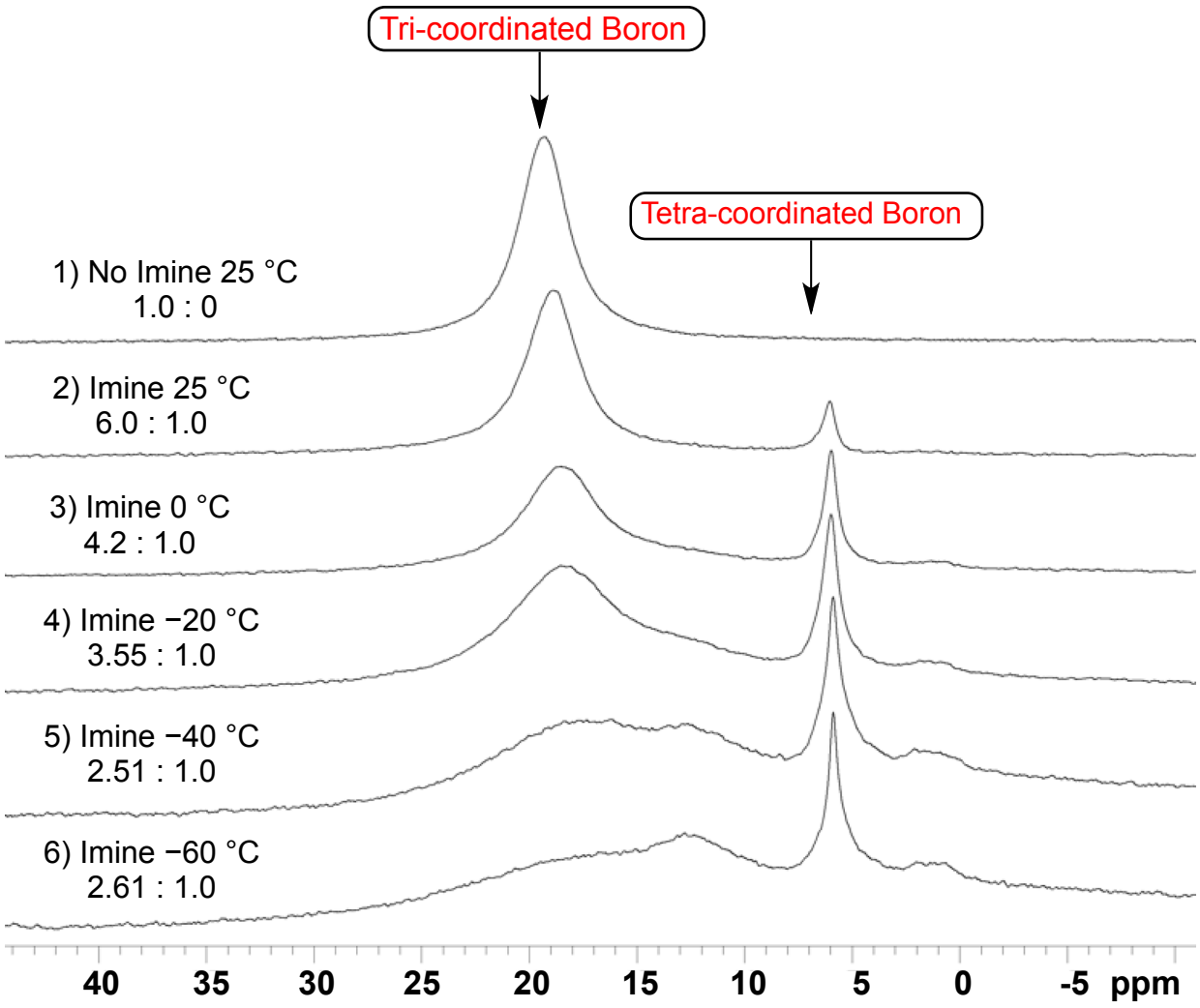

There is an increase in the B3 species as the temperature drops based upon the ratios of the two peaks (entries 2-6). The ratio of tri-coordinated and tetra-coordinated boron species changes from 6.0:1.0 at room temperature to 2.6:1.0 at −60 °C. This could be due to either an increase in the B3 complex as the temperature decreases or an integration error due to the broadening of the peaks at low temperatures.

When returning the sample to room temperature, the peaks become sharp once again and the tri-coordinated and tetra-coordinated boron species return to a 6.9:1.0 ratio, which is similar to the original spectra observed at room temperature (entry 2).

2.7.1.1 Spin saturation transfer study of cyclohexanol B3 catalyst 47a

Once the two B3 bay protons were discovered to lie in different environments at temperatures 0 °C to −60 °C, exchange studies were performed to verify that these two protons were exchanging. The first study attempted was an EXSY1D (exchange spectroscopy, NOESY1D pulse sequence) experiment with a double pulse field gradient spin echo (DPEGSE) NOE sequence. This experiment gave inconclusive results due to a poor signal-to-noise ratio and/or the phase of the NOE and exchange peaks were the same due to the high molecular weight of the compound or possibly the increased viscosity caused by the low temperature.

The second exchange study proved to give more conclusive results. A spin saturation transfer (SST) study was performed where the bay proton at 10.4 ppm was saturated with a continuous wave pulse in order to randomize spin populations. There was transfer of saturation to the bay proton at 11.1 ppm, which appears as a decrease in the size of the peak (Figure 2.13).

Figure 2.13 Spin saturated transfer study Phon catalyst **47a** complexed with imine **8a**

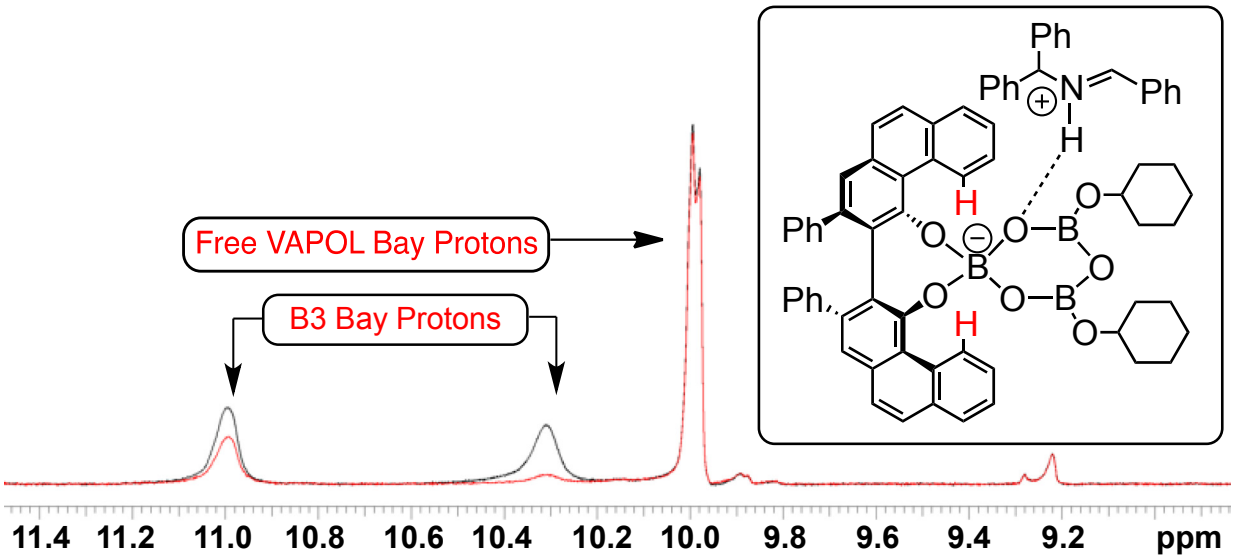

This gives evidence that these two bay protons of the B3 complex are exchanging on the NMR time scale. From this data there are two possible scenarios that could be occurring. Firstly, the imine could be hydrogen binding to one face of the boroxinate ring followed by dissociation and then rotating around the catalyst and rebinding to the opposite face. This would cause the two bay protons to exchange environments. The second scenario is that the imine could be attached to O2 through hydrogen bonding and then swiveling from one face to the other of the B3 catalyst while moving between the two O2 oxygens. Scenario two is a very plausible hypothesis due to previous studies performed on the boroxinate catalyst by a former Wulff group member, Dr. Gang Hu.[39]

Dr. Gang Hu discovered comparable exchange patterns with a similar system. With his system, imine **61** contains a BUDAM protecting group, which is comprised of four tert-butyl groups (Figure 2.14).

When mixing a 1:1 ratio of imine to catalyst the methyls that make up the tert-butyl moieties showed three peaks in the ^{1}H NMR (entry 3, Figure 2.14). One peak (H^{b}) would be the free imine **61**, which appears as a single peak because all four tert-butyl groups are equivalent and therefore appear in the same signal. The second and third peaks would represent the H-bonded imine-B3 complex **62** where two of the tert-butyl groups located on one of the aromatic rings would cause one signal ($H^{b'}$) while the other two tert-butyl groups on the other aromatic ring would cause a separate signal ($H^{b''}$). Both of these peaks are seen at room temperature suggesting that the imine is

bound to the B3 complex causing the two aromatic rings of the protecting group to exist in two different environments while at room temperature (entry 3, Figure 2.14).

Figure 2.14 BUDAM imine-B3 complex with a 1:1 ratio of imine to catalyst

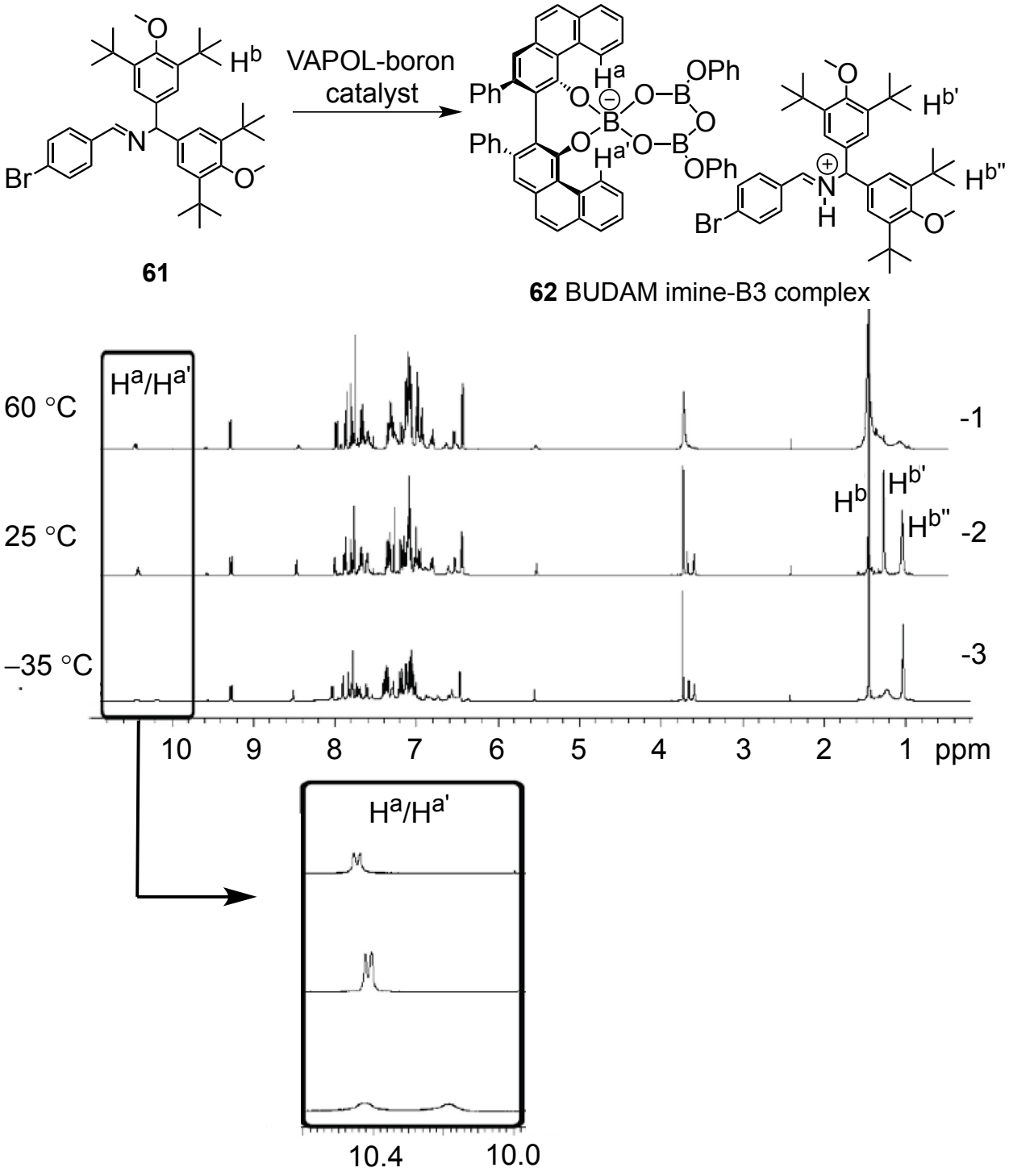

Furthermore, since two peaks appear for the bound imine (complex **62**), this also implies that the aromatic rings can still rotate causing the tert-butyl groups on their respective ring to be equivalent (all $H^{b'}$ are equivalent and all $H^{b''}$ are equivalent). When cooling the B3-BUDAM-imine complex **62**, Hu discovered that two of the tert-butyl groups located on the same aromatic ring (either $H^{b'}$ or $H^{b''}$) started to decoalesce and began to generate a possible fourth peak (broad peak in entry 2, Figure 2.14). This would imply that one of the aromatic rings of the imine is rotating slower than the NMR time scale at cold temperatures, causing two tert-butyl groups on the same aromatic ring to exist in separate environments. In summary of the imine **61/62** protons, Hb, Hb' and Hb'', the tert-butyl groups are in one environment when not bound to the catalyst (Hb), are in two environments when bound to the catalyst at room temperature (Hb' and Hb'') and are beginning to enter three environments at −35 °C (broad peak and sharp peak around Hb' and Hb'' location).

The second portion of evidence needed to determine whether the imine is swiveling from top to bottom of the catalyst versus falling on and off lays in the B3 bay proton region of the proton NMR (10-11 ppm). When looking at the B3 bay protons of complex **62** at room temperature, there is only one signal for the B3 bay protons at 10.4 ppm (entry 3, Figure 2.14). However, when cooling the complex to −35 °C, two signals form for the B3 bay protons at 10.18 and 10.42 ppm (H^{a} and $H^{a'}$, entry 2). These findings suggest that when complex **62** is at room temperature, the bay protons are exchanging faster that the NMR time scale generating one signal and at lower temperatures, the

bay protons are exchanging slower than the NMR times scale (or not at all) to generate two signals (entry 3 vs entry 2).

Therefore, when looking at all of the data, we believe that it is possible for the imine to be swiveling from top to bottom of the B3 catalyst. The reason is that at room temperature, the bay protons H^{a} and $H^{a'}$ are in the same environment (one signal) while the imine protons $H^{b'}$ and $H^{b''}$ are in separate environments (two signals). If the imine in complex **62** was coming on and off, the H^{a} and $H^{a'}$ would come in one signal but so would the $H^{b'}$ and $H^{b''}$. If the imine was not moving from top to bottom of the catalyst, then the H^{a} and $H^{a'}$ would be two signals not one. Therefore, the only other option is that the imine in complex **62** is swiveling from top to bottom allowing the H^{a} and $H^{a'}$ protons to experience both environments while at the same time the imine protecting group is bound enough where the imine protons stay in two separate environments. However, further studies are required to verify these claims, such as low temperature EXSY studies.

2.7.2 NMR analysis of phenol boroxinate catalyst 33a

2.7.2.1 Formation of phenol boroxinate catalyst 33a using borane dimethyl sulfide

Further NMR studies were performed in order to study other alcohols and phenols using various methods. Using an internal standard ($CHPh_3$), the yields of B2, B3, and VAPOL were determined. The first method studied was Method A, which is seen throughout this chapter.

The first variables to be investigated were concentration and temperature. It was determined that both of these factors had an effect on the amount of B3 generated (Table 2.11). Prior to the addition of imine, the amount of B2 formed was dependent on the concentration of the reaction. With a high concentration of 0.10 M, there was 13% B2 generated. (entry 1, Table 2.11). When the concentration was decreased to 0.05 M, the amount of B2 decreased to 5% (entry 3, Table 2.11). Once the imine is added, B3 can then self-assemble in situ. When comparing concentrations, it was observed that with a higher concentration of 0.08 M, 39% B3 was formed where the lower concentration of 0.04 M gave only 24% B3 (entries 2 and 4). When heating the NMR tube within the NMR machine to higher temperatures, the B3 complex begins to decompose resulting in decreased yields of B3 (entries 5 and 6).

Table 2.11 Variations in temperature and concentration in the formation of B3 [a]

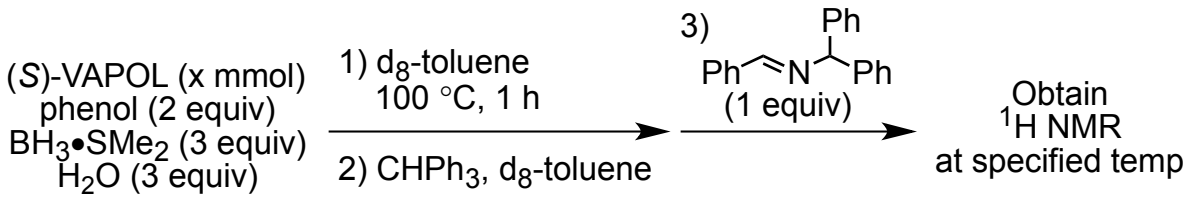

Entry	Concentration (M) [b]	Temp (°C)	B2 (%) [c]	B3 (%) [c]	VAPOL (%) [c]
1 [d]	0.10	25	13	–	70
2	0.08	25	5	39	47
3 [d]	0.05	25	5	–	72
4	0.04	25	3	24	65
5	0.04	50	2	11	59
6	0.04	70	3	6	60

[a] Unless otherwise stated, (*S*)-VAPOL (0.05 or 0.10 mmol), phenol (2.00 equiv), borane dimethyl sulfide (3.00 equiv), and water (3.00 equiv) were stirred in d_8-

toluene (0.5 mL) at 100 °C for 1 h followed by the addition of an internal standard ($CHPh_3$) dissolved in d_8-toluene (0.5 mL). The ^1H NMR was obtained followed by the addition of imine (1.00 equiv dissolved in 0.3 mL d_8-toluene). The ^1H NMR was once again obtained to determine the amount of B3 present. [b] Concentration is determined by the amount of (*S*)-VAPOL present. [c] Percent yield of B2, B3 and VAPOL was done using $CHPh_3$ as an internal standard. [d] ^1H NMR results were taken prior to imine addition.

2.7.2.2 Formation of phenol boroxinate catalyst 33a using triphenyl borate

Aside from using borane dimethyl sulfide to generate the B3 catalyst, it was also produced by using triphenyl borate. Two different methods were studied along with a variation in the amount of imine added. When heating the VAPOL, triphenyl borate, and water followed by removing the volatiles, a decent amount of B2 is generated (entry 1, Table 2.12). When adding in the imine, the B2 decreases from 24% to 5% while also generating 56% yield of B3. This indicates that the B3 is not only generated from B2 but also from VAPOL (entry 2). When the catalyst is generated at room temperature and the volatiles are not removed, the amount of B2 and B3 decrease (entries 4 and 5). Prior to imine addition, there is 14% B2 (entry 4), which decreases to 2% after imine addition (entry 5). There is 34% B3 generated using this method, which is substantially lower than the previous method when the catalyst is generated at 100 °C and the volatiles are removed (entries 4 and 5).

Table 2.12 Variations of imine equivalents and catalyst loading in B3 system [a]

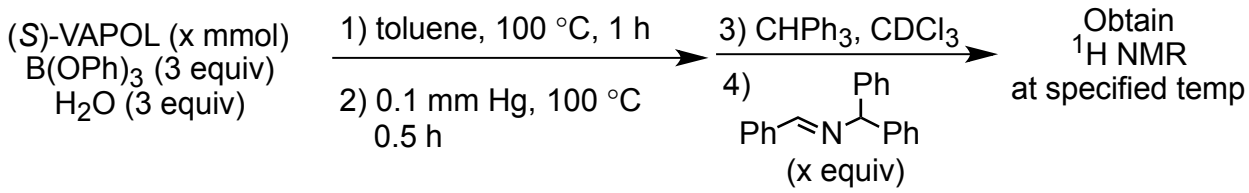

Entry	(*S*)-VAPOL (mmol)	Imine (equiv)	B2 (%)[b]	B3 (%)[b]	VAPOL (%)[b]
1[c]	0.10	0	24	–	64
2	0.10	1.0	5	56	25
3	0.10	2.0	0.5	62	15
4[c,d]	0.05	0	14	–	64
5[d]	0.05	2.0	2	34	22

[a] Unless otherwise stated, (*S*)-VAPOL (x mmol), triphenyl borate (3.00 equiv), and water (3.00 equiv) were stirred in toluene (1 mL) at 100 °C for 1 h followed by the removal of volatiles using 0.1 mmHg at 100 °C. An internal standard ($CHPh_3$) dissolved in $CDCl_3$ (1 mL) was added. The ^1H NMR was obtained followed by the addition of imine **8a** (x equiv dissolved in 0.3 mL $CDCl_3$). The ^1H NMR was once again obtained to determine the amount of B3 present. [b] Percent yield of B2, B3 and VAPOL was done using $CHPh_3$ as an internal standard. [c] ^1H NMR results were taken prior to imine addition. [d] (*S*)-VAPOL (0.05 mmol) and triphenyl borate (3.00 equiv) was stirred in $CDCl_3$ (1 mL) at rt for 10 minutes and directly subjected to ^1H NMR analysis. The imine (2.00 equiv dissolved in 0.3 mL $CDCl_3$) was then added in order to generate the B3 catalyst. The solution was once again subjected to ^1H NMR analysis.

2.7.3 NMR analysis of *n*-butanol boroxinate catalyst 46a

When developing the Wulff AZ reaction, a previous Wulff group member Dr. Jon Antilla discovered that heating VAPOL and BH_3•THF in CH_2Cl_2 followed by removing the volatiles and addition of an imine, EDA, and CH_2Cl_2 resulted in cis-aziridines.[16a] In the current work presented in this chapter, it was discovered that *n*-butanol gave very good results with the cis-aziridination reaction (refer to section 2.4.3). Aliphatic alcohol *n*-butanol was included in these studies because of its connection with the original AZ reaction using borane tetrahydrofuran complex. Borane THF complex is shown to decompose by reductive ring opening of the THF ring to give a variety of borate species including tributyl borate.[40, 16k] For this reason, investigations of the original AZ method and the current Method A were undertaken.

When using the original AZ method, there were multiple peaks seen in the bay proton region. An overview of these peaks is shown in Table 2.13. It was observed that a peak at 10.1 appeared prior to imine addition (entries 1 and 4, Table 2.13) and then disappeared after the imine addition (entries 2,3, and 5). Also, it was seen that a peak at 9.9 ppm appears in each entry and only appears to diminish when excess imine is added (entry 5). Other peaks observed in the presence of excess imine **8a** were 9.95 and 9.56 (entry 5). When using 1 equivalent of imine **8a** and letting the NMR tube containing the solution be stored for 2 days under nitrogen, a peak at 9.4 ppm was observed (entry 3). It is still not clear which of these peaks correspond to the B3 bay protons.

Table 2.13 ^{1}H NMR studies using the original AZ method [a]

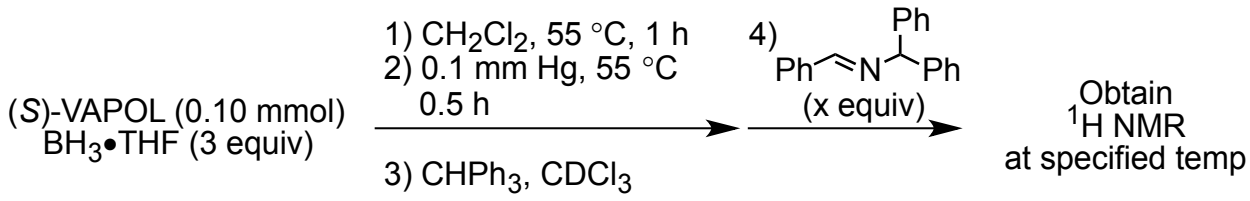

Entry	Imine (equiv)	10.1 ppm (%)[b]	9.9 ppm (%)[b]	9.95 ppm (%)[b]	9.56 ppm (%)[b]	9.4 ppm (%)[b]	VAPOL (%)[b]
1[c]	0	10	29	–	–	2	35
2	1	–	30	–	–	–	35
3[d]	1	–	19	–	–	23	24
4[c]	0	24	33	–	–	–	15
5	10	–	5	45	21	–	13

[a] (*S*)-VAPOL (0.10 mmol) and borane THF (3.00 equiv) were stirred in CH_2Cl_2 at 55 °C for 1 h followed by removal of the volatiles. An internal standard was added followed by the imine (x equiv). ^{1}H NMR analysis was performed. [b] Percent yields were done using $CHPh_3$ as an internal standard. [c] ^{1}H NMR results were taken prior to imine addition. [d] After entry 2 data was obtained, the NMR tube was stored under nitrogen for 2 days and then the proton NMR was obtained once again to give data reported in entry 3.

It was difficult to make any assessment as to what all of these species were. Instead, we moved forward and looked at the currently used method(s) to make the B3 catalyst with *n*-butanol (Tables 2.14 and 2.15).

Table 2.14 ^{1}H NMR studies for butanol catalyst **46a** [a]

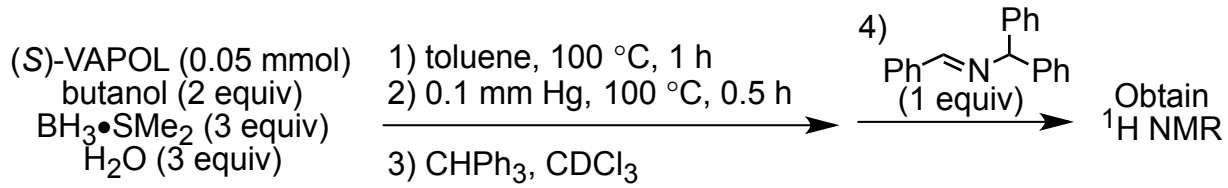

entry	10.15 ppm (%) [b]	9.9 ppm (%) [b]	9.4 ppm (%) [b]	(*S*)-VAPOL (%)[b]	boron NMR (18.6 ppm : 5.2 ppm)
1[c]	0	4	30	40	1.0 : 0
2	27	0	22	29	2.9 : 1.0

[a] Unless otherwise stated, (*S*)-VAPOL (0.05 mmol), butanol (2.00 equiv), borane dimethyl sulfide (3.00 equiv), and water (3.00 equiv) were stirred in toluene (1 mL) at 100 °C for 1 h followed by the removal of volatiles. An internal standard ($CHPh_3$) dissolved in $CDCl_3$ (1 mL) was added. The ^{1}H NMR was obtained followed by the addition of imine (1.00 equiv dissolved in 0.3 mL $CDCl_3$). The ^{1}H NMR was once again obtained to determine the amount of B3 present. [b] Percent yield of B2, B3 and VAPOL was done using $CHPh_3$ as an internal standard. [c] ^{1}H NMR results were taken prior to imine addition.

Several peaks were observed when generating butanol catalyst **46a**. However, the B3 catalyst bay protons were assumed to be the peak that appeared most down field after imine addition due to its broadness (10.15 ppm in Table 2.14 and 10.59 ppm in Table 2.15). It was determined that using vacuum increased the B3 yield by 7% (entry 2, Table 2.14 versus entry 2, Table 2.15). When applying vacuum to generate the pre-

catalyst, a peak at 9.4 was observed and calculated to be 30% yield (entry 1, Table 2.14).

Table 2.15 ^{1}H NMR studies for 6-component AZ protocol using catalyst **46a** [a]

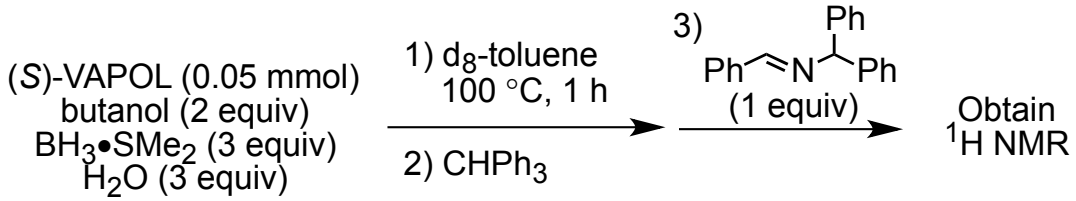

entry	10.59 ppm (%) [b]	10.12 ppm (%) [b]	(*S*)-VAPOL (%)[b]	9.79 ppm (%)[b]	boron NMR (18.7 ppm : 5.9 ppm)
1[c]	0	3	62	13	1.0 : 0
2	20	0	49	7	6.9 : 1.0

[a] Unless otherwise stated, (*S*)-VAPOL (0.05 mmol), butanol (2.00 equiv), borane dimethyl sulfide (3.00 equiv), and water (3.00 equiv) were stirred in d_8-toluene (1 mL) at 100 °C for 1 h. An internal standard ($CHPh_3$) was added. The ^{1}H NMR was obtained followed by the addition of imine (1.00 equiv dissolved in 0.3 mL d_8-toluene). The ^{1}H NMR was once again obtained to determine the amount of B3 present. [b] Percent yield of B2, B3 and VAPOL was done using $CHPh_3$ as an internal standard. [c] ^{1}H NMR results were taken prior to imine addition.

One possible species for this peak could be B2. In the absence of vacuum, a decent size peak appeared at 9.79 ppm giving 13% yield (entry 1, Table 2.15). This peak also has the possibility to be B2. Further studies are required for this catalyst system before any definite assumptions can be made on if these peaks are actually B2 or other VAPOL species.

2.8 Conclusion

An extensive study was undertaken to examine the electronic and steric effects of the B3 catalyst system on the 6-component catalytic asymmetric aziridination reaction. It was discovered that electron donating groups located in the para position of the phenol used to self assemble the B3 catalyst lead to increased enantioselectivity. This may be due to an increase in electron density in the B3 system causing better hydrogen bonding with the substrate and therefore better enantioselectivity. Furthermore, with electron deficient para substituted phenols used in the B3 catalyst, it was seen that the enantioselectivity decreased in the AZ reaction, which may be due to a decrease in hydrogen bonding between the substrate and catalyst. These findings were correlated to show a linear relationship between the enantiomeric ratios of the aziridine products and the sigma para negative Hammett values for the para substituted phenols used in the boroxinate catalyst. Furthermore, computational studies were performed in order to calculate the H-bond distance and electron density associated with the B3-imine complexes.

It was additionally revealed that cyclohexanol was the optimal alcohol to use in the B3 catalysts derived from the VANOL or VAPOL ligand. Computational studies revealed that the C-O hydrogen bond distances for the iminium-boroxinate complex containing cyclohexanol to be 1.72 Å in the case of imine **8a** and 1.67 Å in the case of imine **8b**, which explains an increase in enantioselectivity observed when using catalyst **47** as compared with electron neutral phenol catalyst **33a/33b** and electron deficient phenol catalysts **45a/45b**.

CHAPTER THREE

ONE POT MULTI-COMPONENT CATALYTIC ASYMMETRIC AZIRIDINATION REACTION

3.1 Introduction

Over the past decade, the Wulff catalytic asymmetric aziridination (AZ) reaction has been optimized to be a very robust and diverse reaction. The AZ reaction applies a general procedure in order to generate either cis or trans-aziridines in moderate to high yields and ee's.[16,30] We furthered this universal aziridination reaction by modifying the procedure in order to create a route that allows for the direct assembly of a large B3 catalyst family (refer to chapter 2). This 6-component catalytic asymmetric aziridination reaction allows for the generation of a multiplex of chiral polyborate Brønsted acids to be generated using a generalized procedure.

Although these previously discovered methods are excellent in many ways, they all have the same downfall, which is the need to generate the imine precursor. Imines can be both stable and unstable compounds depending upon the structure. Typically the solid imines are relatively stable and can be purified via crystallization unlike the unstable liquid imines, which generally contain aliphatic moieties and cannot be purified. It is these imines that pose a significant challenge in the previously used AZ reaction methods.

Here, a modified procedure will be revealed that uses a simplified and more efficient multi-component method, which in turn eliminates the problem of unstable imines being synthesized and isolated. Previously, we have used vacuum to remove volatiles, high temperatures, and different precursors in the preparation of the pre-catalyst. These

three factors have been eliminated in the current method described here, which uses a one pot multi-component methodology in order to synthesize cis-aziridines.

3.2 Synthesis of alkyl substituted aziridines using previously established methods

Hitherto, our group has done extensive studies on the aziridination reaction. Both aliphatic and aromatic imines with various nitrogen protecting groups have been used to synthesize cis-aziridines.[16i] When generating aromatic aziridines, the aromatic imine starting reagent is typically crystalline in form. This is very beneficial because the imine can be purified via crystallization and is relatively stable. However, when synthesizing aliphatic aziridines, the aliphatic imines are typically non-crystalline, which poses a problem when attempting to purify them. Non-crystalline imines cannot be purified via crystallization and will normally decompose during column chromatography (silica) or when distillation is attempted. Therefore, these non-crystalline imines are typically synthesized directly prior to the AZ reaction and then used in their crude form.

Some attempts have been made here to synthesize aliphatic aziridines that have remote functionalities using the general AZ reaction. As seen in chapter two, the aliphatic group studied was cyclohexyl. Therefore, here the first substrate to be studied was 4-cyclohexylbutanal **65** as the imine precursor where the cyclohexyl is placed three carbon atoms from the carbonyl carbon. Aldehyde **65** was synthesized starting from the corresponding acid **63**. First, acid **63** was converted into ester **64** via a DCC coupling reaction giving 91% yield followed by DIBAL-H reduction to give aldehyde **65** in 87% yield (Scheme 3.1).

Scheme 3.1 Synthesis of 4-cyclohexylbutanal **65**

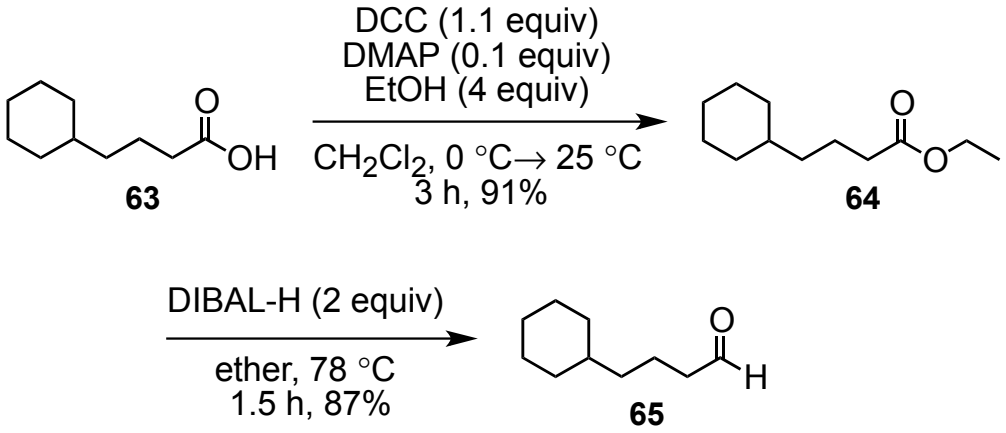

Once synthesized, aldehyde **65** could be used to generate imine **67** and then directly submitted to the AZ reaction (Scheme 3.2).

Scheme 3.2 Synthesis of MEDAM protected imine **67**

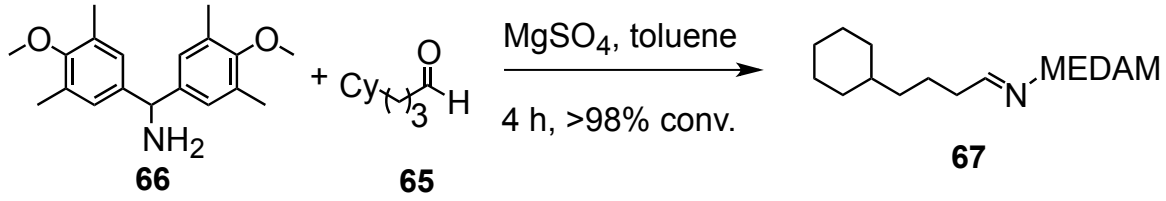

Using previously established methods, MEDAM protected imine **67** was subjected to the AZ reaction to give good to excellent enantioselectivity with poor to moderate yields (Table 3.1).

When evaluating the catalyst loading, it was determined that loading from 2.5-10 mol% did not have any substantial impact on the enantioselectivity with ee's ranging 90-94% (entries 1, 2, and 9, Table 3.1). When using the benzhydryl protecting group instead of MEDAM, the VANOL ligand was found to be superior to the VAPOL ligand (entries 3 and 4). The reaction time was extended for three days to give 89% ee for the VANOL ligand and 96% ee for the VAPOL ligand (entries 5 and 6).

Table 3.1 Synthesis of aziridine **68** via the AZ reaction

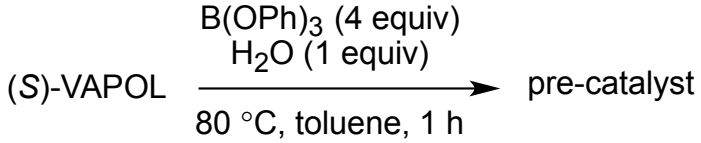

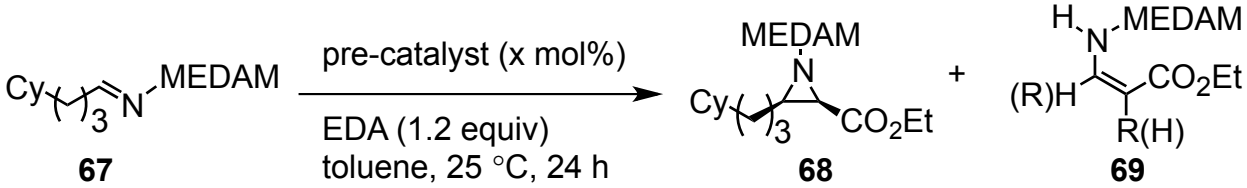

Entry	Catalyst (mol %)	Ligand	Yield **68** (%) [b]	*ee* **68** (%) [c]	Conv. (%) [d]	Enamines **69** (%) [e]
1	10	*(S)*-VAPOL	67	94	94	2.7
2	5	*(S)*-VAPOL	46	90	91	0
3 [f]	5	*(R)*-VANOL	51	79	86	3
4 [f]	5	*(S)*-VAPOL	33	41	100	6.6
5 [g]	5	*(R)*-VANOL	49	89	79	1.5
6 [g]	5	*(S)*-VAPOL	50	96	82	5.5
7 [h]	5	*(S)*-VAPOL	8	ND	91	4.2
8 [i]	5	*(S)*-VAPOL	40	93	66	26
9	2.5	*(S)*-VAPOL	71	94	99	2.1
10 [j]	2.5	*(S)*-VAPOL	31	93	55	27
11 [k]	2.5	*(S)*-VAPOL	38	95	63	18

[a] Unless otherwise specified, all reactions were run at 0.25 M in imine **67** with EDA (1.20 equiv) in the presence of x mol% catalyst in toluene at 25 °C for 24 h. The pre-catalyst was prepared from either (*S*)-VAPOL or (*R*)-VANOL, $B(OPh)_3$ (4.00 equiv) and H_2O (1.00 equiv) in toluene at 80 °C for 1 h followed by removal of volatiles at 80 °C under high vacuum (0.1 mm Hg) for 0.5 h. The enantiomer shown is the product for (S)-VAPOL. (R)-VANOL results in the

opposite enantiomer. ND represents Not Determined. [b] Isolated yield after column chromatography. [c] Determined by HPLC with either a Chiralcel OD-H or Pirkle R,R-(Whelk)-0-1 column. [d] The conversion was determined from the ^{1}H NMR spectrum of the crude reaction mixture using an internal standard ($CHPh_3$). [e] Determined by integration of the enamine protons in ^{1}H NMR. [f] Bh protecting group in place of MEDAM. [g] Reaction ran for 3 days. [h] A different bottle of EDA (not new) was used in the AZ reaction to test for purity effects. [i] A new bottle of EDA was used in the AZ reaction. [j] The catalyst was made without addition of 1.00 equiv of H_2O. [k] Reaction was carried out at 0 °C for 24 h.

When different bottles of EDA were used, including both old and newly purchased bottles, inconsistent results were obtained (entries 7 and 8). Other variables were altered in the reaction such as removal of the water (1.00 equiv) added during pre-catalyst preparation and a decrease in the temperature (entries 10 and 11). These reactions both resulted in ee's in the mid 90's and low yields. Overall, the enantioselectivity appeared to be in the upper 80's and low to mid 90's when using MEDAM imine **67**. However, the yield, amount of enamine, and the extent of conversion were quite unpredictable. This was determined to be primarily due to a side reaction caused by the unstable aliphatic imine **67**. This side reaction side involves a self-

condensation to produce a conjugated imine (Scheme 3.3). A previous group member, Dr. Anil K. Gupta, established that this self-condensation occurs with aliphatic imines.[41]

Scheme 3.3 Self-condensation of aliphatic imines to give conjugated imine byproducts

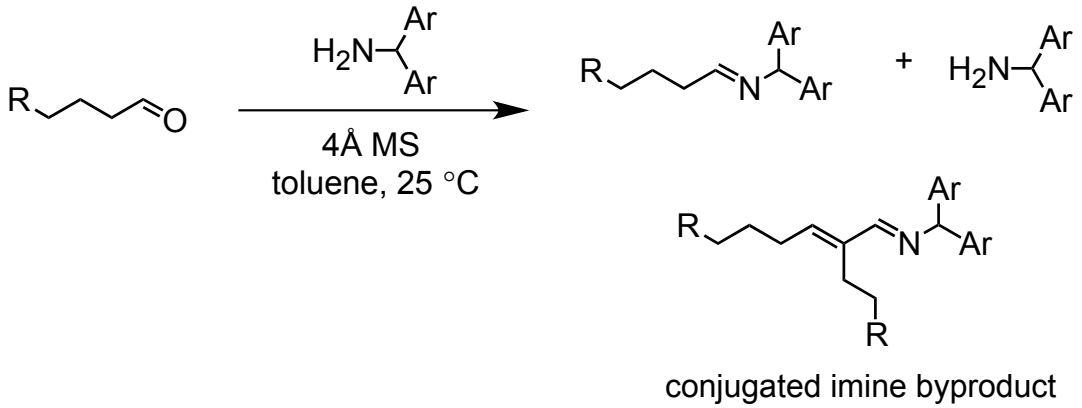

conjugated imine byproduct

Although such a conjugated imine byproduct was not characterized in the reaction involving imine **67**, there was evidence in the ^{1}H NMR of the crude reaction mixture that suggested that this conjugated imine byproduct was being generated. The logical route to follow in order to eliminate this side product from forming is to alter the methodology in order to generate the imine in situ, which allows for the immediate transformation of the imine to the corresponding aziridine. Such methodologies will be discussed in the ensuing sections.

3.3 Multi-component catalytic asymmetric aziridination reaction

When three or more reagents that are all incorporated into the products are added simultaneously to a reaction flask, the reaction is considered multi-component.[42] The first multi-component catalytic asymmetric aziridination (MCAZ) reaction was published by our group in 2011.[41] In these one-pot reactions, all reagents are placed into the same reaction flask without prior synthesis of any intermediates. This allows for the

imine to be generated in situ rather than synthesized, isolated, and in some cases purified prior to the AZ reaction. The two main shortcomings to the currently published MCAZ reaction are the lack of diversity in the B3 catalyst and the use of MEDAM protecting group, which is not commercially available. Therefore, the current study focuses on altering the methodology to generate a large and diverse catalyst family that can be employed in a one pot multi-component AZ reaction and to explore this with the commercially available benzhydryl amine **70**.

3.3.1 Effects of benzoic acid on the one pot multi-component catalytic asymmetric aziridination reaction

In this new methodology, the imine will be synthesized in situ, which requires the starting materials to consist of the corresponding amine and aldehyde. Initially, a method that was developed combined the VANOL or VAPOL ligand, alcohol, borane, water, and amine to generate the B3 catalyst followed by molecular sieves, aldehyde, and EDA to generate cis-aziridines (Scheme 3.4).

Scheme 3.4 General assembly of the boroxinate catalyst using a one pot multi-component AZ reaction

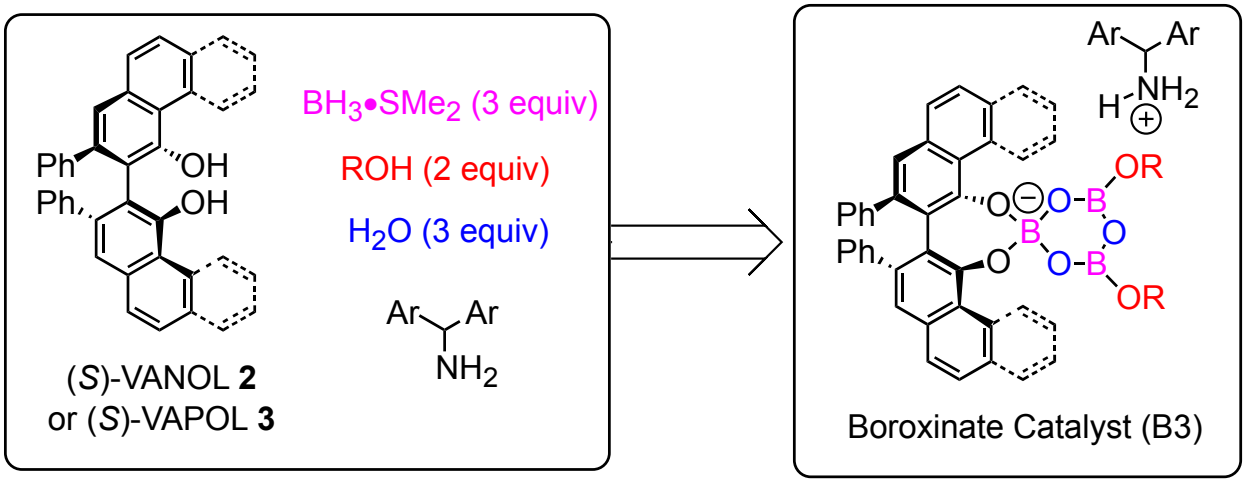

When first attempting to do this type of reaction, low conversions were observed (entries 1 and 4, Table 3.2). Therefore, co-catalysts consisting of various Brønsted acids were added in the attempt to promote the reaction. The rational for adding a co-catalyst stemmed from a protocol developed by Kelly et al., which generates BINOL borate species using BINOL derivatives, acetic acid, borane THF, and juglone.[43] It was suggested that acetic acid accelerates the reaction between BINOL and borane THF.[44] Therefore, both acetic acid and benzoic acid were evaluated to determine if they promoted the reaction in the case of the VANOL and VAPOL ligands. As seen in Table 3.2, when no acid is added, the reaction proceeded with only 9% conversion when using the VAPOL ligand and 54% conversion with the VANOL ligand (entry 1 and 4).

Table 3.2 Effects of Brønsted acids on the one pot multi-component AZ reaction [a]

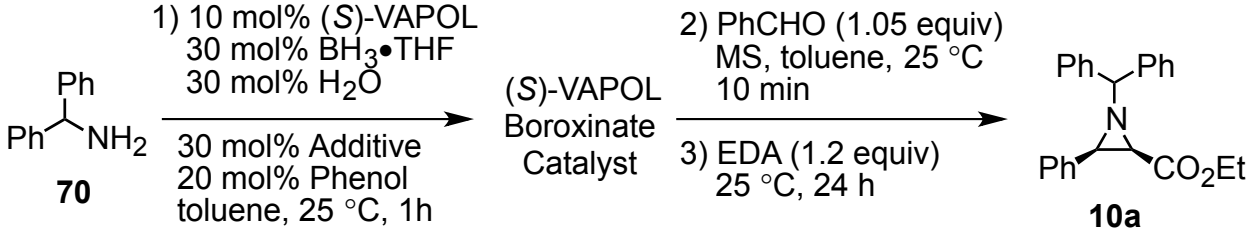

Entry	Additive	Conversion [b] **10a** (%)	Yield **10a** (%) [c]	ee **10a** (%) [d]	*cis/trans* [e]
1	None	9	ND	ND	ND
2	Acetic Acid	75	73	90	25:1
3	Benzoic Acid	90	74	94	25:1
4 [f]	None	54	ND	ND	ND

[a] Unless otherwise stated, the catalyst was prepared by mixing ligand (0.10 equiv), borane (0.30 equiv), water (0.30 equiv), phenol (0.20 equiv), and amine (1.00 equiv) in a 1.0 M toluene solution in amine at room temperature for 1 h. Flame-dried 4Å powder

molecular sieves, benzaldehyde (1.05 equiv), and EDA (1.2 equiv) were then added and diluted to a 0.5 M toluene solution. The reaction was stirred at room temperature for 24 h. ND represents Not Determined. [b] The conversion was determined from the ^{1}H NMR spectrum of the crude reaction mixture using an internal standard ($CHPh_3$). [c] Isolated yield after column chromatography. [d] Determined by HPLC on a Chiralcel OD-H column. [e] Determined from the ^{1}H-NMR spectrum of the crude reaction mixture. [f] (R)-VANOL used as ligand.

However, when acetic acid or benzoic acid is added, the conversion increases drastically to 75 and 90%, respectively (entries 2 and 3, Table 3.2). When comparing the two acids, the slightly more acidic benzoic acid gave both higher conversion and higher enantioselectivity with approximately the same isolated yield as compared to that of acetic acid.

The amount of benzoic acid was then decreased to determine if the results are affected (Table 3.3). The motivation for attempting to decrease the amount of benzoic acid was partially due to the fact that the reagents would crash out of solution when using 30 mol% benzoic acid.

Table 3.3 Various amounts of benzoic acid used in the one pot multi-component AZ reaction [a]

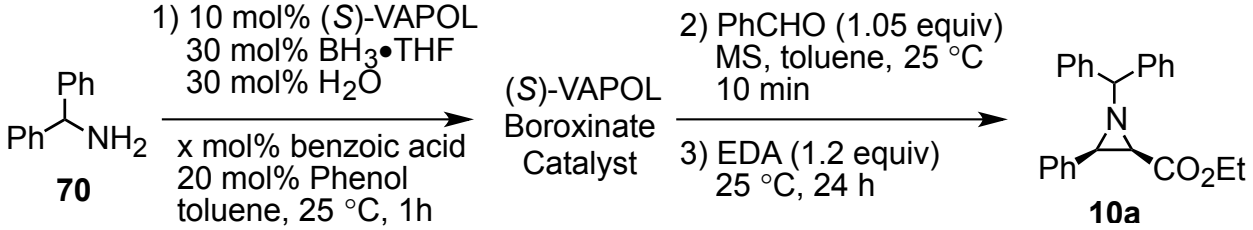

Table 3.3 (Cont'd)

Entry	Benzoic Acid (x mol%)	Conversion (%) [b]	Yield **10a** (%) [c]	ee **10a** (%) [d]	*cis/trans* [e]
1	0	74	ND	ND	ND
2	10	99	90	92	50:1
3	1	98	91	92	100:1

[a] Unless otherwise stated, the catalyst was prepared by mixing (*S*)-VAPOL (0.10 equiv), borane (0.30 equiv), water (0.30 equiv), phenol (0.20 equiv), x mol% benzoic acid, and amine (1.00 equiv) in a 1.0 M toluene solution in amine at room temperature for 1 h. Flame-dried 4Å powder molecular sieves, benzaldehyde (1.05 equiv), and EDA (1.20 equiv) were then added and diluted to a 0.5 M toluene solution. The reaction was stirred at room termperature for 24 h. ND represents Not Determined. [b] The conversion was determined from the ^{1}H NMR spectrum of the crude reaction mixture using an internal standard ($CHPh_3$). [c] Isolated yield after column chromatography. [d] Determined by HPLC on a Chiralcel OD-H column. [e] Determined from the ^{1}H-NMR spectrum of the crude reaction mixture.

Thus it was pleasant to observe that the use of either 10 or 1 mol% benzoic acid resulted in no significant change in conversion, yield or enantioselectivity (entries 2 and 3, Table 3.3). The reaction was then repeated without benzoic acid in order to re-evaluate its significance in this new protocol, which resulted in 74% conversion (entry 1, Table 3.3). However, this result was inconsistent with the previous example that was run in the absence of benzoic acid under the same conditions (entry 1, Table 3.2 vs

entry 1, Table 3.3). Therefore, the reaction was repeated multiple times and non-reproducible results were observed both with and without a co-catalyst (Table 3.4).

Table 3.4 Inconsistent results in the one pot multi-component AZ reaction [a]

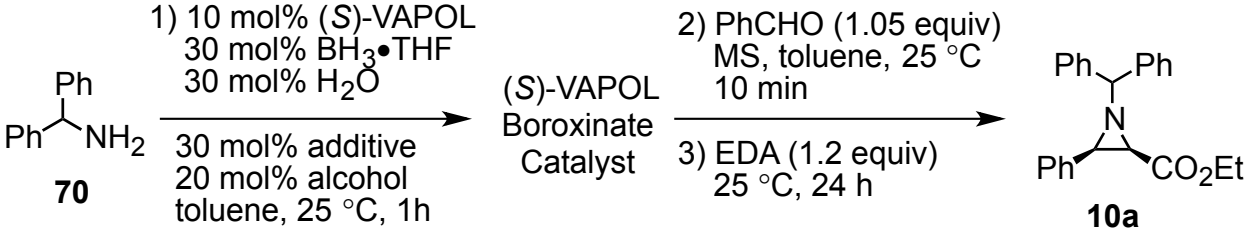

Entry	Alcohol [b]	Additive	Conversion (%) [c]	Yield **10a** (%) [d]	ee **10a** (%) [e]	*cis/trans* [f]
1	CyOH	None	99	87	95	33:1
2	CyOH	None	54	ND	ND	ND
3	PhOH	Benzoic Acid	54	ND	ND	ND
4[g]	PhOH	Benzoic Acid	81	ND	ND	ND
5	PhOH	Acetic Acid	57	ND	ND	ND
6[g]	PhOH	Acetic Acid	62	ND	ND	ND

[a] Unless otherwise stated, the catalyst was prepared by mixing (*S*)-VAPOL (0.10 equiv), borane (0.30 equiv), water (0.30 equiv), phenol (0.20 equiv), and amine (1.00 equiv) in a 1.0 M toluene solution in amine at room temperature for 1 h. Flame-dried 4Å powder molecular sieves, benzaldehyde (1.05 equiv), and EDA (1.20 equiv) were then added and diluted to a 0.5 M solution in toluene. The reaction was stirred at room temperature for 24 h. ND represents Not Determined. [b] Cyclohexanol and phenol are represented by CyOH and PhOH respectively. [c] The conversion was determined from the ^{1}H NMR spectrum of the crude reaction mixture using an internal standard ($CHPh_3$). [d] Isolated yield after column chromatography. [e] Determined by HPLC on a

Chiralcel OD-H column. [f] Determined from the ^{1}H-NMR spectrum of the crude reaction mixture. [g] New bottle of borane tetrahydrofuran complex used.

When using cyclohexanol as the alcohol in the B3 species, we observed nearly full conversion with 87% yield and 95% ee (Table 3.4, entry 1). However, when we repeated this reaction using the same conditions, the conversion dropped to 54% (entry 2). When we repeated the reaction with both benzoic acid and acetic acid, a drastic difference in results appeared. Both reactions resulted in a large drop in conversion, with benzoic acid giving 54% conversion and acetic acid giving 57% conversion (entries 3 and 5 respectively).

We first suspected that the borane had decomposed, since this is one of the more unstable reagents used in the AZ reaction.

Figure 3.1 ^{1}H-NMR spectra for both old and new bottles of borane tetrahydrofuran complex in $CDCl_3$

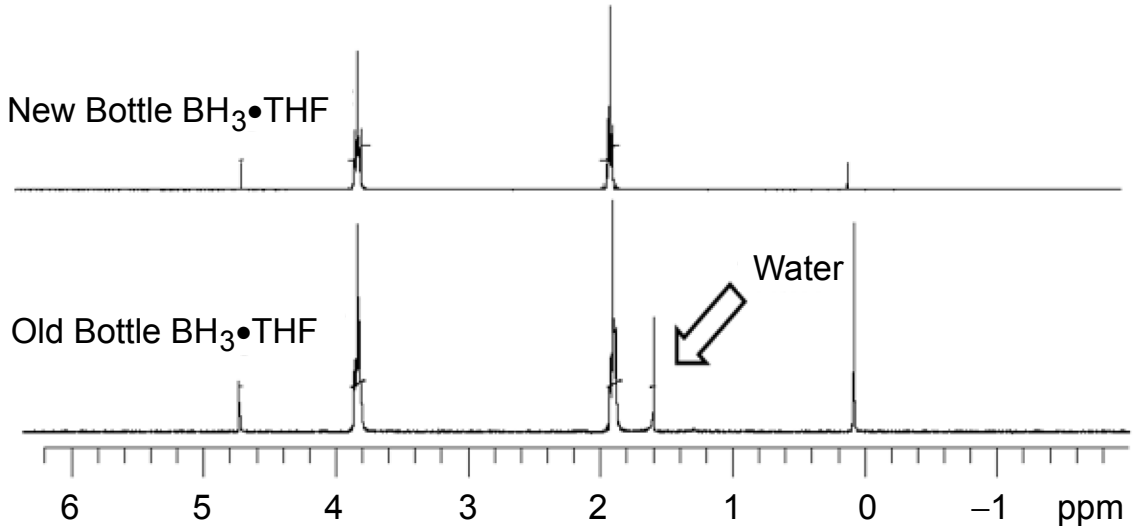

We obtained a new bottle of borane tetrahydrofuran complex and repeated the reactions with a slight increase in conversion (entries 4 and 6, Table 3.4). When looking at the ^{1}H-NMR spectra of the two bottles of borane, we observed only one peak that was different, which we attributed to water (Figure 3.1). After repeating the reaction with several different bottles of borane tetrahydrofuran complex, the results were still inconsistent. Therefore, we moved to alternate possibilities to explain the non-reproducible results. After much consideration, the aldehyde was determined to be the most logical culprit in the inconsistent results. Therefore, we increased the equivalents used from 1.05 equivalents to 1.50 equivalents (Table 3.5).

Table 3.5 Increase in amount of benzaldehyde used in the one pot multi-component AZ reaction [a]

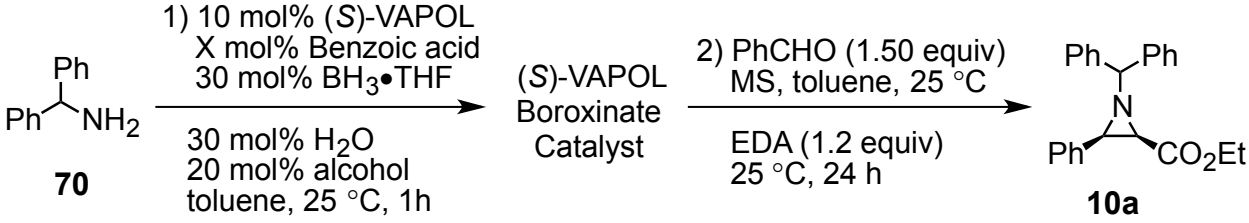

Entry	Alcohol [b]	Benzoic Acid (x mol%)	Conversion (%) [c]	Yield **10a** (%) [d]	ee **10a** (%) [e]	*cis/trans* [f]
1	CyOH	5	99	88	94	50:1
2	CyOH	1	96	ND	ND	ND
3	PhOH	5	99	92	94	100:1
4	PhOH	1	83	ND	ND	ND

[a] Unless otherwise stated, the catalyst was prepared by mixing (*S*)-VAPOL (0.10 equiv), borane (0.30 equiv), water (0.30 equiv), alcohol (0.20 equiv), x mol% benzoic acid, and amine (1.00 equiv) in a 1.0 M toluene solution in amine at room temperature for 1 h. Flame-dried 4Å powder molecular sieves, benzaldehyde (1.50

equiv), and EDA (1.20 equiv) were then added and diluted to a 0.5 M solution in toluene. The reaction was stirred at room temperature for 24 h. ND represents Not Determined. [b] The conversion was determined from the ^{1}H NMR spectrum of the crude reaction mixture using an internal standard ($CHPh_3$). [c] Cyclohexanol and phenol are represented by CyOH and PhOH respectively. [d] Isolated yield after column chromatography. [e] Determined by HPLC on a Chiralcel OD-H column. [f] Determined from the ^{1}H-NMR spectrum of the crude reaction mixture.

We found that the results were reproducible when using excess benzaldehyde (Table 3.5 and Table 3.6). We concluded that when the aldehyde falls short of consuming all of the amine, the amine left behind will in turn poison the catalyst which halts the AZ reaction. In Table 3.5, it was observed that decreasing the amount of benzoic acid from 5 mol% to 1 mol% results in lower conversion of the starting materials to product (Table 3.5, entries 1-4). Furthermore, we eliminated the 10 minutes of stirring prior to adding the EDA since this step appeared unnecessary.

Now that the aziridination reactions were reproducible while using VAPOL as the ligand, the VANOL ligand would now be evaluated in the reaction. Unfortunately, this change in ligand caused a drastic decrease in conversion (entries 1-4, Table 3.6). Further investigation within the Wulff group is currently underway on the inconsistences seen with the VANOL-B3 catalyst. When using VAPOL, the alcohol that is incorporated into the B3 catalyst did not appear to have a significant impact on the enantioselectivity (entries 2 and 4). However, when using phenol, the reaction gave a higher yield than that of cyclohexanol (entries 2 and 4). Now that the reaction has become reproducible

with excess aldehyde, the benzoic acid was removed from the reaction conditions to see the true effect that benzoic acid was having in the one pot multi-component AZ reaction. This resulted in a decrease in conversion (entries 5 and 6). Lastly, when lowering the catalyst loading to 5 mol%, the enantioselectivity remained constant with the yield and conversion decreasing slightly (entry 7).

Table 3.6 VANOL versus VAPOL in the one pot multi-component AZ reaction [a]

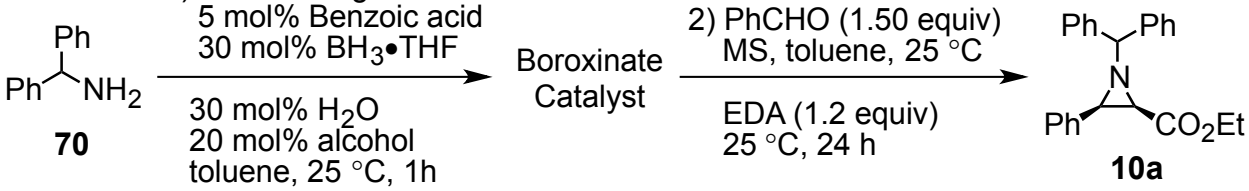

Entry	Ligand	Alcohol [b]	Conversion (%) [c]	Yield **10a** (%) [d]	ee **10a** (%) [e]	*cis/trans* [f]
1	(*R*)-VANOL	CyOH	37	ND	ND	ND
2	(*S*)-VAPOL	CyOH	98	78	94	25:1
3	(*R*)-VANOL	PhOH	29	ND	ND	ND
4	(*S*)-VAPOL	PhOH	98	94	95	100:1
5 [g]	(*S*)-VAPOL	PhOH	69	ND	ND	ND
6 [g]	(*S*)-VAPOL	CyOH	83	ND	ND	ND
7 [h]	(*S*)-VAPOL	PhOH	90	88	96	100:1

[a] Unless otherwise stated, the catalyst was prepared by mixing ligand (0.10 equiv), borane (0.30 equiv), water (0.30 equiv), alcohol (0.20 equiv), benzoic acid (0.05 equiv), and amine (1.00 equiv) in a 1.0 M solution in amine in toluene at room temperature for 1 h. Flame-dried 4Å powder molecular sieves, benzaldehyde (1.50 equiv), and EDA (1.20 equiv) were then added and diluted to a 0.5 M toluene solution. The reaction was stirred at room temperature for 24 h. The enantiomer shown is the product for (S)-VAPOL. (R)-VANOL results in the opposite enantiomer.

ND represents Not Determined. [b] Cyclohexanol and phenol are represented by CyOH and PhOH respectively. [c] Conversion was determined from the ^{1}H NMR spectrum of the crude reaction mixture using an internal standard ($CHPh_3$). [d] Isolated yield after column chromatography. [e] Determined by HPLC on a Chiralcel OD-H column. [f] Determined from the ^{1}H-NMR spectrum of the crude reaction mixture. [g] No benzoic acid was added. [h] Catalyst loading was lowered to 5 mol%: 5 mol% ligand, 15 mol% borane, 15 mol% water, 10 mol% phenol, and 2.5 mol% benzoic acid was used to generate the catalyst in step 1.

The one pot multi-component method was then expanded to the synthesis of aliphatic aziridines (Table 3.7). This resulted in moderate yields and ee's (entries 1 and 2, Table 3.7). However, VAPOL gave a higher conversion of 96% than that of VANOL's 80% conversion.

Table 3.7 Aliphatic aziridine **10b** synthesized via the one pot multi-component AZ reaction

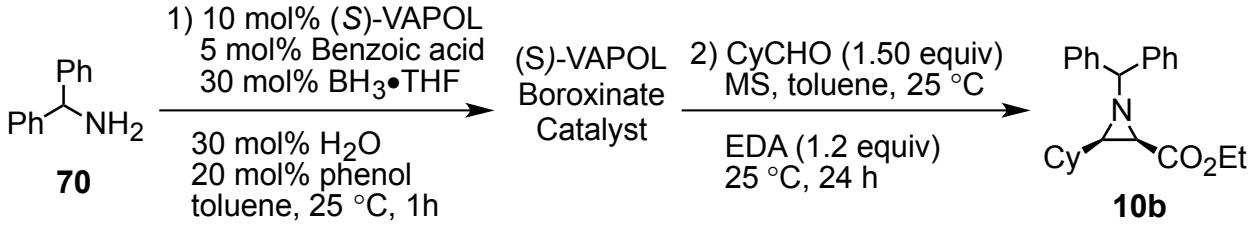

Entry	Conversion (%) [b]	Yield **10b** (%) [c]	ee **10b** (%) [d]	cis/trans [e]
1	96	71 [f]	80	ND
2 [g]	80	78	79	ND

[a] Unless otherwise stated, the catalyst was prepared by mixing (*S*)-VAPOL (0.10 equiv), borane (0.30 equiv), water (0.30 equiv), phenol (0.20 equiv), 5 mol% benzoic acid, and amine (1.00 equiv) in a 1.0 M solution in amine in toluene at room temperature for 1 h. Flame-dried 4Å powder molecular sieves, cyclohexylcarbaldehyde (1.50 equiv), and EDA (1.20 equiv) were then added and diluted to a 0.5 M solution in toluene. The reaction was stirred at room temperature for 24 h. The enantiomer shown is the product for (S)-VAPOL. (R)-VANOL results in the opposite enantiomer. ND represents Not Determined. [b] Conversion was determined from the ^{1}H NMR spectrum on the crude reaction mixture using an internal standard ($CHPh_3$). [c] Isolated yield after column chromatography. [d] Determined by HPLC on a Chiralcel OD-H column. [e] Could not be determined from the ^{1}H NMR spcectrum of the crude reaction mixture due to peak overlap. [f] Purification by column chromatography on silica gel twice was required to isolate the pure aziridine. [g] (*R*)-VANOL was used as the ligand.

3.4 Attempted reductive ring opening of aliphatic aziridines

It has been known that Pearlman's catalyst ($Pd(OH)_2$) can cleave benzhydryl groups from amines.[45] A previous group member Dr. Zhenjie Lu was able to deprotect alkyl substituted aziridines using this methodology.[46] However, when attempting to deprotect aromatic substituted aziridines, reductive ring opening occurred giving alpha amino

esters. Here, attempts to do reductive ring opening of aliphatic aziridines will be discussed.

The first attempt to open the aziridine ring began with the ester substituted aliphatic aziridine **10b**. A methodology was developed by Nimmagadda and McRae to convert aldehydes, ketones and primary, secondary and tertiary alcohols into their corresponding alkanes using $HSi(Et)_3$ and $B(C_6F_5)_3$.[47] This methodology was used in an attempt to reductively open the cis-aziridine **10b**. However, no reaction was observed (Scheme 3.5).

Scheme 3.5 Attempts at reductive ring opening of ester substituted aliphatic aziridine **10b**

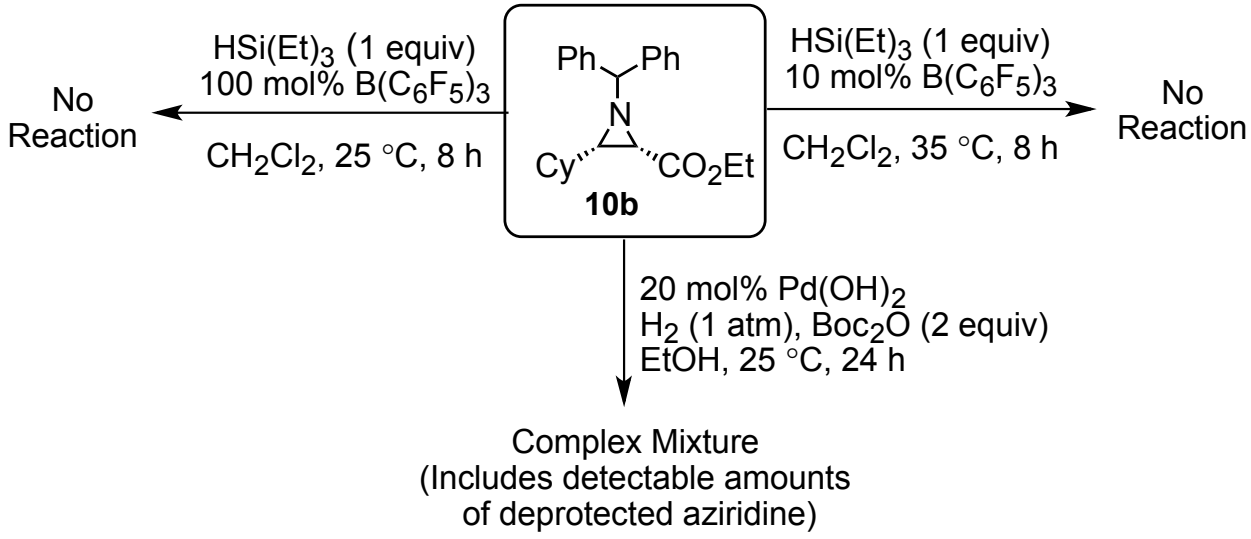

Also, an attempt to open the ring of the ester substituted aliphatic aziridine **10b** with a higher amount of Pearlman's catalyst in the presence of hydrogen gas and Boc_2O was tried. The aspiration of this method was that the aziridine **10b** would be deprotected, reprotected with Boc and finally cleaved open. However, a complex mixture arose, which included deprotected aziridine (Scheme 3.5).

When attempts to open the ester substituted aziridine failed, the ester was then transformed into other moieties that would incorporate stronger hydrogen bonding capabilities. This included changing the ester group to either an alcohol or carboxylic acid (Scheme 3.6).

Scheme 3.6 Synthesis of aziridine derivatives derived from aziridine **10b**

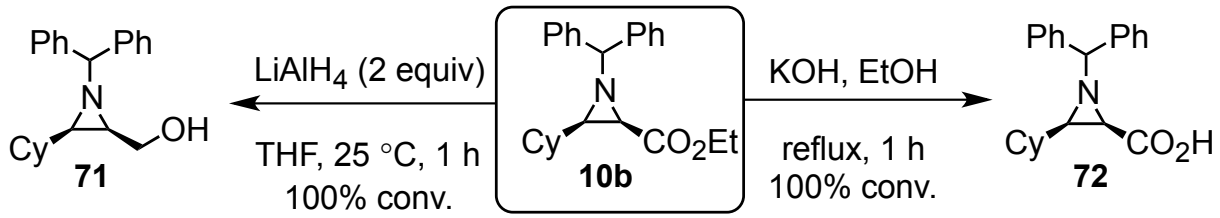

When reacting aziridine **71** with Pearlman's catalyst in the presence of hydrogen gas, the deprotection of the benzhydryl group resulted with the formation of the aziridine **73**. When repeating the reaction with Boc_2O, the reaction gave a complex mixture (Scheme 3.7).

Scheme 3.7 Attempted reductive ring opening of aziridine **71**

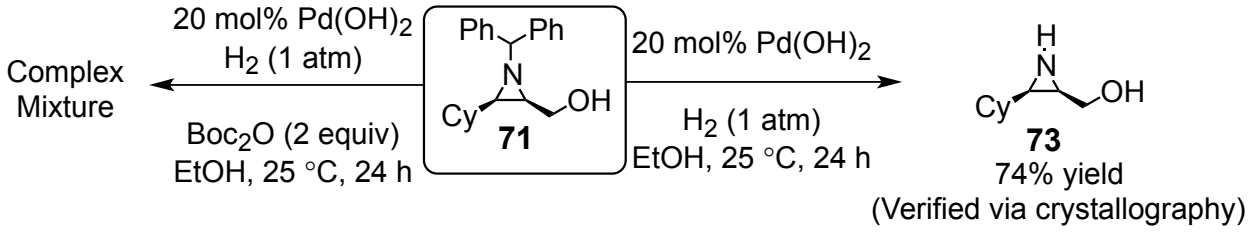

The final method attempted to perform reductive ring opening on an aliphatic aziridine starting from the acid substituted aziridine **72** was a modified procedure that was previously used to reductively open tri-substituted aromatic aziridines to alpha amino esters.[16e] Unfortunately, this reaction resulted in no reaction and starting material was recovered (Scheme 3.8).

Scheme 3.8 Attempted reductive ring opening of aziridine **72**

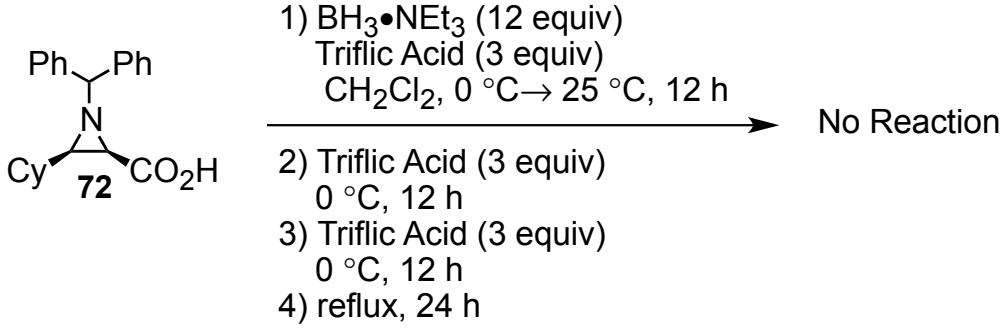

3.5 Conclusion

A methodology to generate aliphatic and aromatic cis-aziridines was developed, which uses a one pot multi-component aziridination reaction. This method proceeded to give high conversion rates when using benzoic acid as a co-catalyst. When using the VAPOL ligand to generate the boroxinate catalyst, cis-aziridines were obtained in moderate to high yields and high ee's for aromatic aziridines and moderate yields and ee's for aliphatic aziridines. Unfortunately, VANOL boroxinate catalysts do not work well with this methodology giving incomplete conversions.

Also, an attempt to develop a method for the reductive ring opening of aliphatic aziridines was undertaken to no avail. Unfortunately, all methods attempted resulted in either no reaction, complex mixtures, or deprotected aziridines. Further pursuits could be made in the future in this area of research by altering the protecting group on the aziridine to a unit such as α-methyl benzyl.

CHAPTER FOUR

BORATE COMPLEXES OF BINOL AND THE LARGE SCALE SYNTHESIS OF THE VANOL MONOMER VIA THE CAEC REACTION

4.1 Introduction

As discussed in chapter one, linear and vaulted biaryl ligands are very important in asymmetric catalysis. Within this chapter, both types of ligands will be studied for different purposes. Firstly, the linear ligand BINOL **1** will be used to synthesize various borate complexes derived from either triphenyl borate or borane-tetrahydrofuran complex using various solvents and ratios of reagents. NMR studies, including proton and boron NMR, were performed in order to aid in the identification of these BINOL derivatives, which include both 3-coordinate and 4-coordinate borate species.

Additionally to be discussed within this chapter are the vaulted biaryl ligands VANOL **2** and VAPOL **3**. The cycloaddition electrocyclization cascade (CAEC) reaction will be discussed with the focus being the large-scale synthesis of the VANOL monomer. The CAEC reaction is both cost effective and efficient when used to synthesize the VANOL monomer. Therefore, a large-scale synthesis of the VANOL monomer was performed using the CAEC reaction. Lastly to be discussed within this chapter is a time study that was performed on both the VANOL and VAPOL ligands to determine the stability and shelf life under various storage conditions.

4.2 BINOL-borate complexes

In 1992, Yamamoto and Hattori published an asymmetric aza Diels-Alder reaction mediated by a chiral borate species. [48] This borate compound was reported to be a B1 species synthesized by mixing a 1:1 molar ratio of BINOL and $B(OPh)_3$ at room

temperature in methylene chloride for 1 h. This chiral Lewis acid (Figure 4.1) was used to catalyze the aza-Diels-Alder reaction between aldimines and Danishefsky's diene.[48] However, no spectroscopic data was reported to support the structure of B1.

Figure 4.1 A multitude of borate species derived from BINOL **1**

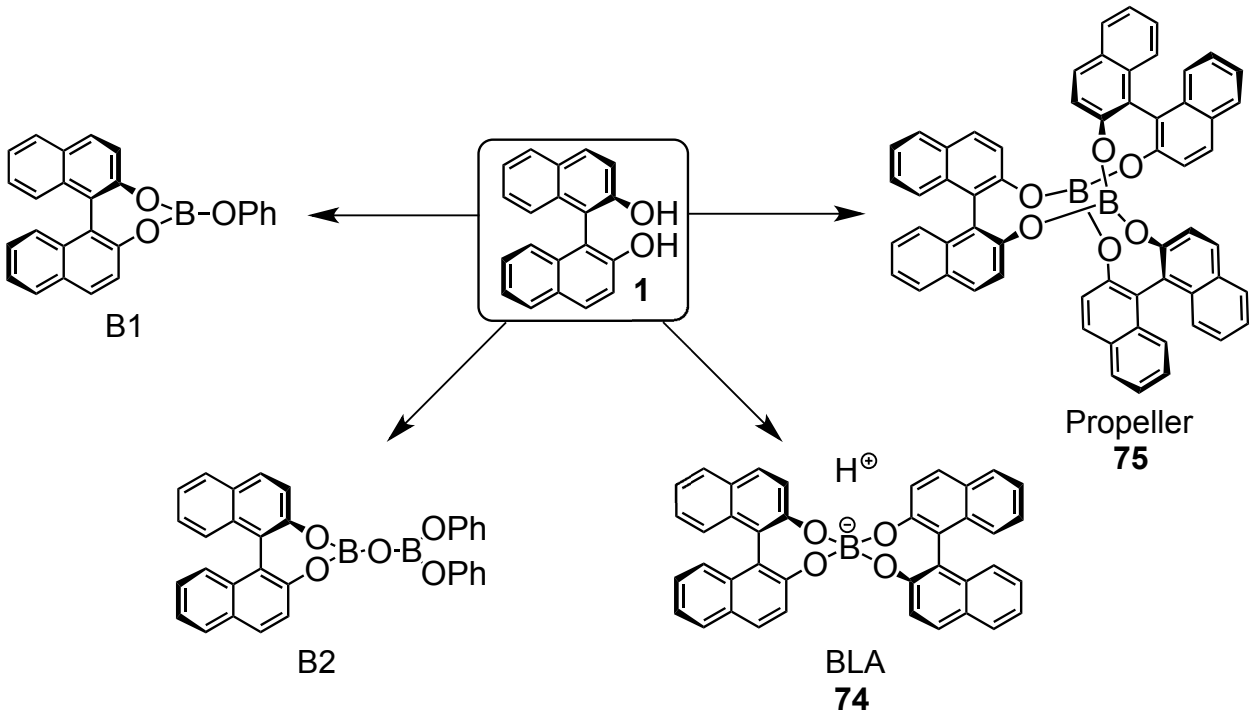

Two years later, Yamamoto et al. reported a second borate species BLA **74**, which incorporated a 2:1 molar ratio of BINOL and triaryl borate to form a tetra-coordinated borate species acting as a Brønsted acid-assisted chiral Lewis acid (BLA) (Figure 4.1).[49] This newly found BLA was employed in both the asymmetric aza Diels-Alder and Aldol-type reactions of imines.[50] Aside from B1 and BLA, other common borate species that can be formed from boranes or borates and BINOL are B2 and Kaufmann's propeller[51] (Figure 4.1).

It was claimed in Yamamoto's paper that BLA was crystallized. However, no spectroscopic data was mentioned aside from optical rotation, molecular weight determined by mass spectrometric and cryoscopic methods and elemental analysis.

It was discovered that when using our own ligands, VANOL and VAPOL, both B1 and B2 species can be generated.[16h] Therefore, BINOL was investigated to determine if similar species were being formed as well.

4.2.1 BINOL-borate complexes generated in deuterated methylene chloride

To begin, Yamamoto's procedures were repeated. Both 1:1 and 2:1 molar ratios of BINOL and $B(OPh)_3$ in methylene chloride were examined to determine if B1 and B2 complexes would form. The mixtures were evaluated by both ^1H NMR (Figure 4.2) and ^{11}B NMR analysis (Figure 4.3). The first spectrum in black represents the free BINOL species in deuterated methylene chloride (entry 1, Figure 4.2). The next two spectra are a mixture of either a 1:1 or 2:1 ratio of BINOL with $B(OPh)_3$ in the presence of molecular sieves at room temperature for one hour. The mixtures were generated with the aspiration of forming B1 and B2 complexes (entry 2 and 3). There is a significant amount of BINOL in both spectra with small peaks appearing in the B1 and B2 region (6.0-6.5 ppm). Unfortunately, both spectra do not appear to form any clear product while the major species observed was BINOL. However, upon addition of one equivalent of imine **8a**, a new species was formed (entries 4 and 5, Figure 4.2). In the presence of imine **8a**, BINOL was assembled into the BLA-imine complex **74a**.

To verify the BLA-imine complex being assembled, the boron NMR was obtained (Figure 4.3). Spectra 1 and 2 were taken prior to imine addition with both a 1:1 and 2:1

ratio of BINOL and $B(OPh)_3$ respectively. It was observed that no BLA-imine complex was being formed (entries 1 and 2).

Figure 4.2 Synthesis of BINOL-borate complexes following Yamamoto's protocol [a]

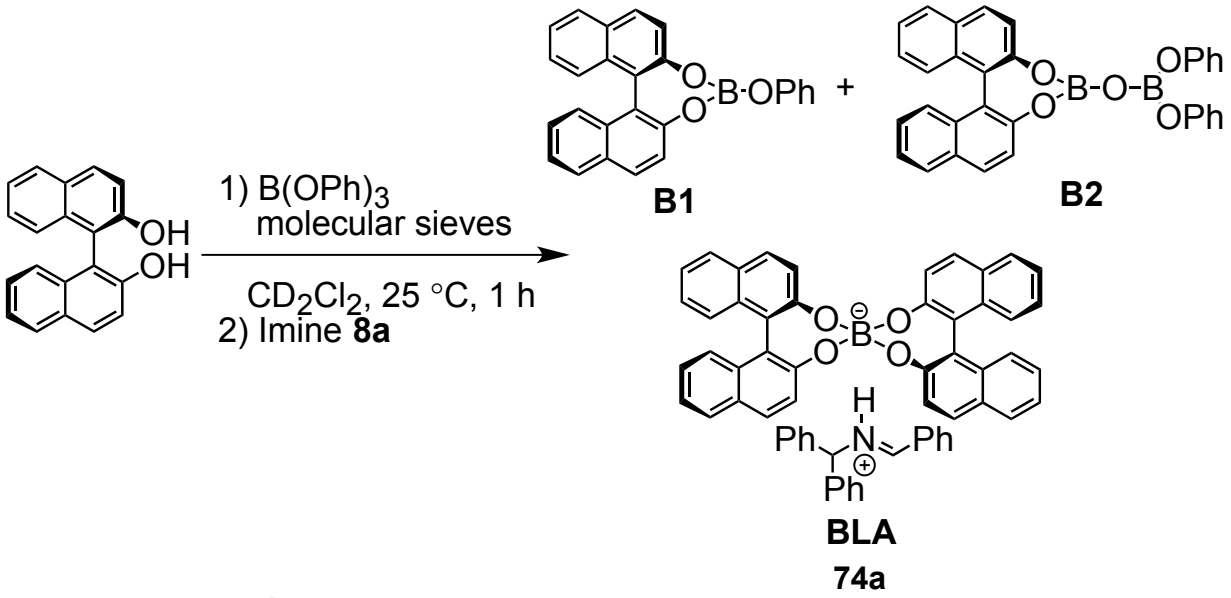

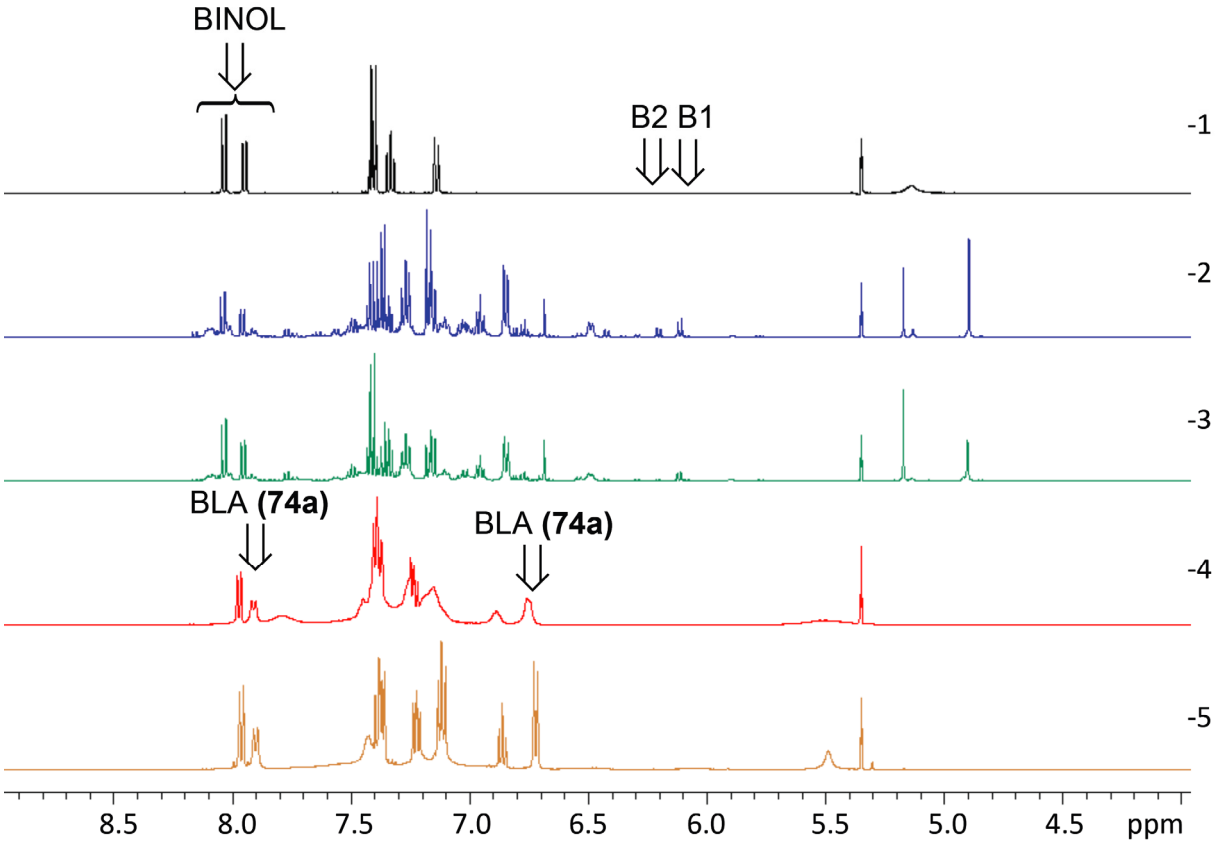

[a] All spectra were taken in CD_2Cl_2: (1) BINOL; (2) BINOL and $B(OPh)_3$ (1:1) with molecular sieves stirred at rt for 1 h (Yamamoto's procedure); (3) BINOL and $B(OPh)_3$ (2:1) with molecular sieves stirred at rt for 1 h (Yamamoto's procedure); (4) BINOL, $B(OPh)_3$ and imine **8a** (1:1:1) with molecular sieves; same NMR tube as entry 2 with imine added; (5) BINOL, $B(OPh)_3$ and imine **8a** (2:1:1) with molecular sieves; same NMR tube as entry 3 with imine added.

Figure 4.3 Boron NMR for BINOL-borate complexes seen in Figure 4.2 [a]

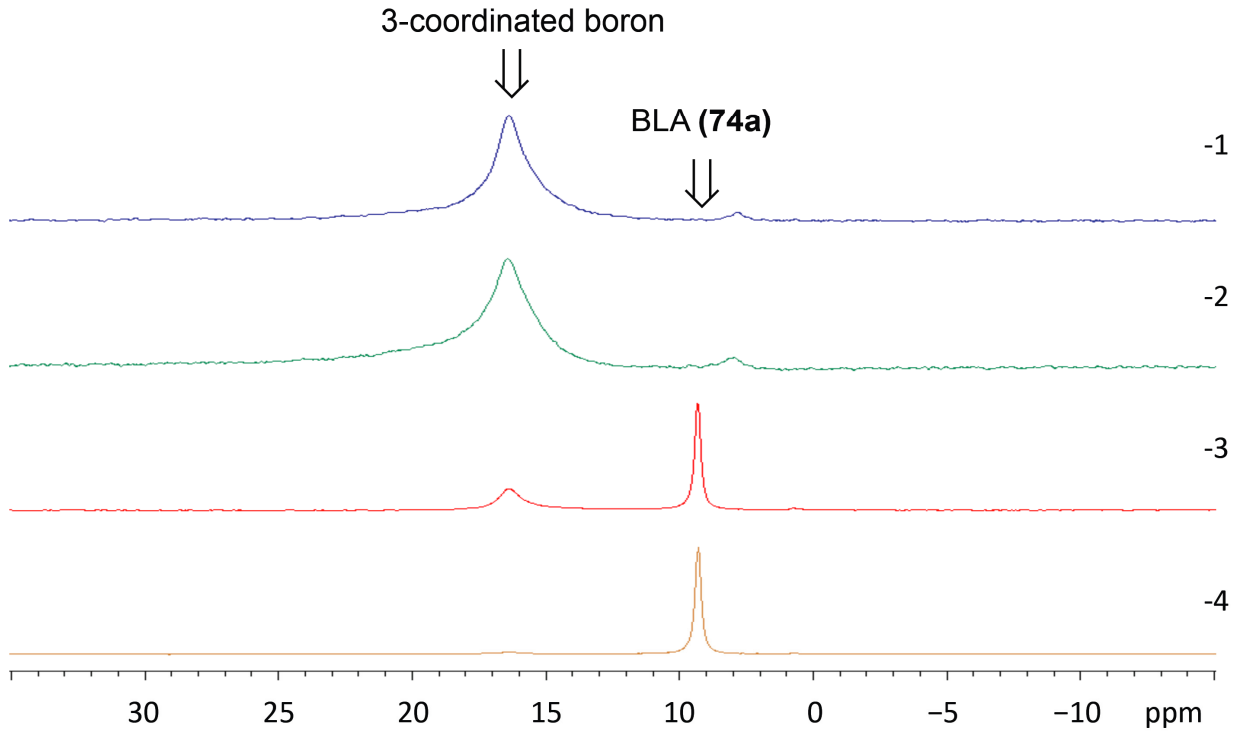

[a] All spectra were taken in CD_2Cl_2. Colors correspond to ^1H NMR's shown in Figure 4.2: (1) BINOL and $B(OPh)_3$ (1:1) with molecular sieves stirred at rt for 1 h (Yamamoto's procedure); (2) BINOL and $B(OPh)_3$ (2:1) with molecular sieves stirred at rt for 1 h

(Yamamoto's procedure); (3) BINOL, $B(OPh)_3$ and imine **8a** (1:1:1) with molecular sieves; same NMR tube as entry 1 with imine added; (4) BINOL, $B(OPh)_3$ and imine **8a** (2:1:1) with molecular sieves; same NMR tube as entry 2 with imine added.

The major peak for both spectra was at 16.5 ppm, which corresponds to the tri-coordinated borate species. However, when adding one equivalent of imine **8a** to the NMR tube and gently shaking, the BLA-imine complex **74a** appeared at 9-10 ppm for both the 1:1 and 2:1 mixture of BINOL and triphenyl borate (entries 3 and 4, Figure 4.3).

The only difference between the two entries was that with the 1:1 ratio, there still existed some tri-coordinated borate species, which appeared as a small peak at 16.5 ppm (entry 3, Figure 4.3). Alternately, with the 2:1 ratio, all of the tri-coordinated borate species appearing at approximately 16-17 ppm was transformed to the tetra-coordinated BLA-imine complex **74a**, which appears at 9-10 ppm in the boron spectrum (entry 4).

In summary, very little B1 or B2 species was generated following Yamamoto's procedure. However, a significant amount of BLA-imine complex **74a** can self assemble when in the presence of an imine.

4.2.2 BINOL-borate complexes generated in deuterated chloroform

4.2.2.1 Generation of BINOL-borate complexes using triphenyl borate

Similar procedures to Yamamoto's protocol were then applied using deuterated chloroform as the reaction solvent, which were evaluated by proton and boron NMR (Figure 4.4 and Figure 4.5). Deuterated chloroform was used as a solvent in order to compare spectra previously obtained in the Wulff group to protocols developed by Yamamoto using methylene chloride. The first spectrum in black shows free BINOL in

$CDCl_3$ (entry 1, Figure 4.4). When mixing BINOL with triphenyl borate in a 1:1 ratio, interesting results were obtained based upon the amount of water in the reaction. When doing the reaction without molecular sieves, B2 was formed in 44% yield, which appears as a doublet at 6.2 ppm (entry 2). However, when adding molecular sieves to the reaction, only trace amounts of B2 (6%) were observed with the major species present being BINOL (37%) (entry 3). These results can be explained due to the trace amounts of water present in the absence of molecular sieves, which promote the B2 formation. The origin of water is presumably the triphenyl borate.

Figure 4.4 BINOL-borate complexes synthesized using $CDCl_3$ as the solvent [a]

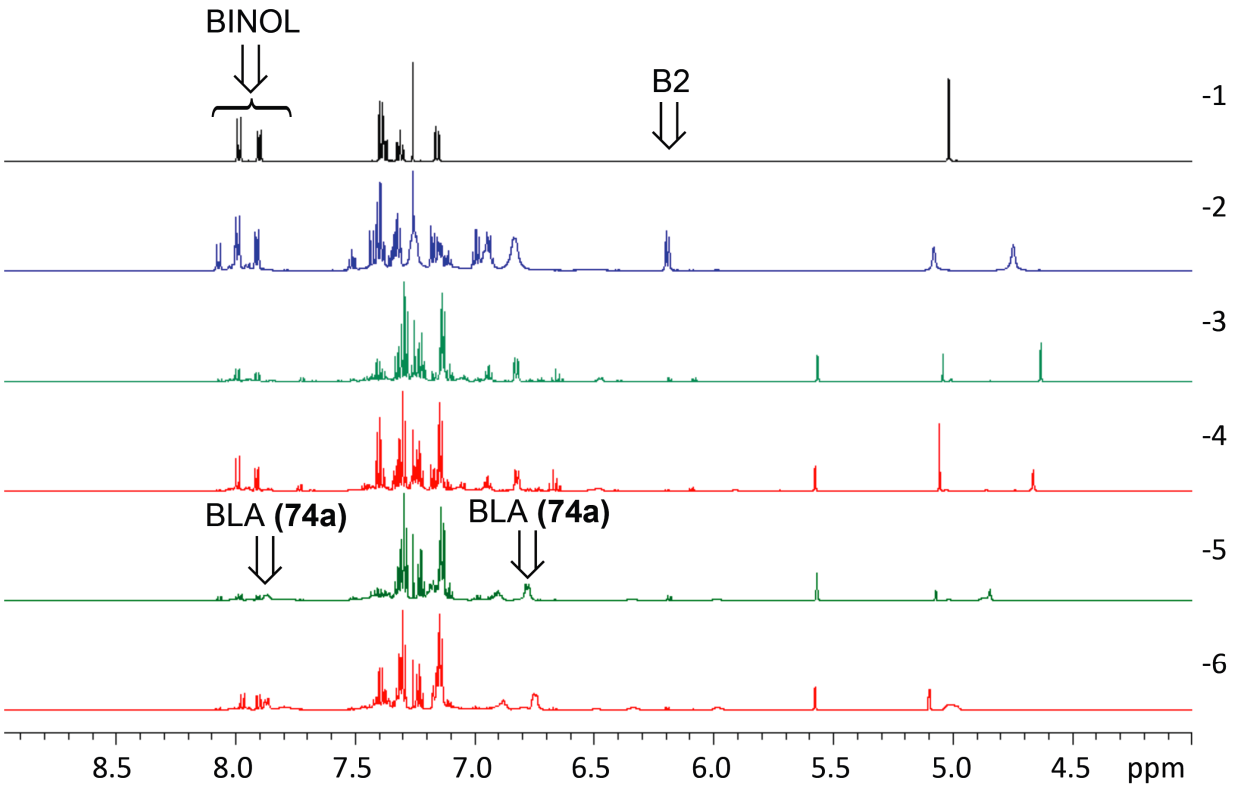

[a] All spectra were taken in $CDCl_3$: (1) BINOL; (2) BINOL and $B(OPh)_3$ (1:1); (3) BINOL and $B(OPh)_3$ (1:1) with molecular sieves (internal standard $CHPh_3$); (4) BINOL and

$B(OPh)_3$ (2:1) with molecular sieves (internal standard $CHPh_3$); (5) BINOL, $B(OPh)_3$, and imine **8a** (1:1:1) with molecular sieves (internal standard $CHPh_3$); same NMR tube as entry 3 with imine added; (6) BINOL, $B(OPh)_3$, and imine **8a** (2:1:1) with molecular sieves (internal standard $CHPh_3$); same NMR tube as entry 4 with imine added.

Figure 4.5 Boron NMR for BINOL-borate complexes seen in Figure 4.4 [a]

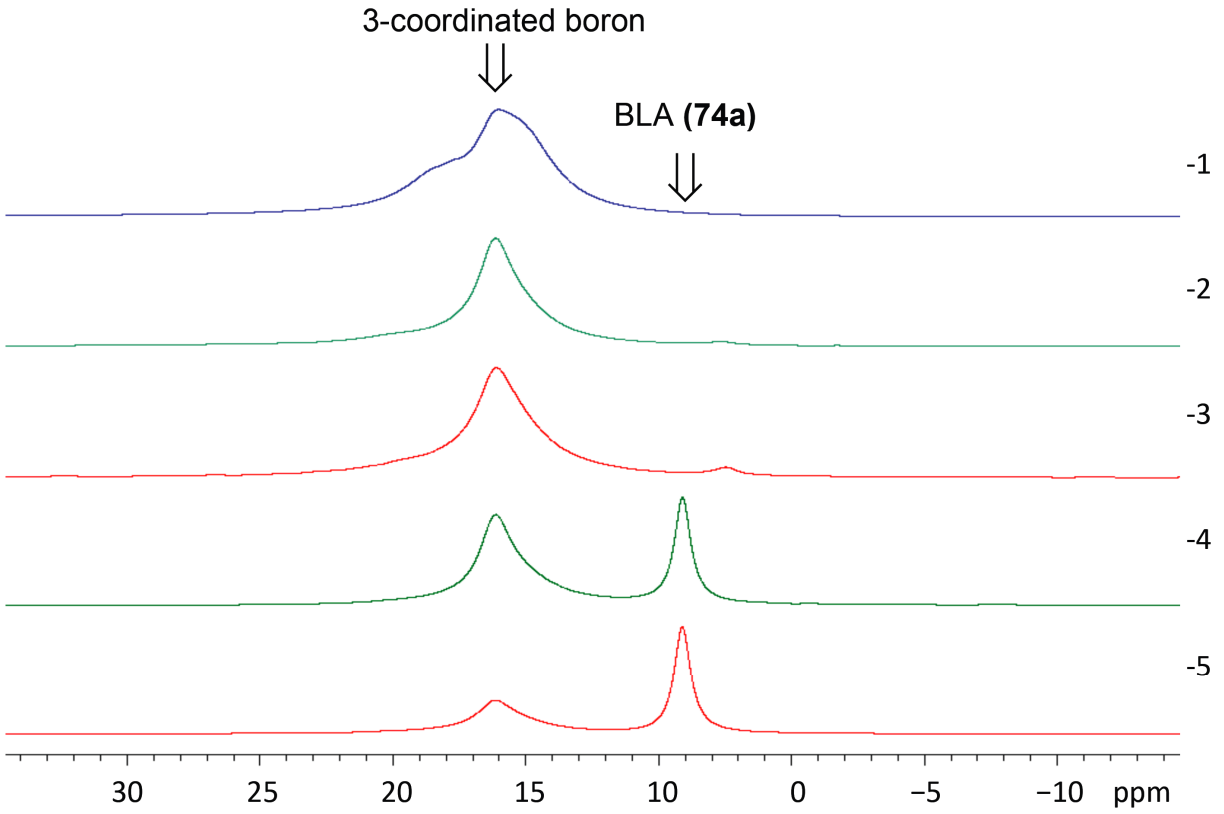

[a] All spectra were taken in $CDCl_3$. Colors correspond to ^1H NMR's shown in Figure 4.4: (1) BINOL and $B(OPh)_3$ (1:1); (2) BINOL and $B(OPh)_3$ (1:1) with molecular sieves (internal standard $CHPh_3$); (3) BINOL and $B(OPh)_3$ (2:1) with molecular sieves (internal standard $CHPh_3$); (4) BINOL, $B(OPh)_3$, and imine **8a** (1:1:1) with molecular sieves

(internal standard $CHPh_3$); same NMR tube as entry 2 (5) BINOL, $B(OPh)_3$, and imine **8a** (2:1:1) with molecular sieves (internal standard $CHPh_3$); same NMR tube as entry 3.

When the ratio of BINOL and triphenyl borate was changed to 2:1, a complex mixture formed with BINOL still present in 47% yield (entry 4, Figure 4.4). Entries 5 and 6 include imine **8a** in the reaction mixture. This results in the generation of the BLA-imine complex **74a** in 75% yield for entry 5 and 94% yield for entry 6. However, the peaks are broad, which causes the calculation of the yields to be less accurate (yields were calculated via ^1H NMR using Ph_3CH as an internal standard).

The boron NMR in Figure 4.5 corresponds to the proton NMR in Figure 4.4. The peaks support the prior assignments made in the proton NMR. The first three entries lack imine and therefore only have tri-coordinated borate species (entries 1, 2 and 3, Figure 4.5). Entry 1 appears unsymmetrical due to the large amount of B2 generated, which incorporates two boron molecules that are asymmetric to one another. However, once imine **8a** is added, the BLA-imine complex is formed, which is seen at 9-10 ppm in the boron NMR (entries 4 and 5).

4.2.2.2 Generation of BINOL-borate complexes using borane tetrahydrofuran

After failure to make B1 in a decent yield using Yamamoto's procedure, a new procedure was sought after. In 1986, Kelly et al. published a procedure to make a chiral Lewis acid by mixing 3,3'-BINOL derivatives, acetic acid, BH_3•THF, and juglone **77** (Scheme 4.1).[43]

Scheme 4.1 Kelly's Lewis acid system Ph

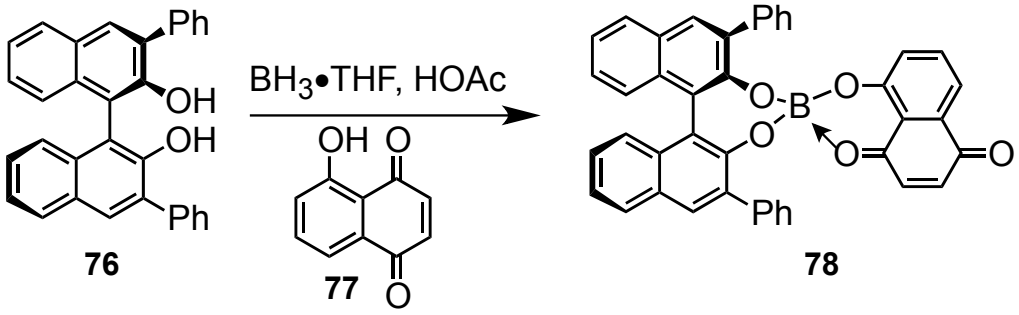

The interesting aspect of this protocol was that an initial borane or borate species was generated prior to the addition of juglone **77** by mixing the BINOL derivative with BH_3•THF and acetic acid.

Figure 4.6 BINOL-borate complexes generated following Kelly's protocol [a]

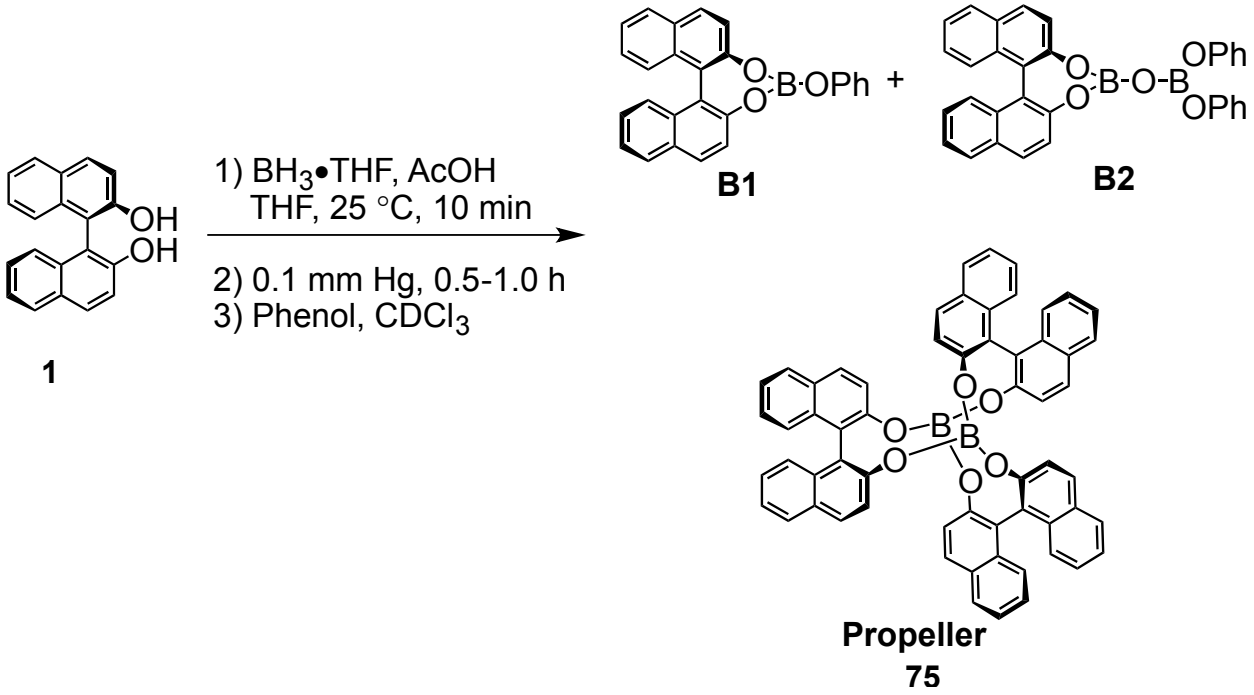

Figure 4.6 (Cont'd)

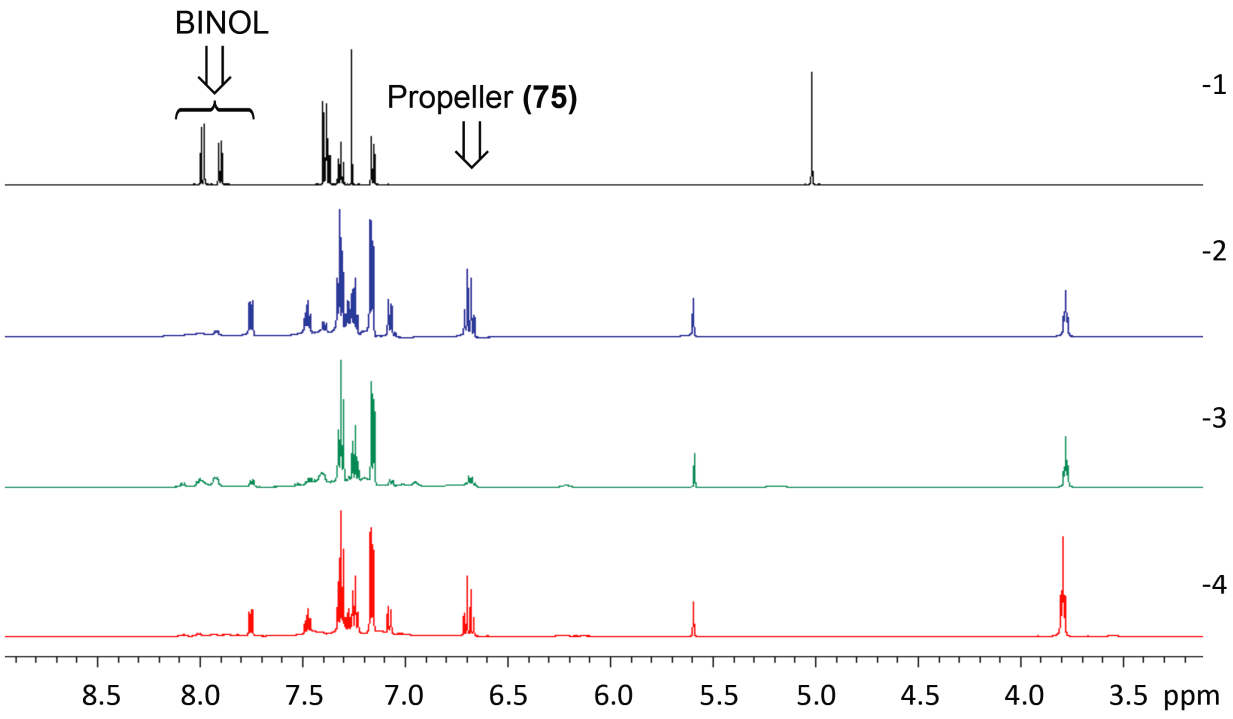

[a] (1) BINOL in $CDCl_3$; (2) BINOL, BH_3•THF, and AcOH (1:1:1) stirred in THF at rt for 10 minutes followed by removal of volatiles with vacuum for 1 h (0.1 mm Hg) and then dissolving in $CDCl_3$; (3) BINOL, BH_3•THF, and AcOH (1:1:1) stirred in THF at rt for 10 minutes followed by removal of volatiles with vacuum for 30 minutes (0.1 mmHg) and then addition of phenol (1 equiv) and dissolving solids in $CDCl_3$; (4) BINOL, BH_3•THF, and AcOH (1:2:2) stirred in THF at rt for 10 minutes followed by removal of volatiles with vacuum for 30 minutes (0.1 mmHg) and then addition of phenol (1.00 equiv) and dissolving solids in $CDCl_3$.

It was suggested that acetic acid accelerates the otherwise very slow reaction between the BINOL derivative and BH_3•THF.[44] We repeated Kelly's procedure in the

absence of juglone to see if B1 could be generated. The reaction was monitored by proton and boron NMR (Figure 4.6 and Figure 4.7). The first spectrum in black represents the free BINOL in $CDCl_3$ (entry 1, Figure 4.6). When mixing a 1:1:1 ratio of BINOL, BH_3•THF, and acetic acid followed by the removal of volatiles via vacuum (0.1 mm Hg) resulted in generating Kaufmann's propeller **75** in 94% yield (entry 2). Once phenol was added to the reaction mixture, the propeller **75** begins to dis-assemble and decreases from 94% (entry 2) to 21% (entry 3).

When changing the ratio to 1:2:2 of BINOL, BH_3•THF, and acetic acid in the presence of phenol (1.00 equiv), the propeller **75** still formed in 84% yield. However, a second species was observed in the boron NMR at 2 ppm (entry 3, Figure 4.7).

Figure 4.7 Boron NMR of BINOL-borate complexes seen in Figure 4.6 [a]

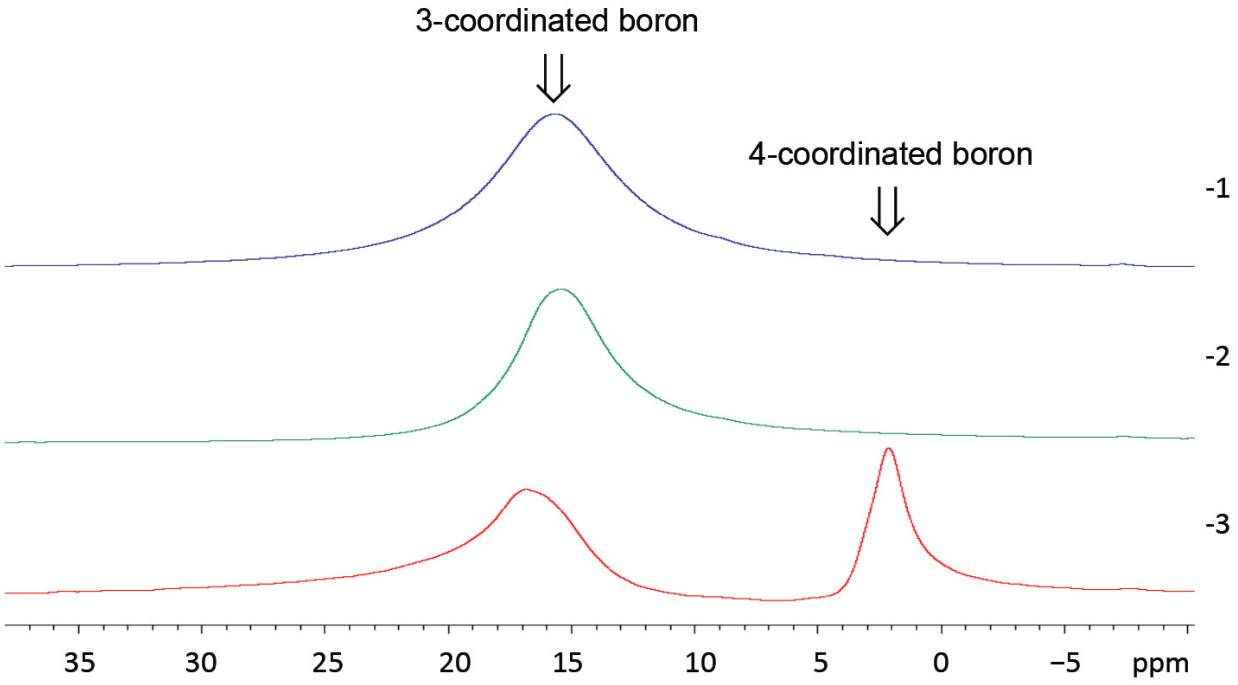

[a] Colors correspond to ^{1}H NMR's shown in Figure 4.6: (1) BINOL, BH_3•THF, and AcOH (1:1:1) stirred in THF at rt for 10 minutes followed by removal of volatiles with vacuum for 1 h (0.1 mmHg) and then dissolving in $CDCl_3$; (2) BINOL, BH_3•THF, and AcOH (1:1:1) stirred in THF at rt for 10 minutes followed by removal of volatiles with vacuum for 30 minutes (0.1 mm Hg) and then addition of phenol (1 equiv) and dissolving solids in $CDCl_3$; (3) BINOL, BH_3•THF, and AcOH (1:2:2) stirred in THF at rt for 10 minutes followed by removal of volatiles with vacuum for 30 minutes (0.1 mmHg) and then addition of phenol (1.00 equiv) and dissolving solids in $CDCl_3$.

There are several possible species that could be in this region. Brown et al. did extensive work on boron and borate species and found that tripivaloxyborane [$B(O_2CC(CH_3)_3)$] comes at 1.5 ppm in the boron NMR.[52] This shift is most likely explained due to the coordination of one of the carbonyls bound to the borate species creating a tetra-coordinated boron. A similar occurrence may be happening here where any number of possible borate species could acquire an acetate group allowing a carbonyl oxygen to coordinate to the boron and shifting the boron peak to 2 ppm due to the boron being tetra-coordinated.

In summary, we were unable to generate a significant amount of B1 when using a modified version of Kelly's protocol. A primary species observed was Kaufmann's propeller **75**. When phenol was added to the reaction, a complex mixture developed that included Kaufmann's propeller **75**, free BINOL **1**, trace amounts of B1 and B2, and in one case an unidentified tetra-coordinated borate species.

4.2.3 BINOL-borate complexes generated in deuterated DMSO

The third solvent employed in the study of BINOL-borate complexes was deuterated DMSO.

Figure 4.8 BINOL-borate complexes generated when using DMSO [a]

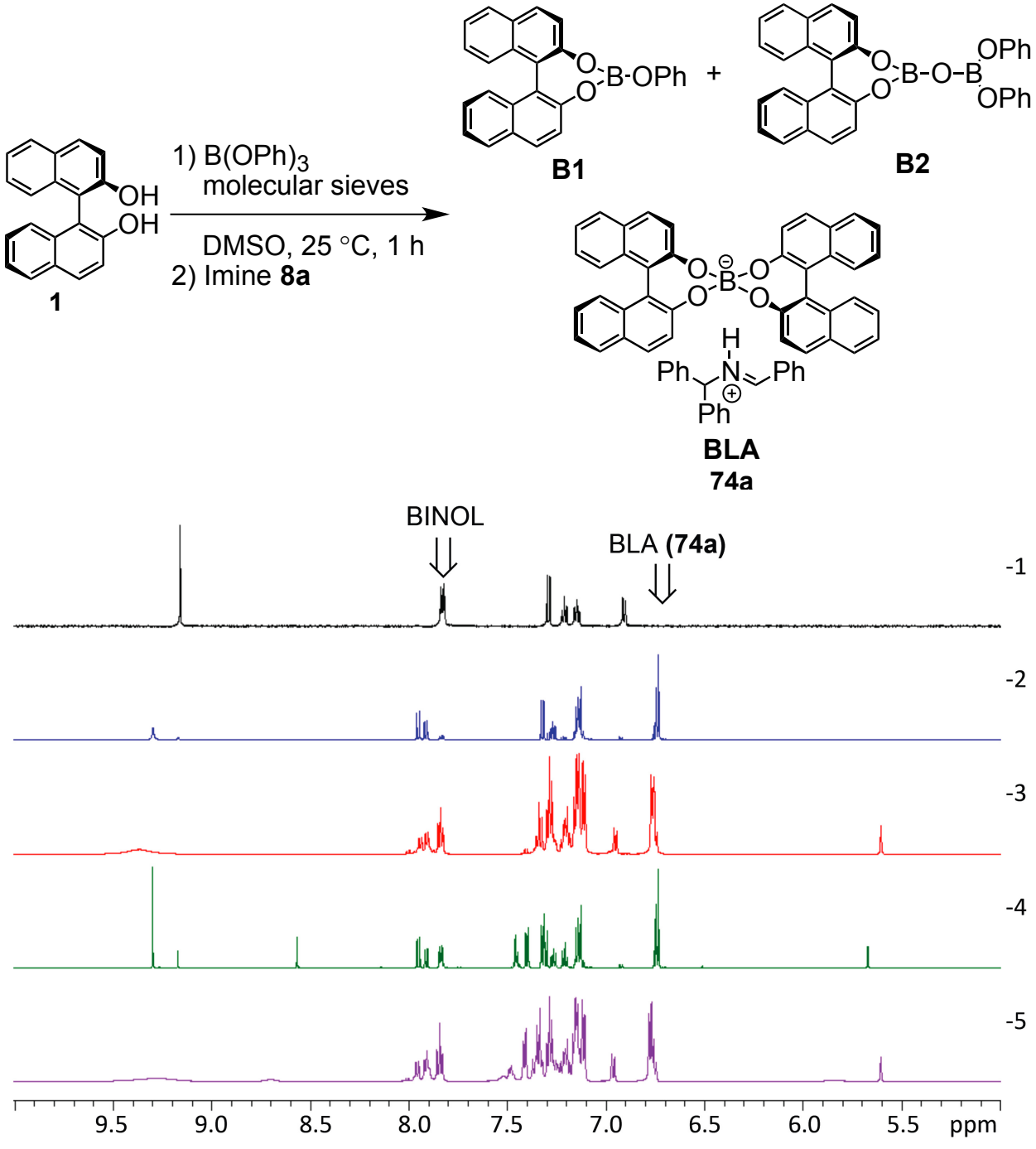

[a] All spectra were taken in deuterated DMSO: (1) BINOL; (2) BINOL and $B(OPh)_3$ (2:1) in the presence of molecular sieves; (3) BINOL and $B(OPh)_3$ (2:1) without molecular sieves (internal standard $CHPh_3$); (4) BINOL, $B(OPh)_3$, and imine **8a** (2:1:1) in the presence of molecular sieves; (5) BINOL, $B(OPh)_3$, and imine **8a** (2:1:1) without molecular sieves (internal standard $CHPh_3$).

Figure 4.9 Boron NMR for BINOL-borate complexes seen in Figure 4.8 [a]

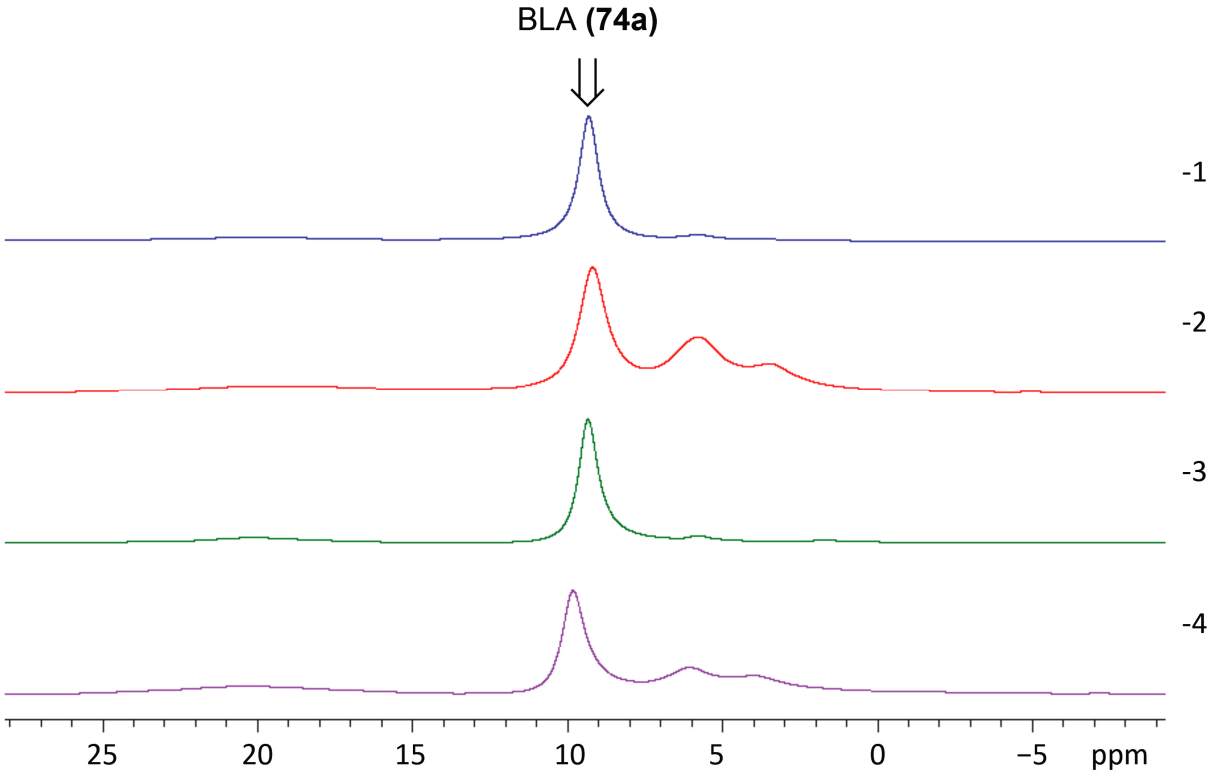

[a] All spectra were taken in deuterated DMSO. Colors correspond to ^1H NMR's shown in Figure 4.8: (1) BINOL and $B(OPh)_3$ (2:1) in the presence of molecular sieves; (2) BINOL and $B(OPh)_3$ (2:1) without molecular sieves (internal standard $CHPh_3$); (3) BINOL,

$B(OPh)_3$, and imine **8a** (2:1:1) in the presence of molecular sieves; (4) BINOL, $B(OPh)_3$, and imine **8a** (2:1:1) without molecular sieves (internal standard $CHPh_3$).

The same ratios were applied here following a similar procedure to Yamamoto's protocol seen in the previous sections. Interesting results were obtained when using DMSO to generate these BINOL-borate species, which were observed via proton and boron NMR (Figure 4.8 and 4.9). The first spectrum in black represents free BINOL in DMSO (entry 1, Figure 4.8). When mixing BINOL and $B(OPh)_3$ both with and without molecular sieves, the BINOL was transformed into BLA in 56% and 72% yields (entries 2 and 3, respectively, Figure 4.8). This was unique because there is no imine to act as a protonated Brønsted base. Therefore, DMSO is capable of coordinating somehow in order to assemble BLA. After addition of imine **8a**, BLA still remained the primary species in 55% and 66% yields (entries 4 and 5, respectively). The boron NMR supports this observation of BLA with a large peak at 9-10 ppm in all spectra (entries 1-4, Figure 4.9). Further attempts are being made in order to identify this newly discovered BLA-DMSO complex.

A subsequent study was performed using deuterated chloroform as the solvent and adding various amounts of DMSO to the NMR tube in order to monitor the amount of DMSO required to generate this DMSO-BLA species (Figures 4.10 and 4.11). When increasing the amount of DMSO, the amount of DMSO-BLA complex increased as shown in Figure 4.10: with no DMSO there was 0% BLA (entry 2), 1 equivalent of DMSO gave 80% BLA (entry 3), 2 equivalents of DMSO gave 89% BLA (entry 4), 5 equivalents of DMSO gave 110% BLA (entry 5), and 10 equivalents of DMSO gave 95%

of BLA (entry 6). These values were calculated using $CHPh_3$ as an internal standard and are not very accurate due to peak overlap in the ^1H NMR.

Figure 4.10 DMSO-BLA complex formed using various amounts of DMSO [a]

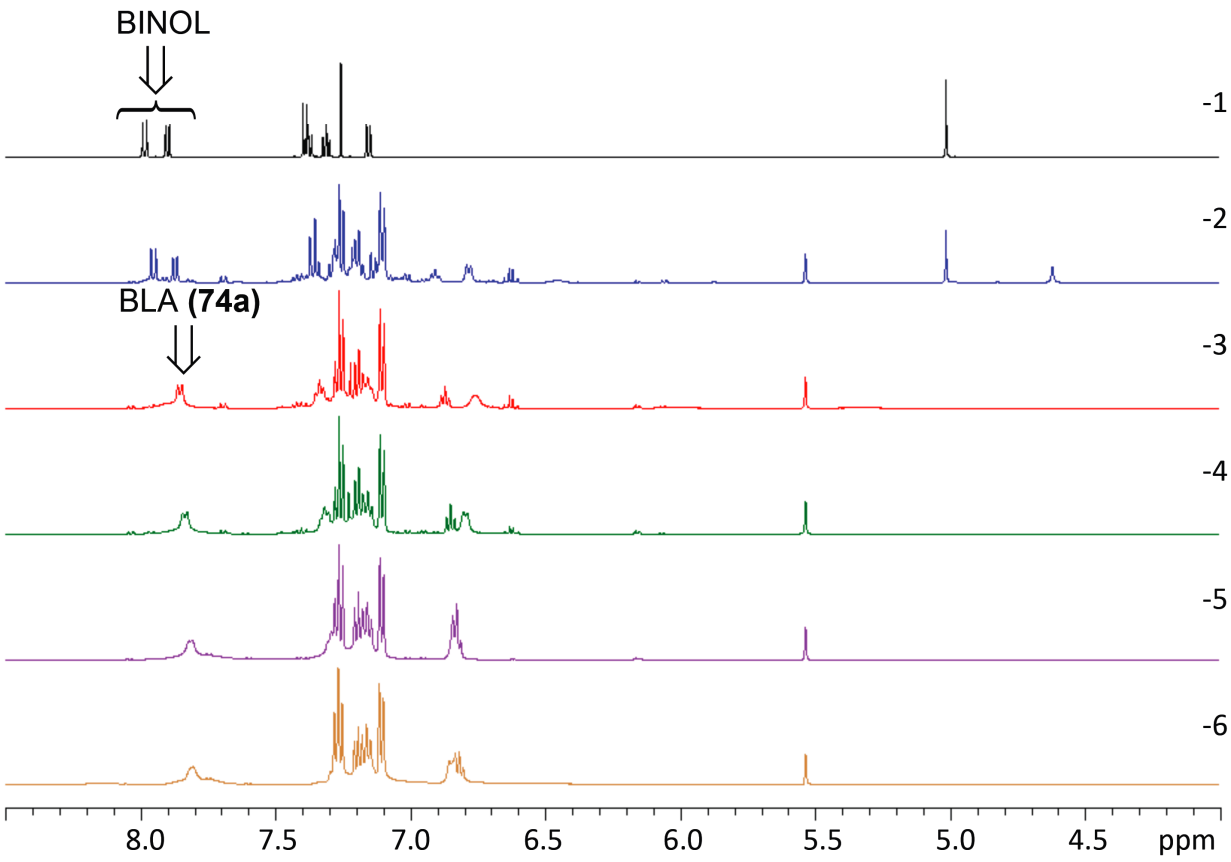

[a] All spectra were taken in $CDCl_3$. (1) BINOL; (2) BINOL and $B(OPh)_3$ (2:1) in the presence of molecular sieves (internal standard $CHPh_3$); (3) BINOL, $B(OPh)_3$, and DMSO (2:1:1) in the presence of molecular sieves (internal standard $CHPh_3$); (4) BINOL, $B(OPh)_3$, and DMSO (2:1:2) in the presence of molecular sieves (internal standard $CHPh_3$); (5) BINOL, $B(OPh)_3$, and DMSO (2:1:5) in the presence of molecular

sieves (internal standard $CHPh_3$); (6) BINOL, $B(OPh)_3$, and DMSO (2:1:10) in the presence of molecular sieves (internal standard $CHPh_3$).

An interesting observation was seen in the boron NMR (Figure 4.11). As the amount of DMSO increased, the BLA peak that typically comes at 9 ppm began to shift towards 6.5 ppm. This could be a solvent issue. However, further studies would need to be performed to verify this assumption.

Figure 4.11 Boron NMR for BINOL-borate complexes seen in Figure 4.10 [a]

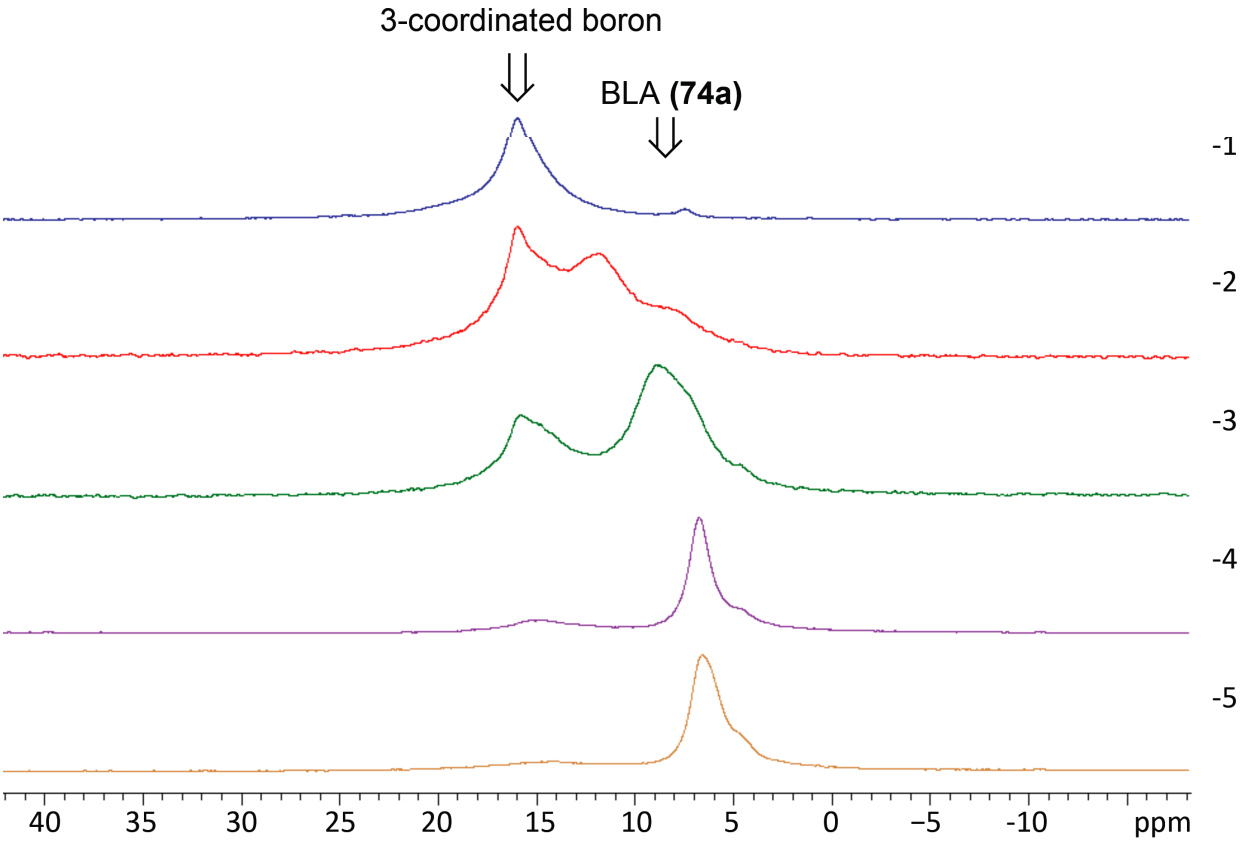

[a] All spectra were taken in $CDCl_3$. Colors correspond to ^1H NMR's shown in Figure 4.10: (1) BINOL and $B(OPh)_3$ (2:1) in the presence of molecular sieves (internal standard $CHPh_3$); (2) BINOL, $B(OPh)_3$, and DMSO (2:1:1) in the presence of molecular

sieves (internal standard $CHPh_3$); (3) BINOL, $B(OPh)_3$, and DMSO (2:1:2) in the presence of molecular sieves (internal standard $CHPh_3$); (4) BINOL, $B(OPh)_3$, and DMSO (2:1:5) in the presence of molecular sieves (internal standard $CHPh_3$); (5) BINOL, $B(OPh)_3$, and DMSO (2:1:10) in the presence of molecular sieves (internal standard $CHPh_3$).

4.3 Synthesis of vaulted biaryl ligand monomers via the CAEC reaction

4.3.1 Synthesis of VANOL monomer via the CAEC reaction

We have previously published efficient routes to synthesize the VANOL monomer using inexpensive materials.[53, 54] The route of interest here is the cycloaddition electrocyclization cascade (CAEC) reaction, which uses a simplistic one pot synthesis to generate the VANOL monomer **84** (Scheme 4.1).

The focus of this study is to exhibit the application of the CAEC reaction on large scale. Therefore, VANOL was synthesized using the CAEC reaction followed by purification via crystallization (Table 4.2).[55] By utilizing crystallization as the purification method, the VANOL monomer synthesis using the CAEC reaction becomes applicable to perform on an industrial scale if ever the need would arise. A previous group member, Dr. Zhensheng Ding, did the majority of the research performed on the CAEC reaction. The current large-scale synthesis of the VANOL ligand was done as a collaborative effort between a previous group member Dr. Hong Ren and myself.

Scheme 4.2 Synthesis of VANOL monomer **84** via the CAEC reaction

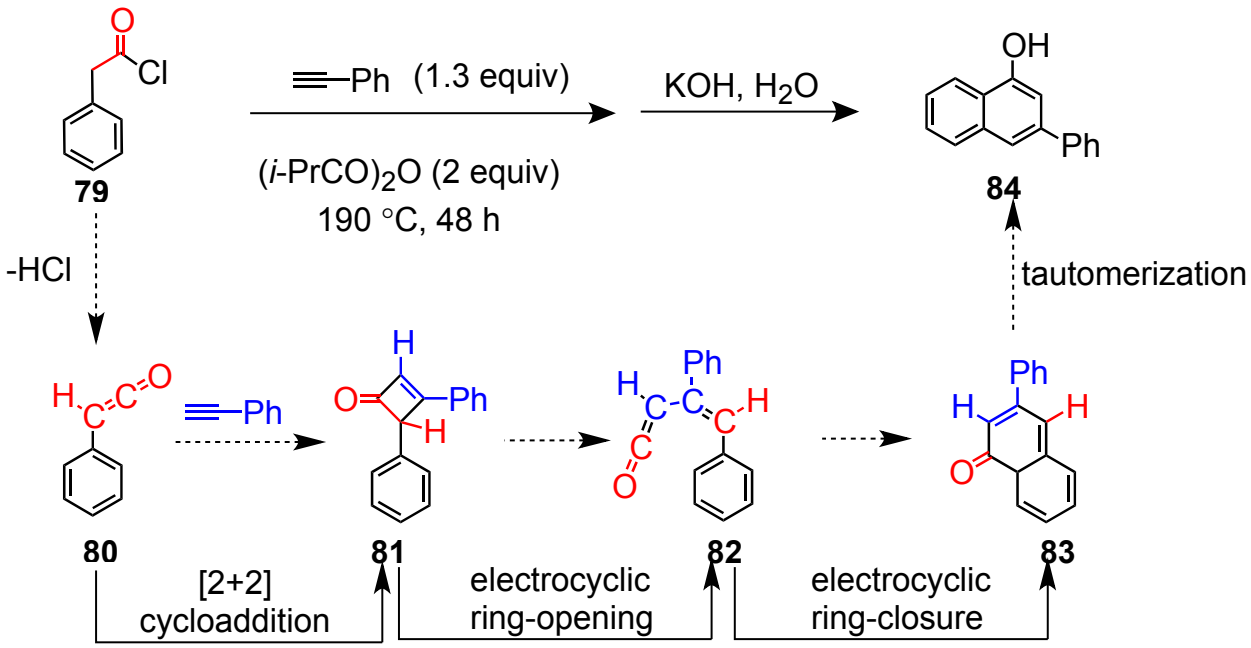

This methodology has a great advantage in that there are a number of commercially available substituted phenyl acetic acid derivatives, which could be used in the CAEC reaction to synthesize a diverse family of VANOL derivatives.

Table 4.1 Large scale synthesis of VANOL monomer using CAEC reaction [a]

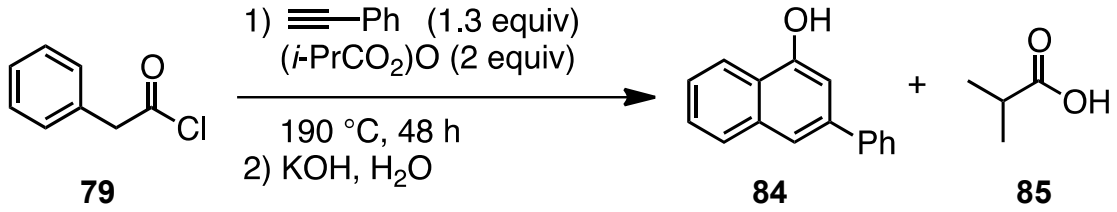

Entry	**79** (mmol)	1st crop [b]	2nd crop [c]	column [d]	total **84** (%) [e]	total **84** (g) [e]
1	74.7	-	-	70f	70	11.5
2	374	43	13	11	67	54.7
3	374	44	17	7	68	56.0

[a] After neutralization, the crude reaction mixture was washed with sat. aq Na_2CO_3 to remove iso-butyric acid **85**. [b] The first crystallization gave **84** from hexanes/CH_2Cl_2 (3-

4:1). [c] The second crystallization gave **84** from hexanes/CH_2Cl_2 (3:1). [d] The mother liquor is stripped of solvent and loaded onto a silica gel column and eluted with hexanes/CH_2Cl_2 (2:1). Collection of fractions containing **84** gave a yellow solid that was not completely pure. Crystallization from hexanes/CH_2Cl_2 (3:1) gave additional pure **84** in the indicated yield. [e] Total isolated yield of **84**. [f] The iso-butyric acid **85** is removed by distillation, and then the entire crude reaction mixture was loaded onto a silica gel column and eluted with hexanes/CH_2Cl_2 (2:1). Collection of the fractions containing **84** gives pure **85** as a biege solid.

4.3.2 Synthesis of tert-butyl VANOL monomer via the CAEC reaction

A similar procedure seen in the synthesis of the VANOL monomer **84** was employed here to synthesize the t-butyl VANOL monomer **89**. The t-butyl VANOL monomer can then be used to synthesize t-butyl VANOL ligand **90** in its enantiopure form. The starting material for the t-butyl VANOL monomer is commercially available. However, to save on cost, the 4-tert-butylphenylacetic acid **88** was synthesized from tert-butyl benzene **86** (Scheme 4.3). Friedel-Crafts acylation of *t*-butylbenzene with acetyl chloride in the presence of $AlCl_3$ afforded 4-*t*-butylacetophenone **87** in 81% yield.[56] Willgerodt-Kindler reaction of 4-*t*-butylacetophenone and subsequent hydrolysis gave 4-*tert*-butyl-phenylacetic acid **88** in 81% yield in a one-pot process.[57,58] Once acid **88** was synthesized, it was then transformed into the acid chloride via thionyl chloride and directly subjected to the CAEC reaction without isolation to give t-butyl VANOL monomer **89** in 25-65% yield (Scheme 4.4).

Scheme 4.3 Synthesis of 4-tert-butylphenylacetic acid **88**

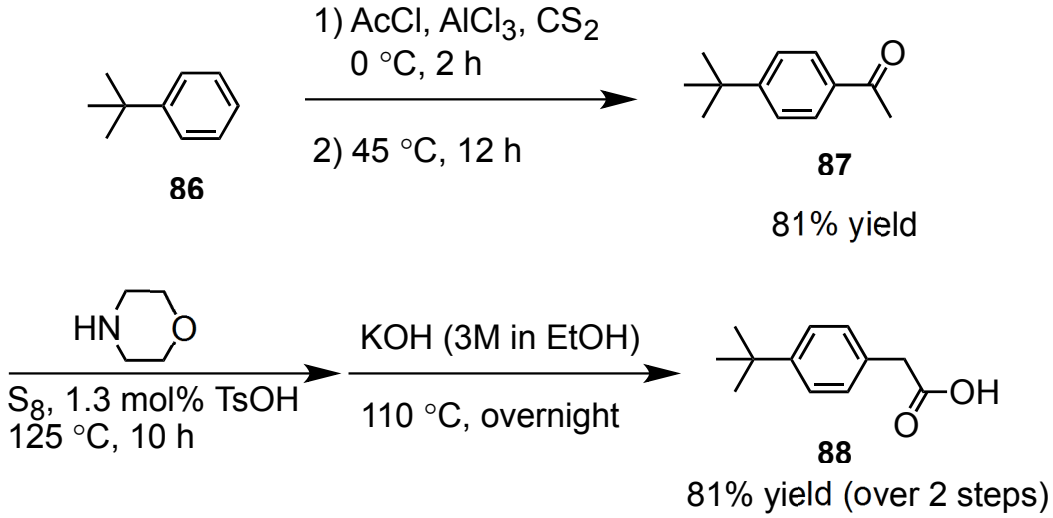

The monomer could then be dimerized via oxidative coupling to give racemic t-butyl VANOL ligand **90** in 65% yield. Deracemization using (+)-Sparteine gave the pure t-butyl VANOL ligand **90** in 67% yield and >99% ee (Scheme 4.4). The reasoning for the wide range in yield seen in the synthesis of monomer **89** is due to purification complications. The monomer synthesis has yet to be completely optimized. Therefore, the crude monomer **89** appears as a black tar and is very difficult to crystallize. Here monomer **89** was purified by a series of columns (silica gel column chromatography). Depending on the number of columns performed, the yield varied drastically as seen in Scheme 4.3. The t-butyl VANOL ligand **90** has been shown to be extremely valuable in the AZ reaction (see chapter 2). Therefore, current group members are trying to optimize the synthesis of this ligand.

Scheme 4.4 Synthesis of t-butyl VANOL ligand **90**

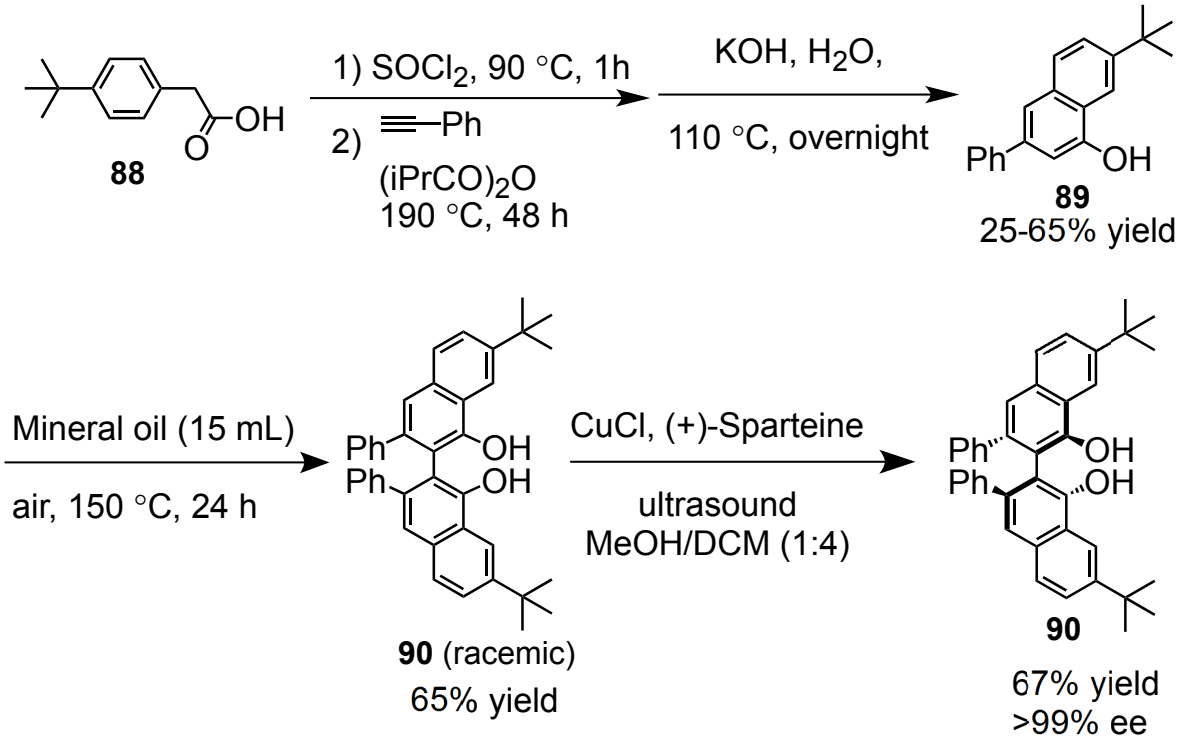

4.4 VANOL and VAPOL shelf life stability testing

In order to test the stability of the VANOL and VAPOL ligands, a series of aziridination reactions were performed over a span of two and a half years using both VANOL and VAPOL ligands that were stored under four different conditions: (A) in a refrigerator under nitrogen; (B) at room temperature under argon and protected from light by aluminum foil; (C) at room temperature under argon; and (D) at room temperature stored in the presence of air. Methods A and D were performed by myself and are reported in Table 4.2. A previous group member Dr. Hong Ren performed the other two methods, B and C. Her results can be seen in Table 4.3.

It was discovered that there was no variation in asymmetric induction in the AZ reaction over the two and a half years using either VANOL or VAPOL from any of the storage conditions. The color of the ligands remained off-white with one exception,

which did not have any affect on the results seen in the AZ reaction (entry 8, Table 4.2).

Table 4.2 Long term stability test of the VANOL and VAPOL ligands [a]

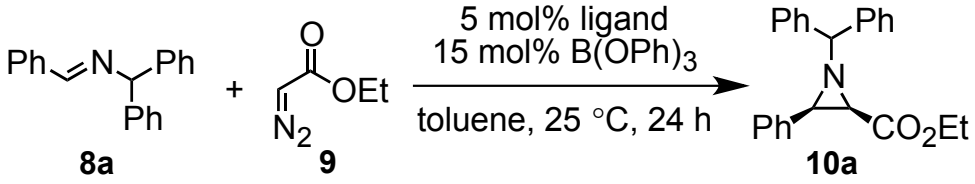

8a **9** **10a**

Entry	Ligand	Time (Years)	Storage Conditions (Condition A or D) [b]	yield **10a** (%) [c]	ee **10a** (%)
1	(*S*)-VANOL	0	Frig/Nitrogen (A)	90	93
2	(*R*)-VAPOL	0	Frig/Nitrogen (A)	84	90
3	(*S*)-VANOL	0	Counter/Air (D)	83	94
4	(*R*)-VAPOL	0	Counter/Air (D)	93	90
5	(*S*)-VANOL	0.5	Frig/Nitrogen (A)	86	93
6	(*R*)-VAPOL	0.5	Frig/Nitrogen (A)	81	92
7	(*S*)-VANOL	0.5	Counter/Air (D)	90	93
8 [d]	(*R*)-VAPOL	0.5	Counter/Air (D)	85	91
9	(*S*)-VANOL	1.5	Frig/Nitrogen (A)	90	93
10	(*R*)-VAPOL	1.5	Frig/Nitrogen (A)	89	92
11	(*S*)-VANOL	1.5	Counter/Air (D)	88	91
12	(*R*)-VAPOL	1.5	Counter/Air (D)	89	92
13	(*S*)-VANOL	2.5	Frig/Nitrogen (A)	87	95
14	(*R*)-VAPOL	2.5	Frig/Nitrogen (A)	86	95
15	(*S*)-VANOL	2.5	Counter/Air (D)	91	94
16	(*R*)-VAPOL	2.5	Counter/Air (D)	91	95

[a] Ligand quality was judged by their performance in the aziridination reactions, which were carried out over a period of 2.5 years. The aziridination catalyst was prepared by mixing 5 mol% ligand, 15 mol% $B(OPh)_3$ in toluene (0.025 M in ligand) at 80 °C for 1 h followed by applying high vacuum (0.1 mmHg) to remove the volatiles at 80 °C for 0.5 h.

Imine **8a** (1.0 mmol) was then added to the catalyst solid followed by toluene (0.5 M in imine) and EDA **9** (1.2 mmol). The reaction was stirred at 25 °C for 24 h to afford aziridine **10a**. Unless otherwise specified, the ligands were all off-white in color, and no change in color or appearance was noted in the course of the study. The VAPOL used in this study was a crystalline form consisting of two molecules of VAPOL and one molecule of CH_2Cl_2. The VANOL did not contain CH_2Cl_2. [b] Condition A: ligands were stored in a refrigerator (3 °C) in a brown bottle under nitrogen and sealed with parafilm. Condition D: ligands were stored on a bench in a brown bottle under air and sealed with parafilm. [c] Isolated yield after chromatography on silica gel. [d] After 6 months of storage, a thin light orange layer appeared on the surface of the VAPOL sample. This was stirred into the sample and was not observed to reappear after 1.5 or 2.5 years. This small amount of orange color appeared after 6 months as a top coating in the bottle. It was stirred into the rest of the ligand and did not reappear over the next two years.

Table 4.3 Long term stability test of the VANOL and VAPOL ligands [a]

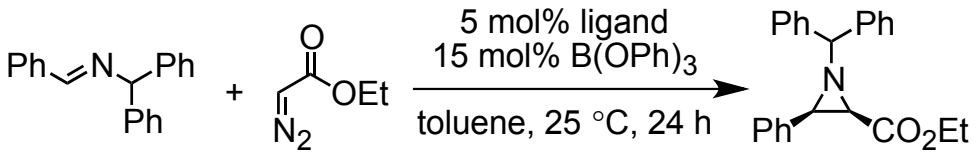

8a **9** **10a**

Entry	Ligand	Time (Years)	Storage Conditions (Condition B or C) [b]	yield **10a** (%) [c]	ee **10a** (%)
1	(*S*)-VANOL	0	Counter/Argon (C)	83	90
2	(*R*)-VAPOL	0	Counter/Argon (C)	83	90
3	(*S*)-VANOL	0	Counter/Argon/Al (B)	91	90
4	(*R*)-VAPOL	0	Counter/Argon/Al (B)	85	90

Table 4.3 (Cont'd)

5	(*S*)-VANOL	0.5	Counter/Argon (C)	86	92
6	(*R*)-VAPOL	0.5	Counter/Argon (C)	85	91
7	(*S*)-VANOL	0.5	Counter/Argon/Al (B)	91	92
8	(*R*)-VAPOL	0.5	Counter/Argon/Al (B)	85	92
9	(*S*)-VANOL	1.5	Counter/Argon (C)	86	92
10	(*R*)-VAPOL	1.5	Counter/Argon (C)	85	94
11	(*S*)-VANOL	1.5	Counter/Argon/Al (B)	87	94
12	(*R*)-VAPOL	1.5	Counter/Argon/Al (B)	83	94
13	(*S*)-VANOL	2.5	Counter/Argon (C)	84	93
14	(*R*)-VAPOL	2.5	Counter/Argon (C)	87	92
15	(*S*)-VANOL	2.5	Counter/Argon/Al (B)	89	91
16	(*R*)-VAPOL	2.5	Counter/Argon/Al (B)	85	92

[a] Ligand quality was judged by their performance in the aziridination reactions which were carried out over a period of 2.5 years. The aziridination catalyst was prepared by mixing 5 mol% ligand, 15 mol% $B(OPh)_3$ in toluene (0.025 M in ligand) at 80 °C for 1 h followed by applying high vacuum (0.1 mmHg) to remove the volatiles at 80 °C for 0.5 h. Imine **8a** (1.0 mmol) was then added to the catalyst solid followed by toluene (0.5 M in imine) and EDA **9** (1.2 mmol). The reaction was stirred at 25 °C for 24 h to afford aziridine **10a**. Unless otherwise specified, the ligands were all off-white in color, and no change in color or appearance was noted in the course of the study. The VAPOL used in this study was a crystalline form consisting of two molecules of VAPOL and one molecule of CH_2Cl_2. The VANOL did not contain CH_2Cl_2. [b] Condition B: ligands were stored in a cabinet in a brown bottle under argon sealed with parafilm and wrapped in aluminum foil. Condition C: ligands were stored on a bench in a brown bottle under

argon and sealed with parafilm. [c] Isolated yield after chromatography on silica gel.

4.5 Purification of non-enantiopure VANOL and VAPOL ligands

Non-racemic mixtures of most enantiomers that are not 100% enantiopure can be purified via crystallization to give enantiopure compounds.[59] Therefore, crystallization was used here to purify scalemic VANOL and VAPOL that ranged from 65-98% ee.

4.5.1 Purification of non-racemic VANOL

Original methods to purify VANOL and VAPOL were accomplished by a previous group member, Dr. Zhensheng Ding.[60] He was able to purify 96% ee (*S*)-VANOL up to >99% (*S*)-VANOL by mixing the non-enantiopure VANOL (30 g, 68.4 mmol) with minimum amount of methylene chloride followed by addition of hexanes (3 L), which was slowly concentrated on vacuum until ca. 500 mL of solvent remained. The solution was flushed with nitrogen and allowed to stand overnight. The yellow solid was filtered, which was enantiopure (*S*)-VANOL (28.3 g, 64.5 mmol, >99% ee). The ee of the (*S*)-VANOL in the mother liquor was 35%. A similar procedure was also followed by Dr. Ding using ethyl acetate and hexanes to afford enantiopure (*S*)-VANOL.

When repeating these purification methods on a small scale, different results appeared. The first attempt made to purify (*R*)-VANOL was using the first method with methylene chloride. (*R*)-VANOL (0.2 g, 0.46 mmol, 74% ee) was dissolved in methylene chloride (5 mL) followed by the addition of hexanes (20 mL). The mixture was subjected to rotary evaporation until ca. 4 mL remained. After filtration, there was no improvement in enantioselectivity.

The second method attempted was using ethyl acetate. A minimal amount of ethyl acetate was used to dissolve the (*R*)-VANOL (0.2 g, 0.46 mmol, 74% ee) followed by

the addition of hexanes (7.5 mL). The solution was shaken vigorously and stored in the freezer overnight. However, after filtration, the ee did not change. Therefore, the procedure was repeated but with removing some of the ethyl acetate via rotary evaporation prior to adding hexanes (7.5 mL). The solution was shaken again and stored overnight in the freezer. After filtration, the mother liquor gave 97.6% ee (*R*)-VANOL (0.142 g, 0.3 mmol) while the solid was racemic. It was noted that the amount of ethyl acetate is crucial in the success of this procedure.

After crystallization was completed, the VANOL ligand was stirred in hexanes and then slowly concentrated via rotary evaporation and placed on high vacuum (0.1 mmHg) for 24 hours. This allowed for the removal of all solvents from the ligand and therefore increased the stability of the ligand over time.

4.5.2 Purificaiton of non-racemic VAPOL

Racemic VAPOL is not soluble in most solvents. Therefore, we can use this to our advantage when purifying non-racemic VAPOL. Following a similar procedure to Dr. Ding, (*R*)-VAPOL (6 g, 11.2 mmol, 65% ee) was stirred in methylene chloride (45 mL) for approximately 5 minutes and then filtered. The mother liquor was concentrated to give (*R*)-VAPOL as an off-white solid in 95% ee (4 g, 7.4 mmol). This 95% ee (*R*)-VAPOL was then subjected once again to stirring in methylene chloride (28 mL) for 5 minutes and then filtered. The mother liquor was stripped of solvents to give >99% ee (1.3 g, 2.4 mmol) of (*R*)-VAPOL.

Other attempts to purify VAPOL that failed included stirring VAPOL (98% ee) in a large amount of hexanes followed by filtration. This resulted in no improvement in enantioselectivity. The procedure was repeated with a small amount of methylene

chloride mixed in with the hexanes. However, the enantioselectivity still did not improve using this methodology.

4.6 Conclusion

In summary, multiple BINOL-borate complexes were synthesized and analyzed using proton and boron NMR spectroscopy. Various procedures were used to synthesize Kaufmann's propeller, BLA-imine complexes and B2. However, there was no clear method to synthesize B1 in a large amount. It was interesting to discover that BLA-DMSO complex can be generated without the assistance of an imine. This suggests that the DMSO must be forming a complex with BLA in order to assemble the tetra-coordinated borate species.

The VANOL monomer was synthesized in large-scale using the CAEC reaction. The ligand was then purified via crystallization to give good yields. Also, the VANOL and VAPOL ligands were stored under various conditions in order to establish the length of time the ligands remain stable. Lastly, scalemic VANOL and VAPOL were purified via crystallization to give their enantiopure forms.

CHAPTER FIVE

EXPERIMENTAL SECTION

General Information: Methylene chloride and acetonitrile were distilled from calcium hydride under nitrogen. Toluene, tetrahydrofuran, and benzene were distilled from sodium under nitrogen. Hexanes and ethyl acetate were ACS grade and used as purchased. All borane reagents and ethyl diazoacetate were purchased from Sigma Aldrich and used as is. Liquid alcohols were purified by distillation under reduced pressure while solid alcohols and/or phenols were purified via sublimation. VANOL and VAPOL were prepared according to a literature procedure and were determined to be at least 99% optically pure.[55]

Melting points were determined on a Thomas Hoover capillary melting point apparatus and were uncorrected. IR spectra were taken on a Mattson Galaxy series FTIR-3000 spectrometer. ^{1}H NMR, ^{13}C NMR, and ^{11}B NMR were recorded on a Varian Inova-300 MHz, Varian UnityPlus-500 MHz, or Varian Inova-600 MHz instrument in $CDCl_3$, unless otherwise noted. $CDCl_3$ was used as an internal standard for both ^{1}H NMR (δ = 7.24) and ^{13}C NMR (δ = 77.0), unless otherwise noted. BF_3•OEt was used as an internal standard for ^{11}B NMR (δ = 0.0). HRMS was performed in the Department of Biochemistry at Michigan State University using either a Waters Xevo G2-S QTof or a Waters QTof Ultima API mass spectrometer. Analytical thin-layer chromatography (TLC) was performed on silica gel IB2-F plates. Visualization was by short wave (254 nm) and long wave (365 nm) ultraviolet light or by staining with phosphomolybdic acid (PMA) in ethanol or potassium permanganate. Column chromatography was performed

with silica gel 60 (230-450 mesh). HPLC analyses were carried out using a Varian Prostar 210 Solvent Delivery Module with a Prostar 330 PDA Detector and a Prostar Workstation. Optical rotations were obtained on a Perkin-Elmer 341 polarimeter at a wavelength of 589 nm (sodium D line) using a 1.0-decimeter cell with a total volume of 1.0 mL. Specific rotations are reported in degrees per decimeter at 20 °C.

Although we have not experienced any problems with either the preparation or use of diazo compounds herein, we note that diazo compounds in general are heat sensitive and potentially explosive and should be handled with due care.

5.1 Experimental for chapter two

5.1.1 General procedure for the preparation of aldimines

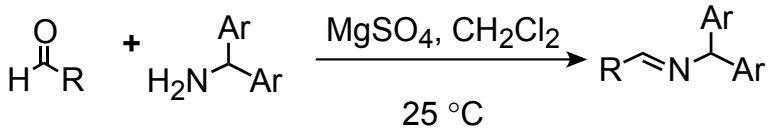

To a flame-dried round bottom flask equipped with a stir bar was added magnesium sulfate (1.50-4.00 equiv). Cotton was placed in the neck of the vacuum adapter to prevent the $MgSO_4$ from entering the vacuum line followed by placing the $MgSO_4$ under vacuum and flame-drying the flask until the $MgSO_4$ stopped bouncing (indication of removal of water). Once cooled, CH_2Cl_2 (2-4 mL/mmol) was added followed by amine (1.00 equiv) and finally aldehyde (1.05 equiv). The reaction flask was sealed with a rubber septum and nitrogen balloon and stirred at room temperature for the specified time. The slurry was then filtered over a pad of Celite 545 on a sintered glass funnel and the filtrate was concentrated by rotary evaporation to give the crude product. Liquid

aldimines were then subjected to the AZ reaction without further purification while solid aldimines were recrystallized prior to the AZ reaction.

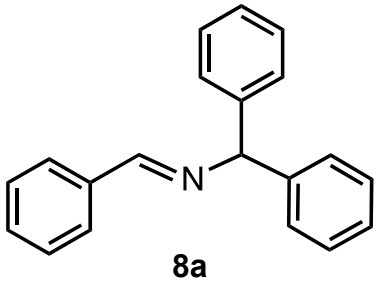

8a

*Preparation of N-benzylidene-1,1-diphenylmethanamine (**8a**):* The general procedure was followed with benzhydryl amine (0.92 g, 5.00 mmol, 1.00 equiv), benzaldehyde (0.56 g, 5.25 mmol, 1.05 equiv), dry CH_2Cl_2 (15 mL), $MgSO_4$ (1.00 g, 8.40 mmol, 1.70 equiv, freshly dried), and a reaction time of 24 hours. The crude product was placed under high vacuum (0.1 mm Hg) for 4-6 hours to give the imine **8a** as a white solid. The imine was purified by crystallization using ethyl acetate and hexanes to give the pure product as white solid crystals (mp = 102-104 °C) in 82% yield (1.11 g, 4.1 mmol).

Spectral data for **8a**: ^{1}H NMR ($CDCl_3$, 500 MHz) δ 5.63 (s, 1H, CH), 7.26 (t, 2H, *J* = 7.0 Hz, Ar-H), 7.35 (t, 4H, *J* = 7.5 Hz, Ar-H), 7.43-7.44 (m, 7H, Ar-H), 7.86-7.88 (m, 2H, Ar-H), 8.45 (s, 1H, CHN) ppm; ^{13}C NMR ($CDCl_3$, 125 MHz) δ 77.89, 126.95, 127.67, 128.41, 128.45, 128.51, 130.73, 136.34, 143.90, 160.75 ppm. These spectra match those previously reported for this compound.[16h]

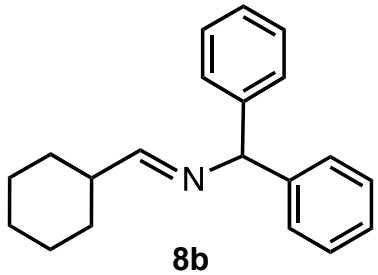

8b

*Preparation of N-(cyclohexylmethylene)-1,1-diphenylmethanamine (**8b**):* The general procedure was followed with benzhydryl amine (9.15 g, 8.6 mL, 50.0 mmol, 1.00 equiv), cyclohexylcarbaldehyde (5.83 g, 6.3 mL, 52.5 mmol, 1.05 equiv), dry CH_2Cl_2 (150 mL), $MgSO_4$ (12.0 g, 100 mmol, 2.00 equiv), and a reaction time of 16 hours. The crude product was placed under high vacuum (0.1 mm Hg) for 4-6 hours to give the imine **8b** as a white solid. The imine was purified by crystallization using ethyl acetate and hexanes to give the pure product as solid white crystals (mp = 52-54 C°) in 72% yield (9.99 g, 36.0 mmol).

Spectral data for **8b**: ^{1}H NMR ($CDCl_3$, 500 MHz) δ 1.20-1.37 (m, 5H), 1.66-1.88 (m, 5H), 2.29-2.33 (m, 1H), 5.32 (s, 1H), 7.20-7.24 (m, 2H), 7.28-7.32 (m, 8H), 7.70 (d, 1H, *J* = 5.0 Hz) ppm; ^{13}C NMR ($CDCl_3$, 125 MHz) δ 25.43, 26.02, 29.72, 43.50, 77.95, 126.77, 127.56, 128.31, 144.02, 169.04 ppm. These spectra match those previously reported for this compound.[16h]

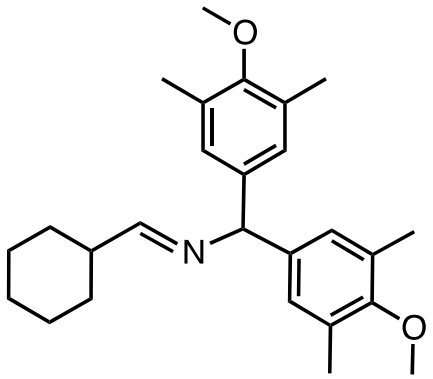

53

*Preparation of (E)-N-(cyclohexylmethylene)-1,1-bis(4-methoxy-3,5-dimethylphenyl) methanamine(**53**):* The general procedure was followed with MEDAM amine (1.5 g, 5.00 mmol, 1.00 equiv), cyclohexylcarbaldehyde (0.59 g, 0.64 mL, 5.25 mmol, 1.05 equiv),

dry CH_2Cl_2 (15 mL), $MgSO_4$ (1.00 g, 8.40 mmol, 1.70 equiv, freshly dried), and a reaction time of 24 hours. The crude product was placed under high vacuum (0.1 mm Hg) for 4-6 hours to give the imine **53** as a white solid. The imine was purified by crystallization (ethyl acetate/hexanes 1:60) to give the pure product as white solid crystals (mp = 107-109 °C) in 70% yield (1.40 g, 3.50 mmol).

Spectral data for **53**: ^{1}H NMR ($CDCl_3$, 500 MHz) δ 1.20-1.32 (m, 5H), 1.64-1.82 (m, 6H), 2.23 (s, 12H), 3.67 (s, 6H), 5.05 (s, 1H), 6.91 (s, 4H), 7.60 (d, 1H, *J* = 5.0 Hz) ppm; ^{13}C NMR ($CDCl_3$, 125 MHz) δ 16.19, 25.42, 26.01, 29.79, 43.51, 59.58, 77.44, 127.73, 130.49, 139.39, 155.68, 168.60 ppm. These spectra match those previously reported for this compound.[38]

5.1.2 Preparation of MEDAM amine

General scheme for the synthesis of MEDAM amine (**59**):

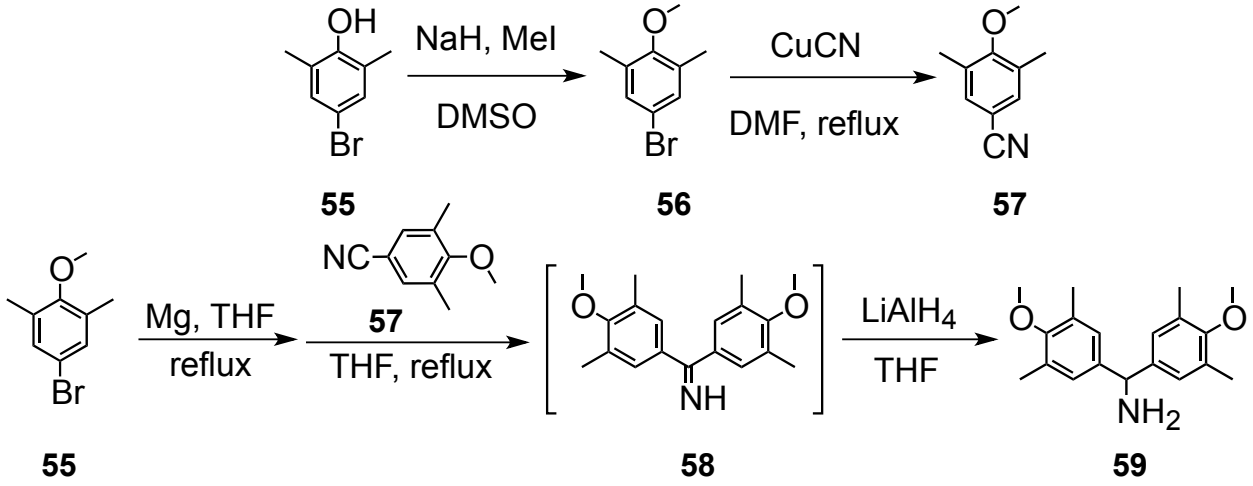

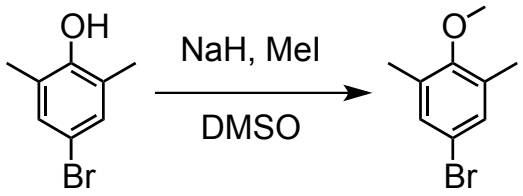

55 **56**

*Preparation of 2,6-dimethyl-4-bromoanisole **(56):*** To a flame-dried 2 L three neck round bottom flask equipped with a mechanical stirrer was added anhydrous DMSO (600 mL) and NaH (24.0 g, 0.59 mol, 60% suspension in oil) under nitrogen. The flask was then transferred to an ice bath at 0° C and stirred at 115 rpm. 4-bromo-2,6-dimethylphenol **55** (50.0 g, 248.5 mmol) was added to the suspension slowly over a period of 30 min and stirred for an additional 15 min at 0° C. MeI (59 mL, 0.95 mol) was then added drop wise to the suspension *via* addition funnel over a period of 20 min. The resulting mixture was stirred at 0° C for 15 min. The reaction mixture was allowed to warm to room temperature (approximately 2 h) and stirred at room temperature overnight. The reaction mixture was cooled to 0° C and diluted with hexanes (200 mL). The mixture was then poured into a 2 L Erlenmeyer flask containing hexanes (215 mL) at 0° C. The mixture was stirred with a mechanical stirrer at 100 rpm while slowly adding water (215 mL) and stirred until two layers appeared. The organic layer was separated, and the aqueous layer was extracted with hexanes (100 mL x 3). The combined organic layer was then washed with water (150 mL x 4), dried over $MgSO_4$, and concentrated under reduced pressure to give the crude product as a yellow liquid. The crude product was purified by simple distillation (0.8 mm Hg pressure/ 80° C) to give the 4-bromo-2,6-dimethylanisole **56** as a colorless liquid in 84% yield (45.1 g, 210 mmol).

Spectral data for **56**: R_f = 0.3 (1:15 EtOAc/ hexanes); ^{1}H NMR (300 MHz, $CDCl_3$) δ 2.21 (s, 6H), 3.64 (s, 3H), 7.15 (s, 2H) ppm; ^{13}C NMR (75 MHz, $CDCl_3$) δ 15.05, 60.73, 126.61, 131.81, 113.22, 155.51 ppm. These spectra match those previously reported for this compound.[16i]

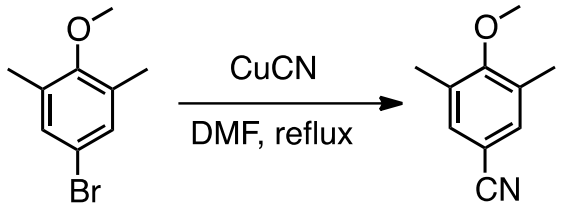

56 **57**

*Preparation of 2,6-dimethyl-4-cyanoanisole **(57):*** A flame-dried 2 L three neck round bottom flask filled with nitrogen and equipped with a refluxing condenser was charged with 4-bromo-2,6-dimethylanisole **56** (27.5 g, 104.5 mmol), CuCN (11.25 g, 125.5 mmol) and anhydrous DMF (250 mL, freshly distilled and stored over 4Å MS). The reaction mixture was purged with nitrogen under the surface of the solution for 15 min. The nitrogen inlet was then replaced with a nitrogen balloon on the top of the condenser through a rubber septum stopper (the flask was sealed with Teflon tape, and stoppers were covered with Teflon sleeves). The mixture was heated to reflux in a 180° C oil bath for 8 h. During the refluxing, the solid CuCN dissolved after approximately 2 h and the reaction turned a dark green color. The reaction mixture was then cooled gradually to room temperature and poured into an Erlenmeyer flask containing a solution of ethylene diamine (45 mL ethylene diamine in 1120 mL water) at 0° C. The ice bath was removed and benzene (340 mL) was added, and the resulting mixture was stirred at room temperature for 20 min and loaded into a separation funnel. The water layer was

extracted with benzene (125 mL x 4). The combined organic layers were washed with 6% NaCN aqueous solution (175 mL) followed by water (200 mL x 2). The organic layer was dried over $MgSO_4$ and concentrated under reduced pressure to give the crude product as an off-white solid. Purification was performed by crystallization from hexanes to give 4-bromo-2,6-cyanoanisole **57** as a white crystalline solid (m.p. = 47.5-49 °C) in 85% yield (14.3 g, 89.0 mmol).

Spectral data for **57**: R_f = 0.35 (1:15 EtOAc/hexanes); ^{1}H NMR ($CDCl_3$, 300 MHz) δ 2.24 (s, 6H), 3.72 (s, 3H), 7.25 (s, 2H) ppm; ^{13}C NMR ($CDCl_3$, 75 MHz) δ 15.93, 59.73, 107.25, 119.00, 132.46, 132.70, 160.75 ppm. These spectra match those previously reported for this compound.[16i]

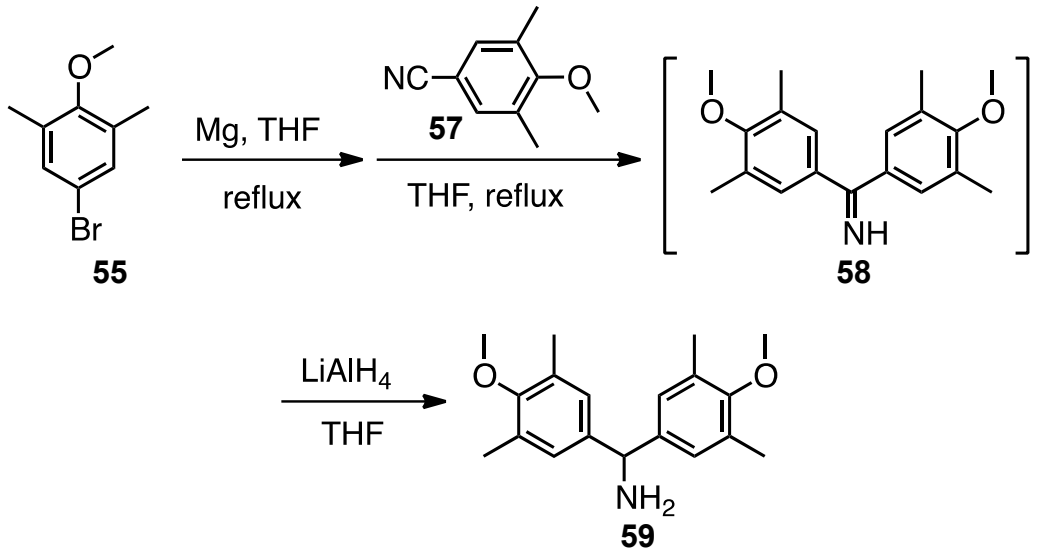

*Preparation of Bis-(2,6-dimethyl-4-methoxyphenyl)methineamine **(59):*** To a flame-dried 2 L three neck round bottom flask filled with nitrogen and equipped with a refluxing condenser was added magnesium (6.10 g, 248.3 mmol, 20 mesh), THF (200mL), 4-bromo-2,6-dimethylanisole **55** (21.3 g, 99.3 mmol) and a few crystals of iodine. The mixture was set to reflux for 3 h under nitrogen. The resulting amber solution was

allowed to cool to room temperature. Meanwhile, to a flame dried 500 mL round bottom flask was added 2,6-dimethyl-4-cyanoanisole **57** (14.5 g, 90.7 mmol) and THF (200 mL). The solution was then added *via* cannula to the 2 L flask containing the freshly prepared Grignard reagent over a period of 20 min at room temperature. The resulting mixture was heated to reflux for 5 h under nitrogen, then allowed to cool to room temperature and finally cooled to 0° C. To this mixture was transferred a suspension of $LiAlH_4$ (3.70 g, 100 mmol) in THF (100 mL) *via* cannula. The $LiAlH_4$ suspension was prepared in a flame-dried 150 mL flask filled with nitrogen and pre-cooled at 0° C. The ice bath was then removed, and the resulting yellow reaction mixture was heated to reflux for 15 h under nitrogen atmosphere. The reaction flask was cooled down to room temperature and carefully quenched with the slow addition of water (4.0 mL), then 10% NaOH solution (4.0 mL), and water (9.0 mL). The resulting suspension was filtered through a pad of Celite (503) and washed with ether until no amine was left (monitored by TLC). Appearance of a white solid in the organic phase shows the formation of the bicarbonate salt (this happens if the filtration takes too much time). This was removed with treatment of 0.5 M NaOH and a subsequent extraction. The combined organic layers were washed with brine, dried over $MgSO_4$, and concentrated under reduced pressure to give the crude product as a dark red viscous liquid. The product was further diluted with ether. Concentrated HCl (10 mL) was then added to form the amine salt. The ether layer was then removed and the salt was washed with ether then finally taken back into the organic layer by addition of saturated NaOH solution. The organic layer was separated and the aqueous layer was washed with ether (100 mL x 3), dried over $MgSO_4$ and concentrated under reduced pressure to give the crude product in a pale

yellow solid. The crude product was then purified once again by crystallization from hexanes to afford bis-(2,6-dimethyl-4-methoxyphenyl)methineamine **59** as white crystals (m.p. = 59-61 °C) in 65% yield (17.63 g, 59.0 mmol).

Spectral data for **59**: ^{1}H NMR ($CDCl_3$, 300 MHz) δ 1.73 (s, 2H), 2.26 (s, 12H), 3.69 (s, 6H), 5.10 (s, 1H), 7.01 ppm (s, 4H); ^{13}C NMR ($CDCl_3$, 75 MHz) δ 16.10, 58.77, 59.50, 126.96, 130.56, 140.88, 155.65 ppm. These spectra match those previously reported for this compound.[16i]

5.1.3 The 6-Component Catalytic Asymmetric Aziridination Reaction

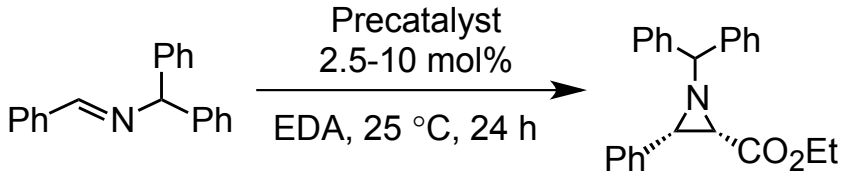

8a **10a**

General Procedures for the 6-Component Catalytic Asymmetric Aziridination Reaction:

Method I (**10a)**: For reactions in Table 2.1. A 50 mL Schlenk flask equipped with a stir bar and Teflon cap was placed under reduced pressure (0.1 mm Hg) and flame-dried. The flask was allowed to cool under vacuum followed by purging the flask with nitrogen. Under a nitrogen atmosphere, 10 mol% (*R*)-VANOL (22 mg, 0.05 mmol, 0.10 equiv) and phenol (14.0 mg, 0.15 mmol, 0.30 equiv) were added. Toluene (2.0 mL) was added and the mixture was stirred to dissolve all solids. Borane dimethyl sulfide (2 M in toluene, 50 μL, 0.10 mmol, 0.20 equiv) was added followed by water (0.9 μL, 0.05 mmol, 0.10 equiv). The Teflon valve was sealed (under nitrogen atmosphere) and the reaction was stirred at the specified temperature (80-100 °C) for 1 h. At 80-100 °C, the Teflon valve was slowly opened to vacuum (0.1 mm Hg) to remove the volatiles. The vacuum

remained open at 80-100 °C for 0.5 h. Once the flask cooled to room temperature, the Teflon valve was opened to a nitrogen line to flush the flask with nitrogen. Imine **8a** (136 mg, 0.50 mmol, 1.00 equiv) was added followed by toluene (2.0 mL). To the stirring reaction, ethyl diazoacetate **9** (62 μL, 0.60 mmol, 1.20 equiv) was added. The Teflon valve was sealed (under nitrogen atmosphere) and the reaction mixture stirred at room temperature for 24 h. Once completed, hexanes (3.0 mL) were added to the Schlenk flask and a precipitate formed. The heterogeneous solution was then transferred to a pre-weighed 25 mL round bottom flask. The Schlenk flask was rinsed with methylene chloride (3 mL x 2) that was transferred to the round bottom flask. The volatiles were removed by rotary evaporation followed by placing the round bottom flask under reduced pressure (0.1 mm Hg) for 4-6 hours. The cis/*trans* ratio, percent conversion, and enamine side products were determined by ^{1}H NMR on the crude reaction mixture. The *cis/trans* ratios were determnined on the crude mixture by putting the integration of the cis-aziridine ring protons to 1.00 H each. The cis (J = 7-8 Hz) and trans (J = 2-3 Hz) coupling constants were used to verify the two diastereomers. The enamines (8.8 and 9.4 ppm) were calculated based upon the isolated yield of pure aziridine and integration of enamines in the crude ^{1}H NMR. Conversion was 100% unless otherwise stated. The aziridine **10a** was purified by column chromatography (silica gel).

Method II (**10a)**: For reactions in Table 2.1. A 50 mL Schlenk flask equipped with a stir bar and Teflon cap was placed under reduced pressure (0.1 mm Hg) and flame-dried. The flask was allowed to cool under vacuum followed by purging the flask with nitrogen. Under a nitrogen atmosphere, x mol% (*R*)-VANOL (mol% is based on imine **8a**) and phenol (2.00 equiv with respect to VANOL) were added. Toluene (2.0 mL) was added

and the mixture was stirred to dissolve all solids. Borane dimethyl sulfide (2 M in toluene, 3.00 equiv with respect to VANOL) was added followed by water (3.00 equiv with respect to VANOL). The Teflon valve was sealed (under nitrogen atmosphere) and the reaction was stirred at the specified temperature (80-100 °C) for 1 h. At 80-100 °C, the Teflon valve was slowly opened to vacuum (0.1 mmHg) to remove the volatiles. The vacuum remained open at 80-100 °C for 0.5 h. Once the flask cooled to room temperature, the Teflon valve was opened to a nitrogen line to flush the flask with nitrogen. Imine **8a** (136 mg, 0.50 mmol, 1.00 equiv) was added followed by toluene (2 mL). To the stirring reaction, ethyl diazoacetate **9** (62 μL, 0.60 mmol, 1.20 equiv) was added. The Teflon valve was sealed (under nitrogen atmosphere) and the reaction mixture stirred at room temperature for 24 h. Once completed, hexanes (3.0 mL) were added to the Schlenk flask and a precipitate formed. The heterogeneous solution was then transferred to a pre-weighed 25 mL round bottom flask. The Schlenk flask was rinsed with methylene chloride (3 mL x 2) that was transferred to the round bottom flask. The volatiles were removed by rotary evaporation followed by placing the round bottom flask under reduced pressure for 4-6 hours. The cis/*trans* ratio, percent conversion, and enamine side products were determined by ^{1}H NMR on the crude reaction mixture. The *cis/trans* ratios were determnined on the crude mixture by putting the integration of the cis-aziridine ring protons to 1.00 H each. The cis (J = 7-8 Hz) and trans (J = 2-3 Hz) coupling constants were used to verify the two diastereomers. The enamines (8.8 and 9.4 ppm) were calculated based upon the isolated yield of pure aziridine and integration of enamines in the crude ^{1}H NMR. Conversion was 100% unless otherwise stated. The aziridine **10a** was purified by column chromatography (silica gel).

Method III (**10a)**: For reactions in Table 2.1. A 50 mL Schlenk flask equipped with a stir bar and Teflon cap was placed under reduced pressure (0.1 mm Hg) and flame-dried. The flask was allowed to cool under reduced pressure followed by purging the flask with nitrogen. Under a nitrogen atmosphere, 10 mol% ligand (0.10 equiv) and phenol (9.4 mg, 0.10 mmol, 0.20 equiv) were added. Toluene (0.5 mL) was added and the mixture was stirred to dissolve all solids. Borane dimethyl sulfide (2 M in toluene, 75 μL, 0.15 mmol, 0.30 equiv) was added followed by water (2.7 μL, 0.15 mmol, 0.30 equiv) and amine **70** (86 μL, 0.5 mmol, 1.00 equiv). The Teflon cap was sealed and the reaction was stirred under nitrogen at the specified temperature (80-100 °C) for 1 h. The reaction was cooled to room temperature over a period of 0.5 h. While the reaction was cooling, 4Å powdered molecular sieves were flame-dried under reduced pressure. To do this, a 10 mL round bottom flask was first flame-dried under reduced pressure and allowed to cool to room temperature while under vacuum. Then a piece of cotton is placed in the glass joint to prevent the sieves from entering the vacuum line. The molecular sieves were then added to the flask (typically measure approximately 10 mg excess molecular sieves to account for the water weight). The flask was once again placed under vacuum and the molecular sieves were flame-dried until the sieves stopped bouncing (indicator that the water had been eliminated). Once at room temperature, the sieves were then ready to be added to the reaction flask. Once the sieves were added, toluene (0.5 mL) was added followed by benzaldehyde (53 μL, 0.525 mmol, 1.05 equiv). To the stirring reaction mixture, ethyl diazoacetate **9** (62 μL, 0.6 mmol, 1.2 equiv) was added. The Teflon valve was sealed (under nitrogen atmosphere) and the reaction mixture stirred at room temperature for 24 h. Once completed, hexanes (6.0 mL) were added to the

Schlenk flask and a precipitate formed. The heterogeneous solution was then filtered through a pad of Celite and rinsed several times with ethyl acetate (dissolves aziridine to allow for filtration of product through Celite). The volatiles were removed by rotary evaporation followed by placing the round bottom flask under reduced pressure (0.1 mm Hg) for 4-6 hours. The cis/*trans* ratio, percent conversion, and enamine side products were determined by ^{1}H NMR on the crude reaction mixture. The *cis/trans* ratios were determnined on the crude mixture by putting the integration of the cis-aziridine ring protons to 1.00 H each. The cis (J = 7-8 Hz) and trans (J = 2-3 Hz) coupling constants were used to verify the two diastereomers. The enamines (8.8 and 9.4 ppm) were calculated based upon the isolated yield of pure aziridine and integration of enamines in the crude ^{1}H NMR. Conversion was 100% unless otherwise stated. The aziridine **10a** was purified by column chromatography (silica gel).

Method IV (10a): For reactions in Table 2.1. A 50 mL Schlenk flask equipped with a stir bar and Teflon cap was placed under reduced pressure (0.1 mm Hg) and flame-dried. The flask was allowed to cool under vacuum followed by purging the flask with nitrogen. Under a nitrogen atmosphere, 10 mol% (*R*)-VANOL (0.10 equiv) and phenol (9.4 mg, 0.10 mmol, 0.20 equiv) were added. Toluene (0.5 mL) was added and the mixture was stirred to dissolve all solids. Borane dimethyl sulfide (2 M in toluene, 75 μL, 0.15 mmol, 0.30 equiv) was added followed by water (2.7 μL, 0.15 mmol, 0.30 equiv). The Teflon valve was sealed (under nitrogen atmosphere) and the reaction was stirred at 100 °C for 1 h. The reaction was then cooled to room temperature and imine **8a** (136 mg, 0.50 mmol, 1.00 equiv) was added followed by toluene (0.5 mL). The reaction was stirred at room temperature for 1 h followed by the addition of ethyl diazoacetate **9** (62 μL, 0.60

mmol, 1.20 equiv). The Teflon valve was sealed (under nitrogen atmosphere) and the reaction mixture stirred at room temperature for 24 h. Once completed, hexanes (3.0 mL) were added to the Schlenk flask and a precipitate formed. The heterogeneous solution was then transferred to a pre-weighed 25 mL round bottom flask. The Schlenk flask was rinsed with methylene chloride (3 mL x 2) that was transferred to the round bottom flask. The volatiles were removed by rotary evaporation followed by placing the round bottom flask under reduced pressure (0.1 mm Hg) for 4-6 hours. The cis/*trans* ratio, percent conversion, and enamine side products were determined by ^{1}H NMR on the crude reaction mixture. The *cis/trans* ratios were determnined on the crude mixture by putting the integration of the cis-aziridine ring protons to 1.00 H each. The cis (*J* = 7-8 Hz) and trans (*J* = 2-3 Hz) coupling constants were used to verify the two diastereomers. The enamines (8.8 and 9.4 ppm) were calculated based upon the isolated yield of pure aziridine and integration of enamines in the crude ^{1}H NMR. Conversion was 100% unless otherwise stated. The aziridine **10a** was purified by column chromatography (silica gel).

Method V (10a): For reactions in Table 2.1. A 50 mL Schlenk flask equipped with a stir bar and Teflon cap was placed under reduced pressure (0.1 mm Hg) and flame-dried. The flask was allowed to cool under vacuum followed by purging the flask with nitrogen. Under a nitrogen atmosphere, 10 mol% (*R*)-VANOL (0.10 equiv), phenol (9.4 mg, 0.10 mmol, 0.20 equiv), and imine **8a** (136 mg, 0.50 mmol, 1.00 equiv) were added. Toluene (1.5 mL) was added and the mixture was stirred to dissolve all solids. Borane dimethyl sulfide (2 M in toluene, 75 μL, 0.15 mmol, 0.30 equiv) was added followed by water (2.7 μL, 0.15 mmol, 0.30 equiv). The Teflon valve was sealed under a nitrogen atmosphere

and the reaction was stirred at 80 °C for 1 h. At 80 °C, the Teflon valve was slowly opened to vacuum (0.1 mmHg) to remove the volatiles. The vacuum remained open at 80 °C for 0.5 h. Once the flask cooled to room temperature, the Teflon valve was opened to a nitrogen line to flush the flask with nitrogen. Toluene (0.5 mL) was added followed by ethyl diazoacetate **9** (62 μL, 0.60 mmol, 1.20 equiv). The Teflon valve was sealed under a nitrogen atmosphere and the reaction mixture stirred at room temperature for 24 h. Once completed, hexanes (3.0 mL) were added to the Schlenk flask and a precipitate formed. The heterogeneous solution was then transferred to a pre-weighed 25 mL round bottom flask. The Schlenk flask was rinsed with methylene chloride (3 mL x 2) and transferred to the round bottom flask. The volatiles were removed by rotary evaporation followed by placing the round bottom flask under reduced pressure for 4-6 hours. The conversion was 25% for this method (entry 11, Table 2.1).

Method A : For reactions in Tables 2.2-2.5. A 50 mL Schlenk flask equipped with a stir bar and Teflon cap was placed under reduced pressure (0.1 mm Hg) and flame-dried. The flask was allowed to cool under vacuum followed by purging the flask with nitrogen. Under a nitrogen atmosphere, 10 mol% ligand (22.0 mg, 0.05 mmol, 0.10 equiv) and phenol (9.4 mg, 0.10 mmol, 0.20 equiv) were added. Toluene (0.5 mL) was added and the mixture was stirred to dissolve all solids. Borane dimethyl sulfide (2 M in toluene, 75 μL, 0.15 mmol, 0.30 equiv) was added followed by water (2.7 μL, 0.15 mmol, 0.30 equiv). The Teflon valve was sealed under a nitrogen atmosphere and the reaction was stirred at 100 °C for 1 h. The reaction was then cooled to room temperature and imine (0.50 mmol, 1.00 equiv) was added followed by toluene (0.5 mL). The reaction was

stirred at room temperature for 0.5 h followed by the addition of ethyl diazoacetate **9** (62 μL, 0.60 mmol, 1.20 equiv). The Teflon valve was sealed under a nitrogen atmosphere and the reaction mixture stirred at room temperature for 24 h. Once completed, hexanes (3.0 mL) were added to the Schlenk flask and a precipitate formed. The heterogeneous solution was then transferred to a pre-weighed 25 mL round bottom flask. The Schlenk flask was rinsed with methylene chloride (3 mL x 2) that was transferred to the round bottom flask. The volatiles were removed by rotary evaporation followed by placing the round bottom flask under reduced pressure (0.1 mm Hg) for 4-6 hours. The cis/*trans* ratio, percent conversion, and enamine side products were determined by ^{1}H NMR on the crude reaction mixture. The *cis/trans* ratios were determnined on the crude mixture by putting the integration of the cis-aziridine ring protons to 1.00 H each. The cis (*J* = 7-8 Hz) and trans (*J* = 2-3 Hz) coupling constants were used to verify the two diastereomers. The enamines (8.8 and 9.4 ppm) were calculated based upon the isolated yield of pure aziridine and integration of enamines in the crude ^{1}H NMR. Conversion was 100% unless otherwise stated. The aziridine was purified by column chromatography (silica gel).

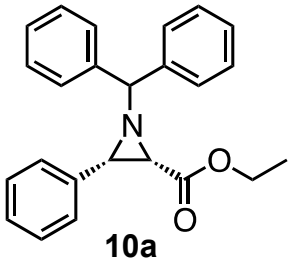

10a

*Preparation of (2S,3S)-ethyl 1-benzhydryl-3-phenylaziridine-2-carboxylate (**10a**) using catalyst **33b**:* Aziridine **10a** was generated from imine **8a** (136 mg, 0.50 mmol, 1.00 equiv) according to Method A using 10 mol% (*R*)-VANOL (22.0 mg, 0.05 mmol, 0.10

equiv) to generate the catalyst **33b**. Upon work-up, the crude ^{1}H NMR indicated a 100:1 cis/trans ratio (cis *J* = 7-8 Hz and trans *J* = 2-3 Hz). The product was purified by column chromatography (silica gel, 3 cm x 30 cm, hexanes/EtOAc 19:1) and **10a** was obtained as a white solid (m.p. = 127-128 °C on 89% ee material) in 83% isolated yield (150.1 mg, 0.42 mmol). The optical purity of **10a** was determined to be 89% *ee* by HPLC analysis (Chiralcel-OD-H column, 95:5 hexane/2-propanol at 222nm, flow-rate: 1.0 mL/min): retention times t_R = 3.401 min (major enantiomer, **10a**) and t_R = 8.358 min (minor enantiomer, *ent*-**10a**).

Spectral data for **10a**: R_f = 0.3 (1:9 EtOAc/hexanes); ^{1}H NMR ($CDCl_3$, 500 MHz) δ 1.01 (t, 3H, *J* = 7.0 Hz), 2.70 (d, 1H, *J* = 6.5 Hz), 3.24 (d, 1H, 6.5 Hz), 3.95-3.99 (m, 3H), 7.21-7.29 (m, 7H), 7.37 (t, 2H, *J* = 7.5 Hz), 7.43 (d, 2H, *J* = 7.0 Hz), 7.52 (d, 2H, *J* = 7.0 Hz), 7.63 (d, 2H, *J* = 7.0 Hz) ppm; ^{13}C NMR ($CDCl_3$, 125 MHz) δ 13.98, 46.42, 48.07, 60.61, 77.74, 127.24, 127.37, 127.45, 127.58, 127.81, 127.83, 128.53, 135.06, 142.43, 142.56, 167.78 ppm. These spectra match those previously reported for this compound.[16h]

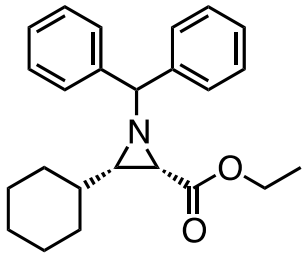

10b

*Preparation of (2S,3S)-ethyl 1-benzhydryl-3-cyclohexylaziridine-2-carboxylate (**10b**) using catalyst **33b**:* Aziridine **10b** was generated from imine **8b** (139 mg, 0.50 mmol,

1.00 equiv) according to Method A using 10 mol% (*R*)-VANOL (22.0 mg, 0.05 mmol, 0.10 equiv) to generate the catalyst **33b**. Upon work-up, the crude ^{1}H NMR indicated a 50:1 cis/trans ratio. The product was purified by column chromatography (silica gel, 3 cm x 30 cm, hexanes/EtOAc 19:1) and **10b** was obtained as a white solid (m.p. = 163-165 °C on 79% ee material) in 78% isolated yield (142 mg, 0.39 mmol). The optical purity of **10b** was determined to be 79% ee by HPLC analysis (Chiralcel-OD-H column, 99:1 hexane/2-propanol at 222nm, flow-rate: 1.0 mL/min): retention times t_R = 3.255 min (major enantiomer, **10b**) and t_R = 6.659 min (minor enantiomer, *ent*-**10b**).

Spectral data for **10b**: R_f = 0.26 (1:9 EtOAc/hexanes); ^{1}H NMR ($CDCl_3$, 500 MHz) δ 0.53-0.55 (m, 1H), 0.97-1.67 (m, 12H), 1.83 (t, 1H, *J* = 8.0 Hz), 2.29 (d, 1H, *J* = 7.0 Hz), 3.64 (s, 1H), 4.20-4.28 (m, 2H), 7.24-7.38 (m, 8H), 7.53 (d, 2H, *J* = 7.0 Hz) ppm; ^{13}C NMR ($CDCl_3$, 125 MHz) δ 14.32, 25.39, 25.57, 30.15, 30.75, 36.31, 43.44, 52.16, 60.72, 78.22, 126.93, 127.10, 127.46, 127.54, 128.31, 128.35, 128.40, 142.37, 142.77, 169.68 ppm. These spectra match those previously reported for this compound.[16h]

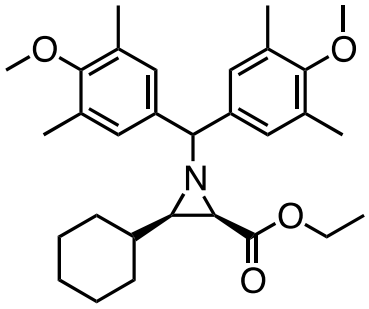

54

*Preparation of (2R,3R)-ethyl 1-(bis(4-methoxy-3,5-dimethylphenyl)methyl)-3-cyclohexylaziridine-2-carboxylate (**54**) using catalyst **47a**:* Aziridine **54** was generated from imine **53** (197 mg, 0.50 mmol, 1.00 equiv) according to Method A using 10 mol% (*S*)-VAPOL (27.0 mg, 0.05 mmol, 0.10 equiv) to generate the catalyst **47a**. Upon work-up, the crude ^{1}H NMR indicated a >100:1 cis/trans ratio. The product was purified by column chromatography (silica gel, 3 cm x 30 cm, hexanes/DCM 2:1) and **54** was obtained as a white solid (m.p. = 48-50 °C on 92% ee material) in 96% isolated yield (231 mg, 0.48 mmol). The optical purity of **54** was determined to be 92% ee by HPLC analysis (Chiralcel-OD-H column, 99:1 hexane/2-propanol at 222nm, flow-rate: 1.0 mL/min): retention times t_R = 3.122 min (major enantiomer, **54**) and t_R = 3.959 min (minor enantiomer, *ent*-**54**).

Spectral datal for **54**: t_R = 0.21 (2:1 hexanes/DCM); ^{1}H NMR ($CDCl_3$, 500 MHz) δ 0.48-0.55 (m, 1H), 0.81-1.14 (m, 4H), 1.23 (t, 3H, *J* = 7.5 Hz), 1.26-1.31 (m, 2H), 1.41-1.60 (m, 4H), 1.71-1.74 (m, 1H), 2.17 (d, 1H, *J* = 7.0 Hz), 2.21 (s, 6H), 2.22 (s, 6H), 3.35 (s, 1H), 3.63 (s, 3H), 3.67 (s, 3H), 4.15-4.23 (m, 2H), 6.94 (s, 2H), 7.10 (s, 2H) ppm; ^{13}C NMR ($CDCl_3$, 75 MHz) δ 13.9, 15.6, 15.7, 24.9, 25.1, 25.7, 29.7, 30.9, 35.9, 43.0, 51.8, 59.0, 59.1, 60.1, 77.0, 126.9, 128.1, 129.8, 130.0, 137.7, 155.3, 155.8, 169.3 ppm. These spectra match those previously reported for this compound.[38]

5.1.4 Preparation of alcohol 52

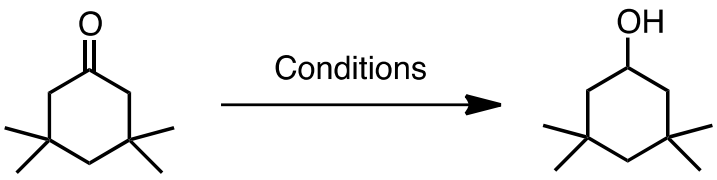

51 **52**

Table 2.6 (Appears in chapter two)

Entry	Conditions	Conversion (%) [b]	Yield (%) [c]
1	$NaBH_4$ (2 equiv), EtOH (2 drops), ether, 25 °C, 12 h	0	-
2	$NaBH_4$ (1.5 equiv), SiO_2, hexanes, 40 °C, 5 h	50	-
3	$NaBH_4$ (1.5 equiv), SiO_2, hexanes, 40 °C, 10 h	98	88

*Procedure for entry 1, Table 2.6 (**52**)*[61]*:* To a flame-dried 25 mL round bottom flask equipped with a stir bar was added anhydrous ether (4.0 mL) and ketone **51** (0.35 mL, 2.00 mmol, 1.00 equiv). The flask was sealed with a rubber septum and a nitrogen balloon was placed on top via a needle. The reaction was taken to 0 °C and stirred for 10 minutes. $NaBH_4$ was added in 2 portions (70 mg x 2 = 140 mg, 3.70 mmol, 1.85 equiv) stirring for 5 minutes between each portion at 0 °C. After both additions were completed, the reaction was slowly brought to room temperature and ethanol (2 drops) was added. The reaction was stirred at room temperature overnight under a nitrogen balloon. Water (2.5 mL) was added to the flask and the mixture was extracted with ether. The organic phases were combined and dried under $MgSO_4$. The drying agent was filtered off and the remaining solution was concentrated via rotary evaporation. The desired product was not formed. Proton NMR analysis revealed only starting material.

*Procedure for entries 2 and 3 (**52**)*[35]: To a flame-dried round bottom flask equipped with a stir bar was added ketone **51** (0.35 mL, 2.00 mmol, 1.00 equiv), hexanes (20 mL), SiO_2 (3.0 g; dried under reduced vacuum (0.1 mm Hg) prior to use), and $NaBH_4$ (114

mg, 3.00 mmol, 1.50 equiv). A condenser was placed on the flask with a rubber septum and nitrogen balloon sealing the top of the condenser. The reaction mixture was stirred at 40 °C for 5-10 h under reflux conditions. The flask was cooled to room temperature and the mixture was poured over a pad of Celite. The flask was rinsed with ether and the Celite was flushed with ether. The solution was then concentrated via rotary evaporation to give the crude alcohol **52** (m.p. = 82-85 °C) in 50-98% conversion as a white solid (5 hours refluxing gave 50% conversion and 10 hours refluxing gave 98% conversion). The alcohol was purified via sublimation (5 mm Hg at 35 °C) to give pure **52** (m.p. = 84-86 °C) in 88% isolated yield (274 mg, 1.80 mmol).

Spectral data for alcohol **52**: ^{1}H NMR ($CDCl_3$, 300 MHz) δ 0.90 (s, 6H), 0.93-1.04 (m, 9H), 1.18 (td, 1H, *J* = 13.5 Hz, 2.1 Hz), 1.42 (s, 1H), 1.70 (d of mult, 2H, *J* = 12.3 Hz), 3.88 (dt, 1H, *J* = 22.4 Hz, 3.3 Hz) ppm; ^{13}C NMR ($CDCl_3$, 125 MHz) δ 27.74, 32.59, 35.16, 48.77, 51.49, 66.13 ppm.

5.1.5 Preparation of aziridine 60 to verify absolute configuration of aziridine 10b

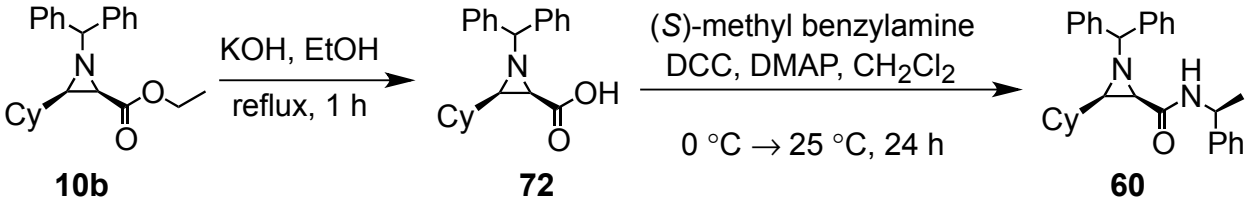

10b **72** **60**

*Preparation of (2R,3R)-1-benzhydryl-3-cyclohexylaziridine-2-carboxylic acid (**72**):* To a flame-dried 25 mL round bottom flask equipped with a stir bar was added aziridine **10b** (210 mg, 0.57 mmol, 1.00 equiv) and ethanol (2.0 mL). To this suspension was added aqueous KOH (164 mg, 2.80 mmol, 4.90 equiv dissolved in 2.0 mL water). A condenser was added to the round bottom and sealed with a rubber septum and nitrogen balloon.

The mixture was refluxed for 1 h (all solid dissolved). The reaction mixture was cooled and aqueous citric acid (2 N, 3.0 mL) was added to generate a precipitate. The precipitate was filtered and rinsed with water. The solid was then dissolved in methylene chloride and dried over $MgSO_4$. The drying agent was filtered off and the solution was concentrated via rotary evaporation. Aziridine **72** was then directly subjected to the following reaction without further purification.

Spectral data for alcohol **72**: ^{1}H NMR ($CDCl_3$, 500 MHz) δ 0.59-0.64 (m, 1H), 0.96-1.30 (m, 6H), 1.49-1.66 (m, 4H), 1.99 (t, 1H, *J* = 8.5 Hz), 2.47 (d, 1H, *J* = 7.0 Hz), 3.76 (s, 1H), 7.26 (q, 2H, *J* = 7.5 Hz), 7.32 (t, 4H, *J* = 4.0 Hz), 7.40 (t, 4H, *J* = 8.5 Hz), 8.80 (br s, 1H) ppm; ^{13}C NMR ($CDCl_3$, 125 MHz) δ 25.29, 25.37, 25.93, 29.88, 30.83, 37.07, 43.14, 53.13, 77.54, 126.80, 127.53, 127.82, 127.90, 128.55, 128.73, 141.27, 141.77, 171.20 ppm.

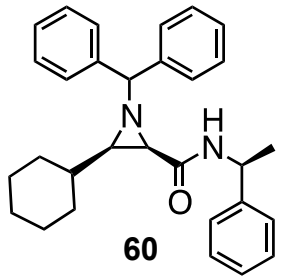

60

Preparation of (2*R*,3*R*)-1-benzhydryl-3-cyclohexyl-*N*-((*S*)-1-phenylethyl)aziridine-2-carboxamide ***60***: To a flame-dried 25 mL round bottom flask equipped with a stir bar was added aziridine **72** (35.5 mg, 0.10 mmol, 1.00 equiv), DMAP (18.3 mg, 0.15 mmol, 1.50 equiv) and methylene chloride (1.0 mL). The reaction was taken to 0 °C followed by the addition of DCC (31.0 mg, 0.15 mmol, 1.50 equiv) and (*S*)-methylbenzyl amine (36.3 mg, 0.30 mmol, 3.00 equiv). The solution solidified directly. However, the reaction

was brought to room temperature and stirred overnight as a slurry. The urea was filtered and the filtrate was washed with HCl (1 M) followed by NaOH (1 M). The organic phase was dried over $MgSO_4$. The drying agent was filtered and the volatiles were removed via rotary evaporation to give the crude aziridine **60**. After purification by column chromatography (silica gel, 2.5 x 25 cm, hexanes/EtOAc 4:1), the product **60** was obtained as a white solid (m.p. = 145.5-148 °C) in 29% yield (13.5 mg, 0.03 mmol), which was recrystallized from hexanes/EtOAc. The solvent evaporated overnight leaving one large crystal, which was submitted to x-ray analysis (see appendices for crystallographic data).

Spectral data for aziridine **60**: R_f = 0.25 (4:1 hexanes/EtOAc); ^1H NMR ($CDCl_3$, 300 MHz) δ 0.45-0.59 (m, 1H), 0.79-1.70 (m, 15H), 2.24 (d, 1H, *J* = 7.2 Hz), 3.57 (s, 1H), 5.05-5.14 (m, 1H), 7.06-7.19 (m, 15H) ppm; ^{13}C NMR ($CDCl_3$, 125 MHz) δ 21.40, 25.61, 26.01, 29.82, 31.09, 37.11, 45.10, 47.69, 52.74, 78.08, 126.20, 127.09, 127.26, 127.39, 127.54, 127.84, 128.35, 128.50, 128.58 (one extra sp^3 carbon peak than expected) ppm; IR (thin film, cm^{-1}) 3389 (m), 2924 (s), 1655 (s), 1510 (s), 700 (s); HRMS (ESI^+) calcd for $C_{30}H_{35}N_2O$ m/z 439.2749 ($[M+H]^+$), meas 439.2739; $[\alpha]^{20}_D$ +31.6° (c = 1.0, $CDCl_3$).

5.1.6 NMR analysis of VAPOL-B3 complexes

*Cold temp NMR studies of cyclohexanol catalyst **47a** seen in Figure 2.11 and 2.12:*

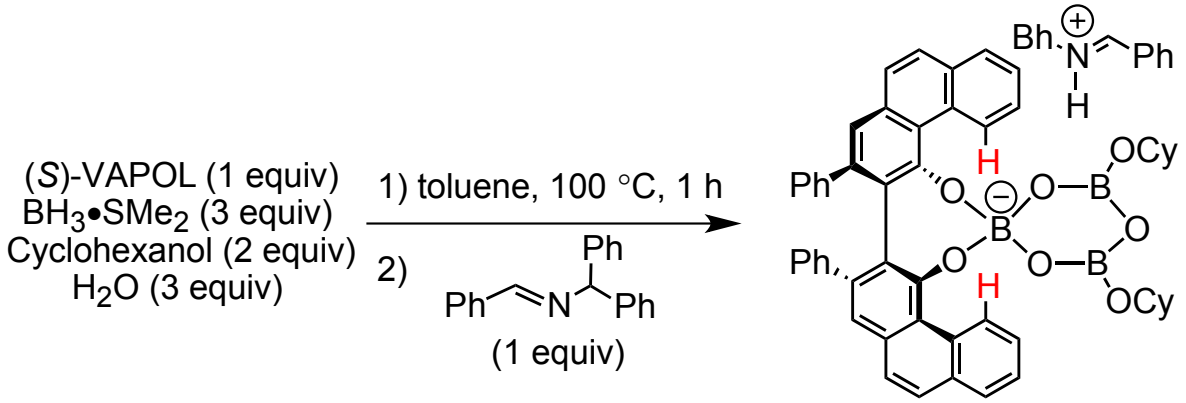

47a-imine **8a** complex

*Preparation of **47a**-imine **8a** complex:* To a flame-dried 50 mL Schlenk flask equipped with a stir bar and Teflon cap was added (*S*)-VAPOL (27.0 mg, 0.05 mmol, 1.00 equiv), cyclohexanol (10.0 mg, 0.10 mmol, 2.00 equiv dissolved in 0.5 mL d_8-toluene), borane dimethyl sulfide (2 M, 75 μL, 0.15 mmol, 3.00 equiv), and H_2O (2.7 μL, 0.15 mmol, 3.00 equiv). The Teflon cap was closed and the reaction was stirred under nitrogen at 100 °C for 1 h. The flask was cooled to room temperature and the Teflon cap was opened to a nitrogen line. An internal standard was added ($CHPh_3$; 12.2 mg, 0.05 mmol, 1.00 equiv) and the solution was transferred to a flame-dried quartz NMR tube. d_8-toluene (0.5 mL) was used to rinse the flask and the solvent was added to the NMR tube (total of 1.0 mL d_8-toluene). The proton and boron NMR were obtained at room temperature. Imine **8a** (13.5 mg, 0.05 mmol, 1.00 equiv dissolved in 0.3 mL d_8-toluene) was then added to the NMR tube and slowly mixed by inverting the tube several times. The proton and boron

NMR were acquired at room temperature once again. The NMR machine was then cooled and the proton and boron NMR were acquired at −60, −40, −20, and 0 °C. The yields of B2 and B3 were then calculated using the internal standard and the boron ratios at 19, 6, and 2 ppm were determined.

Table 5.1 Cold temp study of catalyst **47a** and imine **8a** complex

Entry	Conditions	Temp (°C)	VAPOL (%)	B2 (%)	B3/B3' (%)	Boron Ratio (19 / 6 / 2 ppm)
1	No imine	25	73	−	−	1 : 0 : 0
2	Imine	25	66	−	−	6 : 1 : 0.3
3	Imine	60	79	3	10/14	2.61 : 1 : 0.75
4	Imine	40	73	3	12/14	2.51 : 1 : 0.73
5	Imine	20	65	3	13/14	3.55 : 1 : 0.38
6	Imine	0	43	2	6/7	4.2 : 1 : 0.36
7	Imine	return to 25	48	2	−	6.85 : 1 : 0

NMR studies of catalyst 33a-imine 8a complex:

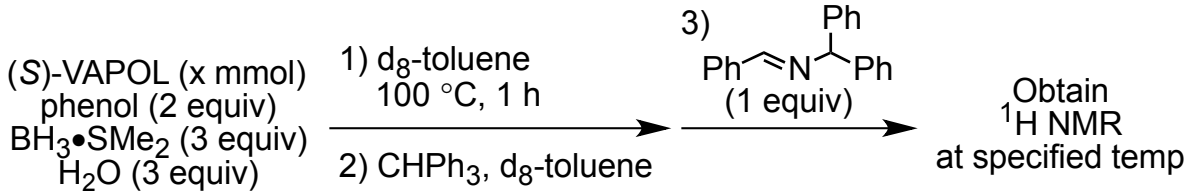

*Preparation of catalyst **33a**-imine **8a** complex (Table 2.11):* To a flame-dried 50 mL Schlenk flask equipped with a stir bar and Teflon cap was added (*S*)-VAPOL (x mmol, 1.00 equiv), phenol (2.00 equiv), d_8-toluene (0.5 mL), borane dimethyl sulfide (2 M, 3.00 equiv), and H_2O (3.00 equiv). The Teflon cap was closed and the reaction was stirred under nitrogen at 100 °C for 1 h. The flask was cooled to room temperature and the Teflon cap was opened to a nitrogen line. An internal standard was added ($CHPh_3$; 1.00

equiv) and the solution was transferred to a flame-dried quartz NMR tube. d_8-toluene (0.5 mL) was used to rinse the flask and the solvent was added to the NMR tube (total of 1.0 mL d_8-toluene). The proton and boron NMR were obtained at room temperature. Imine **8a** (1 equiv dissolved in 0.3 mL d_8-toluene) was then added to the NMR tube and slowly mixed by inverting the tube several times. The proton and boron NMR were acquired at the specified temperatures. Refer to Table 2.11 for results.

Note: The scale of the reaction was done at both 0.05 and 0.10 mmol (see Table 2.11). This was to determine if concentration factors were affecting the amount of catalyst formed.

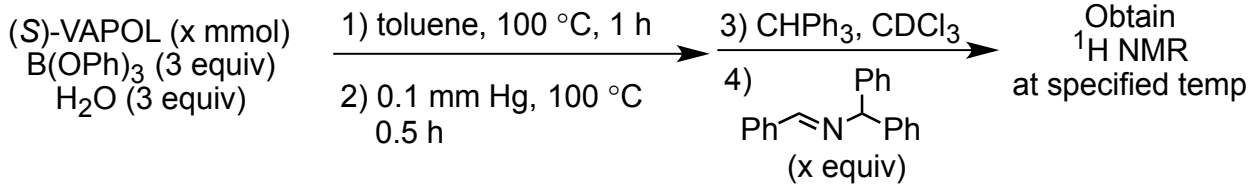

*Preparation of catalyst **33a**-imine **8a** complex using triphenyl borate (Table 2.12):* To a flame-dried 50 mL Schlenk flask equipped with a stir bar and Teflon cap was added (*S*)-VAPOL (x mmol, 1.00 equiv), $B(OPh)_3$ (3.00 equiv), toluene (1.0 mL), and H_2O (3.00 equiv). The Teflon cap was closed and the reaction was stirred under nitrogen at 100 °C for 1 h. At 100 °C, the Teflon cap was slowly released and the vacuum (0.1 mm Hg) was applied at 100 °C for 0.5 h. The flask was cooled to room temperature and the Teflon cap was opened to a nitrogen line. An internal standard was added ($CHPh_3$; 1.00 equiv) and the solids were dissolved in $CDCl_3$ (1.0 mL). The solution was then transferred to a flame-dried quartz NMR tube. The proton and boron NMR were

obtained at room temperature. Imine **8a** (x equiv) was then added to the NMR tube and slowly mixed by inverting the tube several times. The proton and boron NMR were once again acquired. Refer to Table 2.12 for equivalents used and percent yields calculated via the internal standard.

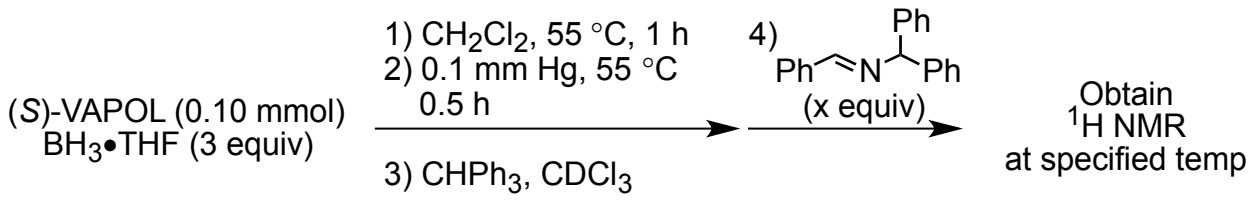

*Preparation of catalyst **33a**-imine **8a** complex using borane tetrahydrofuran (Table 2.13):* To a flame-dried 50 mL Schlenk flask equipped with a stir bar and Teflon cap was added (*S*)-VAPOL (53.0 mg, 0.10 mmol, 1.00 equiv), CH_2Cl_2 (2.0 mL), and BH_3•THF (300 μL, 0.30 mmol, 3.00 equiv). The Teflon cap was closed and the reaction was stirred under nitrogen at 55 °C for 1 h. At 55 °C, the Teflon cap was slowly released and the vacuum (0.1 mm Hg) was applied at 100 °C for 0.5 h. The flask was cooled to room temperature and the Teflon cap was opened to a nitrogen line. An internal standard was added ($CHPh_3$; 24.4 mg, 0.10 mmol, 1.00 equiv) and the solids were dissolved in $CDCl_3$ (1.0 mL). The solution was then transferred to a flame-dried quartz NMR tube. The proton and boron NMR were obtained at room temperature. Imine **8a** (x equiv) was then added to the NMR tube and slowly mixed by inverting the tube several times. The proton and boron NMR were once again acquired. Refer to Table 2.13 for results.

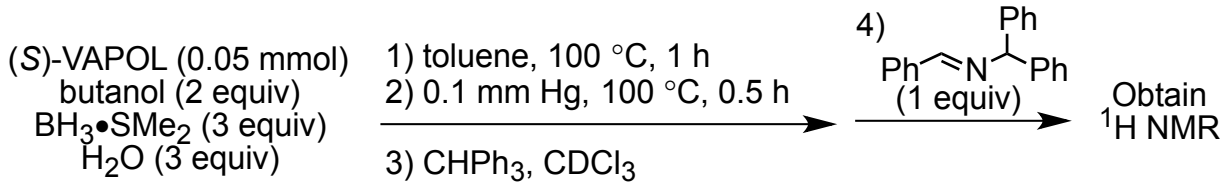

*Preparation of butanol catalyst **46a**-imine **8a** complex (Table 2.14):* To a flame-dried 50 mL Schlenk flask equipped with a stir bar and Teflon cap was added (*S*)-VAPOL (27.0 mg, 0.05 mmol, 1.00 equiv), n-butanol (9.2 mg, 0.10 mmol, 2.00 equiv dissolved in 0.5 mL d_8-toluene), borane dimethyl sulfide (2 M, 75 μL, 0.15 mmol, 3.00 equiv), and H_2O (2.7 μL, 0.15 mmol, 3.00 equiv). The Teflon cap was closed and the reaction was stirred under nitrogen at 100 °C for 1 h. The flask was cooled to room temperature and the Teflon cap was opened to a nitrogen line. An internal standard was added ($CHPh_3$; 12.2 mg, 0.05 mmol, 1.00 equiv) and the solution was transferred to a flame-dried quartz NMR tube. d_8-toluene (0.5 mL) was used to rinse the flask and the solvent was added to the NMR tube (total of 1.0 mL d_8-toluene). The proton and boron NMR were obtained at room temperature. Imine **8a** (13.6 mg, 0.05 mmol, 1.00 equiv dissolved in 0.3 mL d_8-toluene) was then added to the NMR tube and slowly mixed by inverting the tube several times. The proton and boron NMR were acquired at room temperature once again. Refer to Table 2.14 for results.

5.1.7 Computational studies seen in Table 2.7

Figure 5.1 Catalyst-imine structures used to determine the H-bond distances seen in Table 2.7

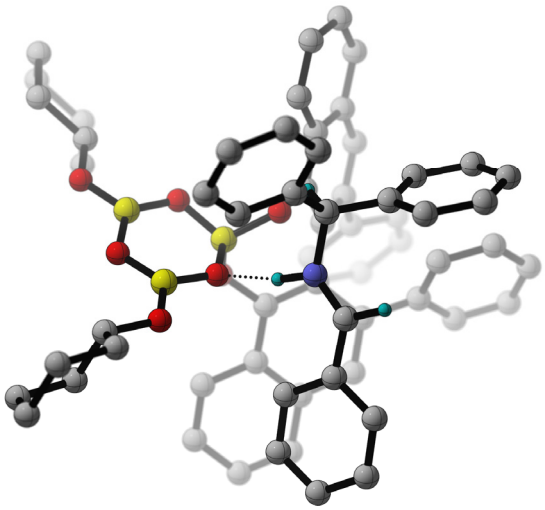

Catalyst **47b**-Imine **8a**

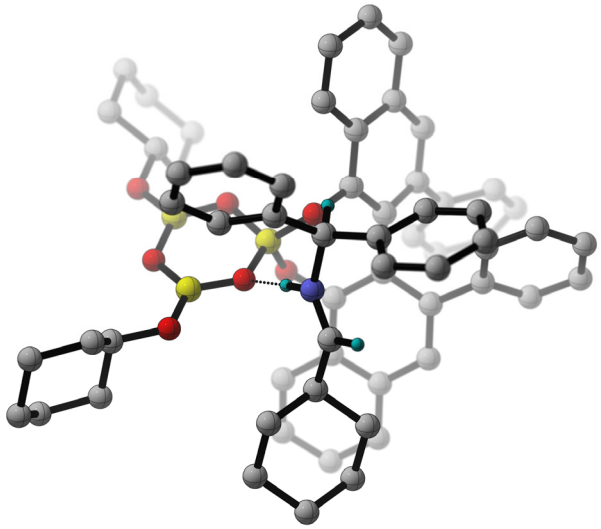

Catalyst **47b**-Imine **8a**

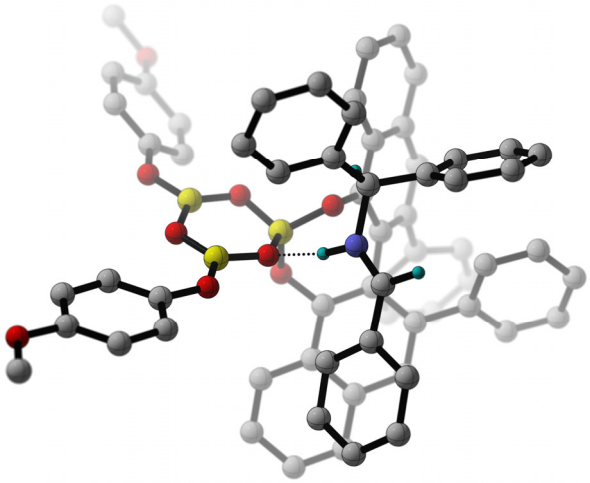

Catalyst **41b**-Imine **8a**

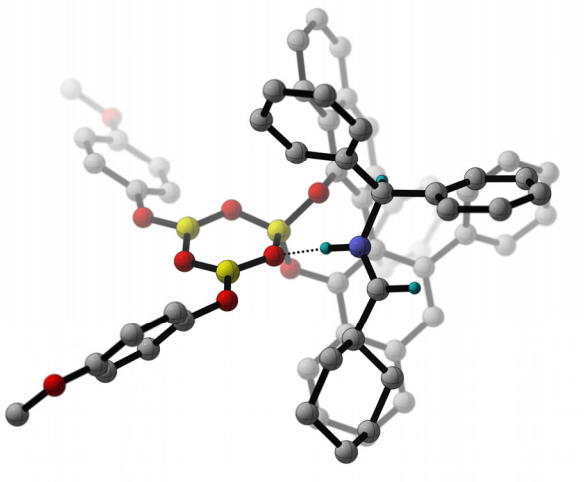

Catalyst **41b**-Imine **8b**

Figure 5.1 (Cont'd)

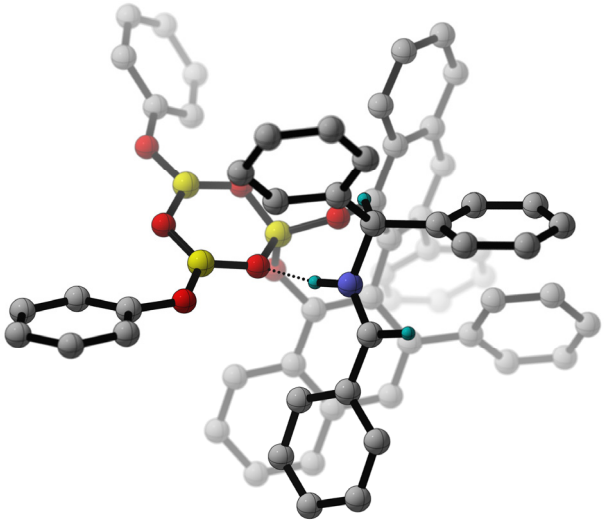

Catalyst **33b**-Imine **8a**

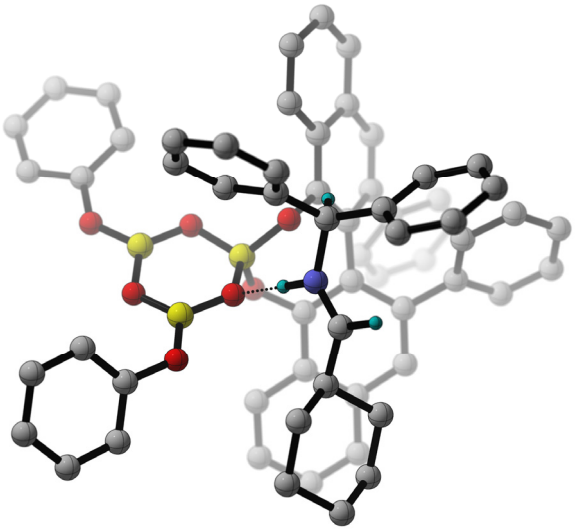

Catalyst **33b**-Imine **8b**

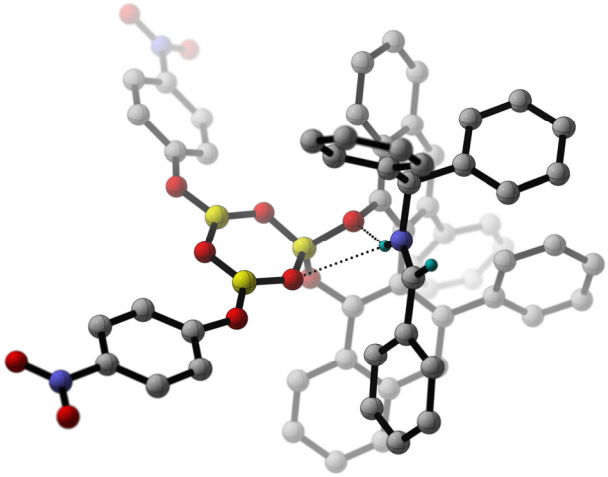

Catalyst **45b**-Imine **8a**

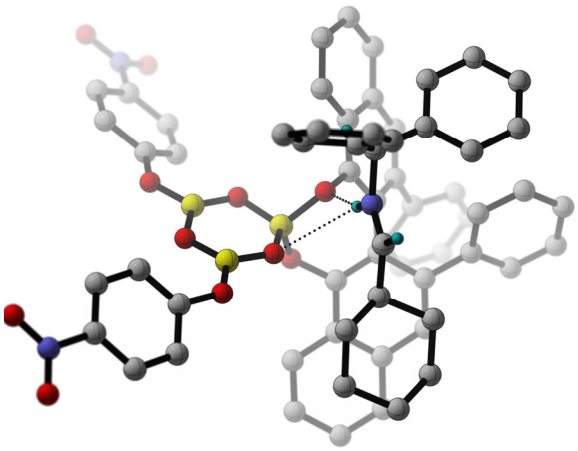

Catalyst **45b**-Imine **8b**

*For the synthesis of t-butyl VANOL ligand refer to chapter four experimental section.

5.2 Experimental for chapter three

5.2.1 Synthesis of imine 67

*Preparation of aldehyde **65**:*

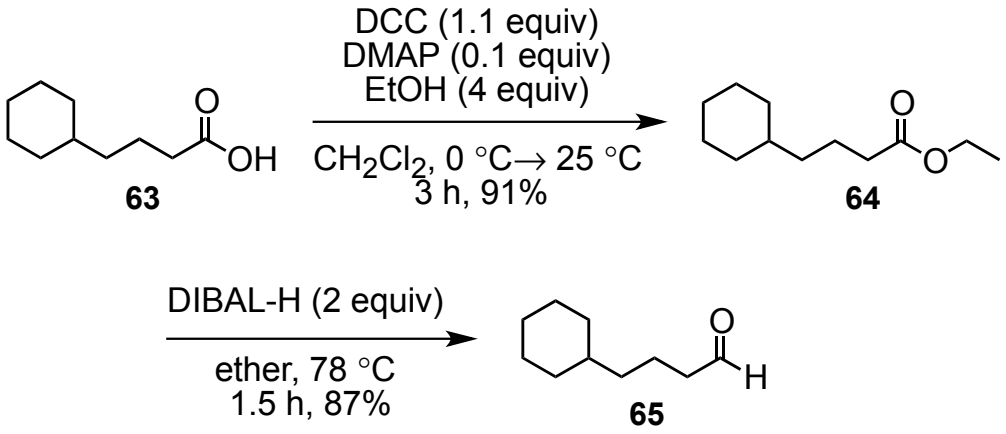

*Preparation of ethyl 4-cyclohexylbutanoate **(64):*** To a flame-dried 100 mL round bottom flask equipped with a stir bar was added 4-cyclohexylbutanoic acid (1.70 g, 10.0 mmol, 1.00 equiv) and CH_2Cl_2 (10 mL). To the stirred solution was added ethanol (2.34 mL, 40.0 mmol, 4.00 equiv) and DMAP (0.12 g, 1.00 mmol, 0.10 equiv). The reaction was cooled to 0 °C (NaCl ice slurry) and DCC (2.27 g, 11.0 mmo, 1.10 equiv) was added. The reaction stirred at 0 °C for 5 minutes and was then warmed to room temperature. The reaction continued to be stirred at room temperature for 3 h. The urea was filtered and rinsed with CH_2Cl_2 (20 mL). The product was washed with HCl (0.5 N, 50 mL x 2) followed by sat. aq. $NaHCO_3$ (50 mL). The organic layer was dried over $MgSO_4$ and concentrated via rotary evaporation to give the crude product. Ester **64** was then purified by column chromatography (silica gel, 2.5 cm x 25 cm, 1:5 CH_2Cl_2/hexanes) to give the pure ester as a colorless liquid in 91% yield (1.80 g, 9.10 mmol). Similar yields were observed when using distillation as the purification method.

Spectral data for **64**: R_f = 0.55 (1:1 CH_2Cl_2/hexanes); ^1H NMR ($CDCl_3$, 300 MHz) δ 0.76-0.89 (m, 2H), 1.04-1.24 (m, 9H), 1.52-1.70 (m, 7H), 2.22 (t, 2H, *J* = 7.6 Hz), 4.08 ppm (q, 2H, *J* = 7.1 Hz) ppm; ^{13}C NMR ($CDCl_3$, 75 MHz) δ 14.13, 22.27, 26.24, 26.56, 33.15, 34.53, 36.81, 37.29, 59.95, 173.66 ppm.

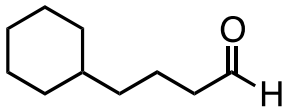

65

*Preparation of 4-cyclohexylbutanal **(65)**:* To a 500 mL flame-dried round bottom flask was added ethyl 4-cyclohexylbutanoate **64** (3.97 g, 20.0 mmol, 1.00 equiv) and anhydrous ether (40 mL). The flask was cooled to -78 °C. DIBAL-H (1 M in hexanes; 40 mL, 40.0 mmol, 2.00 equiv) was added slowly over a period of 10 min. The reaction was stirred for an additional 1.5 h at -78 °C under nitrogen atmosphere followed by quenching with methanol/H_2O (12 mL, 1:1 (v/v)). The flask was warmed to room temperature and ether (100 mL) was added followed by sat. aq. sodium potassium tartrate (120 mL). The mixture was stirred for 5.5 h. The aqueous layer was extracted with ether (100 mL x 3). The organic layers were combined, dried over $MgSO_4$ and concentrated *in vacuo* to afford the crude aldehyde **65**. The crude aldehyde was distilled (0.5mm/71°C) to give the pure product **65** as a colorless oil in 69% yield (30.14 g, 0.20 mmol).

Spectral data for **65**: ^{1}H NMR ($CDCl_3$, 300 MHz) δ 0.63-0.84 (m, 2H), 0.94-1.22 (m, 8H), 1.42-1.72 (m, 5H), 2.29 (td, 2H, *J* = 7.3, 1.9 Hz), 9.64 (s, 1H, *J* = 1.7 Hz) ppm; ^{13}C NMR ($CDCl_3$, 75 MHz) δ 19.34, 26.19, 26.51, 33.09, 36.79, 37.33, 44.03, 202.67 ppm.

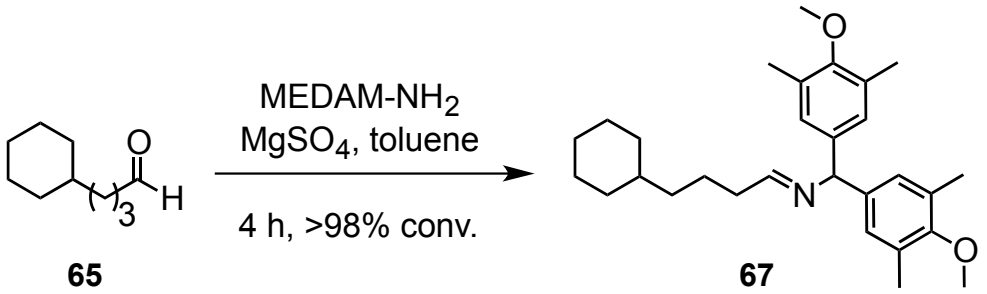

65 **67**

*Preparation of N-(4-cyclohexylbutylidene)-1,1-bis(4-methoxy-3,5-dimethylphenyl) methanamine **(67)**:* To a 50 mL flame-dried round bottom flask was added $MgSO_4$ (0.30 g, 2.50 mmol, 2.5 equiv), which was then flame-dried a second time under vacuum (0.1 mm Hg). Anhydrous CH_2Cl_2 (2.0 mL) and MEDAM amine **66** (0.299 g, 1.00 mmol, 1.00 equiv) were added and stirred for 5 min. To the reaction flask was added 4-cyclohexylbutanal **65** (0.174 g, 1.15 mmol, 1.15 equiv) and the reaction was stirred at room temperature for 4 h under a nitrogen atmosphere. The product was filtered via a filter syringe (syringe and filter were previously flushed with nitrogen prior to use) and subjected directly to the AZ reaction without isolation or purification.

Spectral Data for **67**: ^{1}H NMR (300 MHz, $CDCl_3$) δ 0.89-0.96 (m, 2H), 1.22-1.32 (m, 4H), 1.62 (quint, 3H, *J* = 7.5, 5.8 Hz), 1.73-1.76 (m, 5H), 2.21 (quint, 2H, *J* = 2.2, 2.3 Hz), 2.22-2.30 (m, 1H), 2.31 (s, 6H), 2.32 (s, 6H) 3.46 (s, 6H), 5.31 (s, 1H), 7.10 (s, 2H), 7.14 (s, 2H), 7.78 ppm (t, 1H, *J* = 4.7 Hz) ppm; ^{13}C NMR ($CDCl_3$, 75 MHz) δ 16.18,

23.36, 26.32, 26.67, 33.30, 36.07, 59.59, 77.71, 127.74, 130,56, 139.20, 155.70, 165.16 ppm.

5.2.2 Synthesis of cis-aziridines having remote functionalities using a previously established method

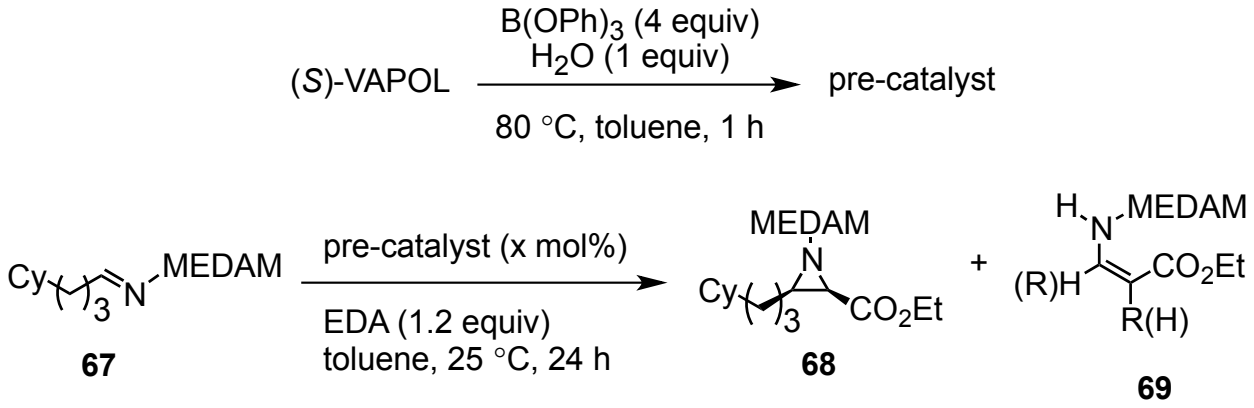

Preparation of (2*R*,3*R*)-ethyl 1-(bis(4-methoxy-3,5-dimethylphenyl)methyl)-3-(3-cyclohexylpropyl)aziridine-2-carboxylate ***(68)****: Pre-catalyst formation:* To a 25 mL flame-dried Schlenk flask flushed with nitrogen was added (*S*)-VAPOL (54.0 mg, 0.10 mmol) and $B(OPh)_3$ (111 mg, 0.40 mmol, 4.00 equiv). Under nitrogen flow, dry toluene (2.0 mL) was added to dissolve the two reagents and this was followed by the addition of water (1.8 μL, 0.10 mmol, 1.00 equiv). The flask was sealed under nitrogen and stirred at 80°C for 1 h. After 1 h, a vacuum (0.1 mm Hg) was carefully applied to remove all volatiles. The vacuum was maintained for a period of 30 min at 80°C. The flask was then filled with nitrogen and the catalyst mixture was allowed to cool to room temperature.

Aziridination reaction: To the flask containing 10 mol% catalyst was added imine **67** (436 mg, 1.00 mmol) and dry toluene (2 mL). The reaction mixture was stirred for 5 min

then EDA **9** (124 μL, 1.20 mmol, 1.20 equiv) was added. The mixture was stirred for 24 h at room temperature. Immediately upon addition of EDA, the reaction mixture became an intense yellow and the formation of bubbles from the release of nitrogen was noted. The reaction was quenched by addition of hexanes (6 mL) after 24 h. The reaction mixture was then transferred to a 100 mL round bottom flask. The reaction Schlenk flask was rinsed with CH_2Cl_2 (5 mL x 2) and the rinse was added to the 100 mL round bottom flask. The resulting solution was then concentrated by rotary evaporation followed by exposure to high vacuum (0.55 mm Hg) for 5 min to afford the crude aziridine **68** as an off-white solid. The conversion was determined from the crude ^{1}H NMR spectrum and the isolated yield of the aziridine. The yields of the enamine side products were determined by ^{1}H NMR analysis of the crude reaction mixture by integration of the *N*-H proton relative to that of the *cis*-aziridine ring protons (integrated to 1.00 H) with the aid of the isolated yield of the *cis*-aziridine. Purification of the crude aziridine by silica gel chromatography (4.5 x 45 mm column, 1:25 ethyl acetate/hexanes as eluent, under gravity) afforded pure aziridine **68** as an off white solid in 67% yield (348 mg, 0.67 mmol). Two column chromatography runs were required for the complete isolation of the aziridine **68**. The optical purity of **68** was determined to be 94% ee by HPLC analysis (Pirkle R,R-(whelk)-01 column, 99:1 hexanes/*i*PrOH at 222 nm, flow-rate: 1.0 mL/min). Retention times, t_R = 11.329 min (major enantiomer, **68**) and t_R = 18.335 min (minor enantiomer, *ent*-**68**).

Spectral data for **68:** R_f = 0.19 (1:9 EtOAc/hexanes); ^{1}H NMR ($CDCl_3$, 500 MHz) δ 0.92-1.18 (m, 8H), 1.27 (t, 2H, *J* = 7.1 Hz), 1.38-1.66 (m, 9H), 1.93 (q, 1H, *J* = 5.9, 7.1

Hz), 2.16 (d, 1H, *J* = 4.4 Hz), 2.21 (s, 12H), 3.38 (s, 1H), 3.65 (d, 6H, *J* = 4.9 Hz), 4.15-4.19 (m, 2H), 5.28 (s, 1H), 6.99 (s, 2H), 7.07 (s, 2H) ppm. ^{13}C NMR ($CDCl_3$, 125 MHz) δ 14.29, 16.07, 16.11, 24.55, 26.31, 26.33, 26.62, 28.23, 33.03, 33.25, 36.94, 37.58, 43.54, 47.04, 59.48, 59.50, 60.59, 77.37, 127.34, 128.09, 130.37, 130.41, 137.77, 138.15, 155.76, 156.17, 169.64 ppm. $[\alpha]^{20}_D$ = +36 (c = 1.0, EtOAc) on 91 % *ee* material.

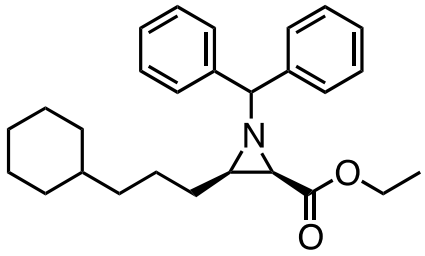

92

*Preparation of (2R,3R)-ethyl 1-benzhydryl-3-(3-cyclohexylpropyl)aziridine-2-carboxylate **(92):*** Purification of the crude aziridine by silica gel chromatography (4.5 x 45 mm column, 1:25 ethyl acetate/hexanes as eluent, under gravity) afforded pure aziridine **92** as an off white solid in 31% yield (125 mg, 0.31 mmol). Three column chromatography runs were required for the complete isolation of the aziridine **92**. The optical purity of **92** was determined to be 41% ee by HPLC analysis (CHIRALCEL OD-H column, 90:10 hexanes/*i*PrOH at 222 nm, flow-rate: 1.0 mL/min). Retention times, t_R = 3.938 min (major enantiomer **92**) and t_R = 2.933 min (minor enantiomer, *ent*-**92**).

Spectral data for **92**: R_f = 0.12 (1:25 EtOAc/Hexanes); ^1H NMR ($CDCl_3$, 500 MHz) δ 0.64-0.78 (m, 2H), 0.92-1.14 (m, 8H), 1.23 (t, 3H, *J* = 7.1 Hz), 1.38-1.68 (m, 9 H), 2.00 (q, 1 H, *J* = 6.6, 13 Hz), 2.25 (d, 1 H, *J* = 6.8 Hz), 3.64 (s, 1 H), 4.11-4.28 (m, 2 H), 7.18

(m, 2 H), 7.23-7.32 (m, 4 H), 7.37 (dd, 2 H, *J* = 1.7, 8.3 Hz), 7.45 ppm (dd, 2 H, *J* = 1.5, 8.8 Hz); ^{13}C NMR ($CDCl_3$, 75 MHz) δ 14.28, 24.41, 26.34, 26.35, 26. 68, 28.15, 33.04, 36.86, 37.50, 43.42, 46.92, 60.68, 77.98, 126.98, 127.16, 127.33, 127.91, 128.34, 128.34, 142.49, 142.87, 169.53 ppm; IR (thin film): v = 1196s, 1448w, 1456w, 1732s, 2851m, 2929s cm^{-1}; CHN (%) for $C_{27}H_{35}NO_2$: 81.33 (C%), 8.45 (H%), and 3.37 (N%).

5.2.3 General procedure for the one pot multi-component reaction

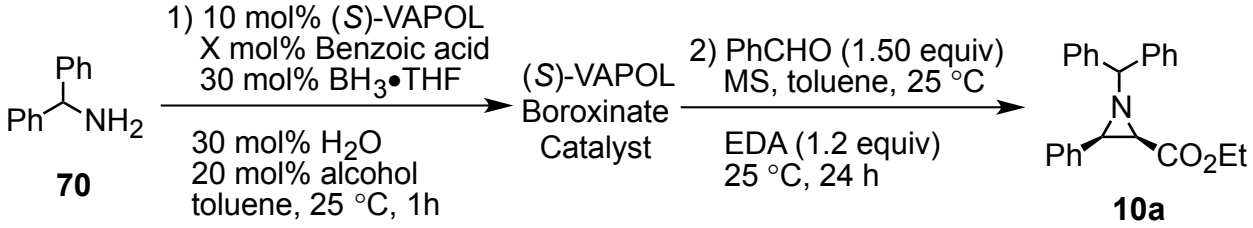

*General procedure using phenol to generate catalyst **33a** to synthesize aziridine **10a**:* To a flame-dried 25 mL round bottom flask equipped with a stir bar was added (*S*)-VAPOL (27.0 mg, 0.05 mmol, 0.10 equiv), phenol (9.4 mg, 0.10 mmol, 0.20 equiv), benzoic acid (3.0 mg, 0.025 mmol, 0.05 equiv), and toluene (0.5 mL). While the reaction stirred, borane tetrahydrofuran complex (1 M, 150 μL, 0.15 mmol, 0.30 equiv), H_2O (2.7 μL, 0.15 mmol, 0.30 equiv), and benzhydryl amine (86 μL, 0.5 mmol, 1.00 equiv) were added in that order. The reaction flask was sealed with a rubber septum and nitrogen balloon and stirred at room temperature for 1 h. While the reaction is stirring, 4Å powdered molecular sieves were flame-dried and cooled under reduced pressure (0.1 mm Hg). After the 1 h of stirring, the molecular sieves were added followed by benzaldehyde (73 μL, 0.75 mmol, 1.50 equiv) and toluene (0.5 mL). The reaction stirred for ca. 1 min while the EDA was being measured. EDA (62 μL, 0.60 mmol, 1.20 equiv) was added and the flask was sealed once again with a rubber septum and nitrogen

balloon. The reaction stirred under nitrogen at room temperature for 24 h. The slurry was then filtered over a pad of Celite and rinsed with EtOAc (20 mL x 2). The volatiles were removed by rotary evaporation to give the crude aziridine **10a** as an off-white solid. The crude product was purified by column chromatography (silica gel, 3 cm x 30 cm, 1:19 EtOAc/hexanes) to give aziridine **10a** as a white solid. See chapter two experimental section for characterization of aziridines **10a** and **10b**.

5.2.4 Attempted reductive ring opening of aliphatic aziridines

Synthesis of aziridines **71** and **72**: *For preparation of (2R,3R)-1-benzhydryl-3-cyclohexylaziridine-2-carboxylic acid (**72**): See section 5.1.5 of experimental.*

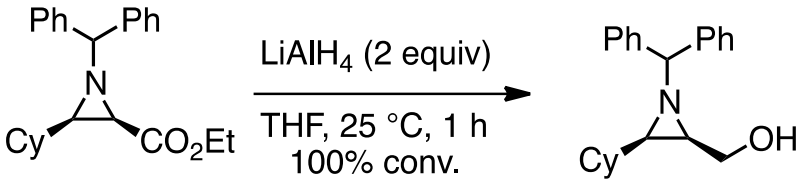

10b **71**

*Preparation of ((2R,3R)-1-benzhydryl-3-cyclohexylaziridin-2-yl)methanol (**71**):* To a flame-dried 25 mL round bottom flask equipped with a stir bar was added aziridine **10b** (20.3, 0.56 mmol, 1.00 equiv) and THF (4.0 mL). A suspension of $LiAlH_4$ (43.0 mg, 1.12 mmol, 2.00 equiv, in 1.2 mL THF) was added to the reaction flask via syringe drop wise at room temperature. The reaction stirred under a nitrogen balloon at room temperature for 1 h (the reaction was monitored by TLC). H_2O (0.4 mL) was added slowly to the reaction vessel followed by KOH (0.15 M, 0.4 mL), and once again H_2O (0.4 mL). The slurry was filtered through a pad of Celite and rinsed with ether followed by CH_2Cl_2. The

volatiles were removed by rotary evaporation to give the crude product (m.p. = 103-108 °C). The aziridine was purified by column chromatography (silica gel, 2.5 cm x 25 cm, 1:3 EtOAc/hexanes) to give the pure aziridine **71** as a white solid (m. p. = 108-111.5 °C) in 90% yield (162 mg, 0.50 mmol).

Spectral data for **71:** R_f = 0.29 (1:3 EtOAc/hexanes); ^{1}H NMR ($CDCl_3$, 500 MHz) δ 0.22-0.41 (m, 1H), 0.88-1.59 (m, 12H), 1.71-1.79 (m, 1H), 3.51 (s, 1H), 3.51-3.56 (m, 1H), 3.64-3.69 (m, 1H), 7.12-7.28 (m, 6H), 7.33 (d, 2H, *J* = 7.5 Hz), 7.39 (d, 2H, *J* = 7.5 Hz); ^{13}C NMR ($CDCl_3$, 125 MHz) δ 25.65, 25.77, 26.21, 30.96, 31.45, 36.96, 44.70, 50.62, 60.70, 78.94, 127.09, 127.20, 127.27, 127.97, 128.25, 128.62, 143.17, 143.58 ppm; IR (thin film, cm^{-1}) 3314 (br), 3030 (m), 2917 (s), 2848 (s), 1449 (m); HRMS (ESI$^+$) calcd for $C_{22}H_{28}NO$ m/z 322.2171 ($[M+H]^+$), meas 322.2168; $[\alpha]^{20}_D$ = −5.9 (c = 1.0, $CDCl_3$).

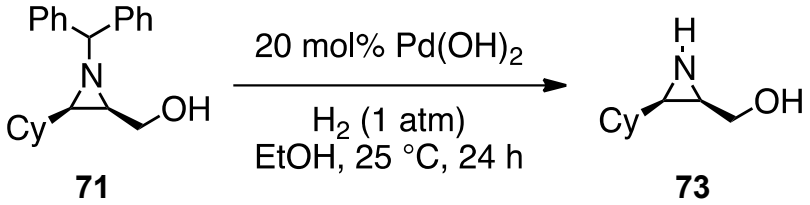

71 **73**

*Preparation of ((2R,3R)-3-cyclohexylaziridin-2-yl)methanol (**73**):* To a flame-dried 50 mL round bottom flask equipped with a stir bar was added aziridine **71** (80.0 mg, 0.25 mmol), 20 mol% $Pd(OH)_2$ (7.0 mg, 0.05 mmol), and ethanol (15 mL). The reaction was applied to vacuum (0.1 mm Hg) for ca. 2-3 seconds and flushed with H_2. This process was repeated three times. The reaction was then sealed under H_2 (1 atm) via a

hydrogen filled balloon and stirred at room temperature for 24 h. The slurry was filtered over a pad of Celite to and the volatiles were removed by rotary evaporation to give the crude aziridine **73**. The crude product was purified by crystallization from EtOAc and hexanes to give the pure aziridine as white solid crystals (m. p. = 80-81 °C) in 74% yield (28.5 mg, 0.18 mmol). For crystallographic data see appendices.

Spectral data for **73**: R_f = 0.72 (1:4 EtOAc/hexanes); ^{1}H NMR ($CDCl_3$, 500 MHz) δ 0.98-1.32 (m, 6H), 1.62-1.79 (m, 6H), 1.91 (dd, 1H, *J* = 9.0, 6.0 Hz), 1.97-1.99 (m, 1H), 2.36-2.40 (m, 1H), 3.52 (dd, 1H, *J* = 11.5, 7.0 Hz), 3.81 (dd, 1H, 11.5, 5.0 Hz) ppm; ^{13}C NMR ($CDCl_3$, 125 MHz) δ 25.80, 26.36, 31.02, 32.01, 36.37, 37.64, 41.11, 41.97, 61.24 ppm; IR (thin film, cm^{-1}) 3371 (m), 3200 (br), 2920 (s), 2847 (s), 1447 (s), 1041 (s), 867 (m); HRMS (ESI^+) calcd for $C_9H_{18}NO$ m/z 156.1388 ($[M+H]^+$), meas 156.1396; $[\alpha]^{20}_D$ = −2.2 (c = 1.0, $CDCl_3$).

5.3 Experimental for chapter four

General information: For all BINOL studies, there was a reference number assigned to each spectrum that is linked with the files for the original data collected. Within this reference number are five digits with the first two representing the research book number and the last three representing the page. An example is **Reference # 01281**, which represents research book 1 (first two digits are 01) and page 281 (last three digits are 281). The spectra were taken in three different solvents, which include CD_2Cl_2, $CDCl_3$ and deuterated DMSO. Pure (*R*)-BINOL was subjected to ^{1}H NMR using all three of these solvents. The three spectra are shown below.

Figure 5.2 BINOL in CD_2Cl_2

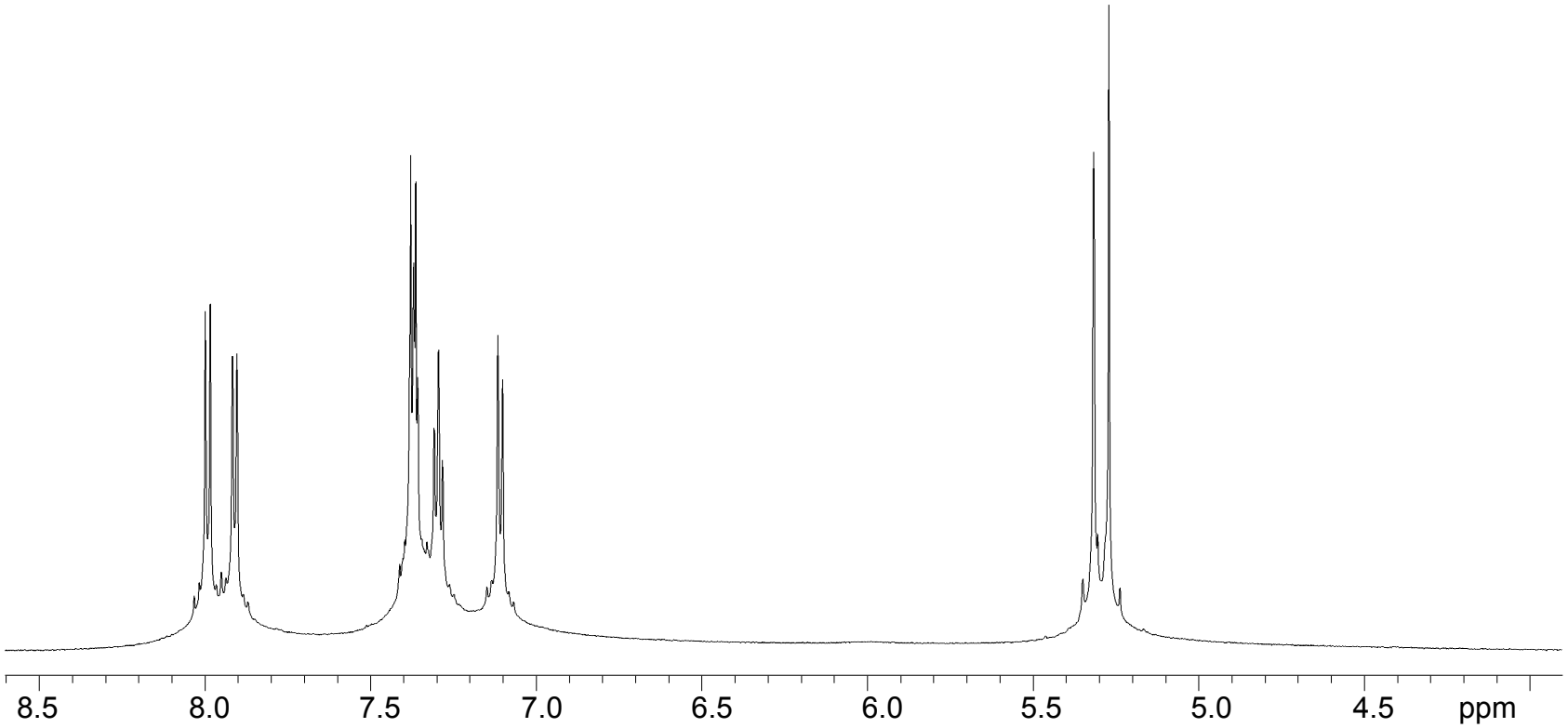

Figure 5.3 BINOL in $CDCl_3$

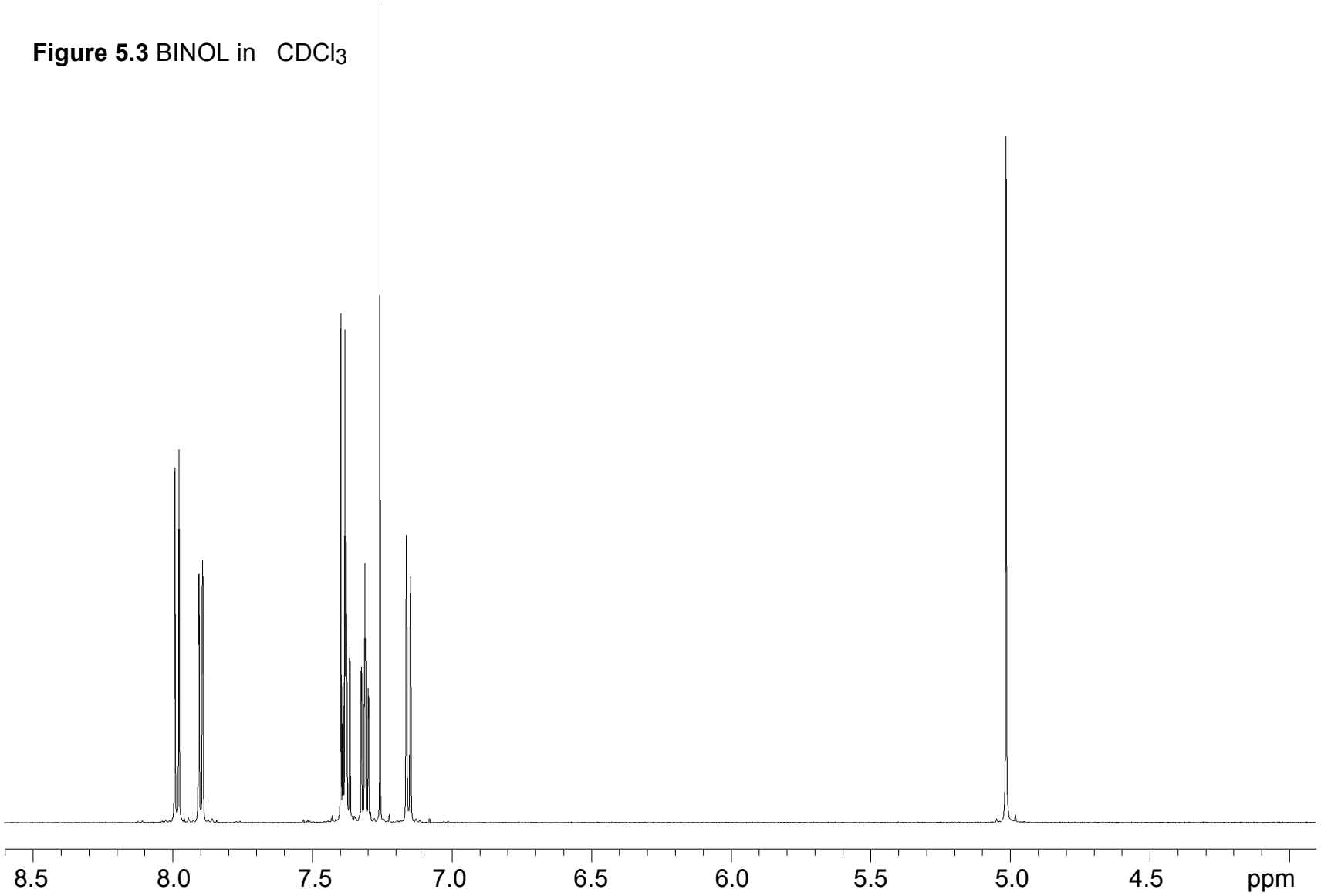

Figure 5.4 BINOL in DMSO

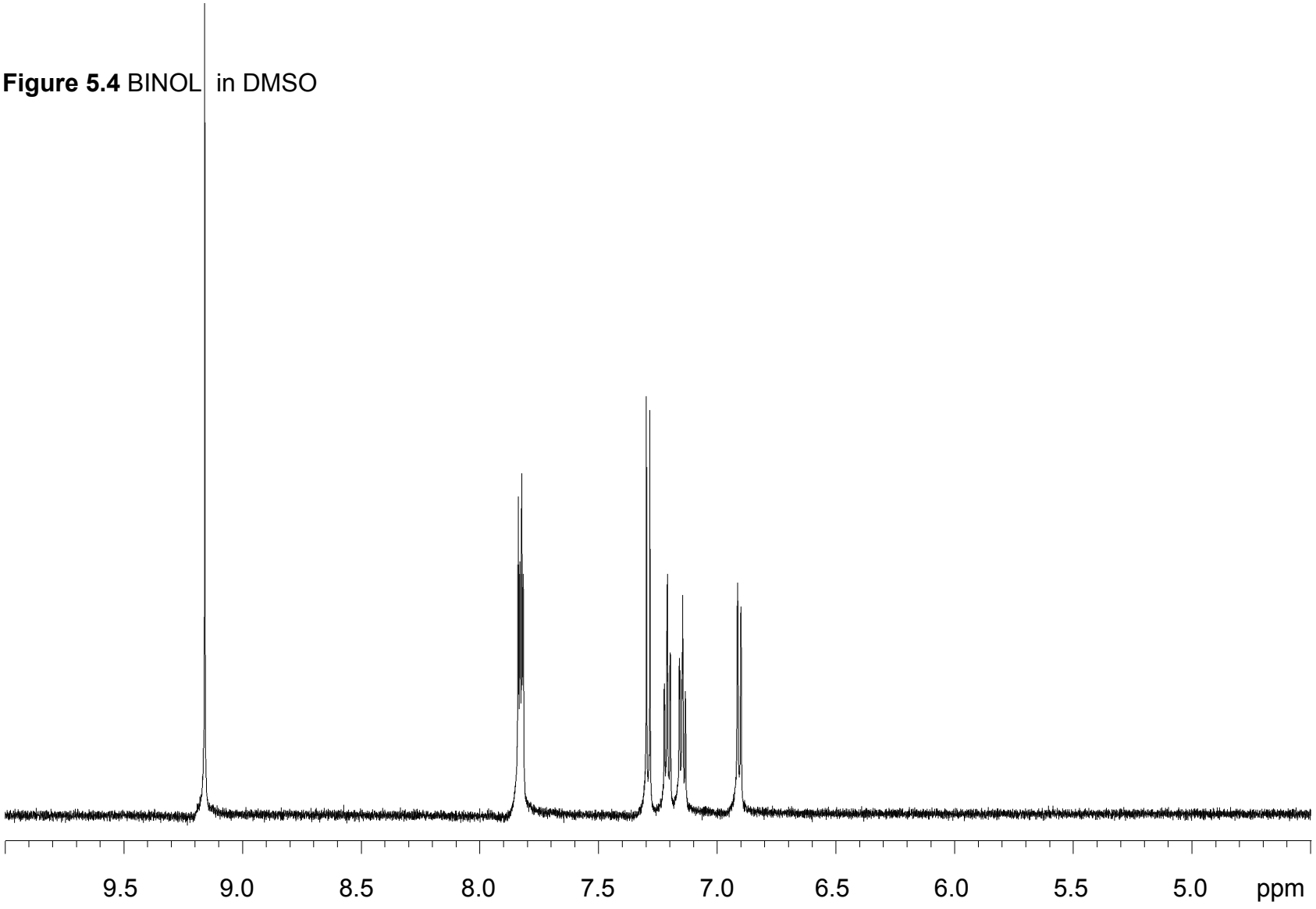

5.3.1 General procedure for the synthesis of BINOL-borate complexes in CD_2Cl_2 via Yamamoto's protocol (Figures 4.2 and 4.3)

Procedure for Reference # 01281: To a flame-dried round bottom flask equipped with a stir bar was added 4Å molecular sieves (flame-dried powder MS under reduced pressure) (200 mg), CD_2Cl_2 (2 mL), (*R*)-binaphthol (20 mg, 0.07 mmol, 1.00 equiv), and $B(OPh)_3$ (20.2 mg, 0.07 mmol, 1.00 equiv) at room temperature under a nitrogen atmosphere. The mixture was stirred at room temperature for 1 h. The solution was then transferred to a flame-dried quartz NMR tube using a filter syringe (25 mm membrane diameter, PTFE 0.45 μm) in order to remove the molecular sieves. An internal standard was added ($CHPh_3$; 17.5 mg, 0.07 mmol, 1.00 equiv) followed by ^1H and ^{11}B NMR analysis. Imine **8a** (19 mg, 0.07 mmol, 1.00 equiv) was added and the NMR tube was inverted several times to ensure the solution was homogeneous. Once again, ^1H and ^{11}B NMR analysis was performed. **Results**: Prior to imine addition = 41% BINOL, 14% B2, 12% B1, 44% phenol. After imine addition = 0% BINOL and 60% BLA

Experiment **Ref. # 02020** is repeating experiment **01281** but without internal standard. Experiment **Ref. #02020** is represented in Figure 4.2 as entries 2 and 4. Spectra for **01281** and **02020** are shown below.

Figure 5.5 01281

Binol :$B(OPh)_3$ 1:1 CD_2Cl_2 w/ MS and $CHPh_3$

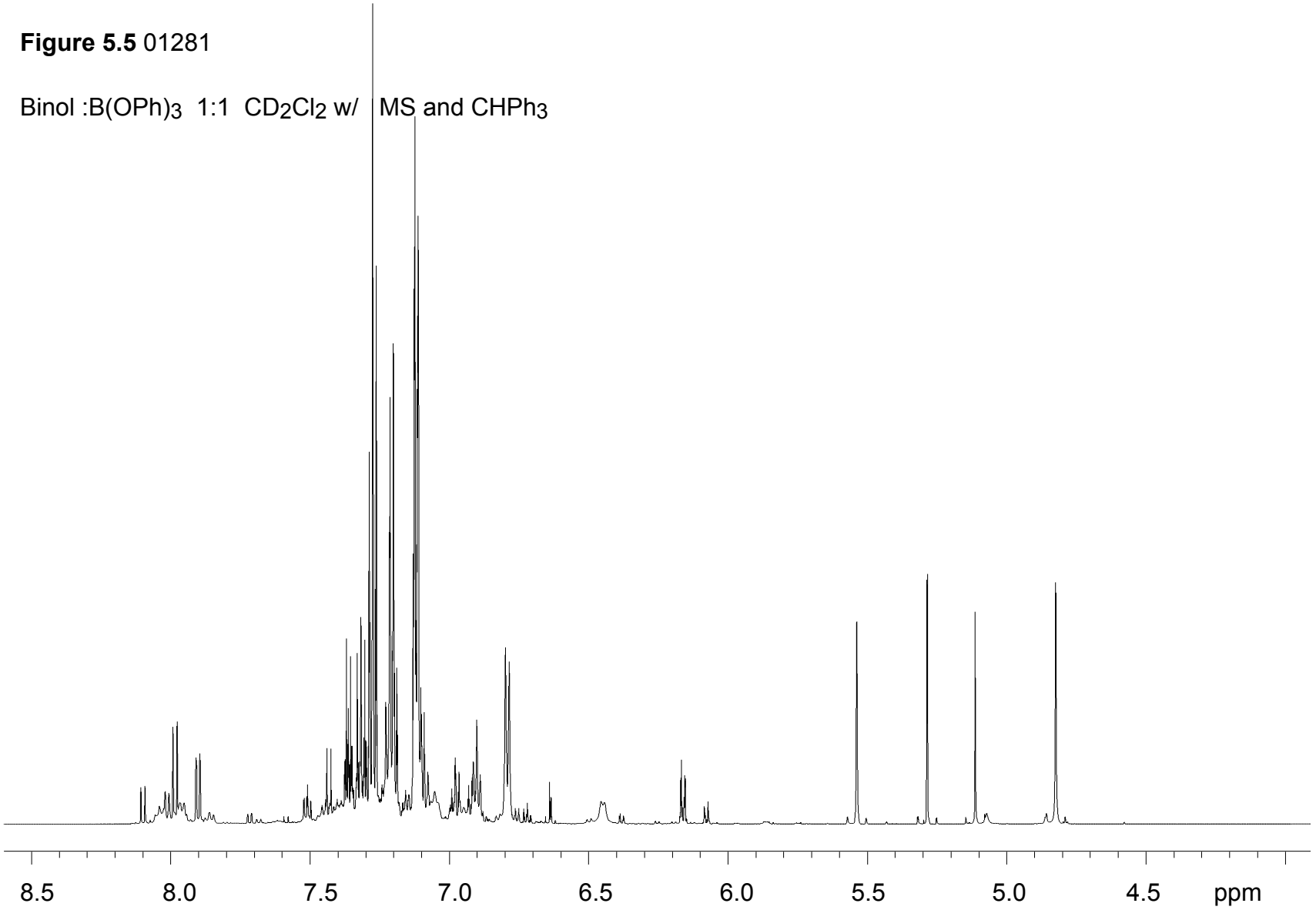

Figure 5.6 01281 Binol : $B(OPh)_3$ 1:1

CD_2Cl_2 w/ MS and $CHPh_3$

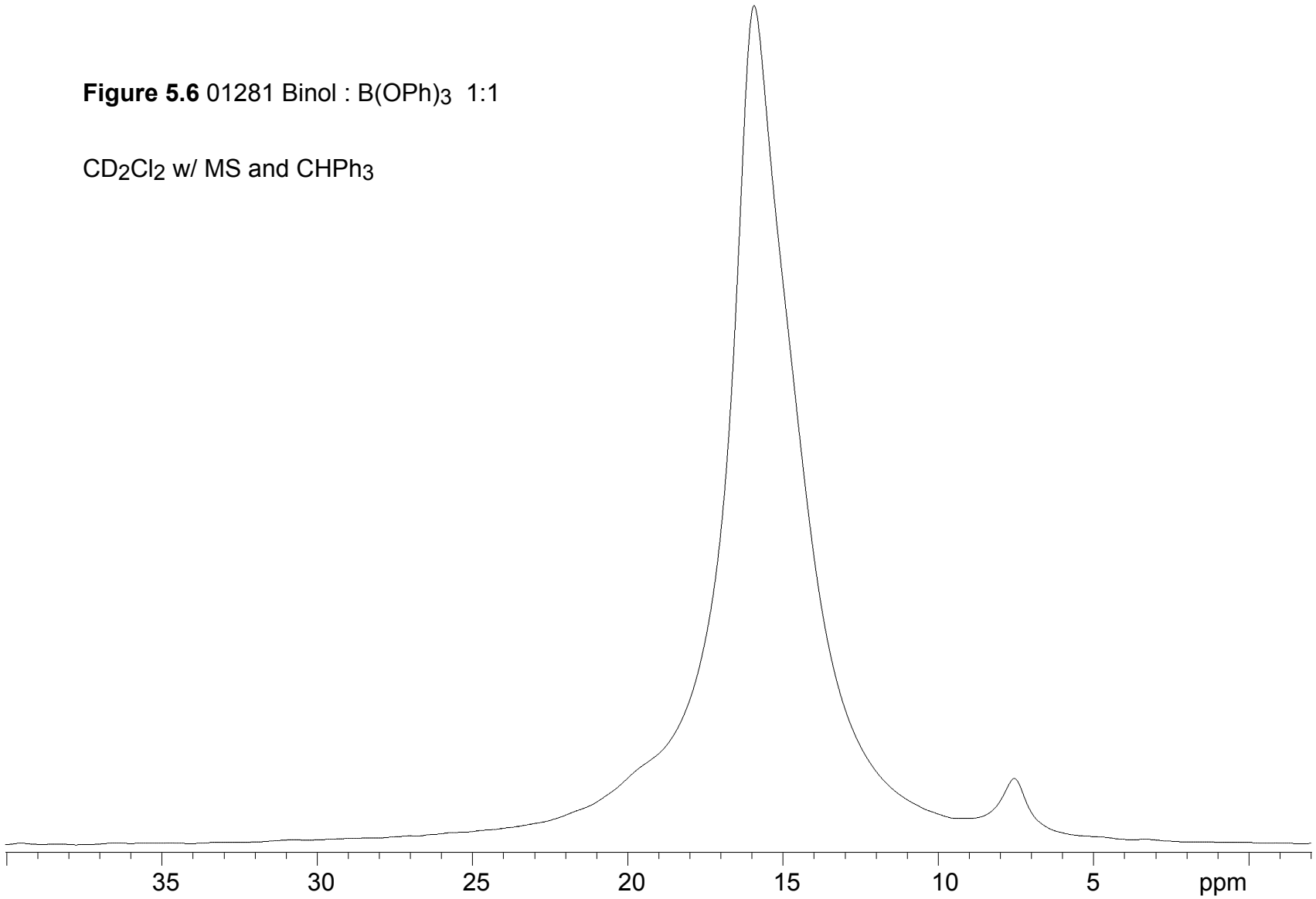

Figure 5.7 01281

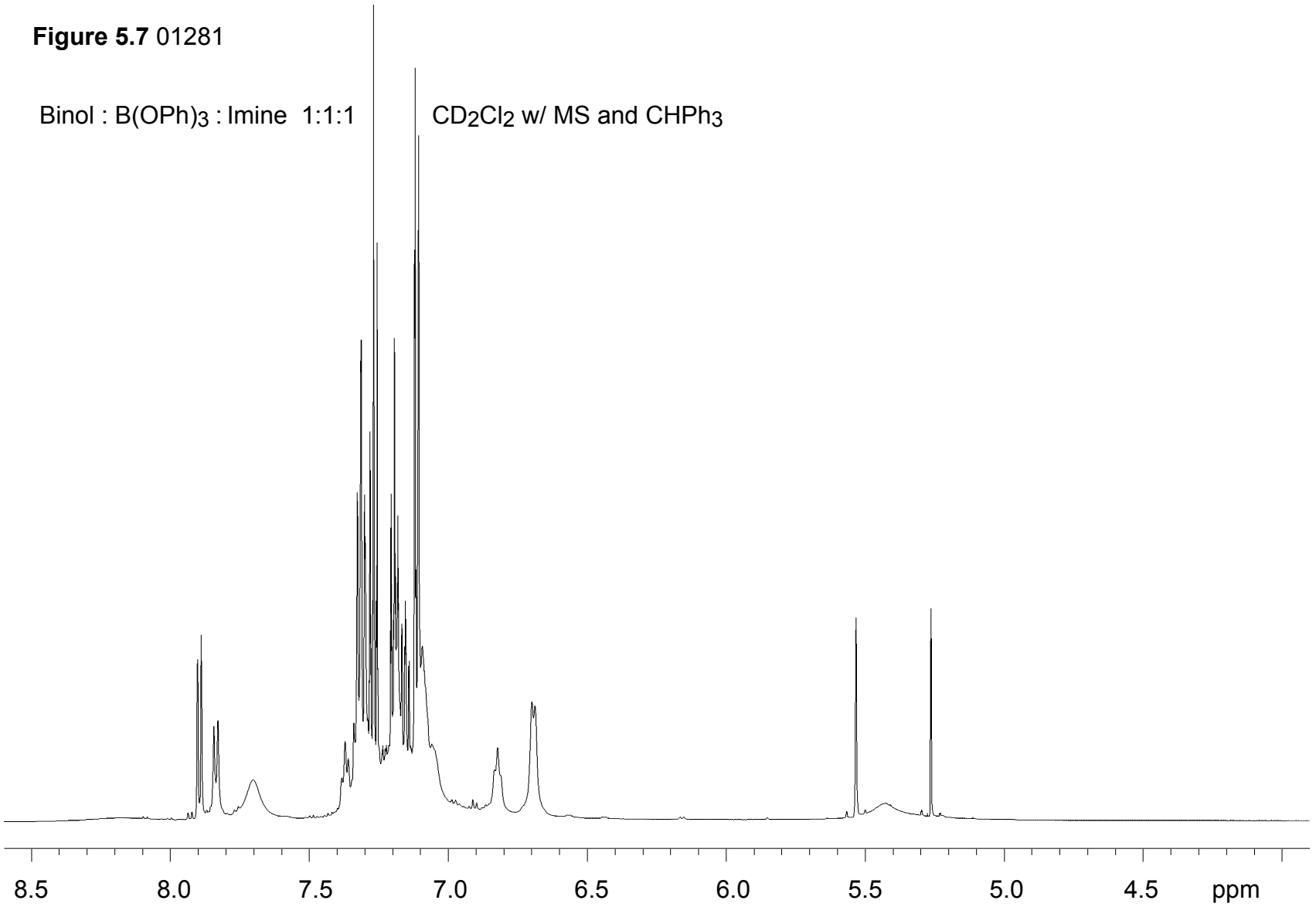

Figure 5.8 01281 Binol : $B(OPh)_3$: Imine 1:1:1

CD_2Cl_2 w/ MS and $CHPh_3$

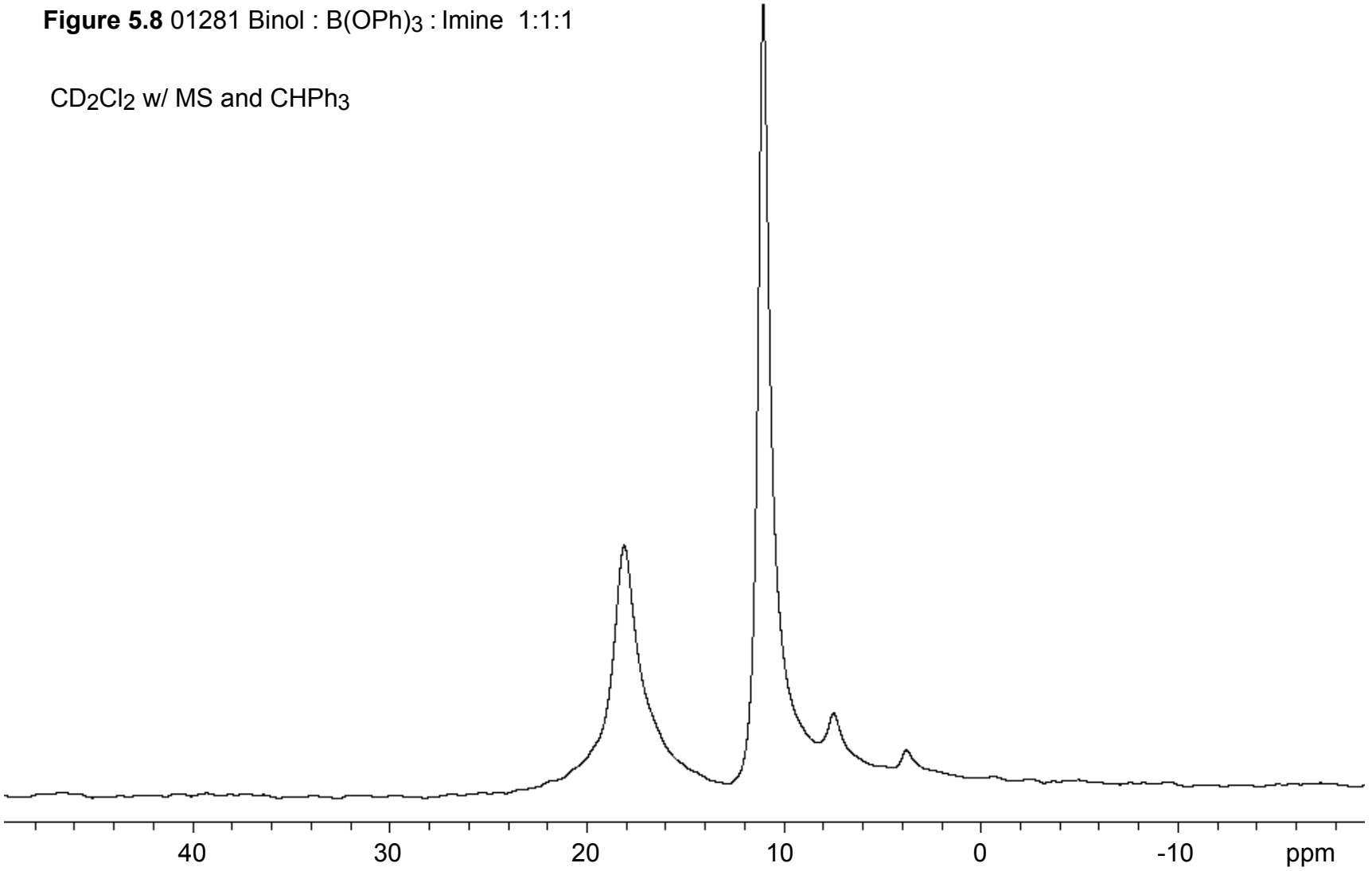

Figure 5.9 02020 Binol : $B(OPh)_3$ 1:1

CD_2Cl_2 w/ MS (no $CHPh_3$)

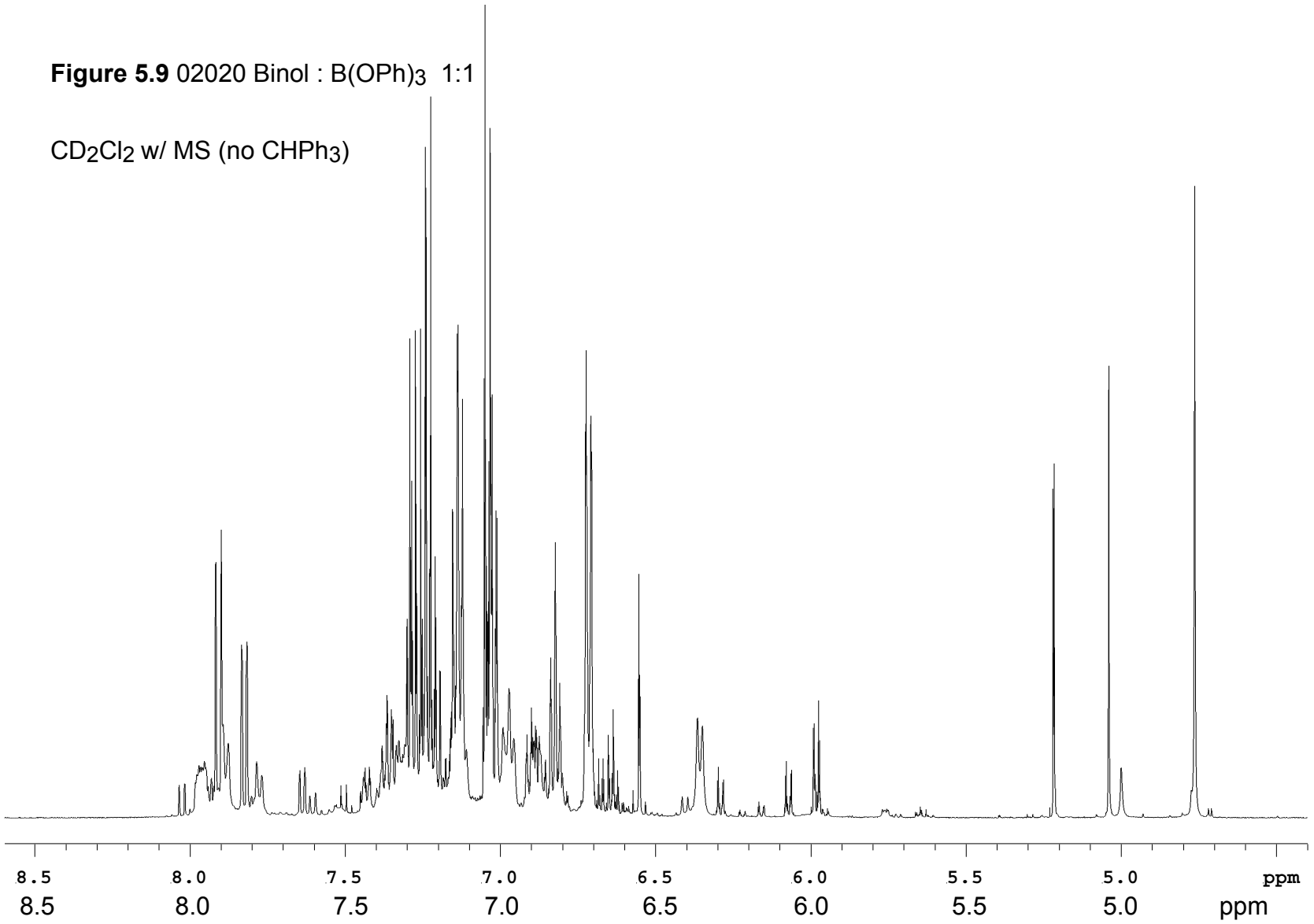

Figure 5.10 02020 Binol : $B(OPh)_3$ 1:1 CD_2Cl_2

w/ MS (no $CHPh_3$)

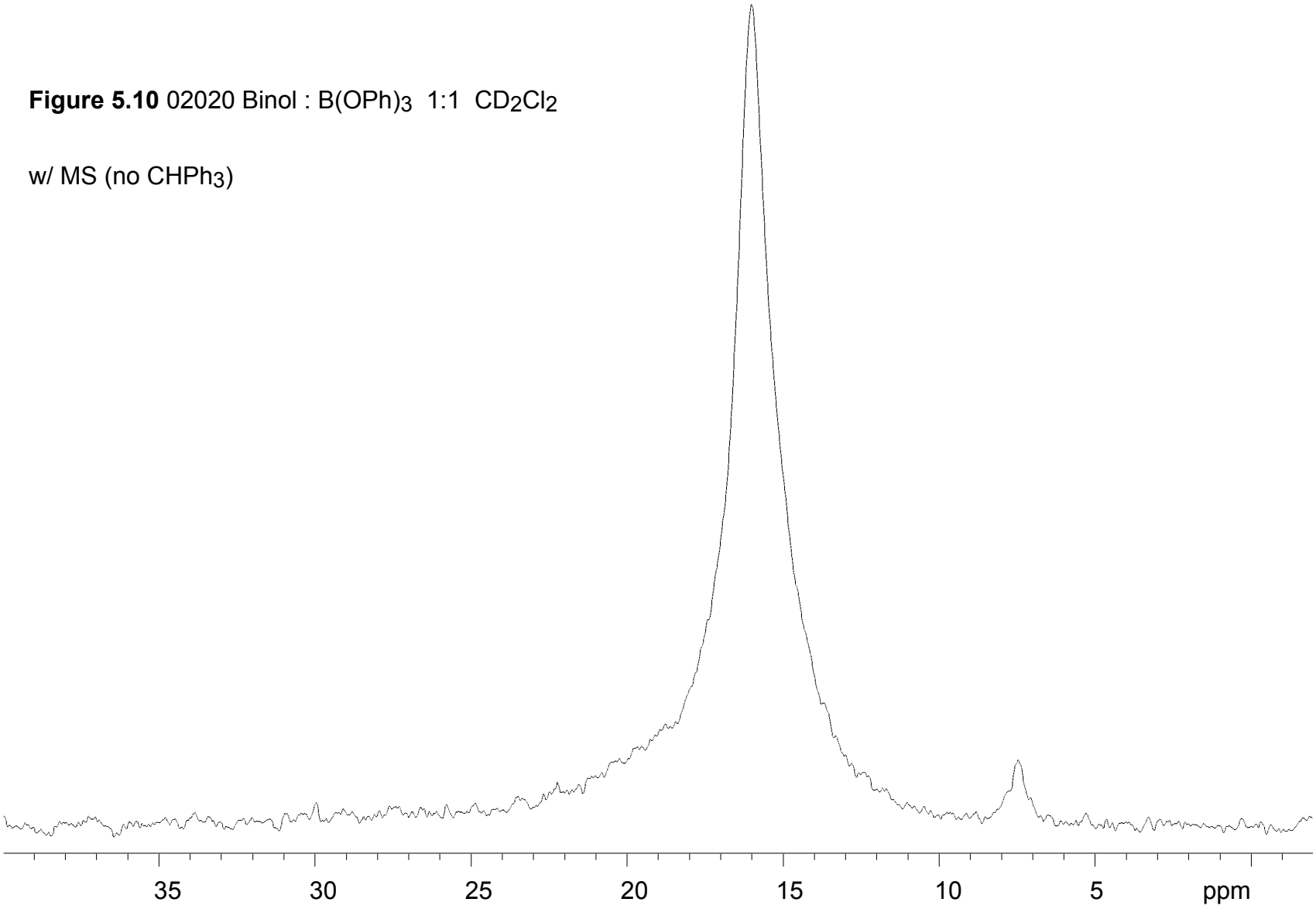

Figure 5.11 02020

Binol : $B(OPh)_3$: Imine 1:1:1 CD_2Cl_2

w/ MS (no $CHPh_3$)

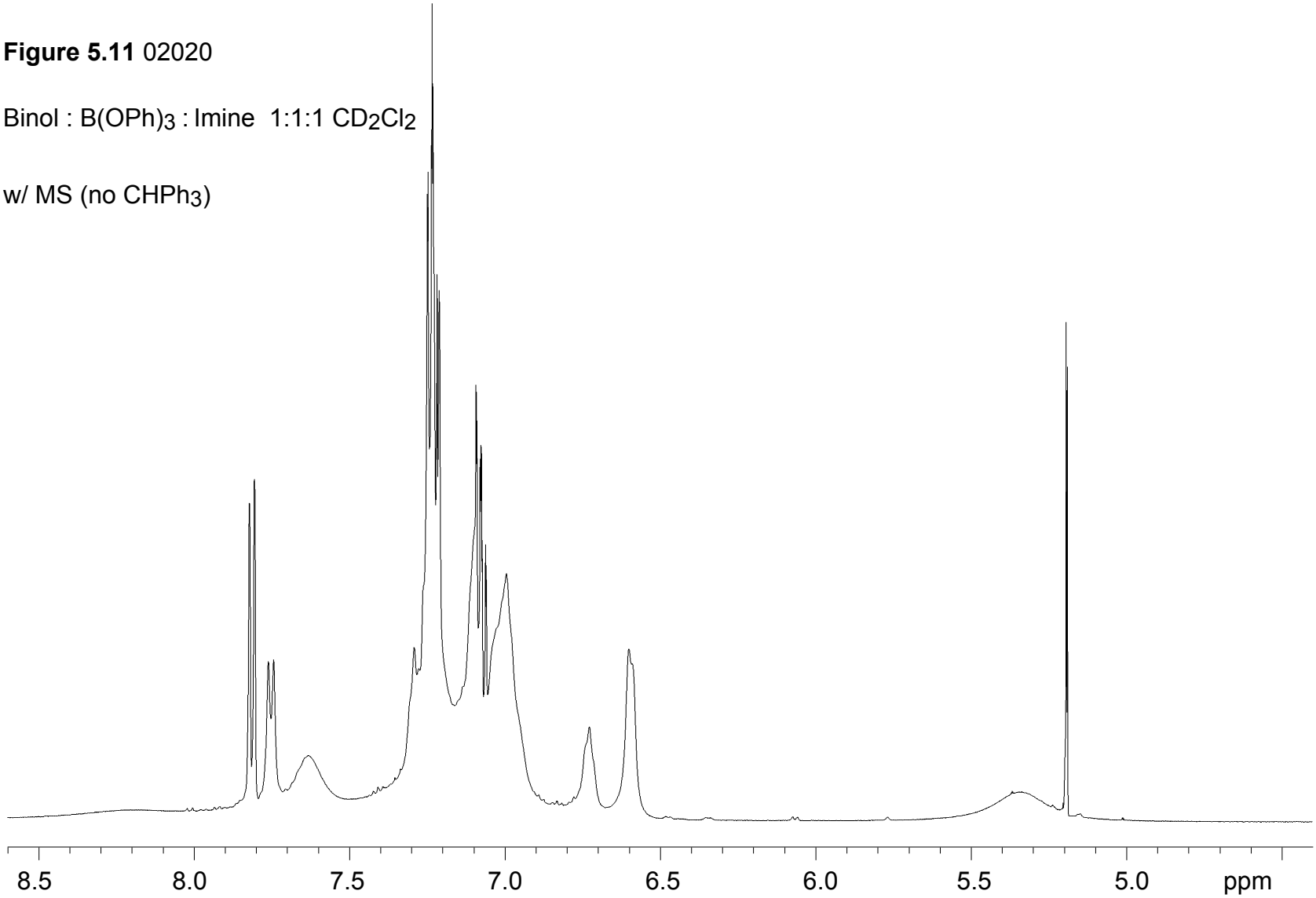

Figure 2.12 02020 Binol : $B(OPh)_3$: Imine 1:1:1

CD_2Cl_2 w/ MS (no $CHPh_3$)

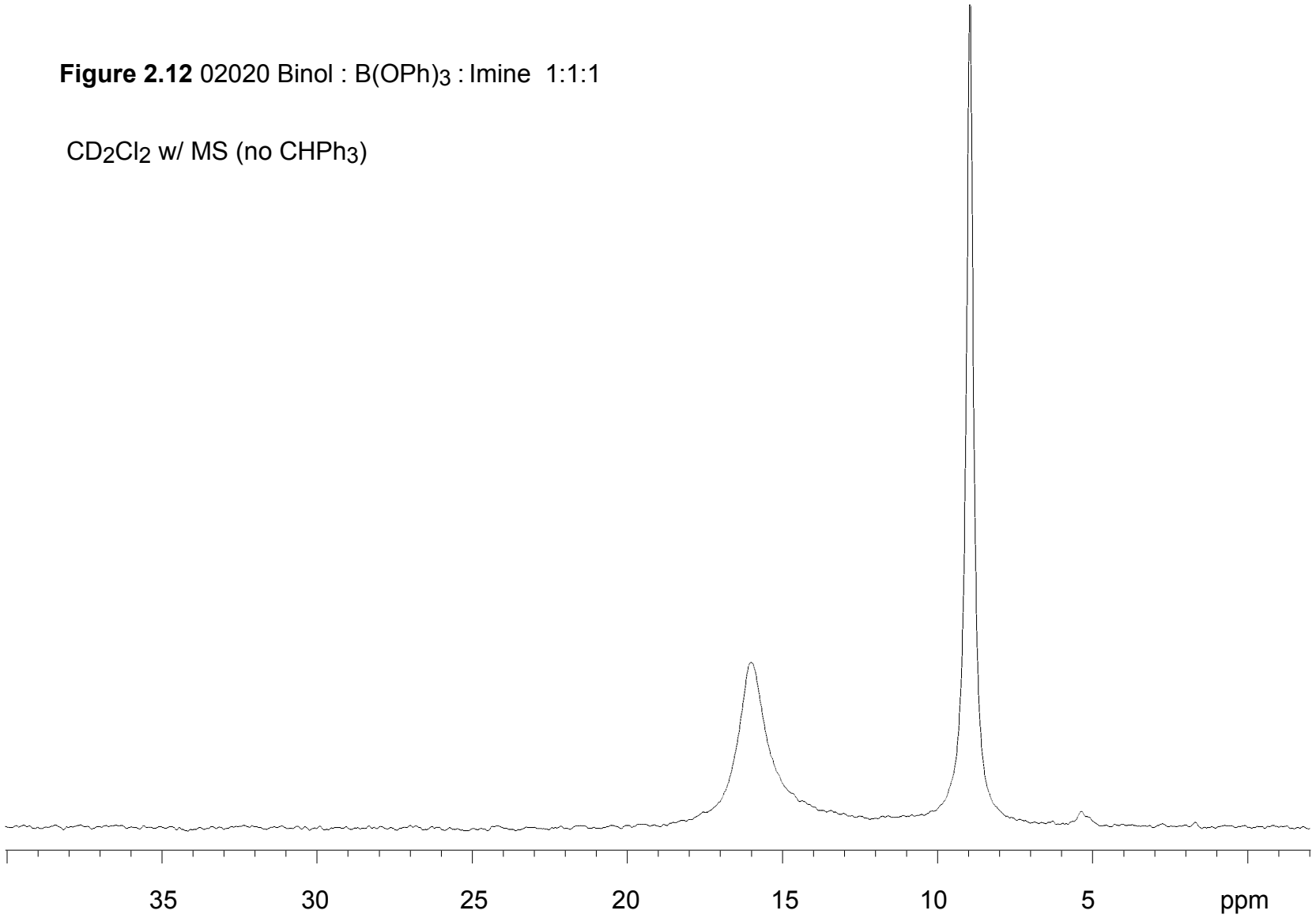

Procedure for 01282: To a flame-dried round bottom flask equipped with a stir bar was added 4 Å molecular sieves (flame-dried powder MS under reduced pressure) (200 mg), CD_2Cl_2 (2 mL), (*R*)-binaphthol (40 mg, 0.14 mmol, 2.00 equiv), and $B(OPh)_3$ (20.2 mg, 0.07 mmol, 1.00 equiv) at room temperature under a nitrogen atmosphere. The mixture was stirred at room temperature for 1 h. The solution was then transferred to a flame-dried quartz NMR tube using a filter syringe (25 mm membrane diameter, PTFE 0.45 µm) in order to remove the molecular sieves. An internal standard was added ($CHPh_3$; 17.5 mg, 0.07 mmol, 1.00 equiv) followed by ^1H and ^{11}B NMR analysis. Imine **8a** (19 mg, 0.07 mmol, 1.00 equiv) was added and the NMR tube was inverted several times to ensure the solution was homogeneous. Once again, ^1H and ^{11}B NMR analysis was performed. **Results**: Prior to imine addition = 53% BINOL, 46% phenol, 3% B2, 5% B1. After imine addition = quantitative yield for BLA

Experiment **Ref. # 02021** is repeating experiment **01282** but without internal standard. Experiment **Ref. #02021** is represented in Figure 4.2 as entries 3 and 5. Spectra for **01282** and **02021** are shown below.

Figure 5.13 01282

Binol : $B(OPh)_3$ 2:1 CD_2Cl_2

w/ MS and $CHPh_3$

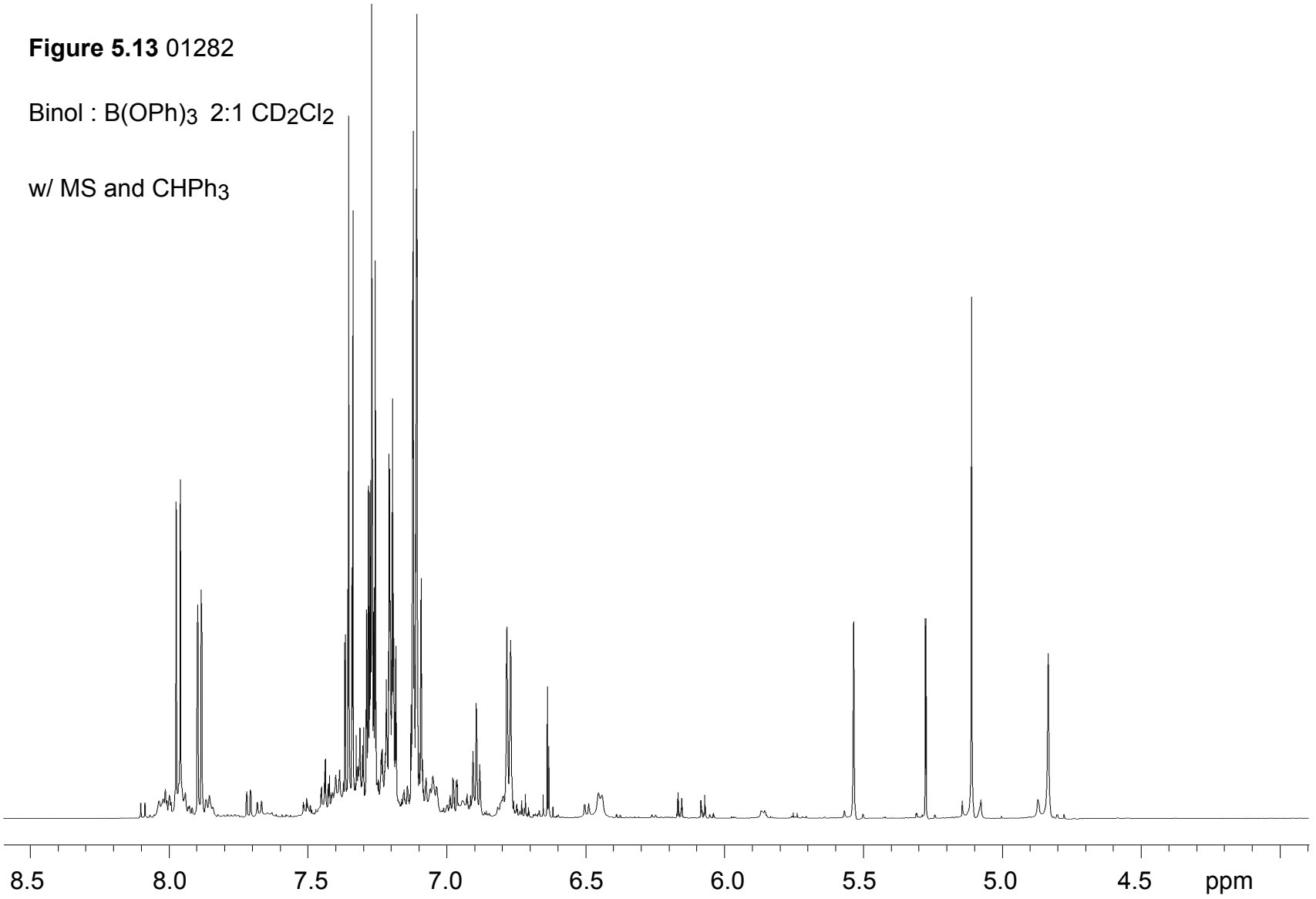

Figure 5.14 01282

Binol : $B(OPh)_3$: Imine 2:1:1

CD_2Cl_2 w/ MS and $CHPh_3$

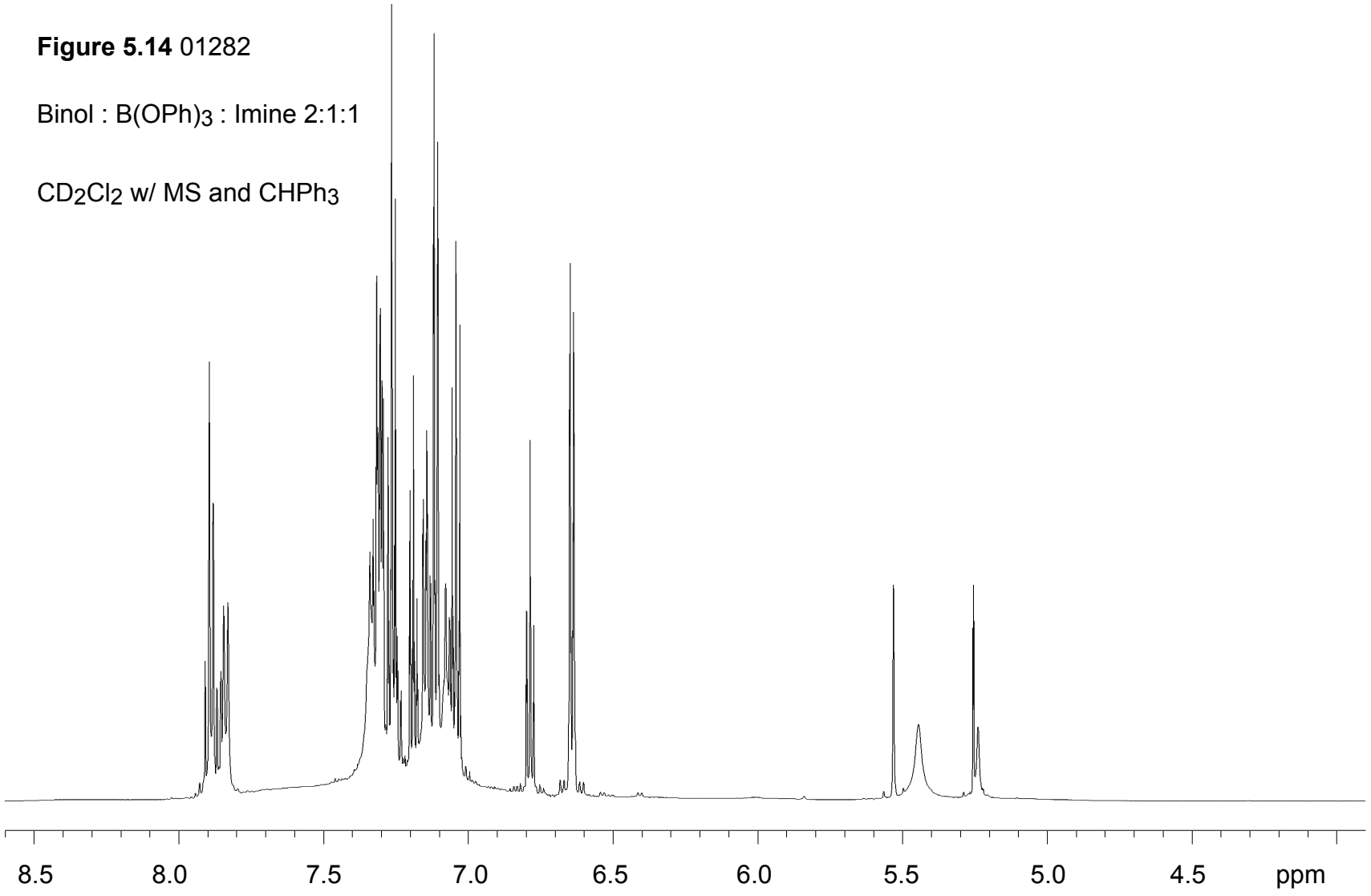

Figure 5.15 01282 Binol : $B(OPh)_3$: Imine 2:1:1

CD_2Cl_2 w/ MS and $CHPh_3$

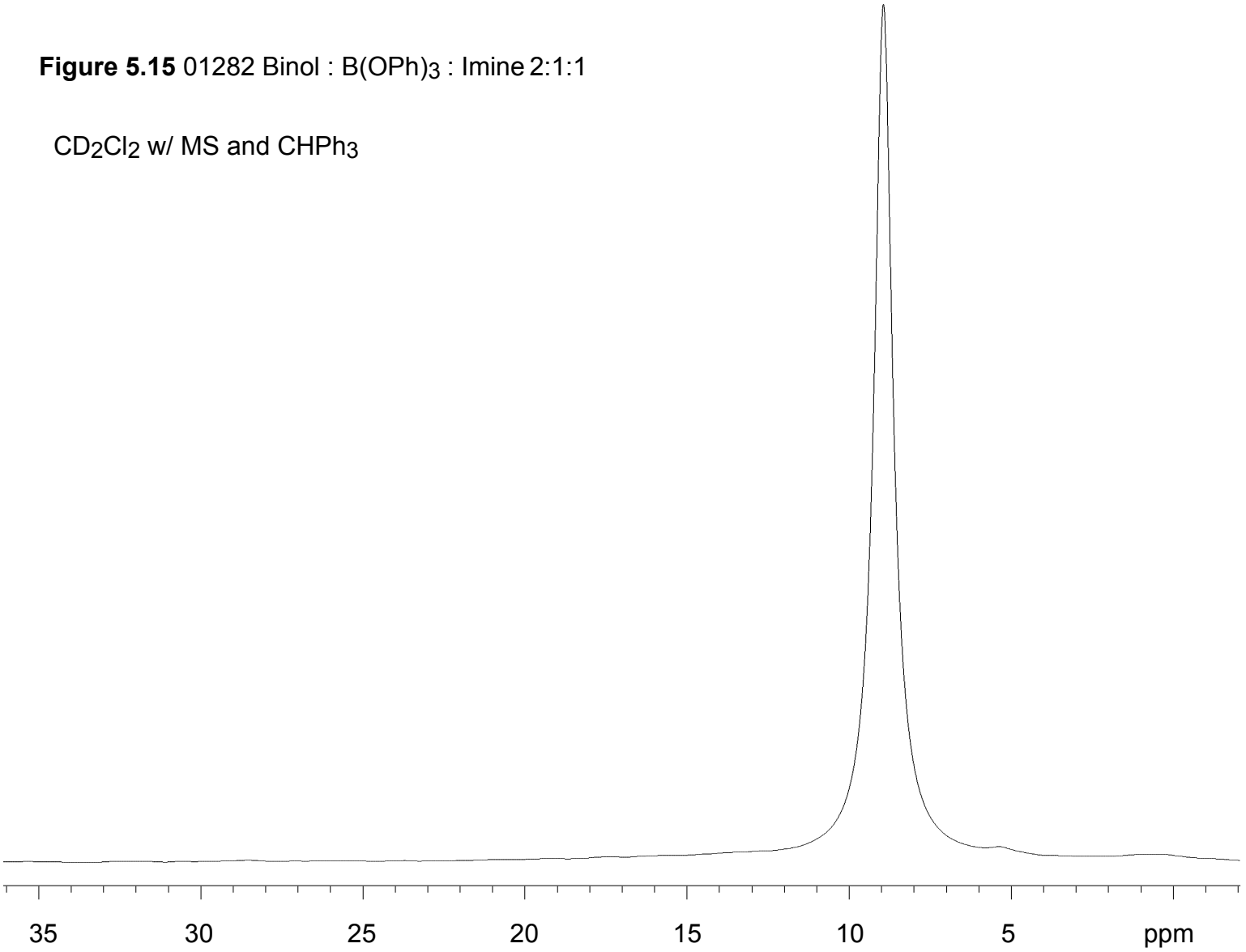

Figure 5.16 02021

Binol : $B(OPh)_3$ 2:1

CD_2Cl_2 w/ MS (no $CHPh_3$)

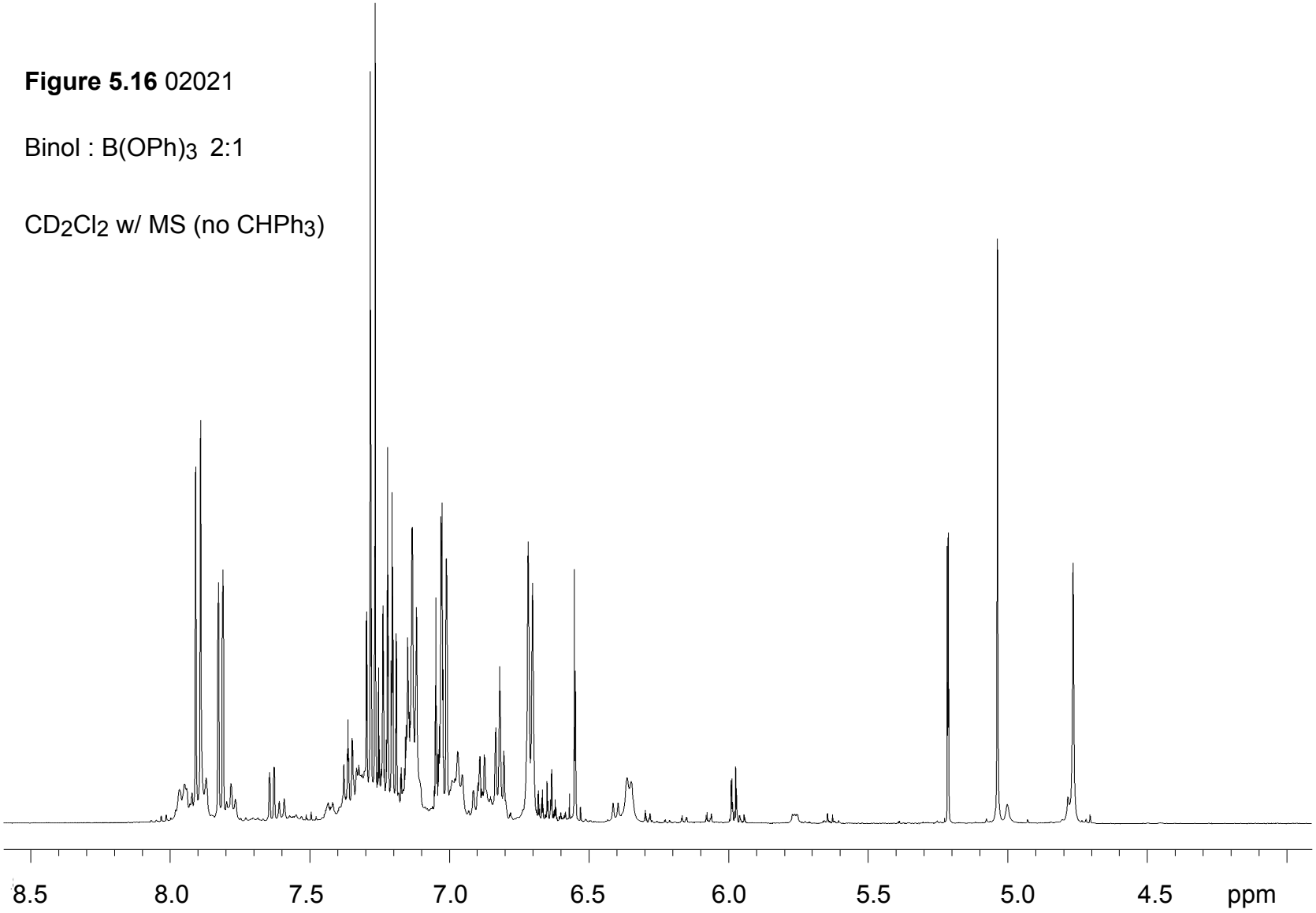

Figure 5.17 02021 Binol : $B(OPh)_3$ 2:1

CD_2Cl_2 w/ MS (no $CHPh_3$)

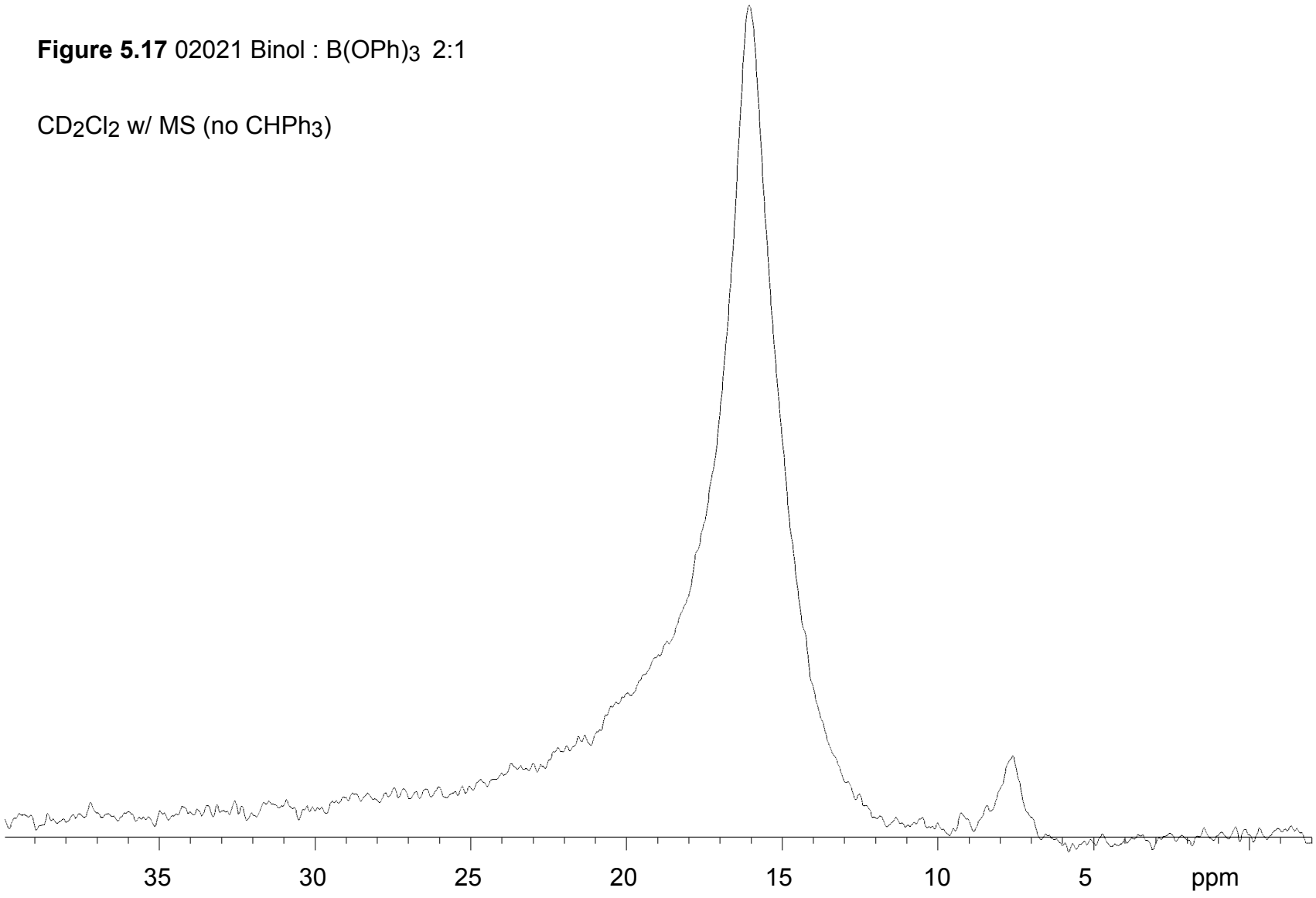

Figure 5.18 02021

Binol : $B(OPh)_3$: Imine 2:1:1

CD_2Cl_2 w/ MS (no $CHPh_3$)

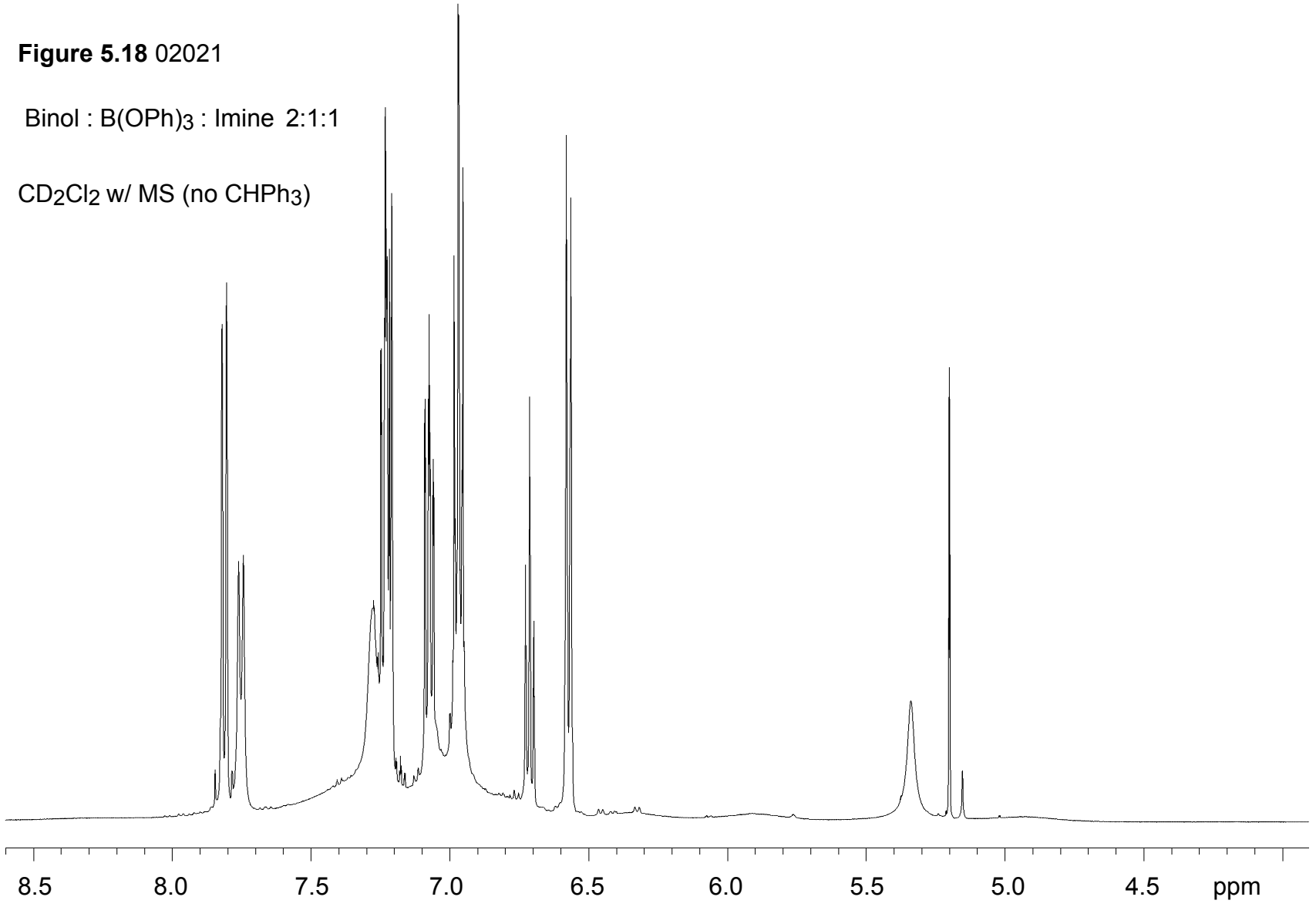

Figure 5.19 02021 Binol : $B(OPh)_3$: Imine 2:1:1

CD_2Cl_2 w/ MS (no $CHPh_3$)

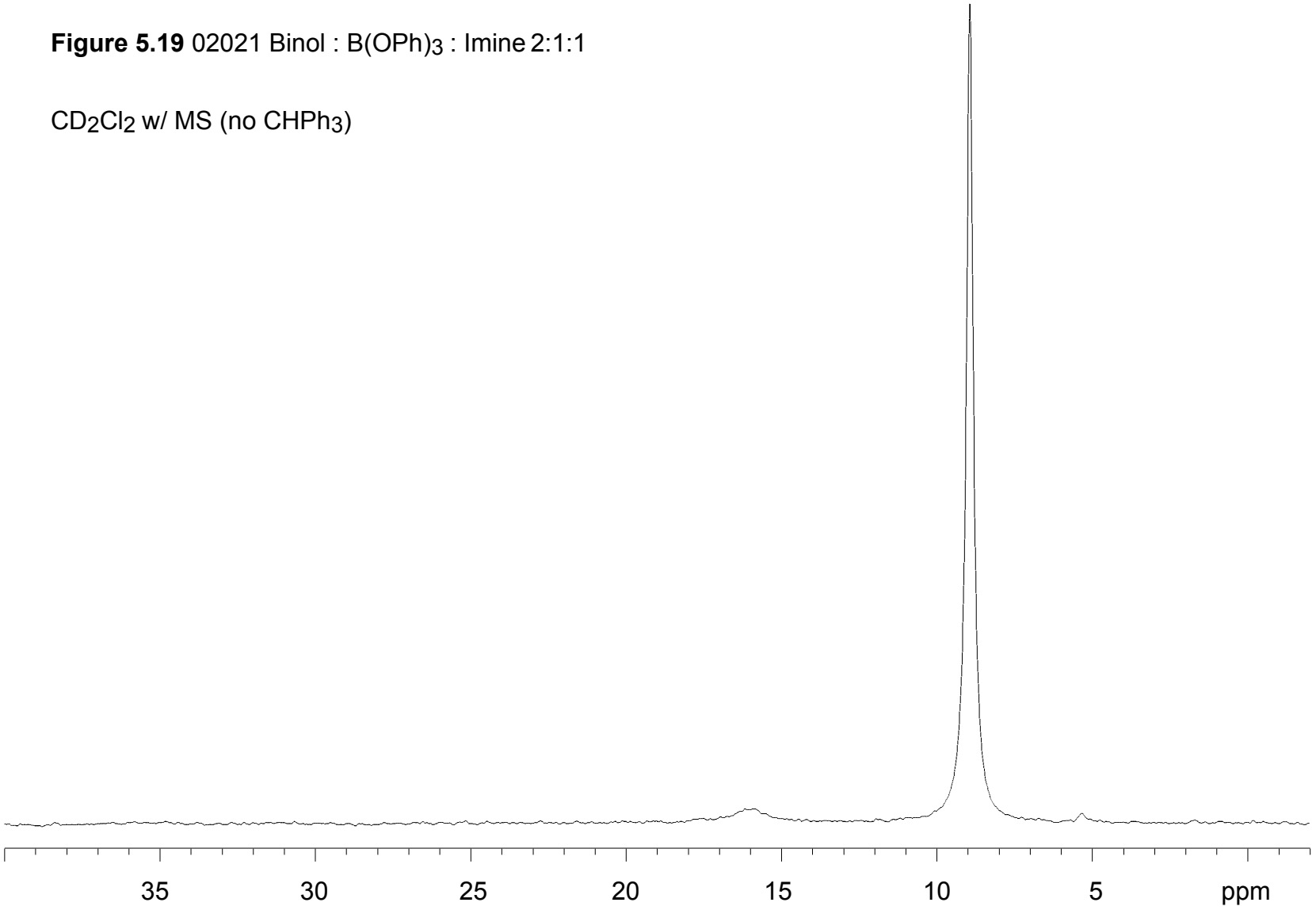

5.3.2 General procedure for the synthesis of BINOL-borate complexes in $CDCl_3$ (Figures 4.4, 4.5, 4.6, 4.7, 4.10, and 4.11)

5.3.2.1 Synthesis of BINOL-borate complexes using triphenyl borate (Figures 4.4, 4.5, 4.10, and 4.11)

Procedure for 02008: To a flame-dried round bottom flask was added (*R*)-binaphthol (20 mg, 0.07 mmol, 1.00 equiv), $B(OPh)_3$ (20.2 mg, 0.07 mmol, 1.00 equiv), and $CDCl_3$ (1 mL) at room temperature under a nitrogen atmosphere. The mixture was swirled and immediately transferred to a flame-dried quartz NMR tube. ^{1}H and ^{11}B NMR analysis was then performed followed by the addition of an internal standard ($CHPh_3$; 17.5 mg, 0.07 mmol, 1.00 equiv). Once again, ^{1}H and ^{11}B NMR analysis was performed. **Results**: 23% BINOL and 44% B2

Experiment **Ref. #02008** is represented in Figure 4.4 as entry 2. Spectra for **02008** are shown below.

Figure 5.20 02008

Binol : $B(OPh)_3$ 1:1 $CDCl_3$

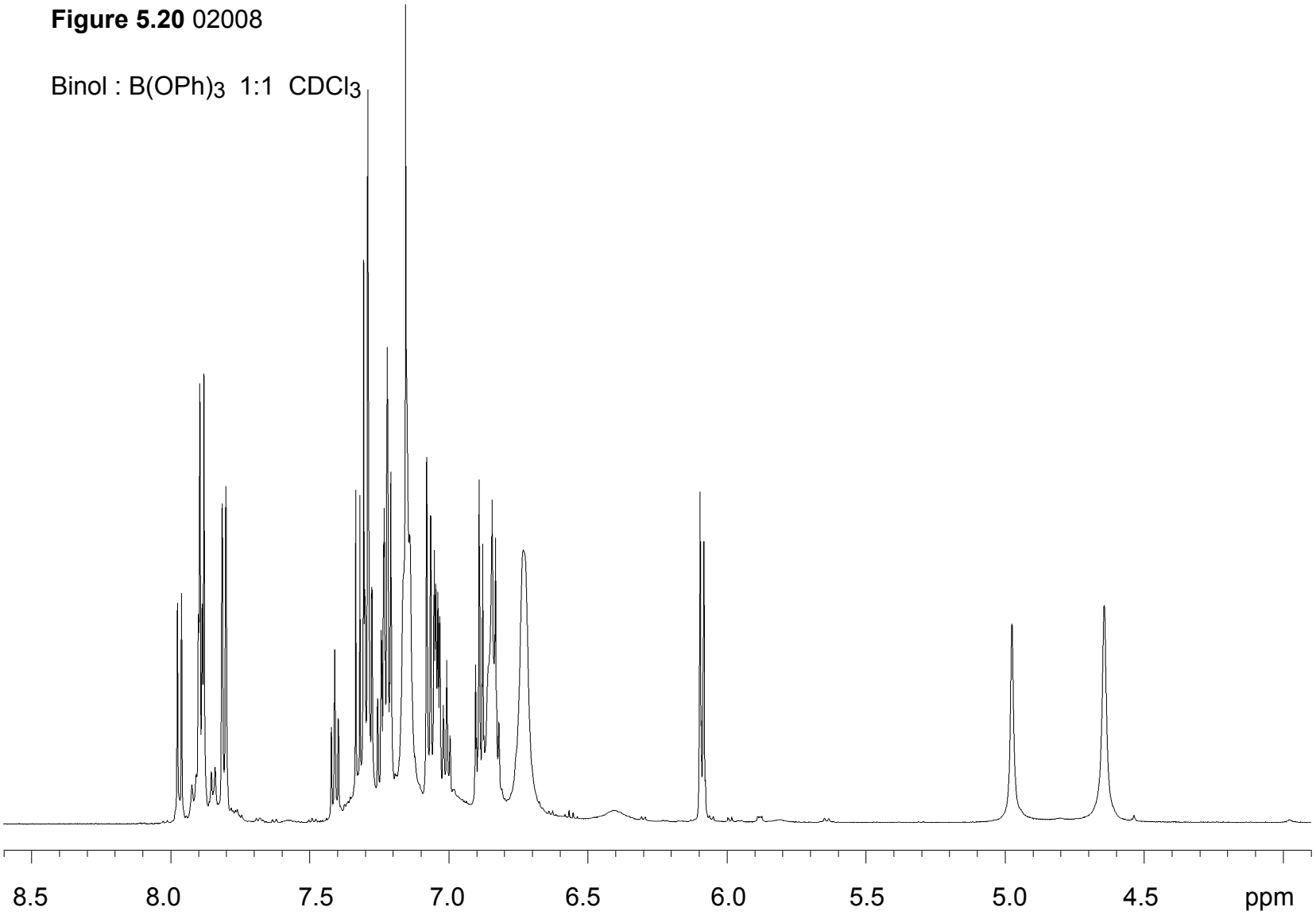

Figure 5.21 02008 Binol : $B(OPh)_3$ 1:1 $CDCl_3$

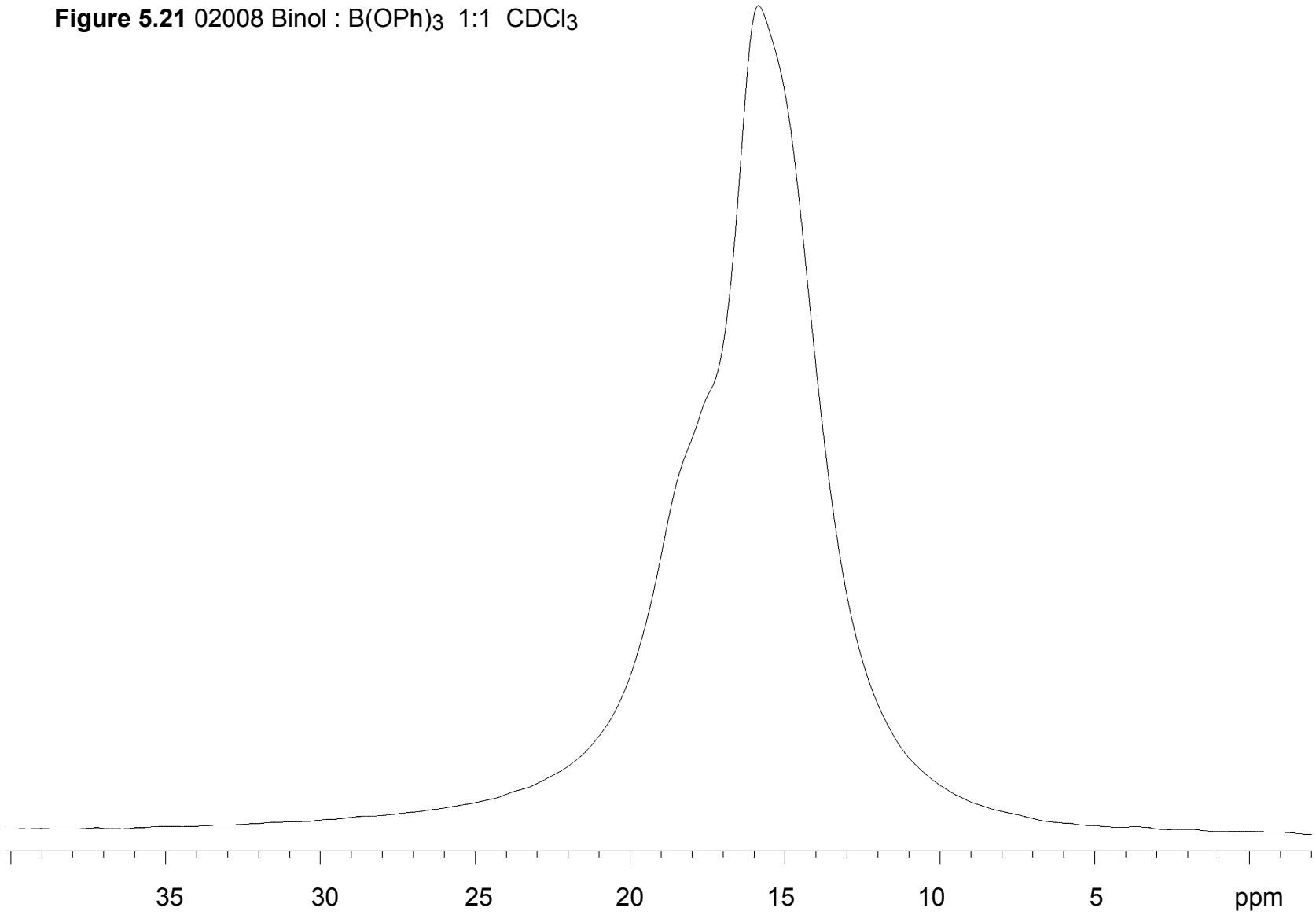

Procedure for 02003: To a flame-dried round bottom flask equipped with a stir bar was added 4Å molecular sieves (flame-dried powder MS under reduced pressure) (200 mg), $CDCl_3$ (2 mL), (*R*)-binaphthol (20 mg, 0.07 mmol, 1.00 equiv), and $B(OPh)_3$ (20.2 mg, 0.07 mmol, 1.00 equiv) at room temperature under a nitrogen atmosphere. The mixture was stirred at room temperature for 1 h. The solution was then transferred to a flame-dried quartz NMR tube using a filter syringe (25 mm membrane diameter, PTFE 0.45 μm) in order to remove the molecular sieves. An internal standard was added ($CHPh_3$; 17.5 mg, 0.07 mmol, 1.00 equiv) followed by ^{1}H and ^{11}B NMR analysis. Imine **8a** (19 mg, 0.07 mmol, 1.00 equiv) was dissolved in 0.3 mL $CDCl_3$ and added to the NMR tube, which was then inverted several times to ensure the solution was homogeneous. Once again, ^{1}H and ^{11}B NMR analysis was performed. **Results**: Prior to imine addition = 37% BINOL, 6% B2, 11% B1, 15% propeller. After imine addition = 20% BINOL, 57% BLA, 2.5% propeller, 9% B2, and 3.5% B1.

Experiment **Ref. #02003** is represented in Figure 4.4 as entries 3 and 5. Spectra for **02003** are shown below.

Figure 5.22 02003

Binol : $B(OPh)_3$ 1:1 $CDCl_3$

w/ MS and $CHPh_3$

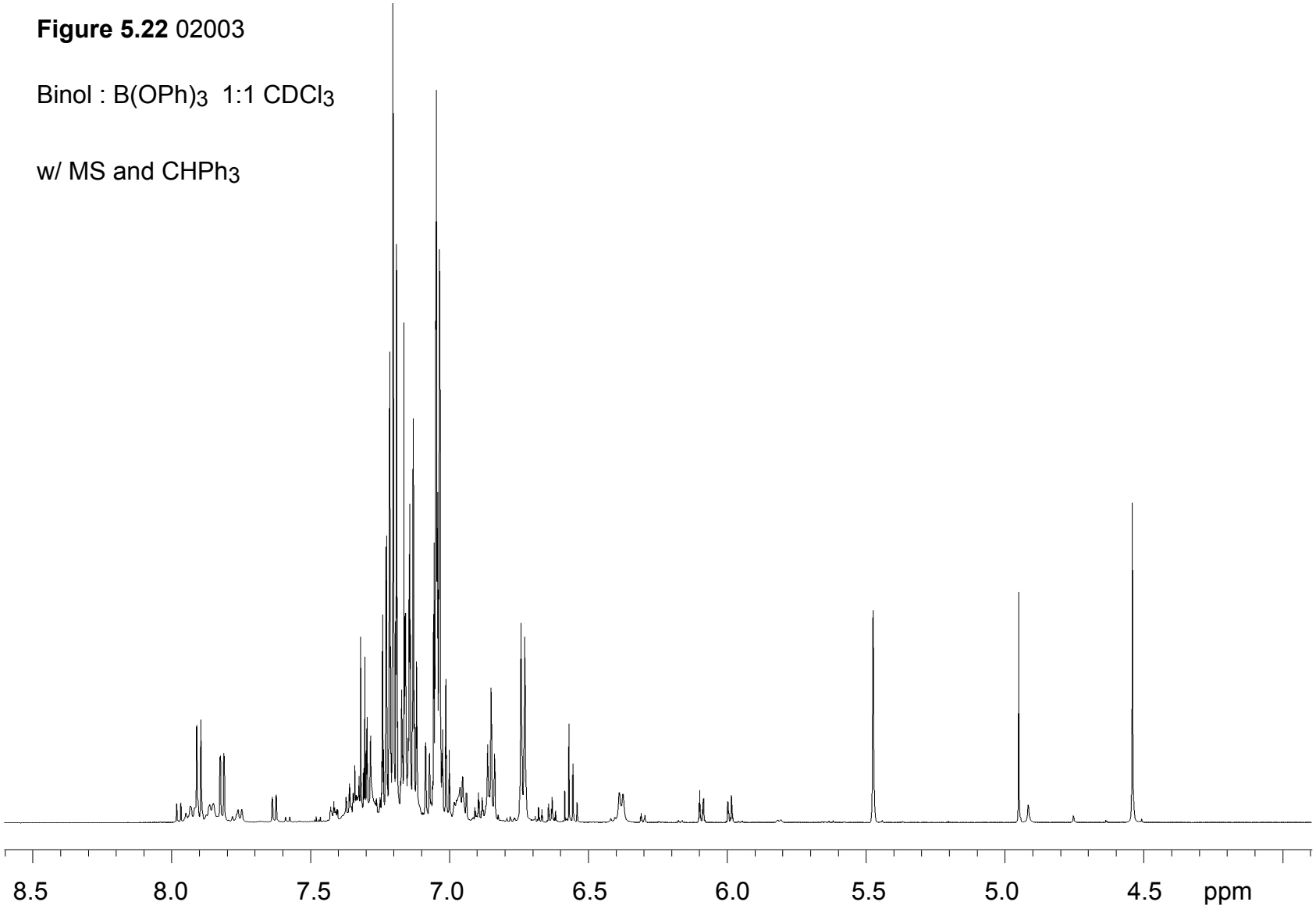

Figure 5.23 02003 Binol : $B(OPh)_3$ 1:1

$CDCl_3$ w/ MS and $CHPh_3$

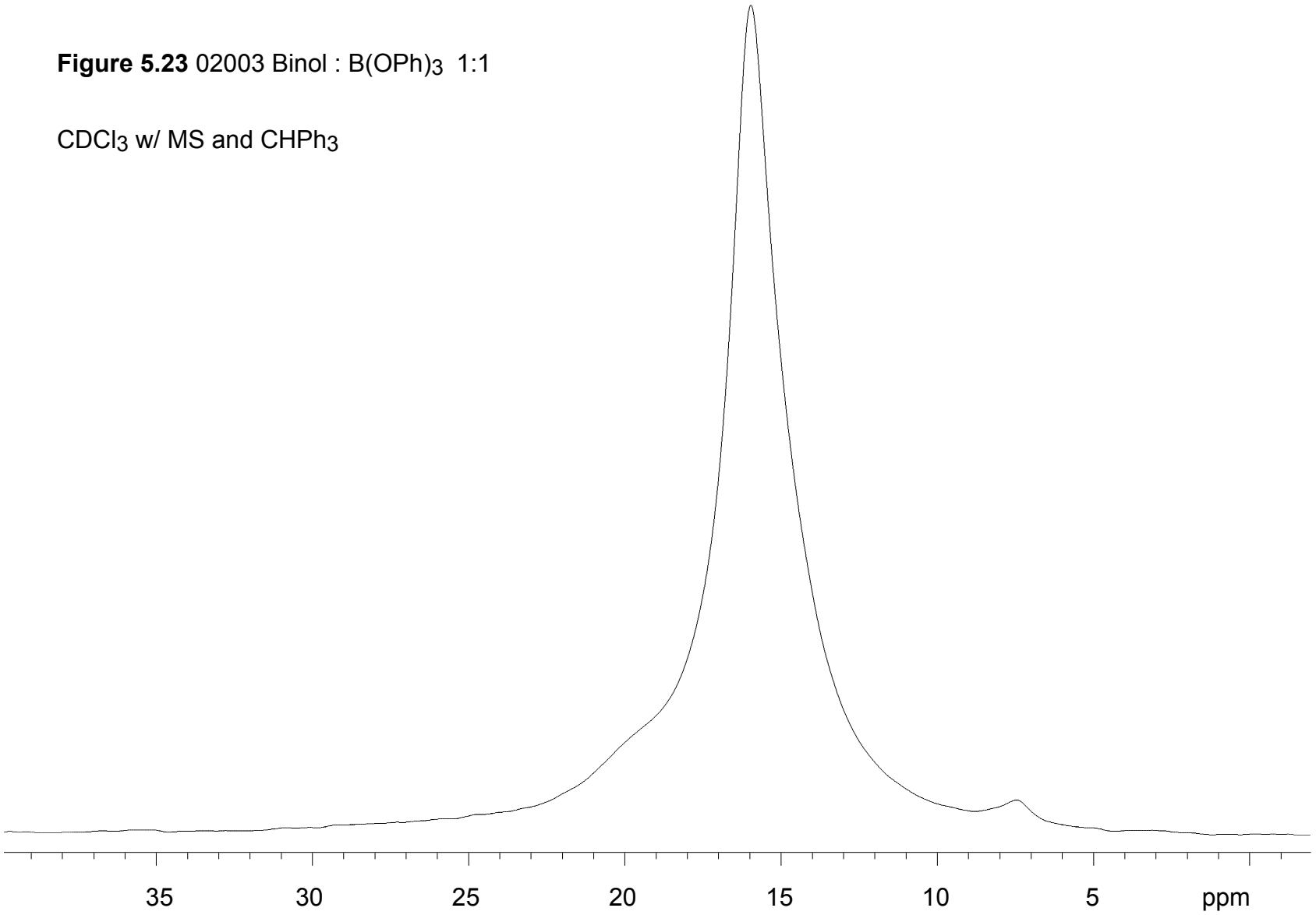

Figure 5.24 02003

Binol : $B(OPh)_3$: Imine 1:1:1

$CDCl_3$ w/ MS and $CHPh_3$

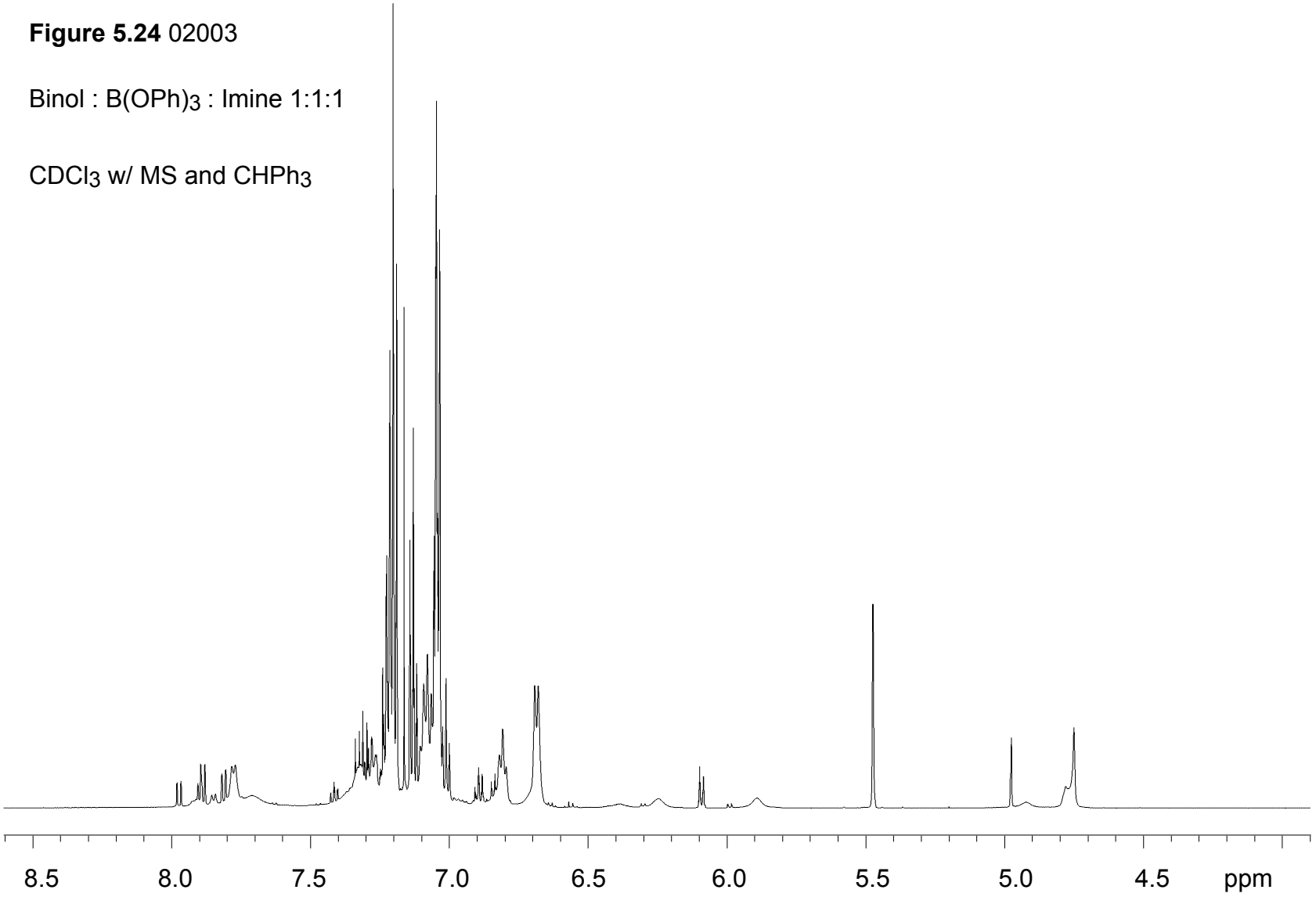

Figure 5.25 02003 Binol : $B(OPh)_3$: Imine 1:1:1

$CDCl_3$ w/ MS and $CHPh_3$

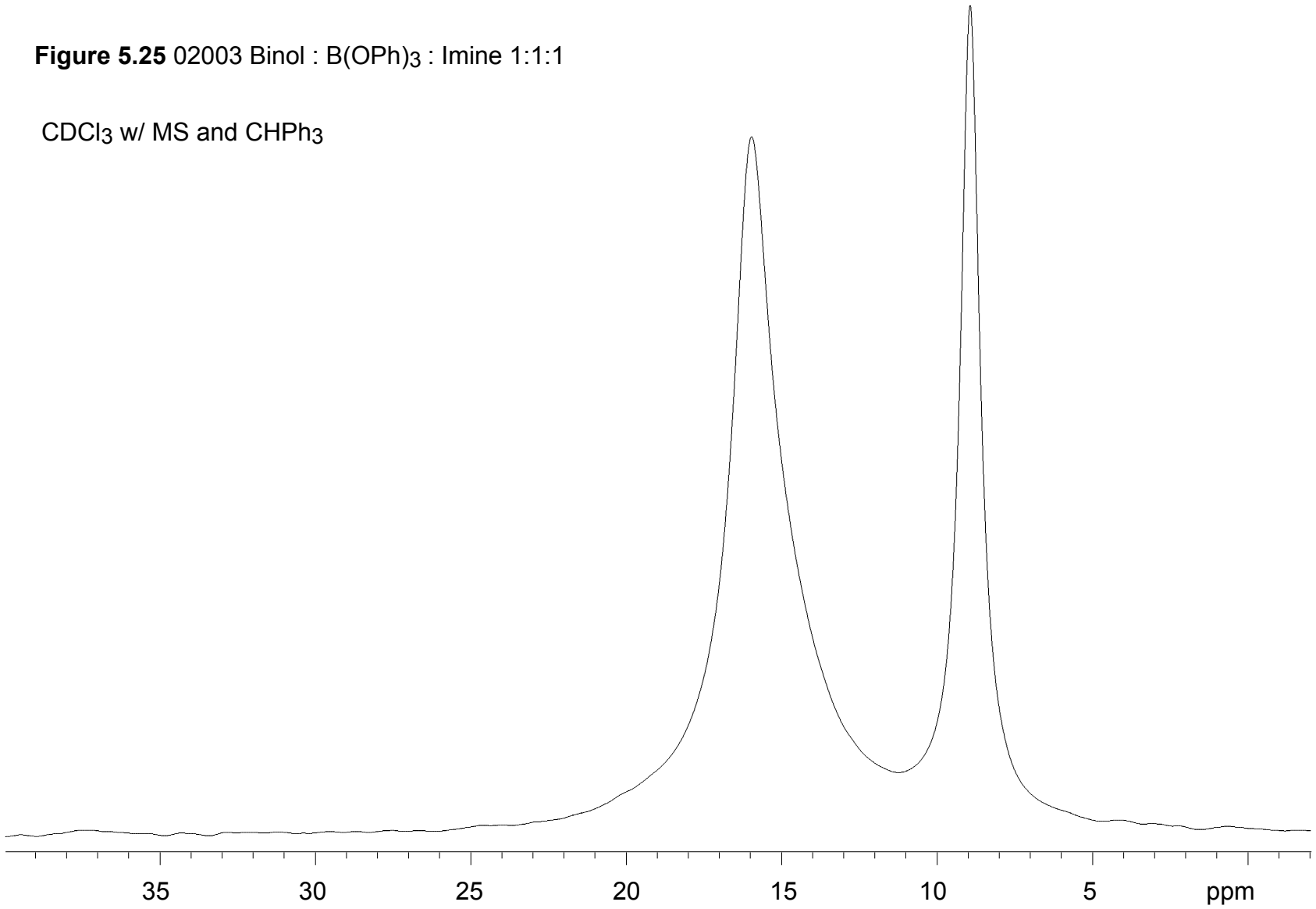

Procedure for 02004: To a flame-dried round bottom flask equipped with a stir bar was added 4 Å molecular sieves (flame-dried powder MS under reduced pressure) (200 mg), $CDCl_3$ (2 mL), (*R*)-binaphthol (40 mg, 0.14 mmol, 2.00 equiv), and $B(OPh)_3$ (20.2 mg, 0.07 mmol, 1.00 equiv) at room temperature under a nitrogen atmosphere. The mixture was stirred at room temperature for 1 h. The solution was then transferred to a flame-dried quartz NMR tube using a filter syringe (25 mm membrane diameter, PTFE 0.45 μm) in order to remove the molecular sieves. An internal standard was added ($CHPh_3$; 17.5 mg, 0.07 mmol, 1.00 equiv) followed by ^{1}H and ^{11}B NMR analysis. Imine **8a** (19 mg, 0.07 mmol, 1.00 equiv) was dissolved in 0.3 mL $CDCl_3$ and added to the NMR tube, which was then inverted several times to ensure the solution was homogeneous. Once again, ^{1}H and ^{11}B NMR analysis was performed. **Results**: Prior to imine addition = 47% BINOL, 12% propeller, 2% B2, and 6% B1. After imine addition = 40% BINOL (messy and broad area of spectrum), 94% BLA, <1% propeller, <5% B2, and <5% B1.

Experiment **Ref. #02004** is represented in Figure 4.4 as entries 4 and 6. Spectra for **02004** are shown below.

Figure 5.26 02004

Binol : $B(OPh)_3$ 2:1 $CDCl_3$

w/ MS and $CHPh_3$

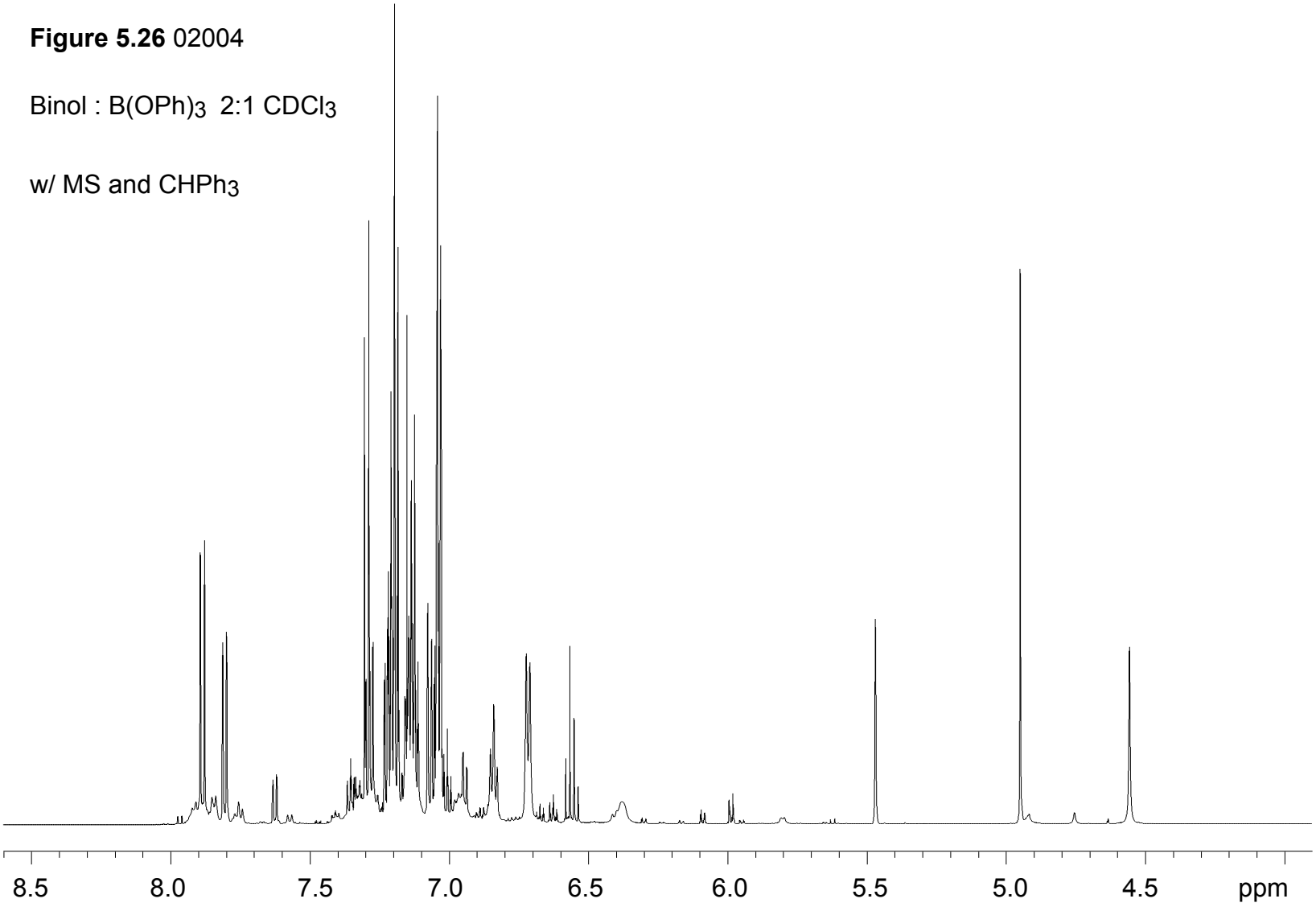

Figure 5.27 02004 Binol : $B(OPh)_3$ 2:1

$CDCl_3$ w/ MS and $CHPh_3$

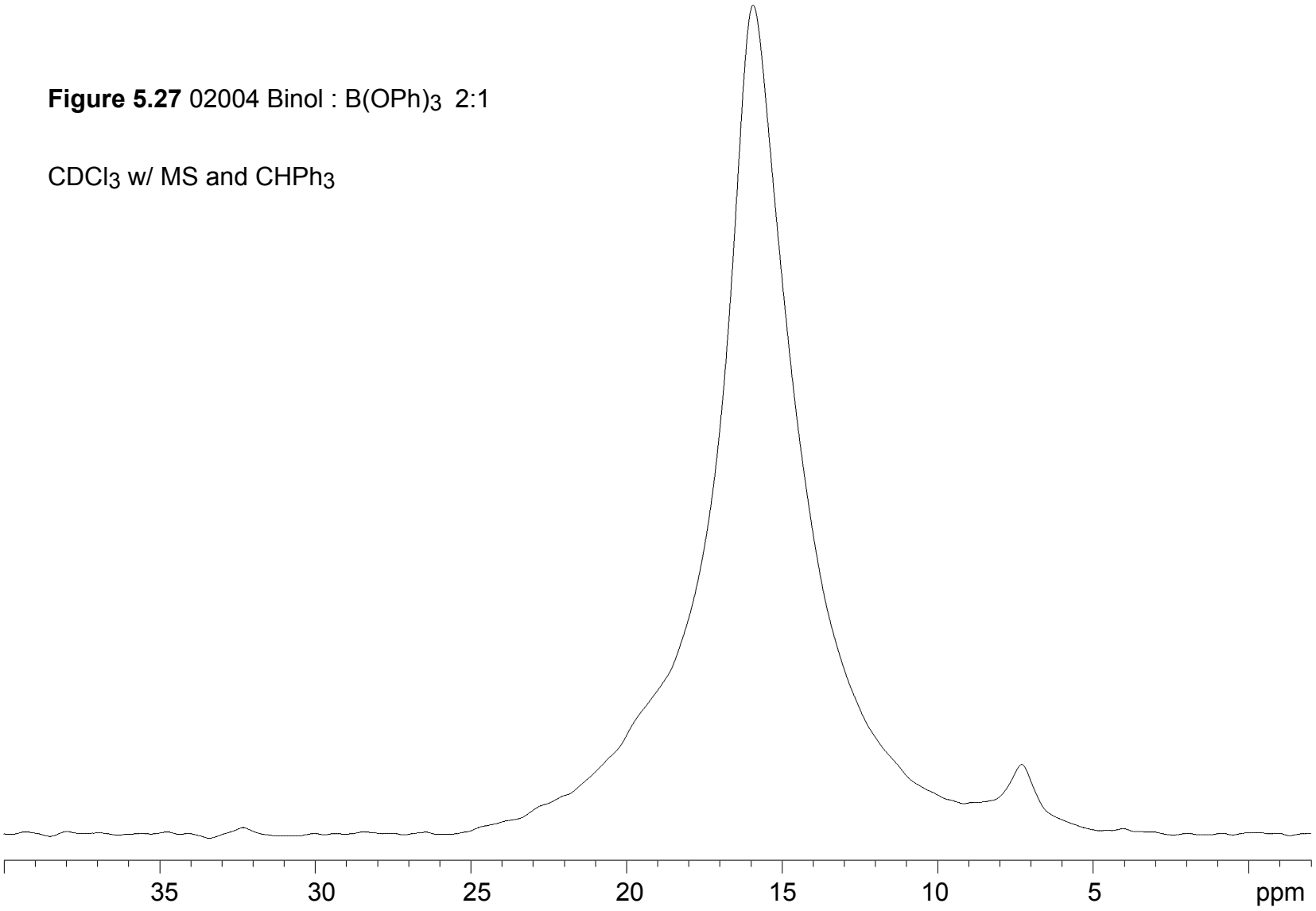

Figure 5.28 02004

Binol : $B(OPh)_3$: Imine 2:1:1

$CDCl_3$ w/ MS and $CHPh_3$

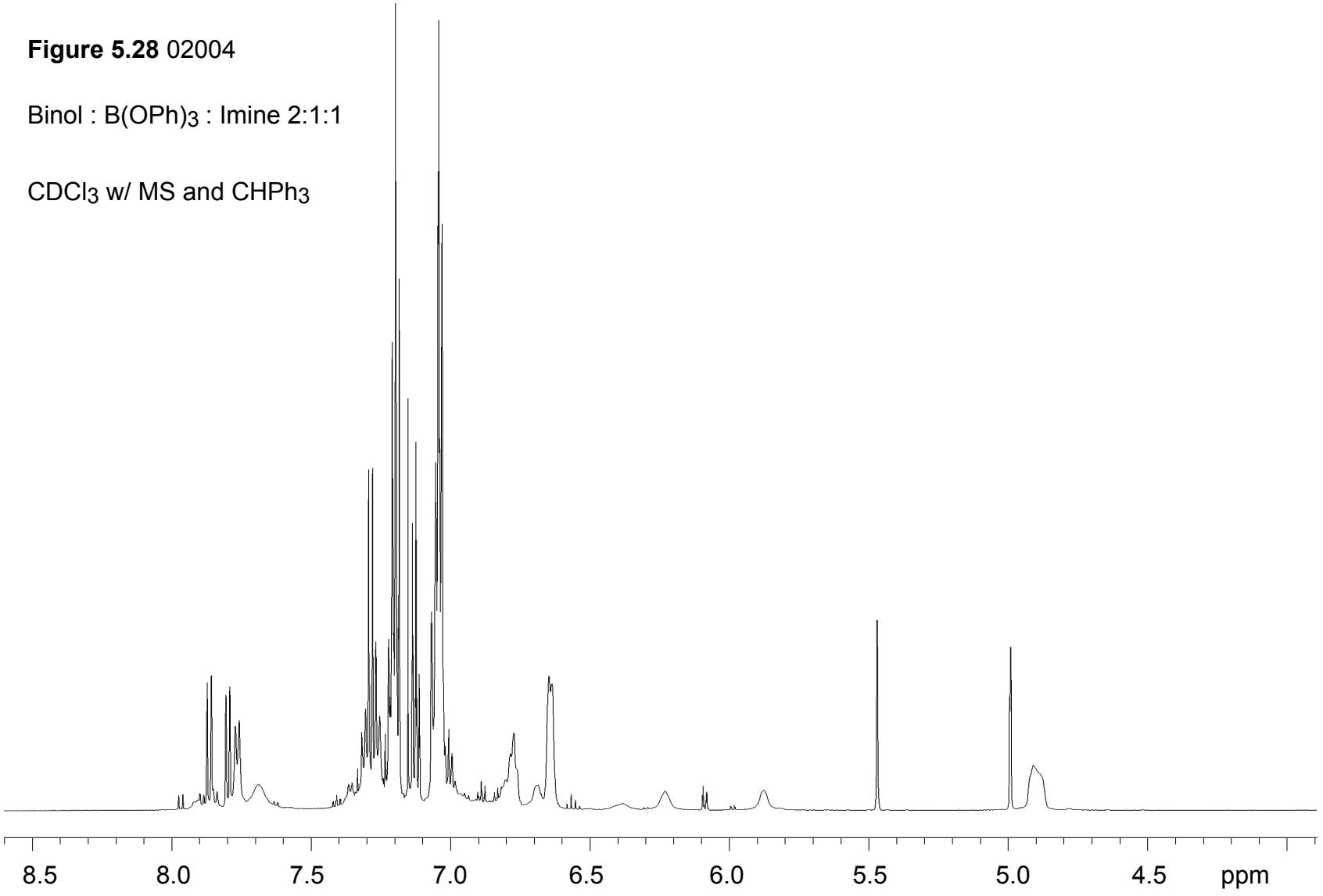

Figure 5.29 02004 Binol : $B(OPh)_3$: Imine 2:1:1

$CDCl_3$ w/ MS and $CHPh_3$

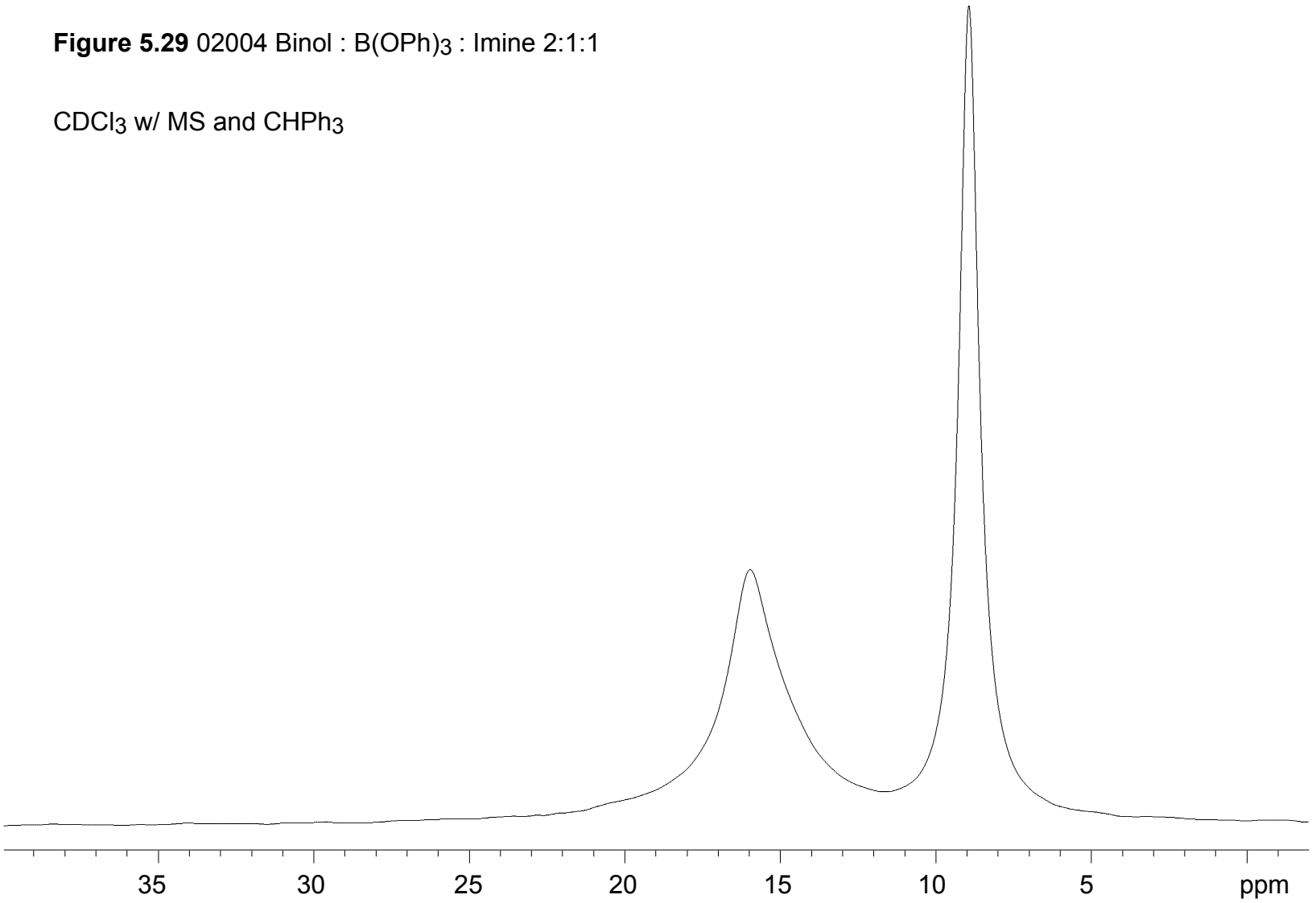

NMR study on the amount of BLA generated using various amounts of DMSO:

Procedure for 02251: To a flame-dried round bottom flask equipped with a stir bar was added 4 Å molecular sieves (flame-dried powder MS under reduced pressure) (200 mg), $CDCl_3$ (2 mL), (*R*)-binaphthol (40 mg, 0.14 mmol, 2.00 equiv), and $B(OPh)_3$ (20.2 mg, 0.07 mmol, 1.00 equiv) at room temperature under a nitrogen atmosphere. The mixture was stirred at room temperature for 1 h. The solution was then transferred to a flame-dried quartz NMR tube using a filter syringe (25 mm membrane diameter, PTFE 0.45 μm) in order to remove the molecular sieves. An internal standard was added ($CHPh_3$; 17.5 mg, 0.07 mmol, 1.00 equiv) followed by ^1H and ^{11}B NMR analysis. One equivalent of DMSO (5 μL, 0.07 mmol) was then added to the NMR tube and inverted several times to mix the solution followed by ^1H and ^{11}B NMR analysis. This was repeated with 2 equivalents, 5 equivalents, and 10 equivalents of DMSO. Each time ^1H and ^{11}B NMR analysis was obtained.

Results: Prior to DMSO addition = 0% BLA; 1 equivalent DMSO = 80%, 2 equivalents DMSO = 89%, 5 equivalents of DMSO = 110%, 10 equivalents of DMSO = 95%. These yields are not extremely accurate due to peak overlap in the region of integration (~7.8 ppm)

Experiment **Ref. #02251** is represented in Figures 4.10 and 4.11. Spectra for **02251** are shown below.

Figure 5.30 02251 Binol : $B(OPh)_3$ 2:1

$CDCl_3$ w/ MS and $CHPh_3$

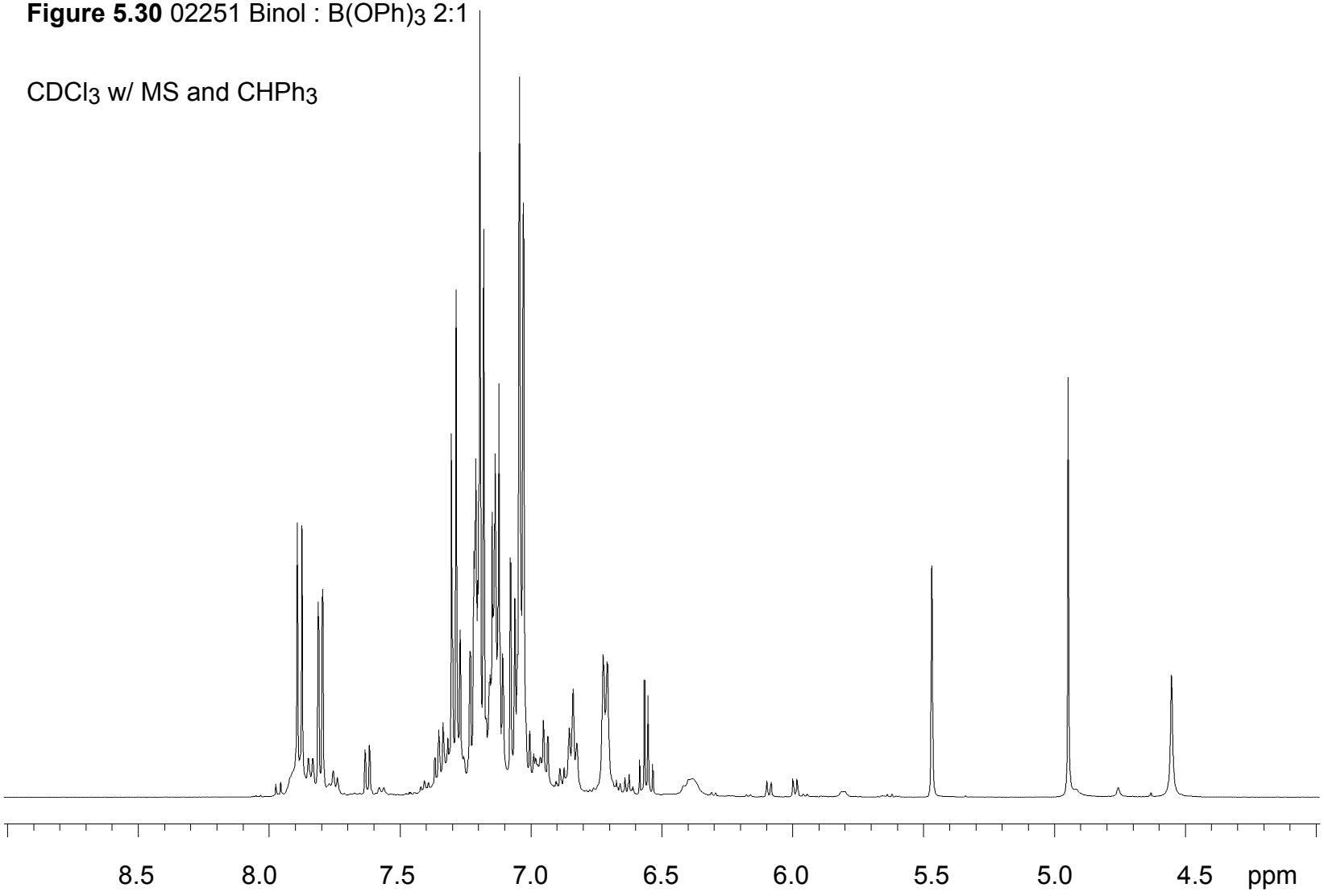

Figure 5.31 02251 Binol : $B(OPh)_3$ 2:1

$CDCl_3$ w/ MS and $CHPh_3$

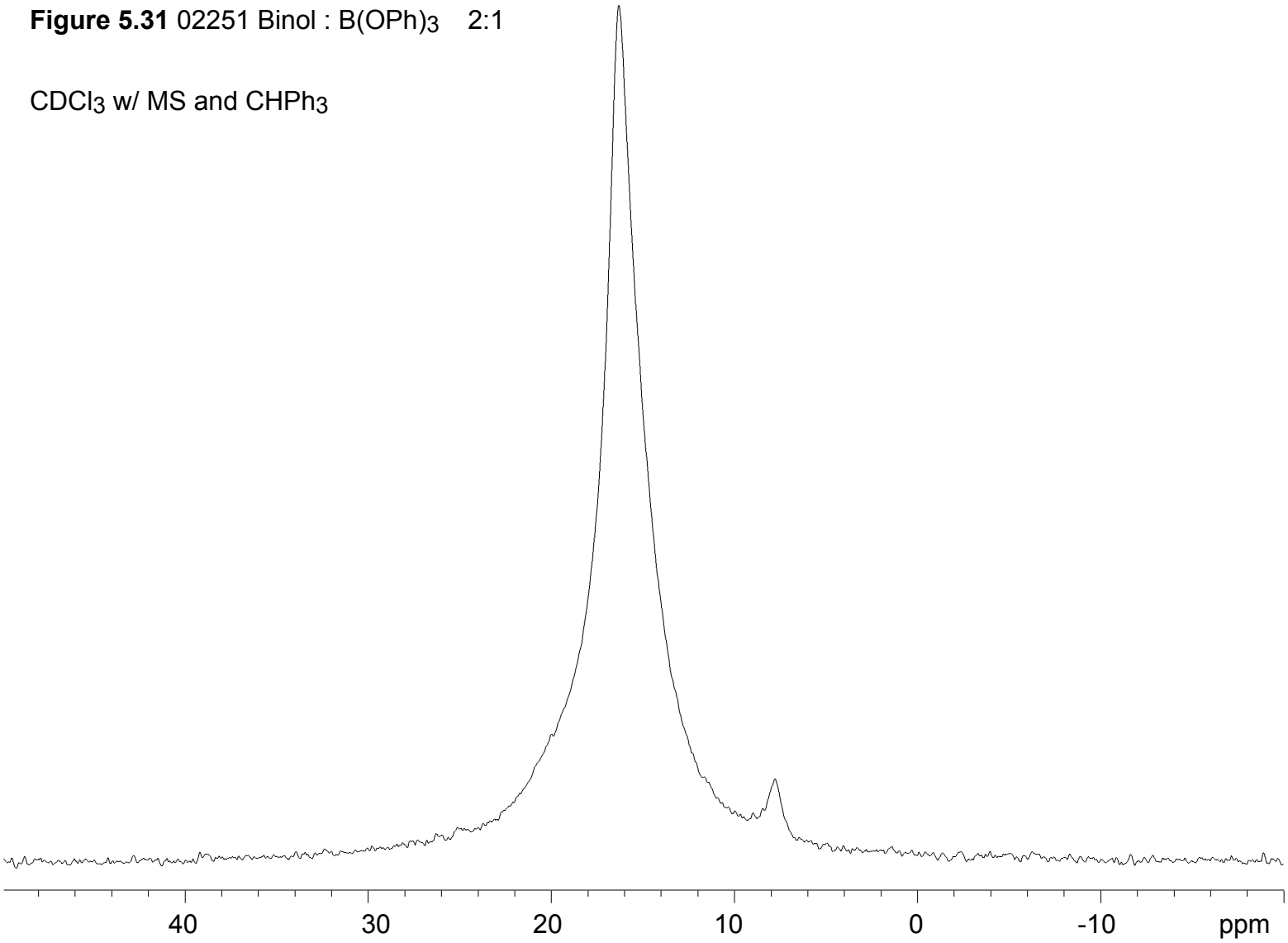

Figure 5.32 02251

Binol : $B(OPh)_3$: DMSO 2:1:1 $CDCl_3$

w/ MS and $CHPh_3$

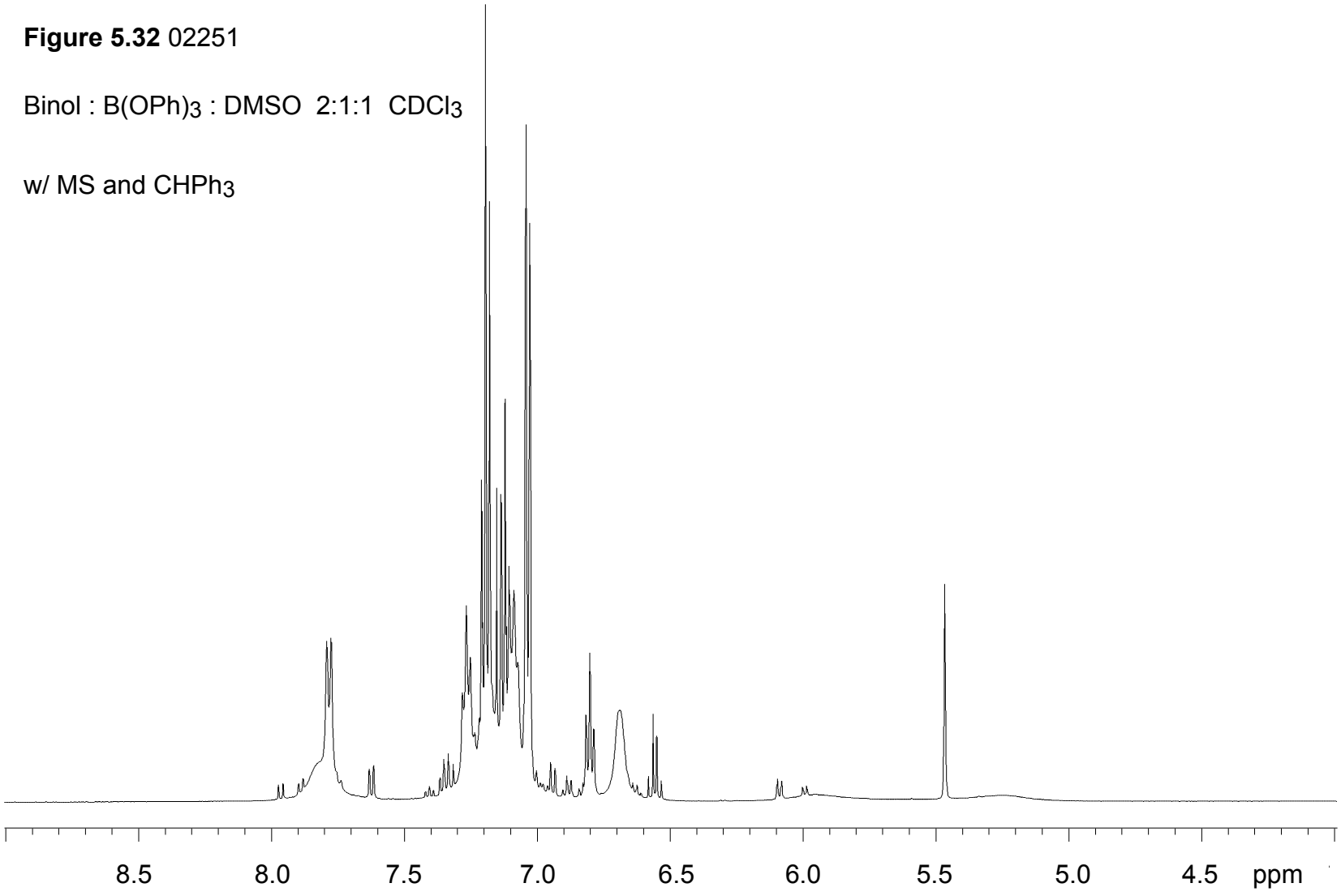

Figure 5.33 02251 Binol : $B(OPh)_3$: DMSO 2:1:1

$CDCl_3$ w/ MS and $CHPh_3$

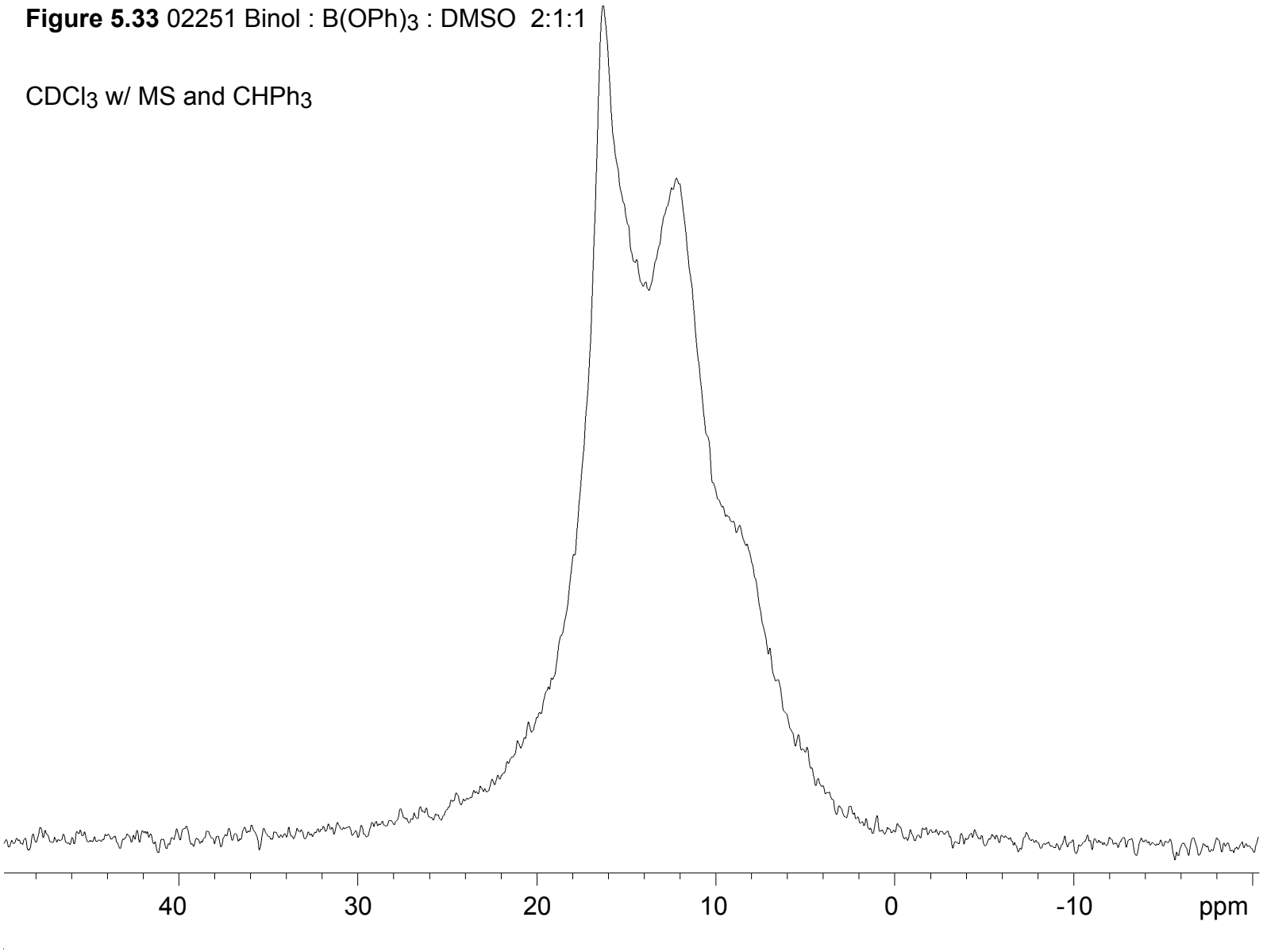

Figure 5.34 02251

Binol : $B(OPh)_3$: DMSO 2:1:2 $CDCl_3$

w/ MS and $CHPh_3$

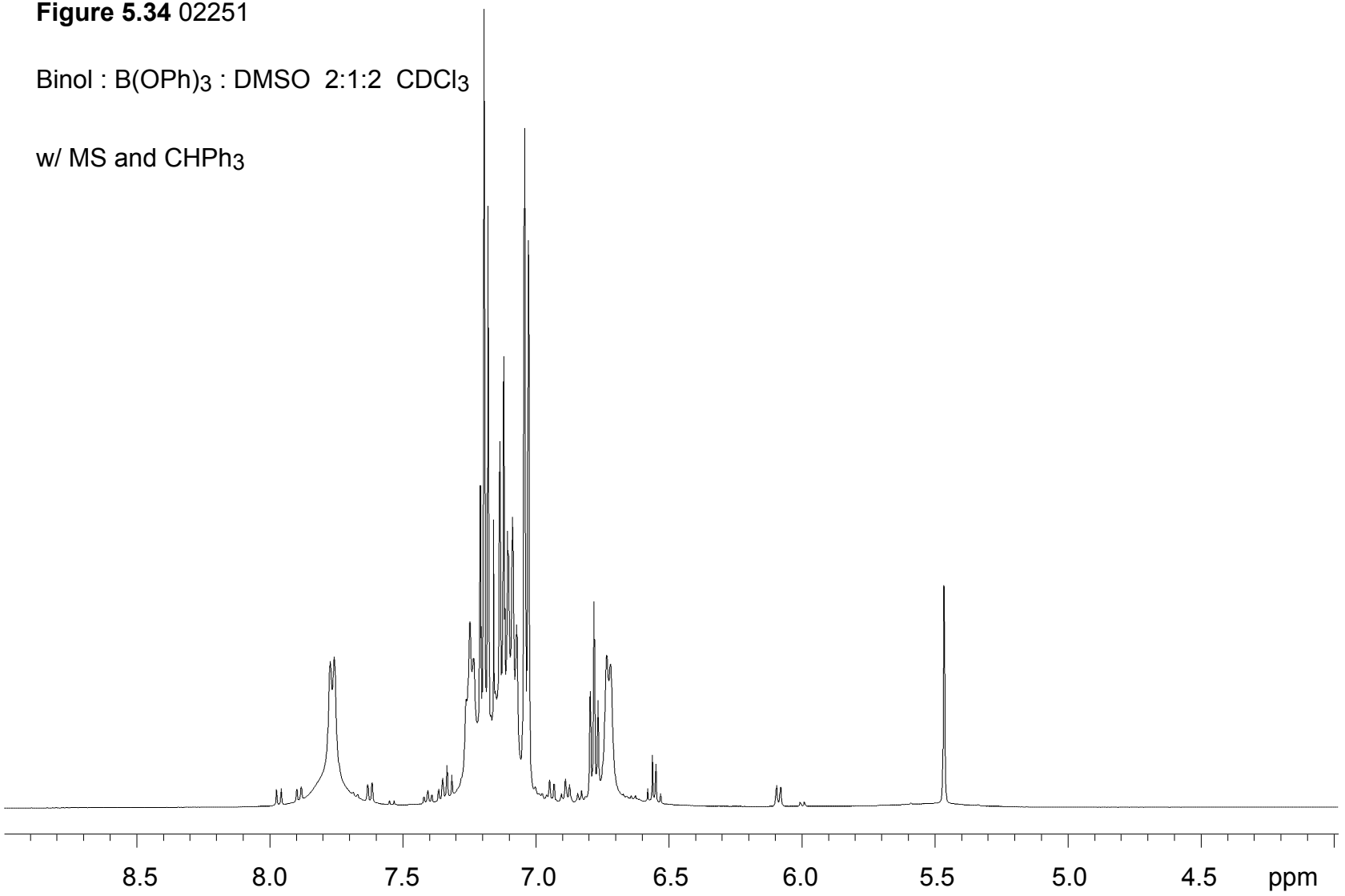

Figure 5.35 02251 Binol : $B(OPh)_3$: DMSO 2:1:2

$CDCl_3$ w/ MS and $CHPh_3$

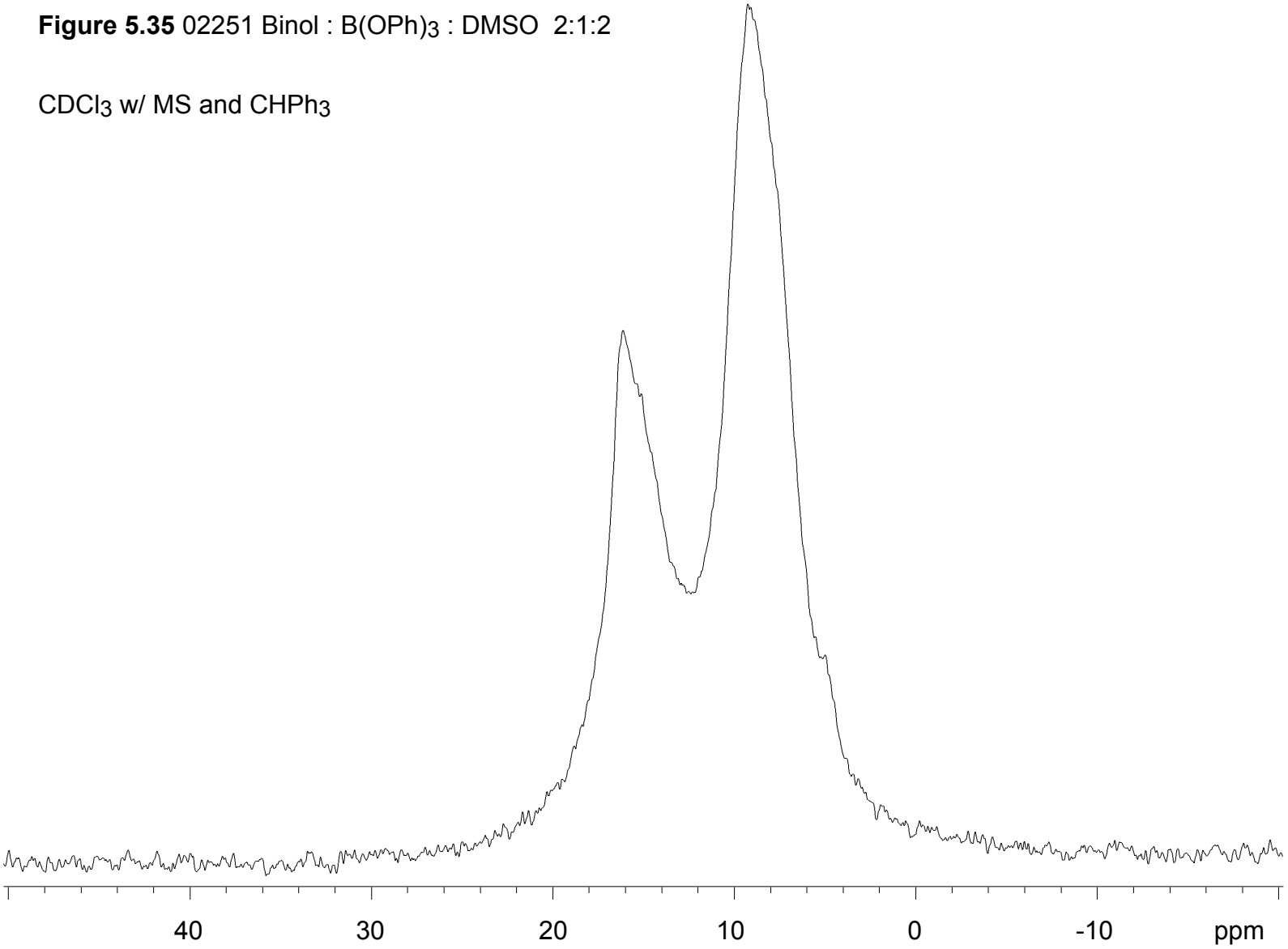

Figure 5.36 02251

Binol : $B(OPh)_3$: DMSO 2:1:5 $CDCl_3$

w/ MS and $CHPh_3$

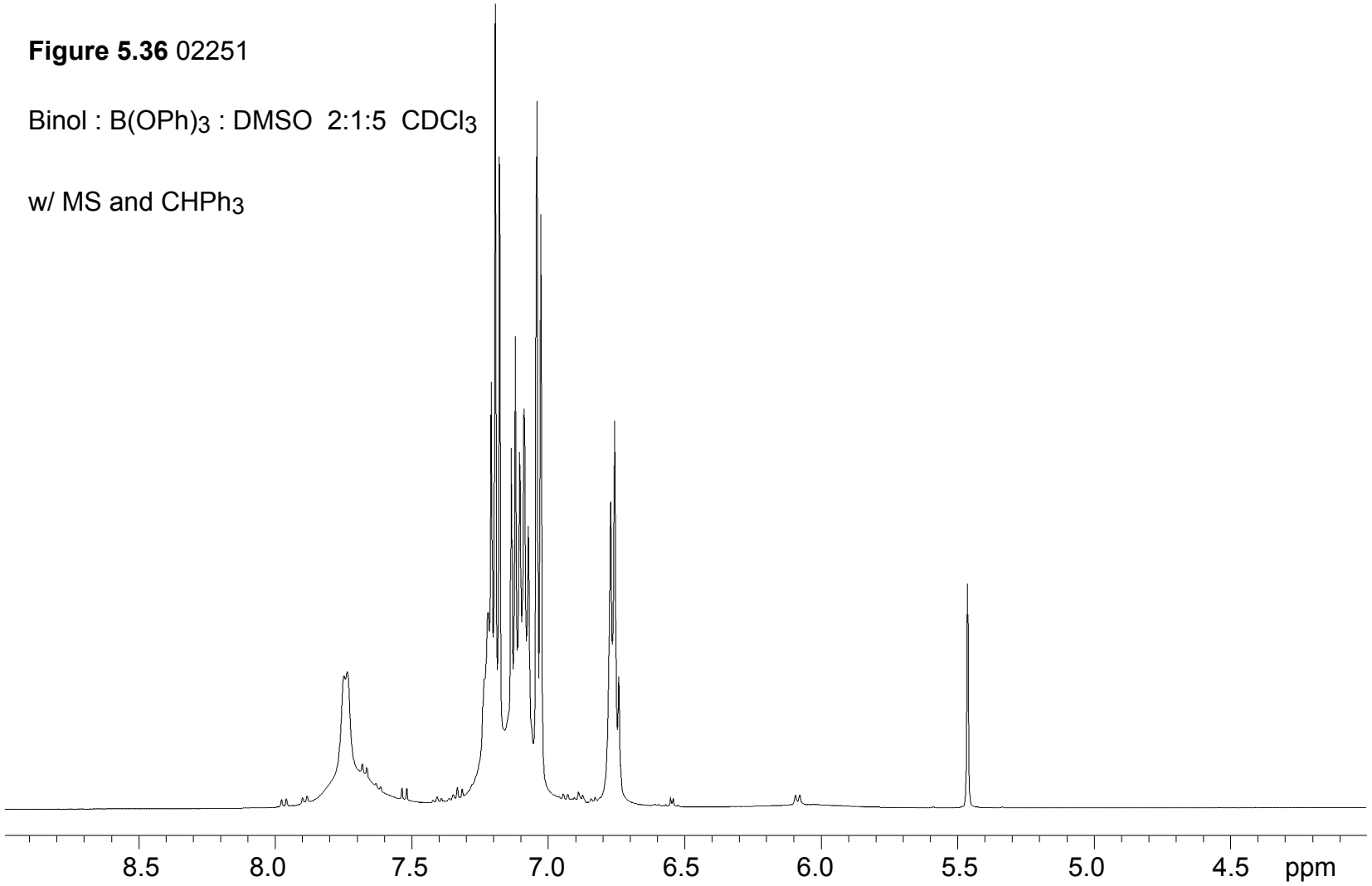

Figure 5.37 02251 Binol : $B(OPh)_3$: DMSO 2:1:5

$CDCl_3$ w/ MS and $CHPh_3$

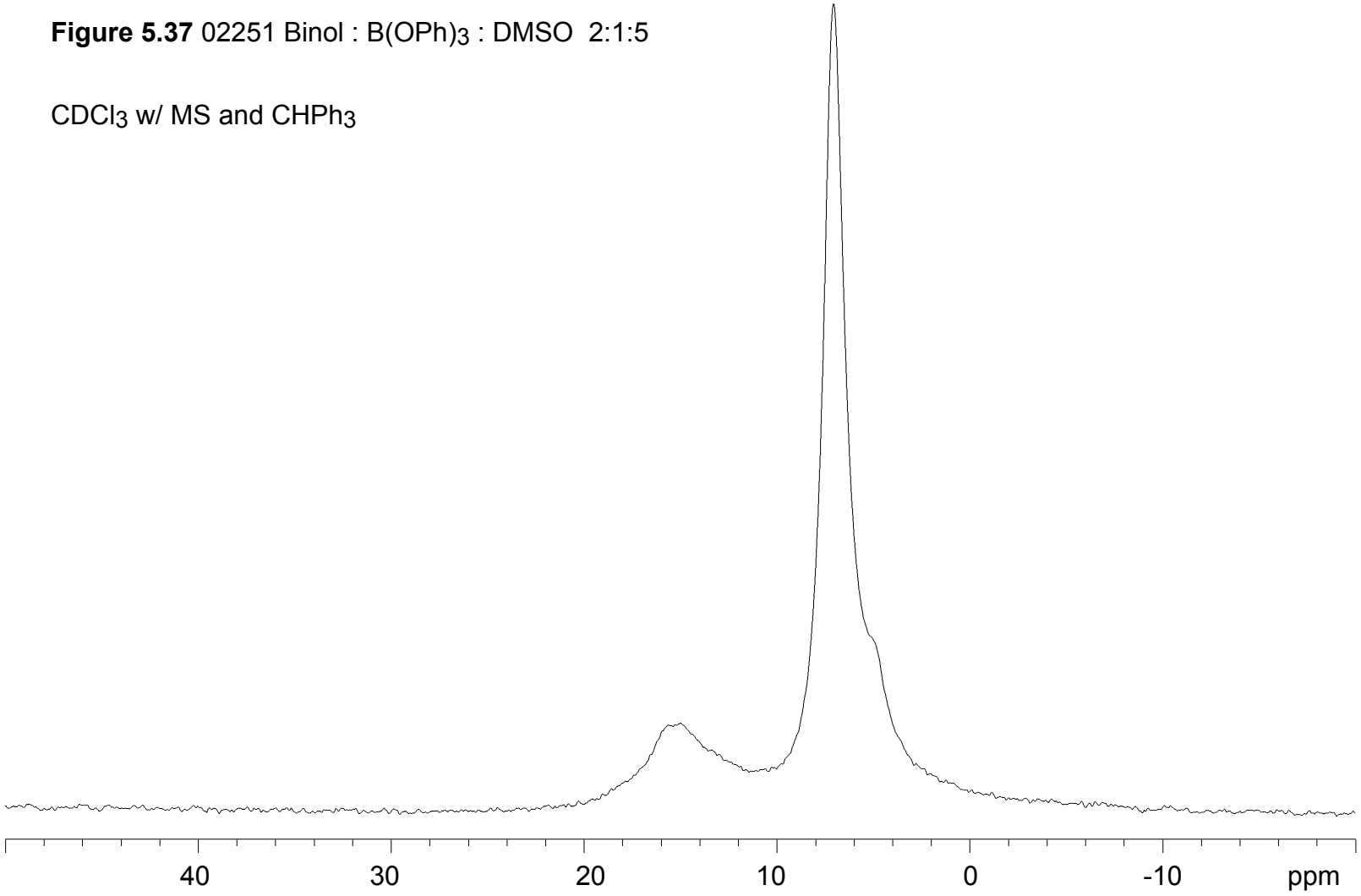

Figure 5.38 02251

Binol : $B(OPh)_3$: DMSO 2:1:10 $CDCl_3$

w/ MS and $CHPh_3$

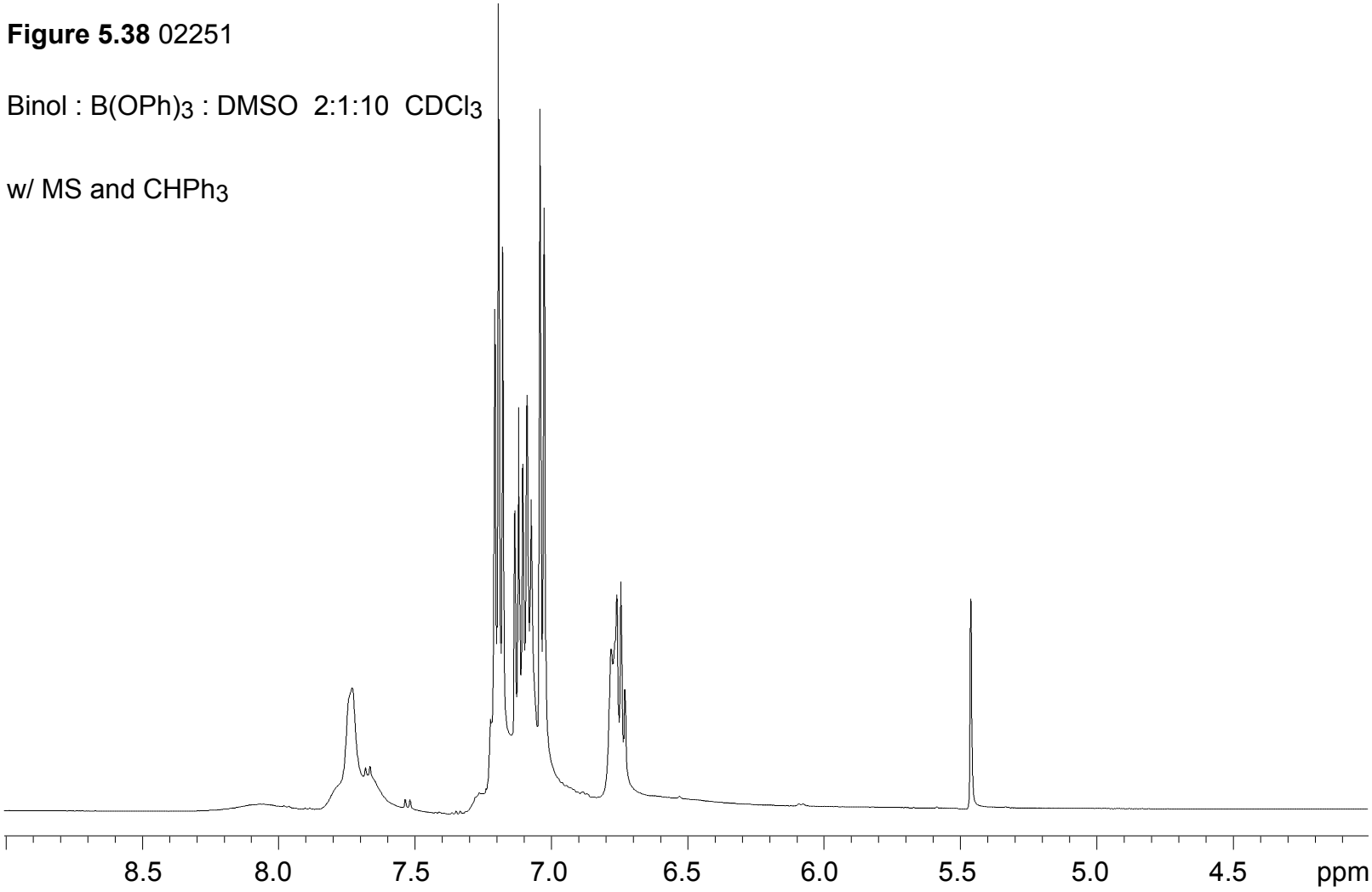

Figure 5.39 02251 Binol : $B(OPh)_3$: DMSO 2:1:10

$CDCl_3$ w/ MS and $CHPh_3$

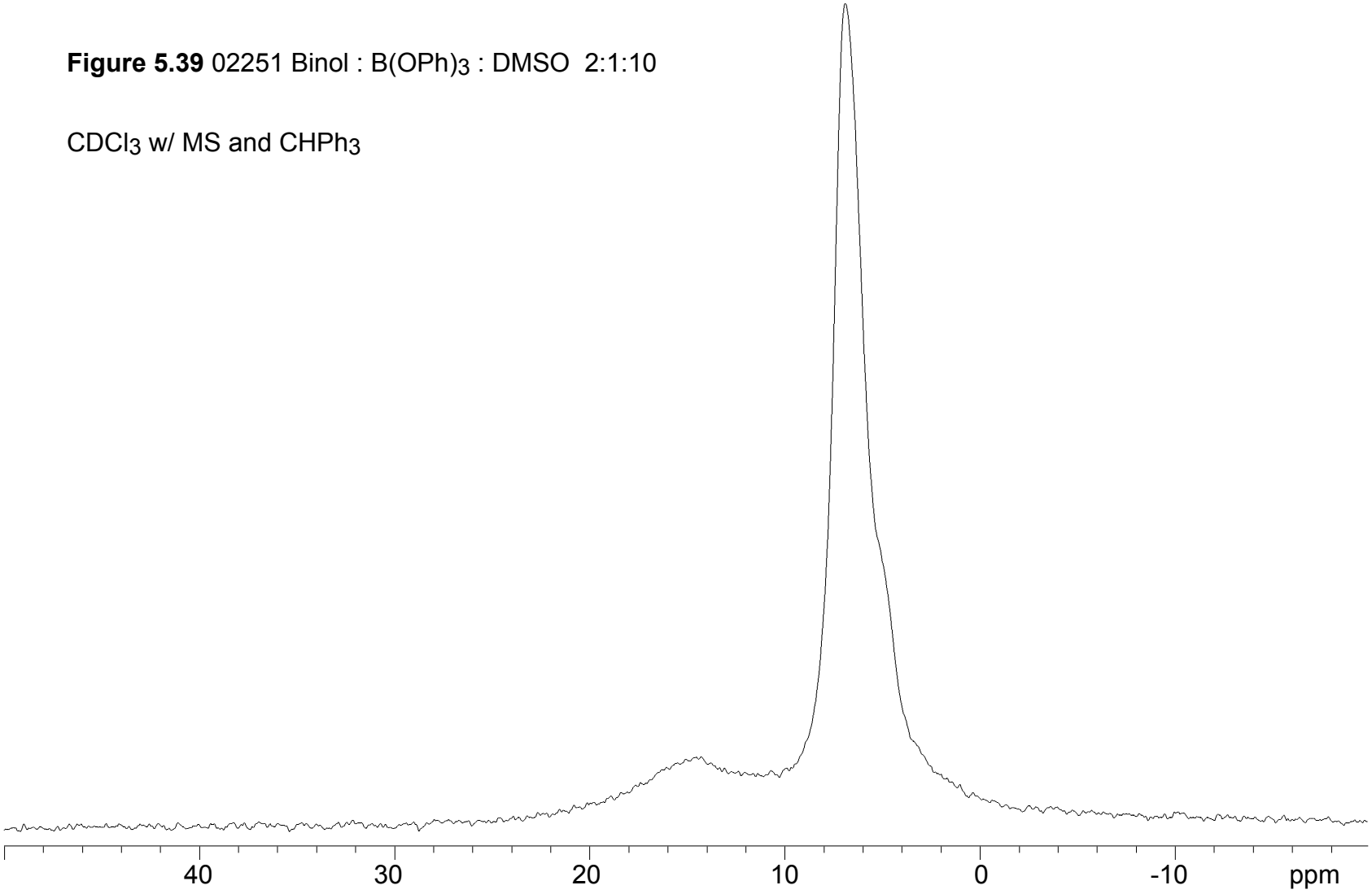

5.3.2.2 Synthesis of BINOL-borate complexes using borane dimethyl sulfide (Figures 4.6 and 4.7)

Procedure for 02007: To a flame-dried 50 mL Schlenk flask was added (*R*)-binaphthol (50 mg, 0.115 mmol) and THF (2.5 mL). To the stirred solution was added BH_3•THF (115 µL, 0.115 mmol) and acetic acid (6.5 µL, 0.115 mmol). The reaction was stirred at room temperature for 10 minutes followed by removing the volatiles under reduced pressure (0.1 mmHg) for 1 h. An internal standard ($CHPh_3$; 28.0 mg, 0.115 mmol, 1.00 equiv) was then added and the solids were dissolved in $CDCl_3$ (1 mL) and transferred to a flame-dried quartz NMR tube. ^1H and ^{11}B NMR analysis were then performed. Lastly, phenol (11 mg, 0.115 mmol) was added to the NMR tube as a 0.23 M solution in $CDCl_3$ and once again, ^1H and ^{11}B NMR analysis was performed. **Results**: Prior to phenol addition = 94% propeller. After imine addition = 42% propeller and 26% BINOL.

NOTE: Acetic acid was purified by refluxing acetic acid with 2% CrO_3 and 5% acetic anhydride followed by distillation.

Experiment **Ref. #02007** is represented in Figure 4.6 as entry 2. Spectra for **02007** are shown below.

Figure 5.40 02007

BINOL : BH_3 : AcOH 1:1:1

No phenol added $CDCl_3$

w/ $CHPh_3$

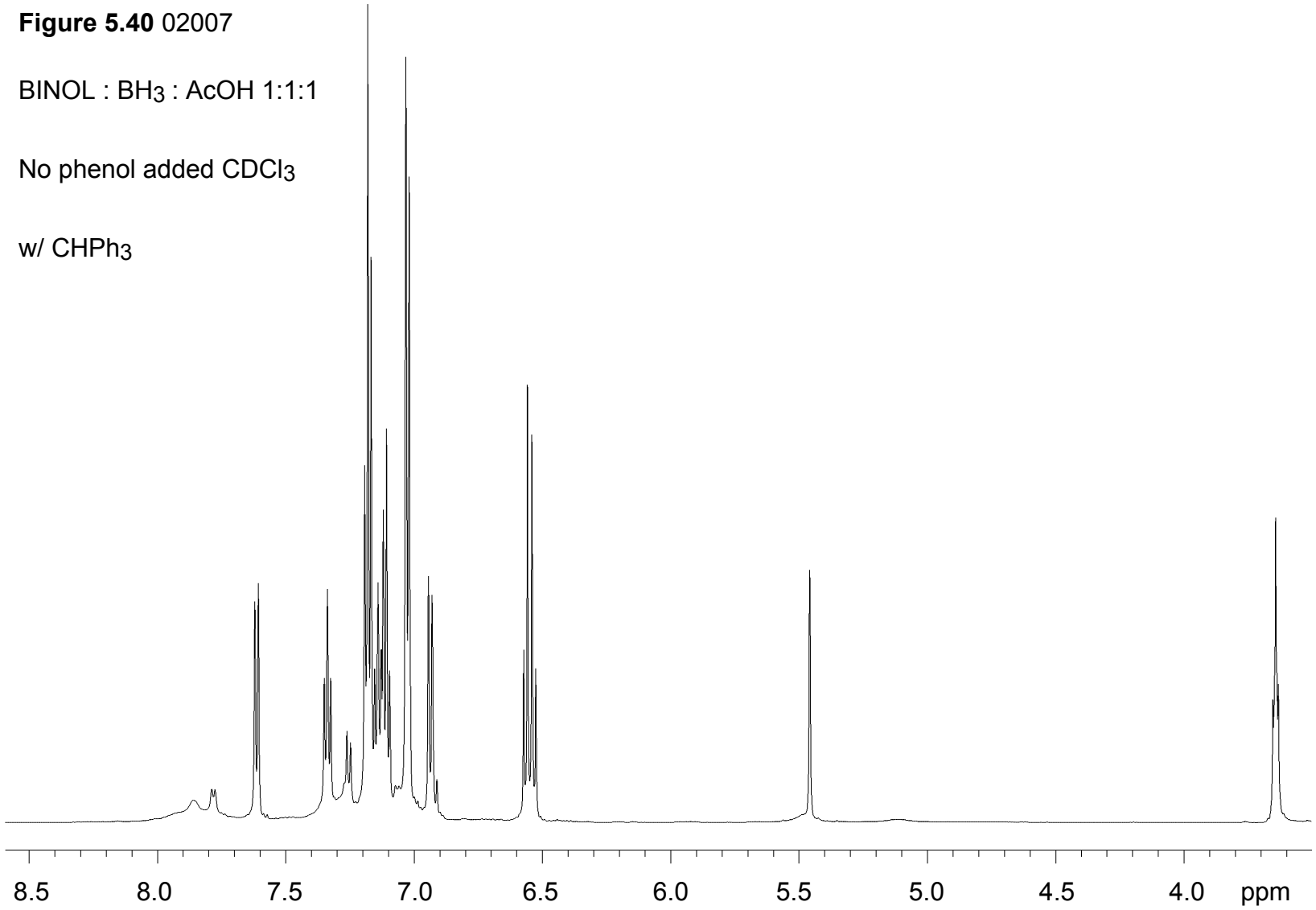

Figure 5.41 02007 BINOL : BH_3 : AcOH 1:1:1

No Phenol; $CDCl_3$ with $CHPh_3$

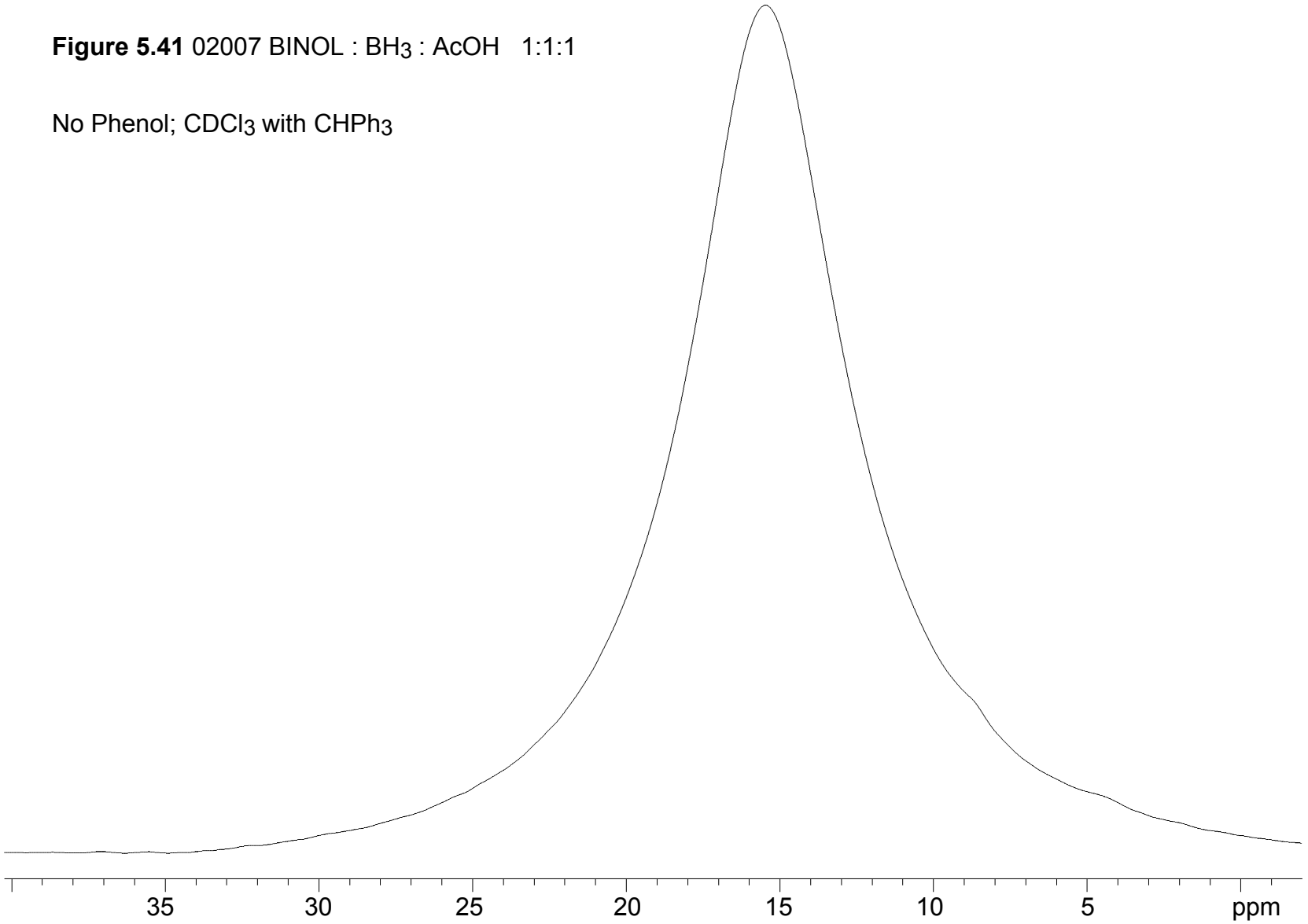

Figure 5.42 02007

BINOL : BH_3 : AcOH 1:1:1 w/ phenol added $CDCl_3$ with $CHPh_3$

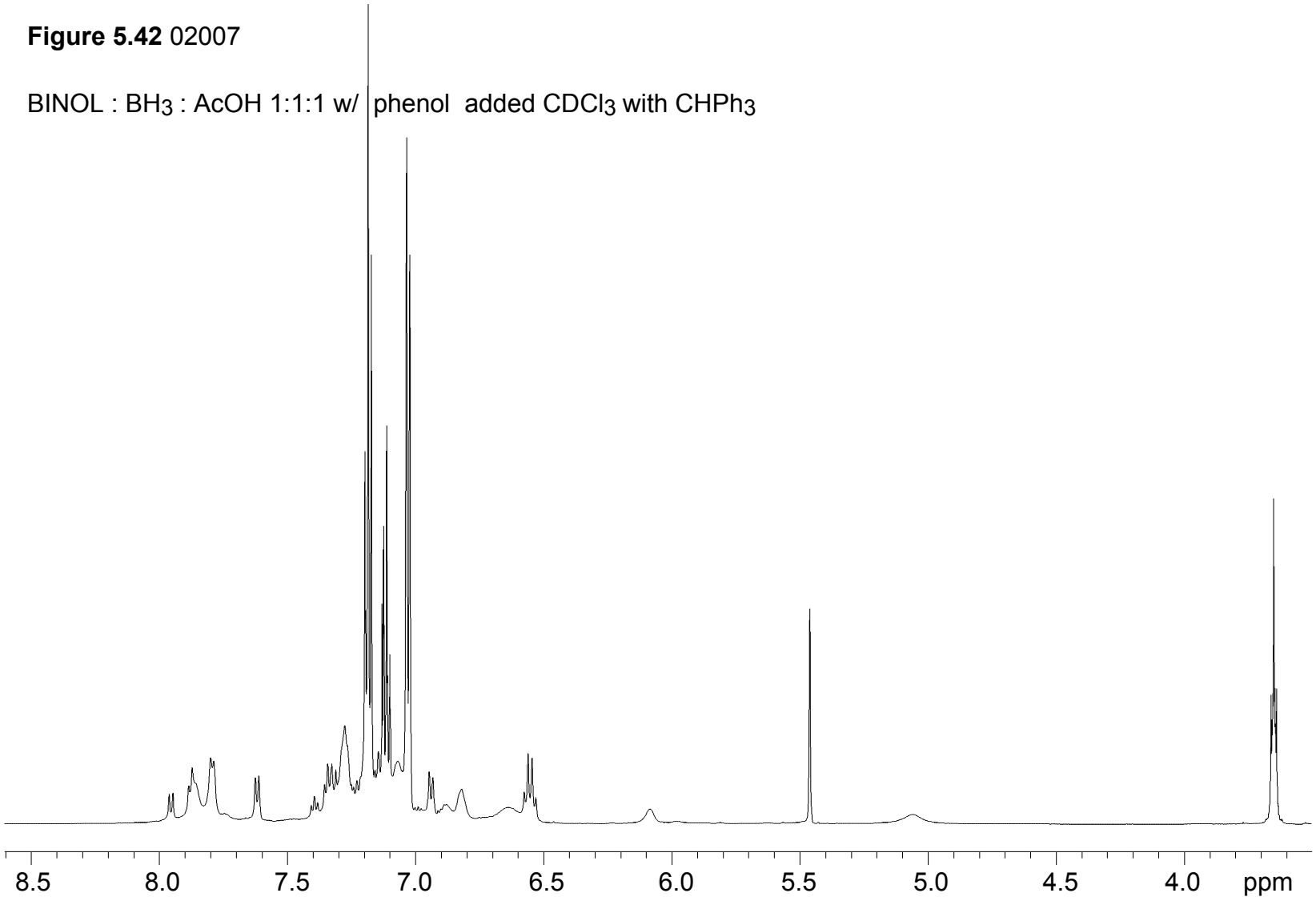

Figure 5.43 02007 BINOL : BH_3 : AcOH 1:1:1

w/ phenol added; $CDCl_3$ w/ $CHPh_3$

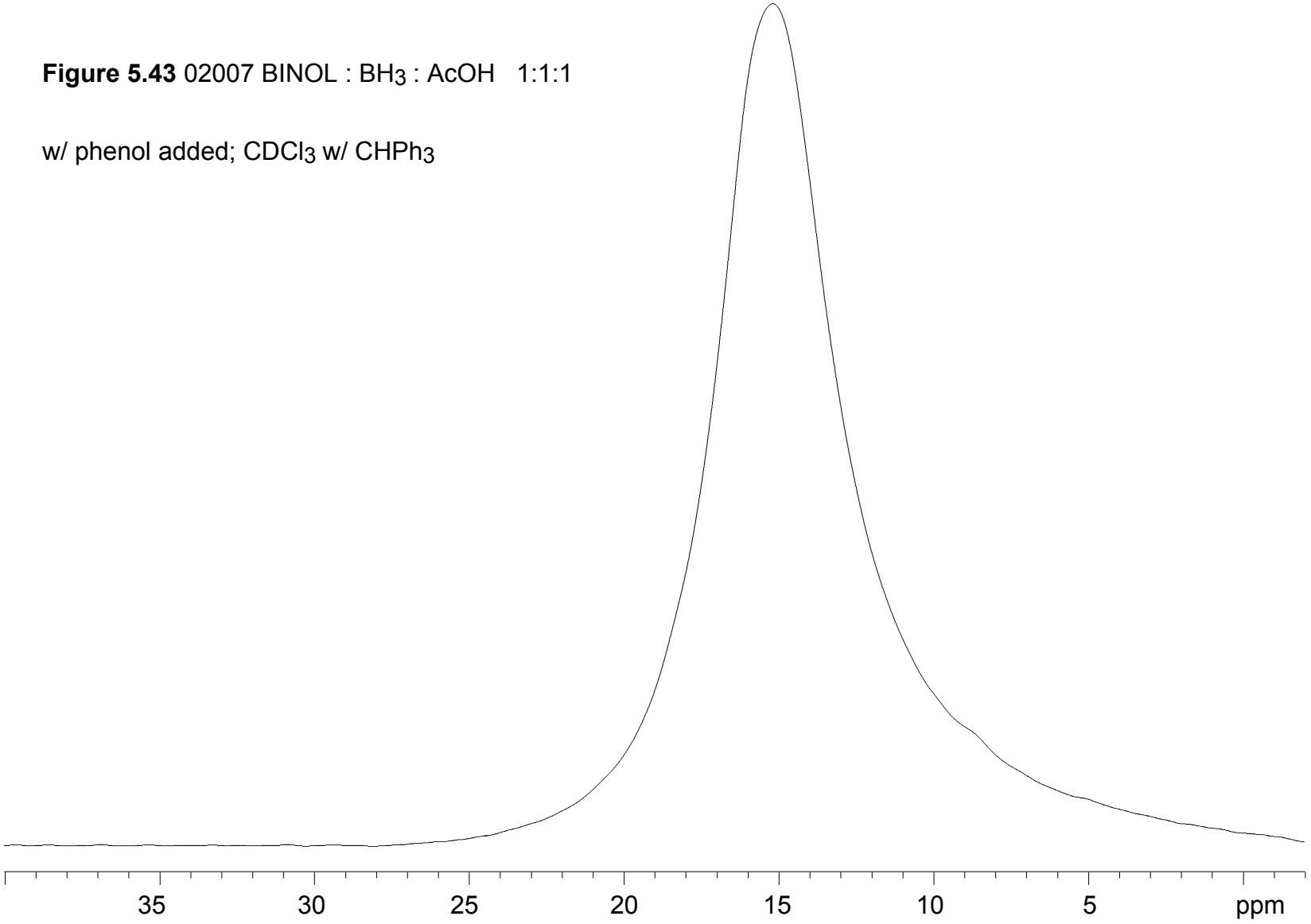

Procedure for 02005: To a flame-dried 50 mL Schlenk flask was added (*R*)-binaphthol (50 mg, 0.115 mmol) and THF (2.5 mL). To the stirred solution was added BH_3•THF (115 µL, 0.115 mmol) and acetic acid (6.5 µL, 0.115 mmol). The reaction was stirred at room temperature for 10 minutes followed by removing the volatiles under reduced pressure (0.1 mmHg) for 30 minutes. Phenol (11 mg, 0.115 mmol) was added as a 0.23 M solution in $CDCl_3$. An internal standard ($CHPh_3$; 28.0 mg, 0.115 mmol, 1.00 equiv) was then added and the solution was transferred to a flame-dried quartz NMR tube. ^1H and ^{11}B NMR analysis was then performed. **Results:** 23% BINOL, 21% propeller, 2% B2, and 5% B1.

NOTE: Acetic acid was purified by refluxing acetic acid with 2% CrO_3 and 5% acetic anhydride followed by distillation.

Experiment **Ref. #02005** is represented in Figure 4.6 as entry 3. Spectra for **02005** are shown below.

Figure 5.44 02005

BINOL : BH_3 : AcOH 1:1:1

$CDCl_3$ with $CHPh_3$

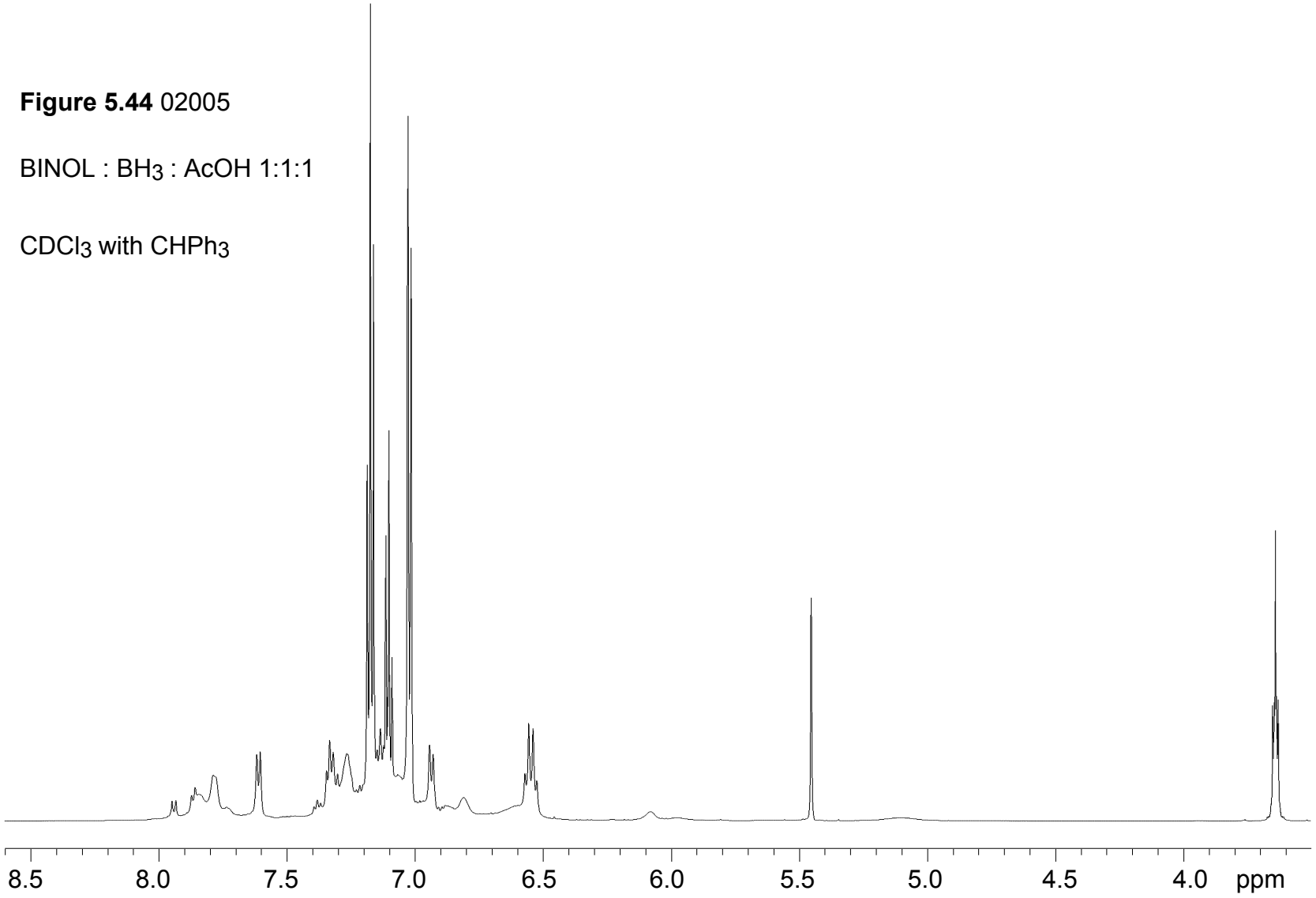

Figure 5.45 02005 BINOL : BH_3 : AcOH 1:1:1

$CDCl_3$ with $CHPh_3$

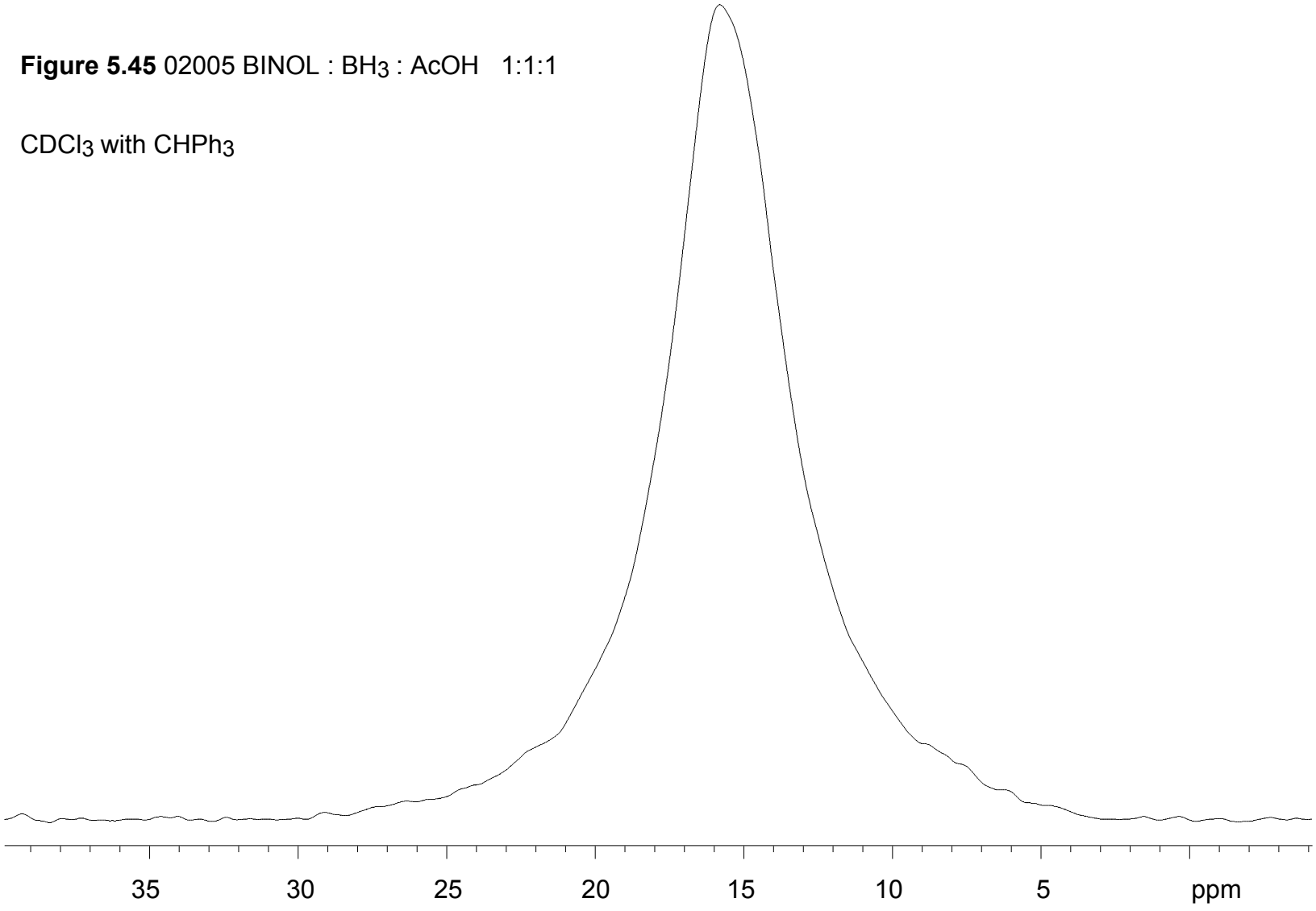

Procedure for 02006: To a flame-dried 50 mL Schlenk flask was added (*R*)-binaphthol (50 mg, 0.115 mmol) and THF (2.5 mL). To the stirred solution was added BH_3•THF (230 µL, 0.23 mmol) and acetic acid (13.0 µL, 0.23 mmol). The reaction was stirred at room temperature for 10 minutes followed by removing the volatiles under reduced pressure (0.1 mmHg) for 30 minutes. Phenol (11 mg, 0.115 mmol) was added as a 0.23 M solution in $CDCl_3$. An internal standard ($CHPh_3$; 28.0 mg, 0.115 mmol, 1.00 equiv) was then added and the solution was transferred to a flame-dried quartz NMR tube. ^1H and ^{11}B NMR analysis was then performed. **Results**: 32% BINOL (messy area in spectrum) and 84% propeller.

NOTE: Acetic acid was purified by refluxing acetic acid with 2% CrO_3 and 5% acetic anhydride followed by distillation.

Experiment **Ref. #02006** is represented in Figure 4.6 as entry 4. Spectra for **02006** are shown below.

Figure 5.46 02006

BINOL : BH_3 : AcOH 1:2:2

$CDCl_3$ with $CHPh_3$

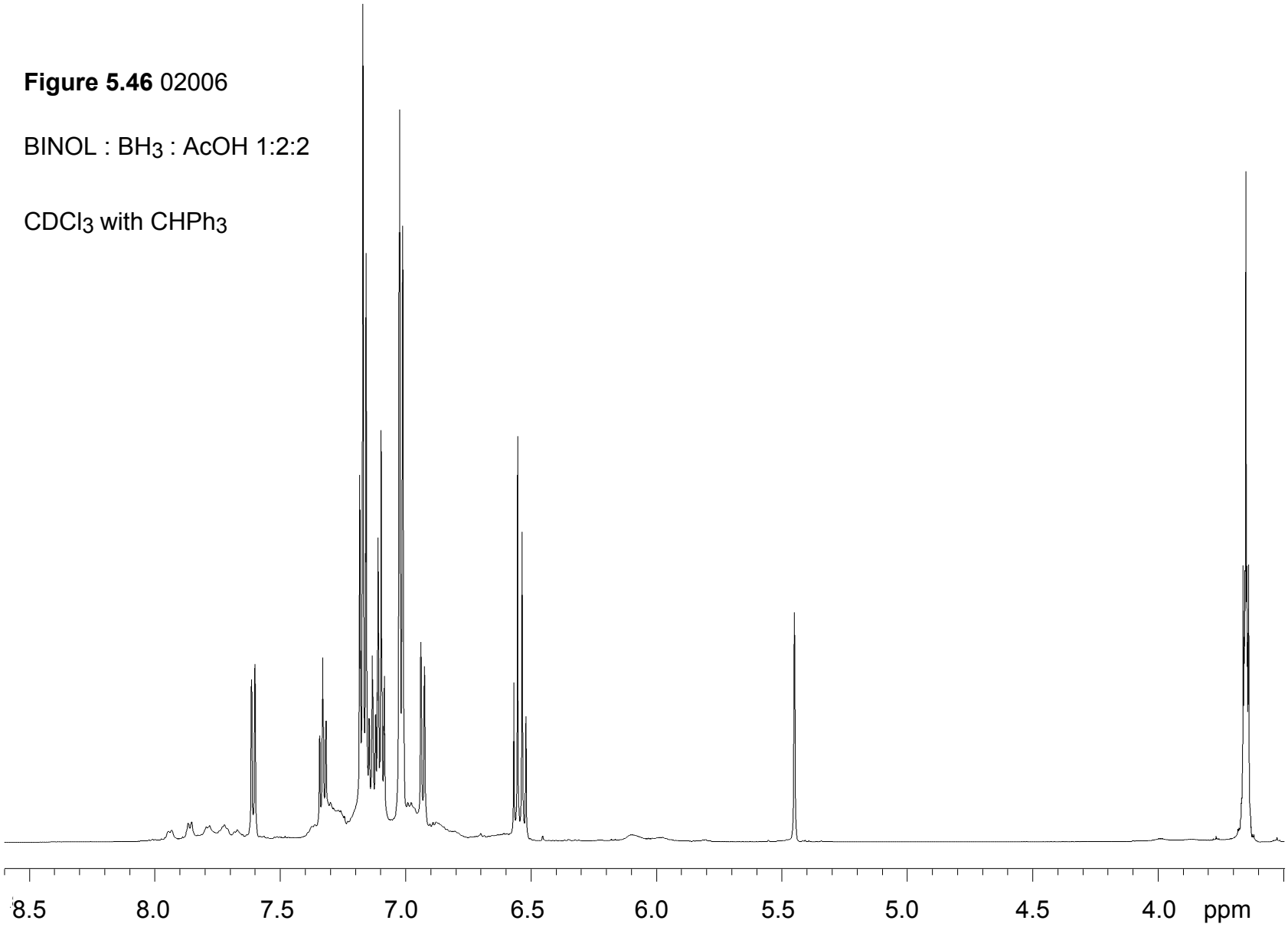

Figure 5.47 02006 BINOL : BH_3 : AcOH 1:2:2

$CDCl_3$ with $CHPh_3$

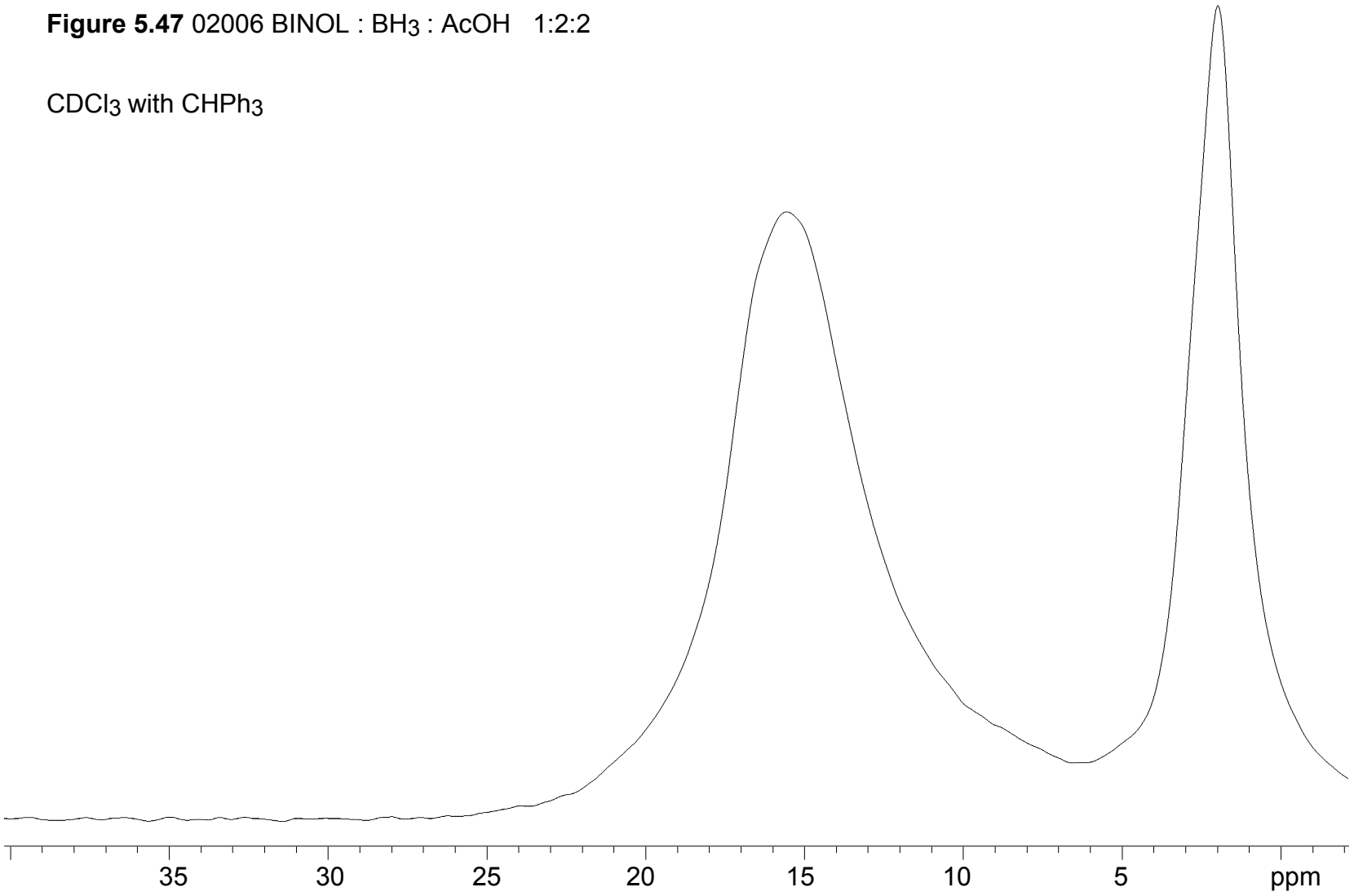

5.3.3 General procedure for the synthesis of BINOL-borate complexes in deuterated DMSO (Figures 4.8 and 4.9)

Procedure for 02010: To a flame-dried round bottom flask equipped with a stir bar was added 4 Å molecular sieves (flame-dried powder MS under reduced pressure) (200 mg), DMSO (2 mL), (*R*)-binaphthol (40 mg, 0.14 mmol), and $B(OPh)_3$ (20.2 mg, 0.07 mmol) at room temperature under a nitrogen atmosphere. The mixture was stirred at room temperature for 1 h. The solution was then transferred to a flame-dried quartz NMR tube using a filter syringe (25 mm membrane diameter, PTFE 0.45 µm) in order to remove the molecular sieves. An internal standard was added ($CHPh_3$; 17.5 mg, 0.07 mmol, 1.00 equiv) followed by ^{1}H and ^{11}B NMR analysis. Imine **8a** (19 mg, 0.07 mmol) was dissolved in 0.3 mL $CDCl_3$ and added to the NMR tube, which was then inverted several times to ensure the solution was homogeneous. Once again, ^{1}H and ^{11}B NMR analysis was performed. **Results**: Prior to imine addition = 29% BINOL and 56% BLA. After imine addition = 27% BINOL and 55% BLA.

Experiment **Ref. # 02011** is repeating experiment **02010** but without $CHPh_3$. Experiment **Ref. #02011** is represented in Figure 4.8 as entries 2 and 4. Spectra for **02010** and **02011** are shown below.

Figure 5.48 02010 BINOL : $B(OPh)_3$ 2:1 DMSO w/ MS and $CHPh_3$

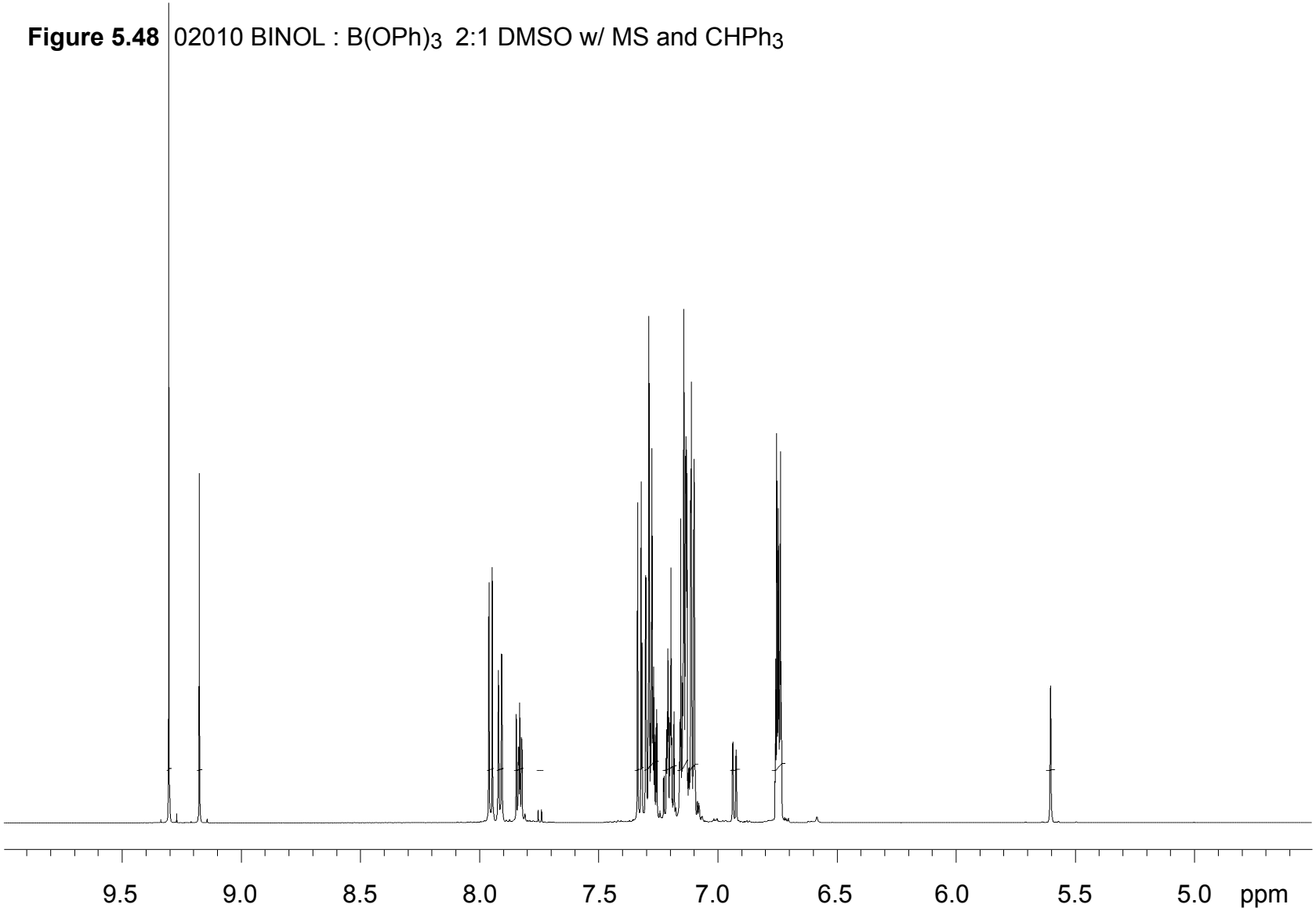

Figure 5.49 02010 BINOL : $B(OPh)_3$ 2:1

DMSO w/ MS and $CHPh_3$

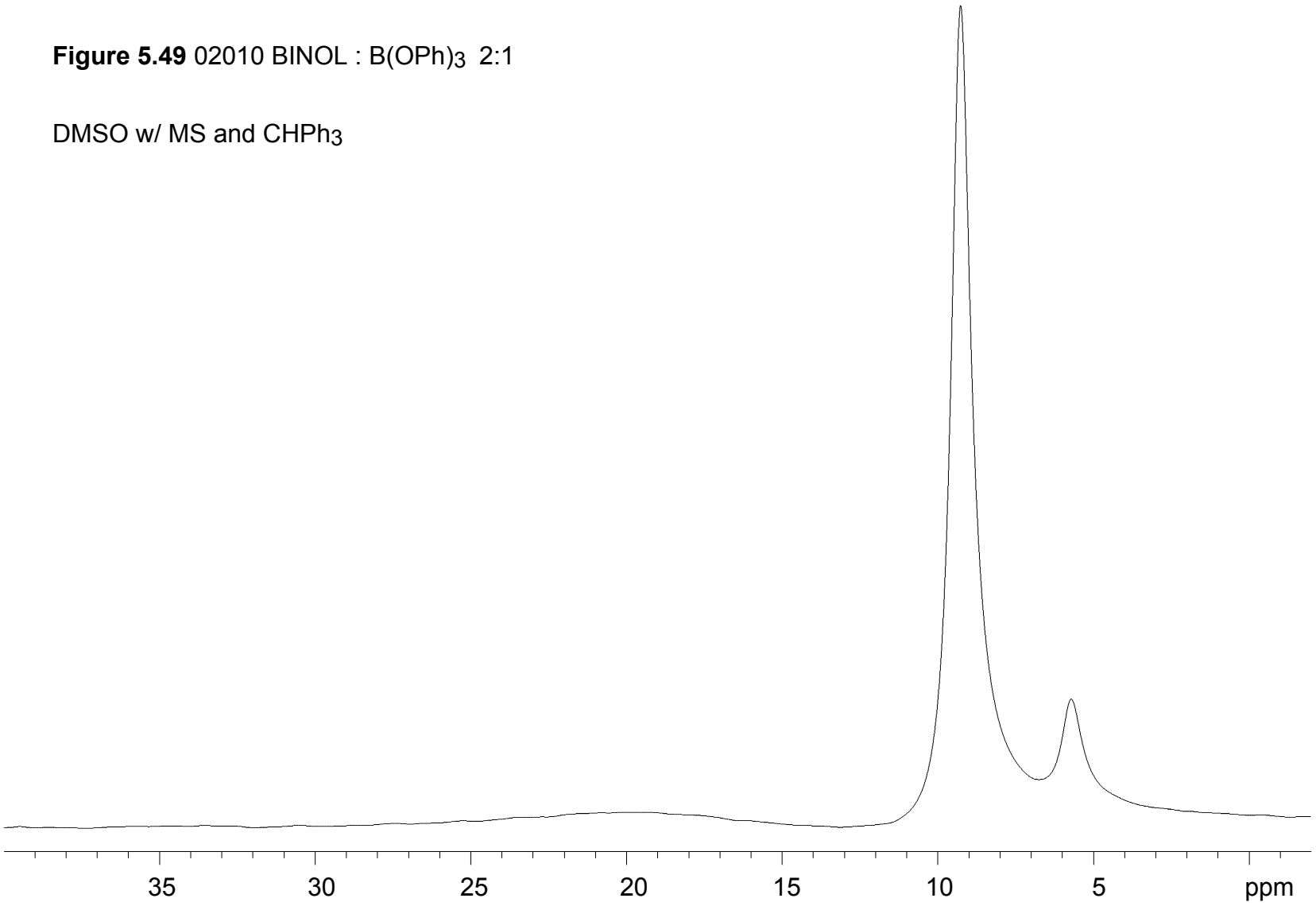

Figure 5.50 02010 BINOL : $B(OPh)_3$: Imine 2:1:1 DMSO w/ MS and $CHPh_3$

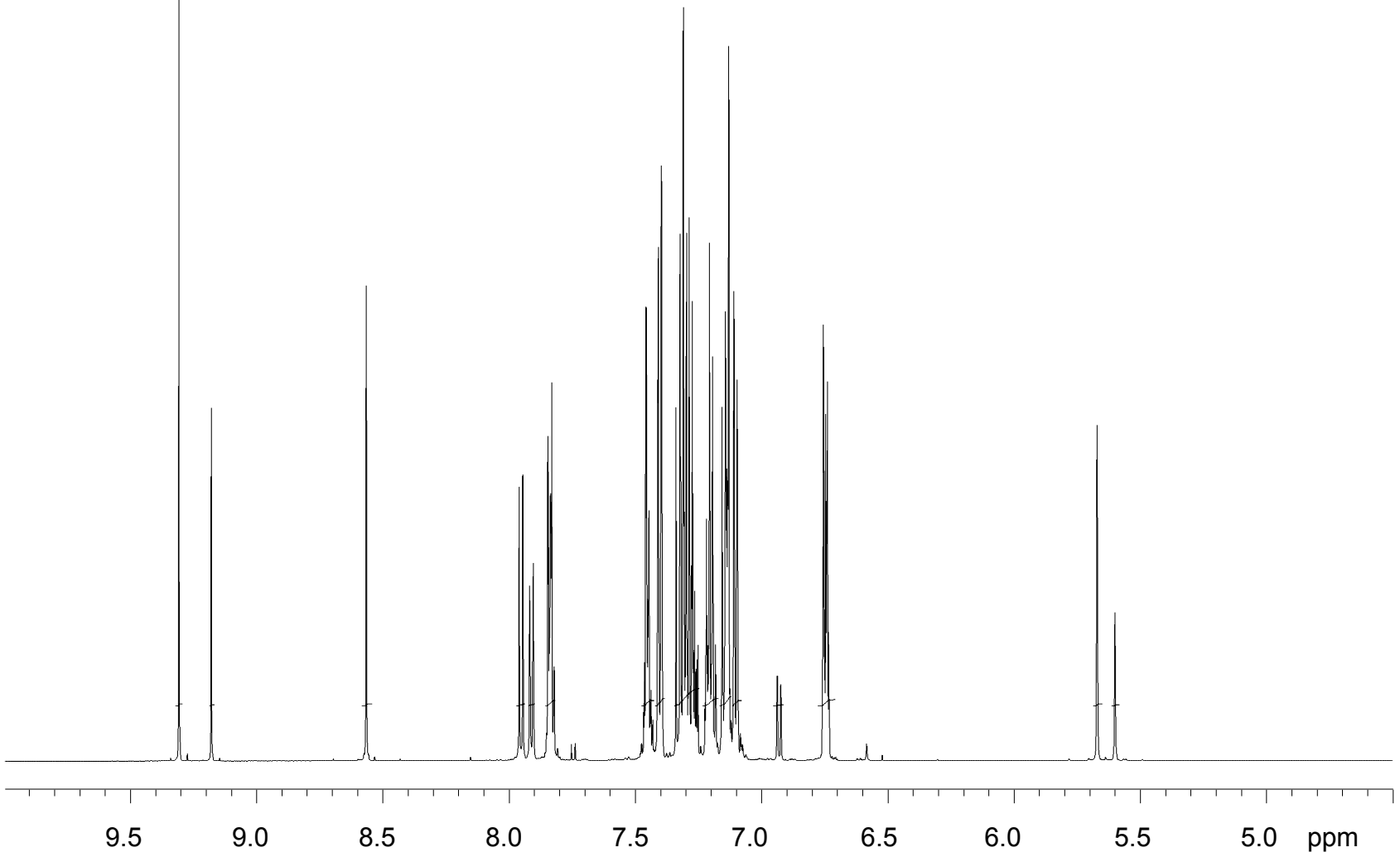

Figure 5.51 02010 BINOL : $B(OPh)_3$: Imine 2:1:1

DMSO w/ MS and $CHPh_3$

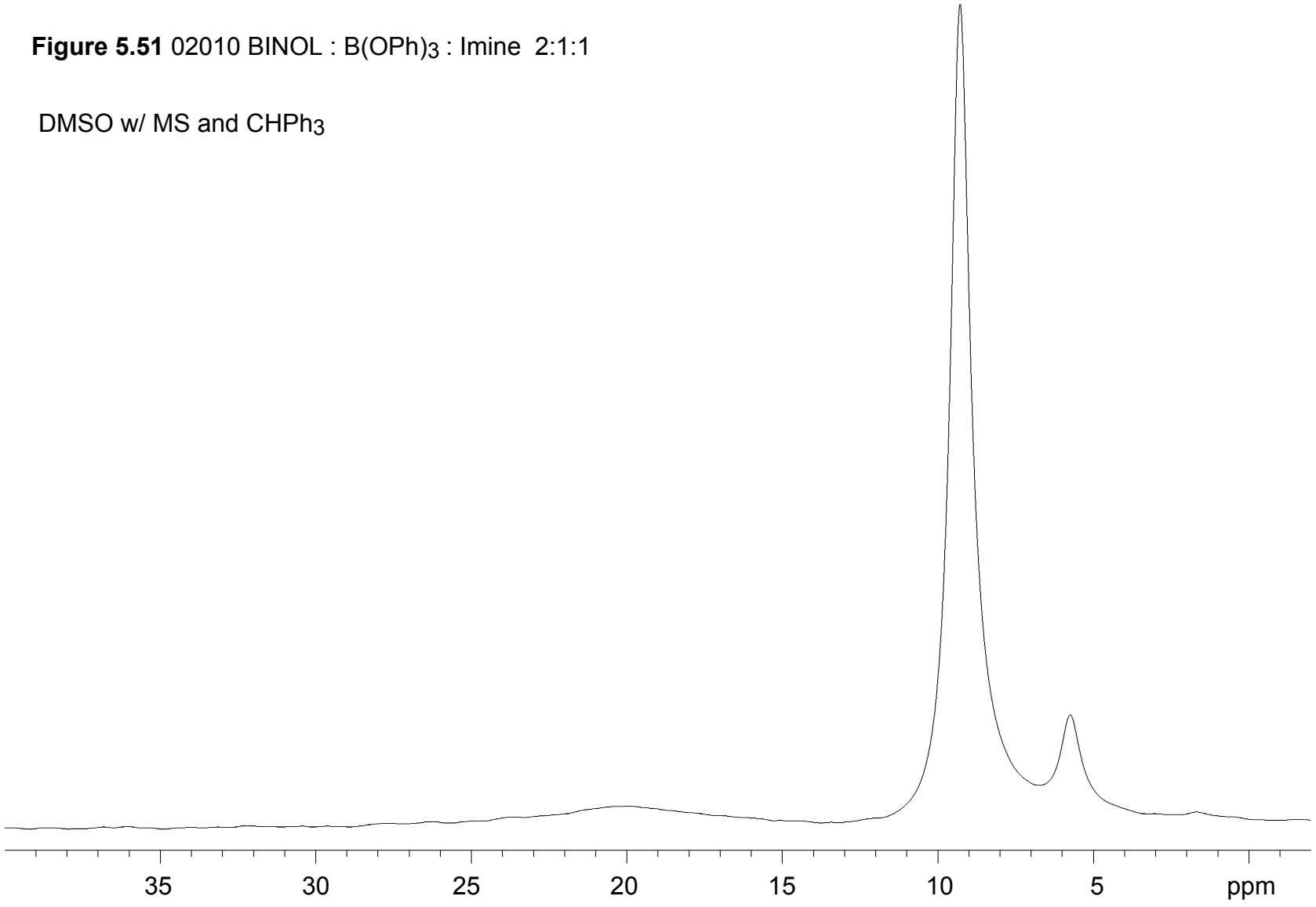

Figure 5.52 02011 BINOL : $B(OPh)_3$ 2:1 DMSO w/ MS

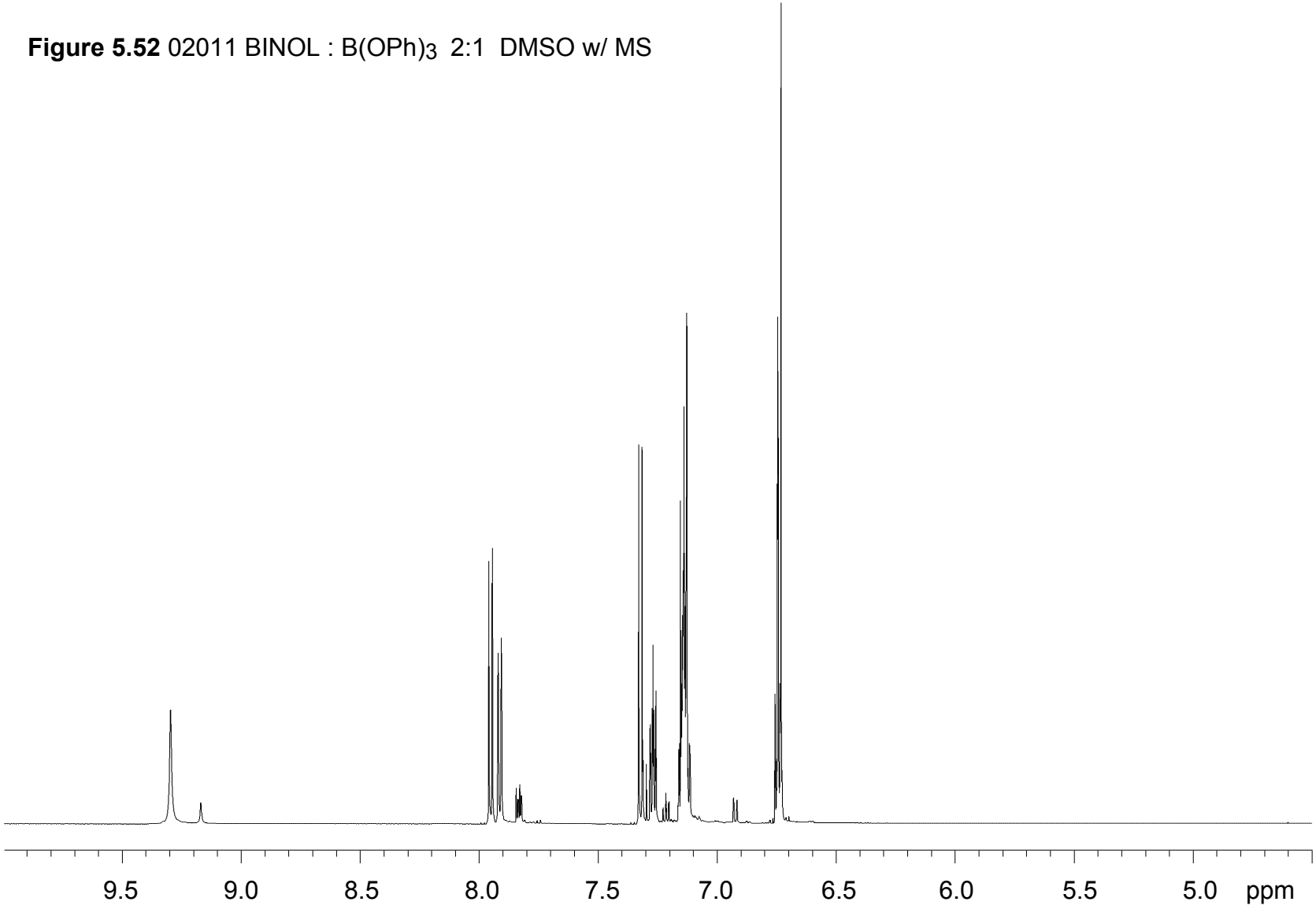

Figure 5.53 02011 BINOL : $B(OPh)_3$ 2:1 DMSO w/ MS

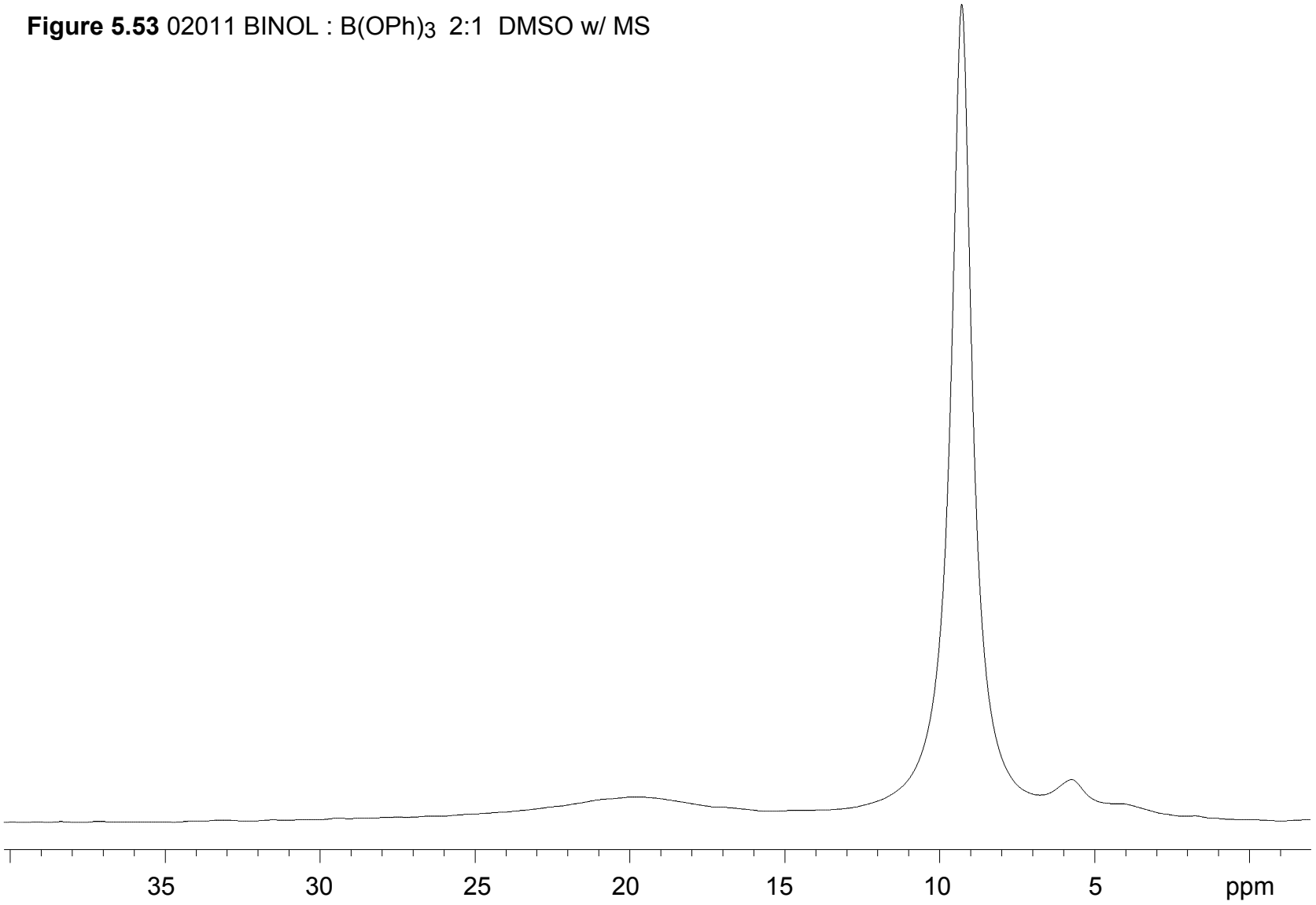

Figure 5.54 02011 BINOL : $B(OPh)_3$: Imine 2:1:1 DMSO w/ MS

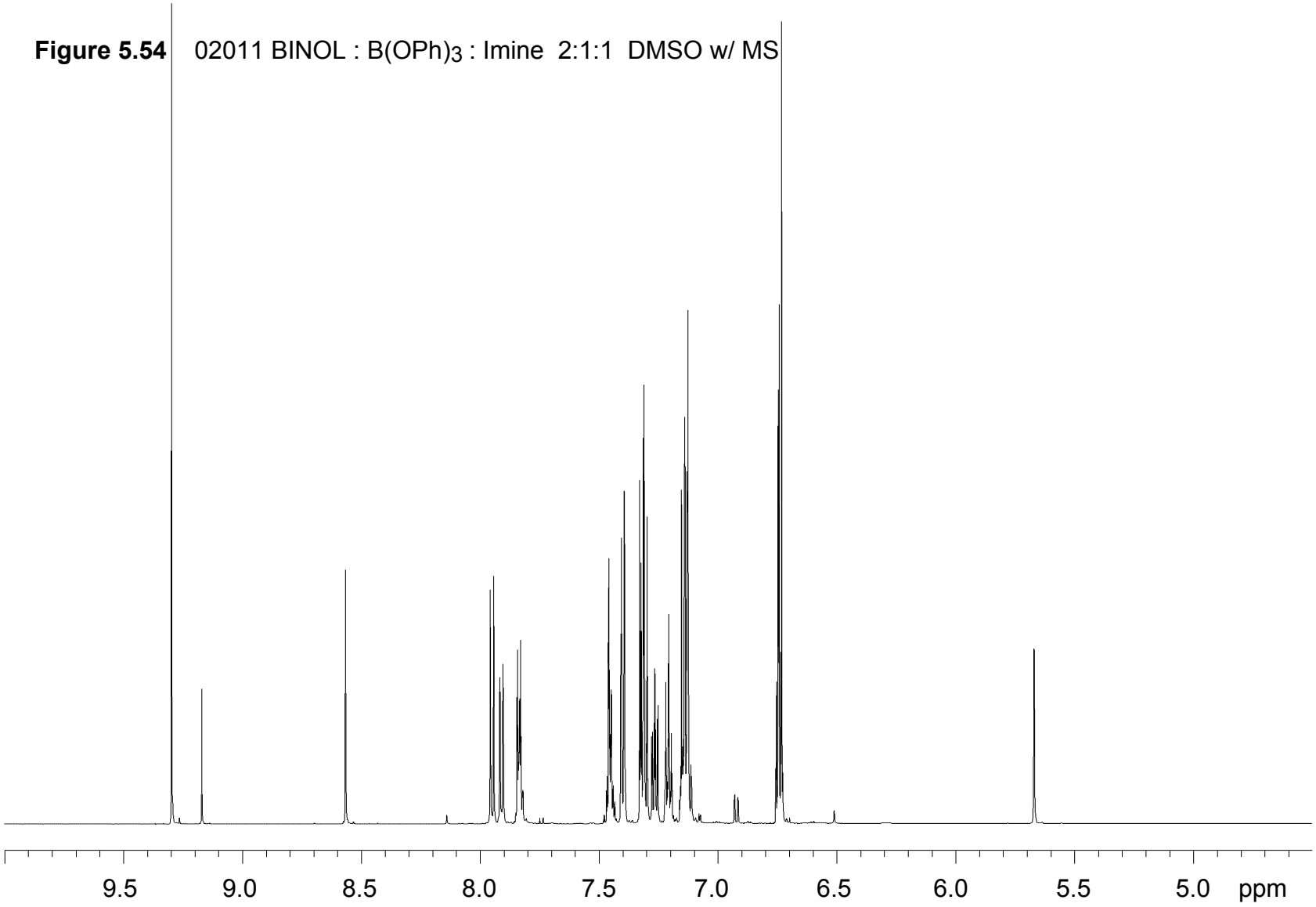

Figure 5.55 02011 BINOL : $B(OPh)_3$: Imine 2:1:1 DMSO w/ MS

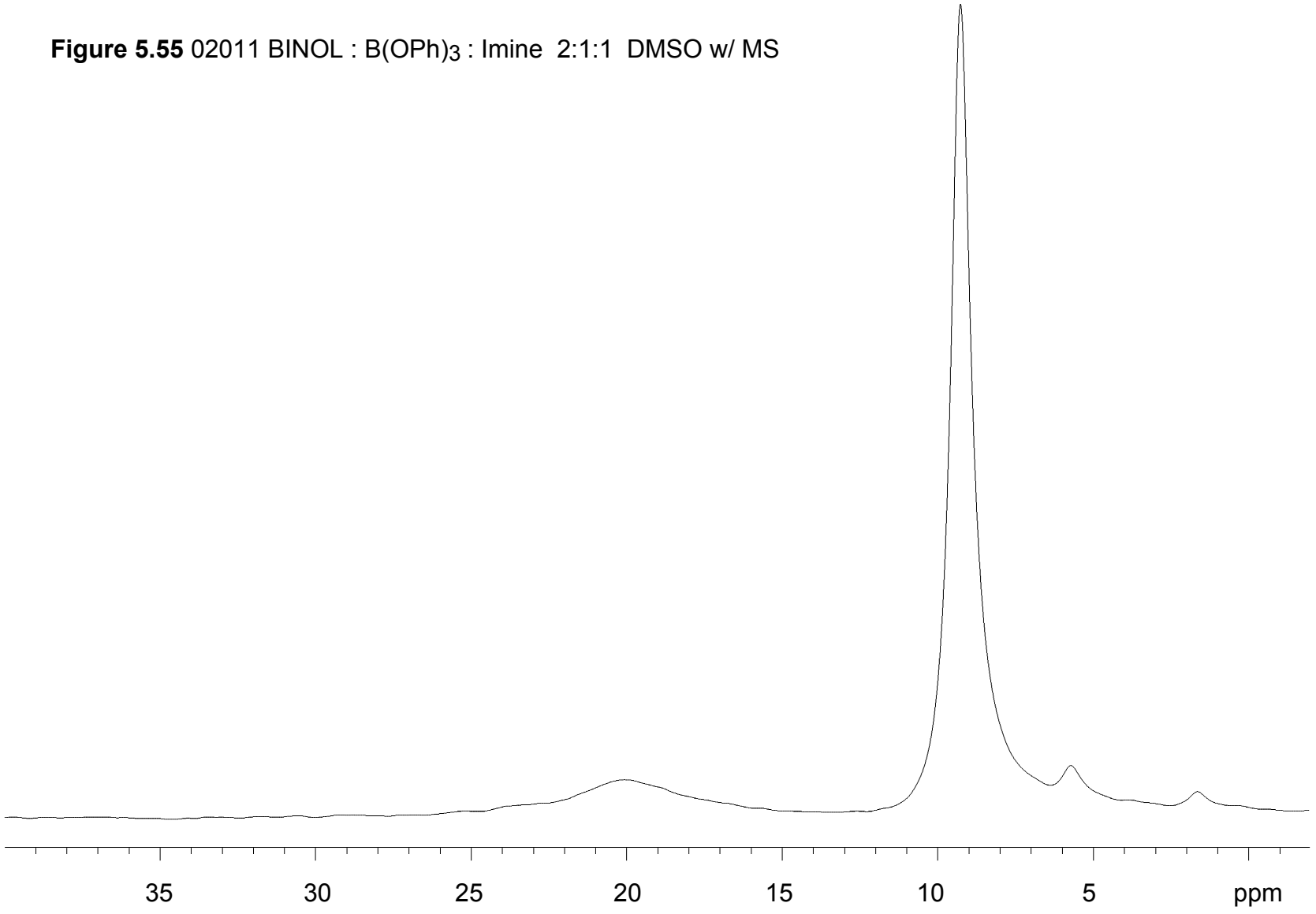

Procedure for 02012: To a flame-dried round bottom flask was added (*R*)-binaphthol (40 mg, 0.14 mmol), $B(OPh)_3$ (20.2 mg, 0.07 mmol), internal standard ($CHPh_3$; 17.5 mg, 0.07 mmol, 1.00 equiv), and DMSO (1 mL) at room temperature under a nitrogen atmosphere. The mixture was swirled and immediately transferred to a flame-dried quartz NMR tube. ^{1}H and ^{11}B NMR analysis was then performed followed by the addition of imine **8a** (19 mg, 0.07 mmol). The NMR tube was inverted several times to ensure the solution was homogeneous. Once again, ^{1}H and ^{11}B NMR analysis was performed. **Results**: Prior to imine addition = 72% BLA and 7% BINOL. After imine addition = 66% BLA and 7% BINOL.

Experiment **Ref. #02012** is represented in Figure 4.8 as entries 3 and 5. Spectra for **02012** are shown below.

Figure 5.56 02012 BINOL : $B(OPh)_3$ 2:1 in DMSO w/ $CHPh_3$

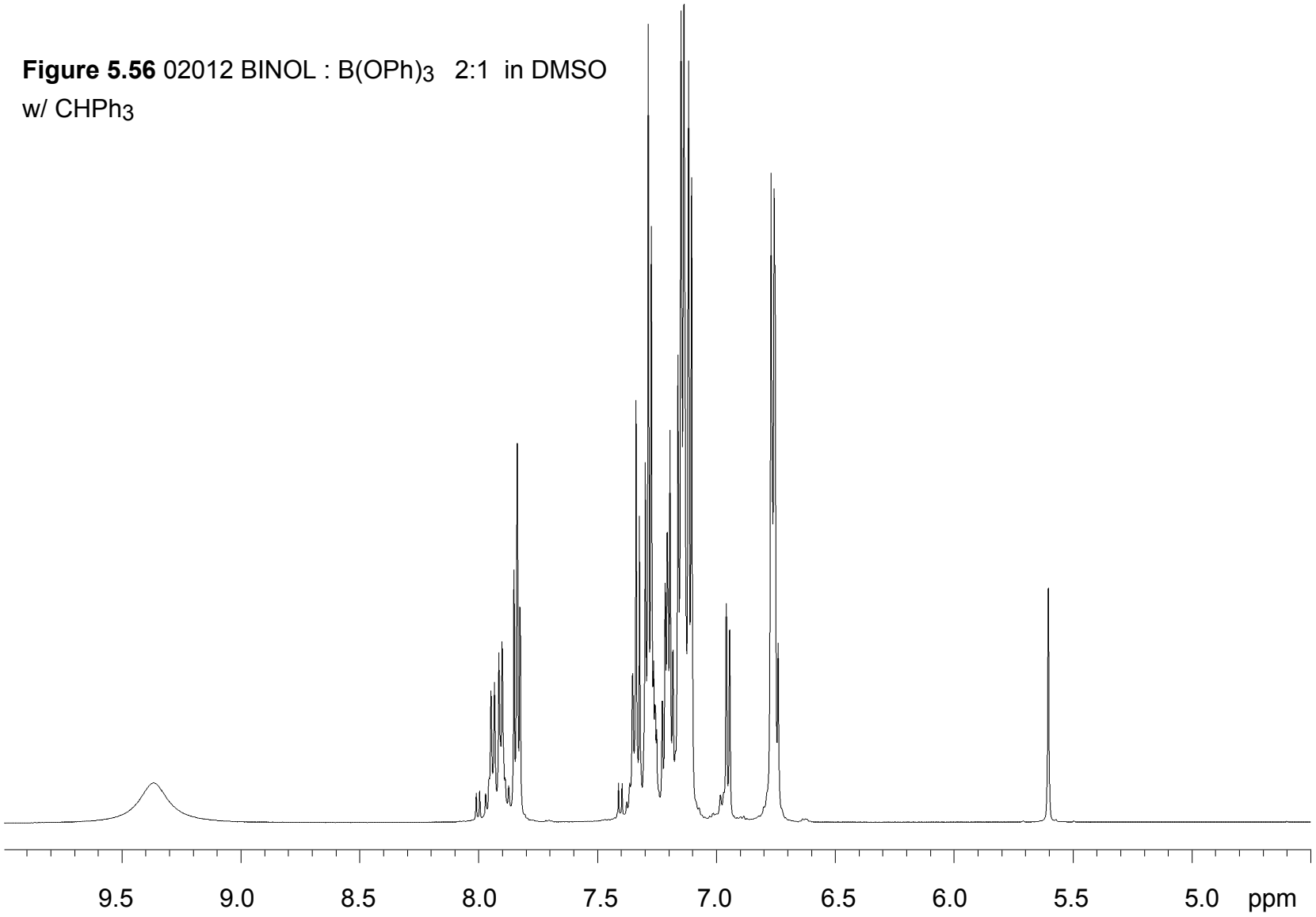

Figure 5.57 02012 BINOL : $B(OPh)_3$ 2:1 DMSO and $CHPh_3$

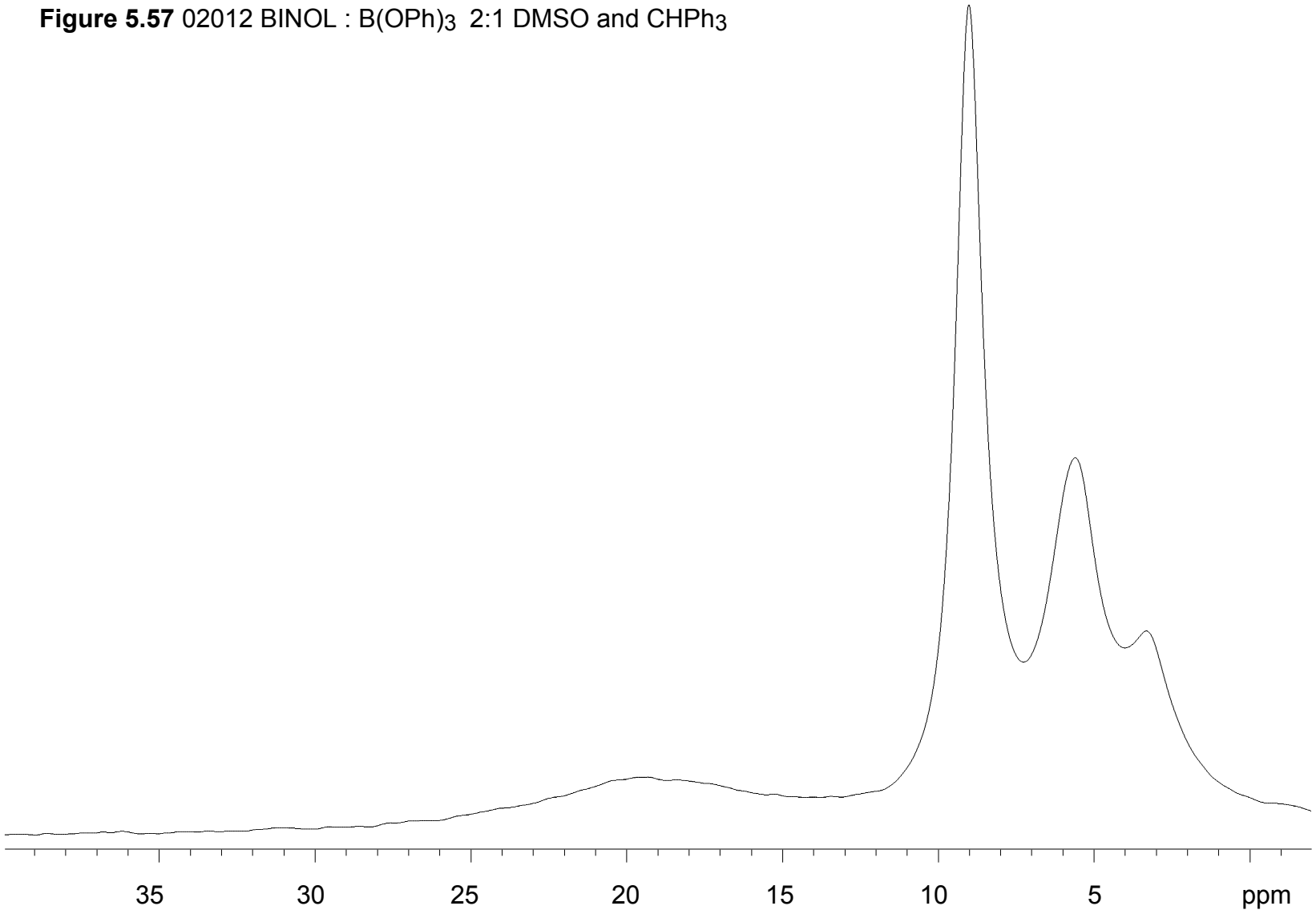

Figure 5.58 02012 BINOL : $B(OPh)_3$: Imine 2:1:1

DMSO and $CHPh_3$

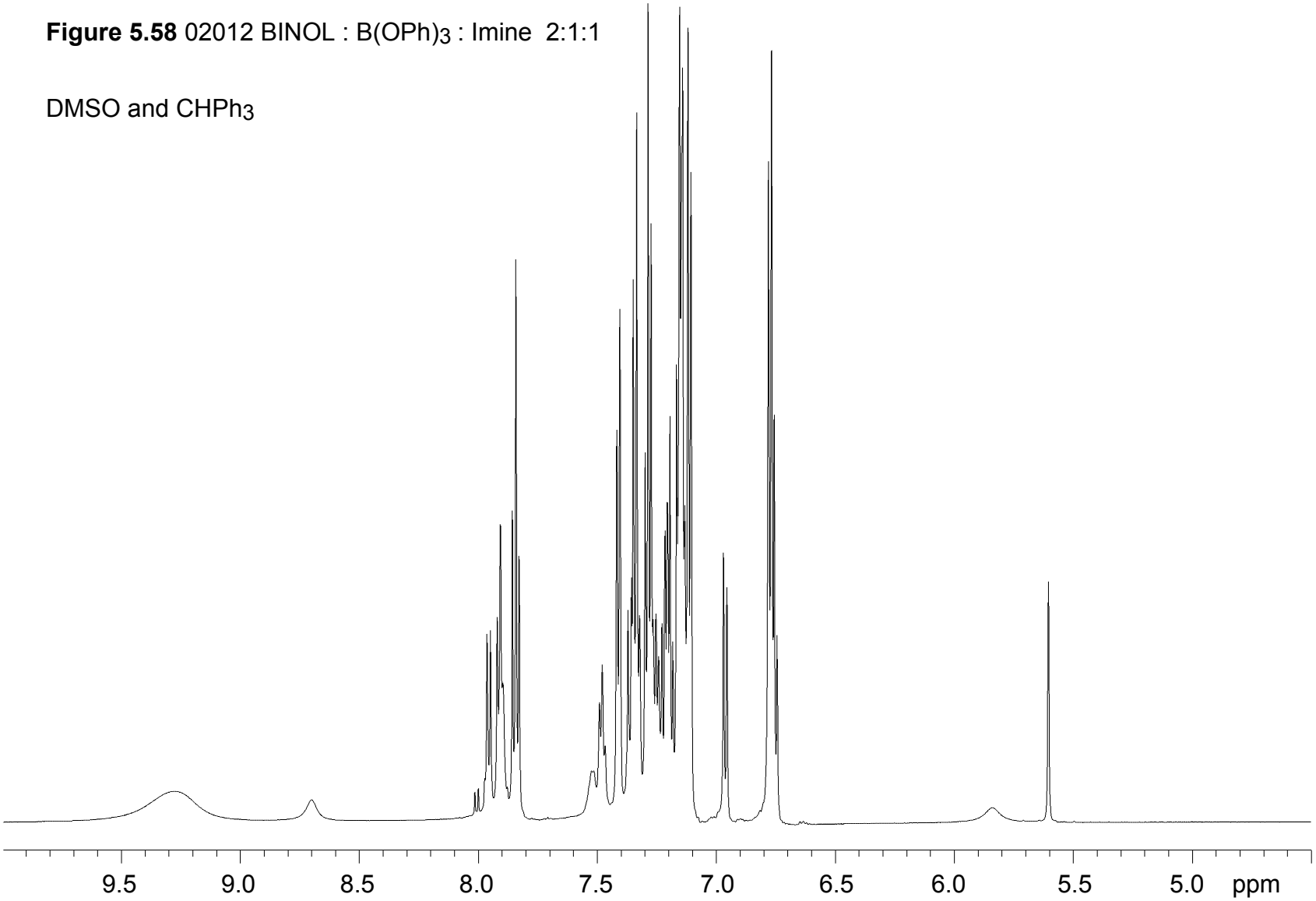

Figure 5.59 02012 BINOL : $B(OPh)_3$: Imine 2:1:1 DMSO and $CHPh_3$

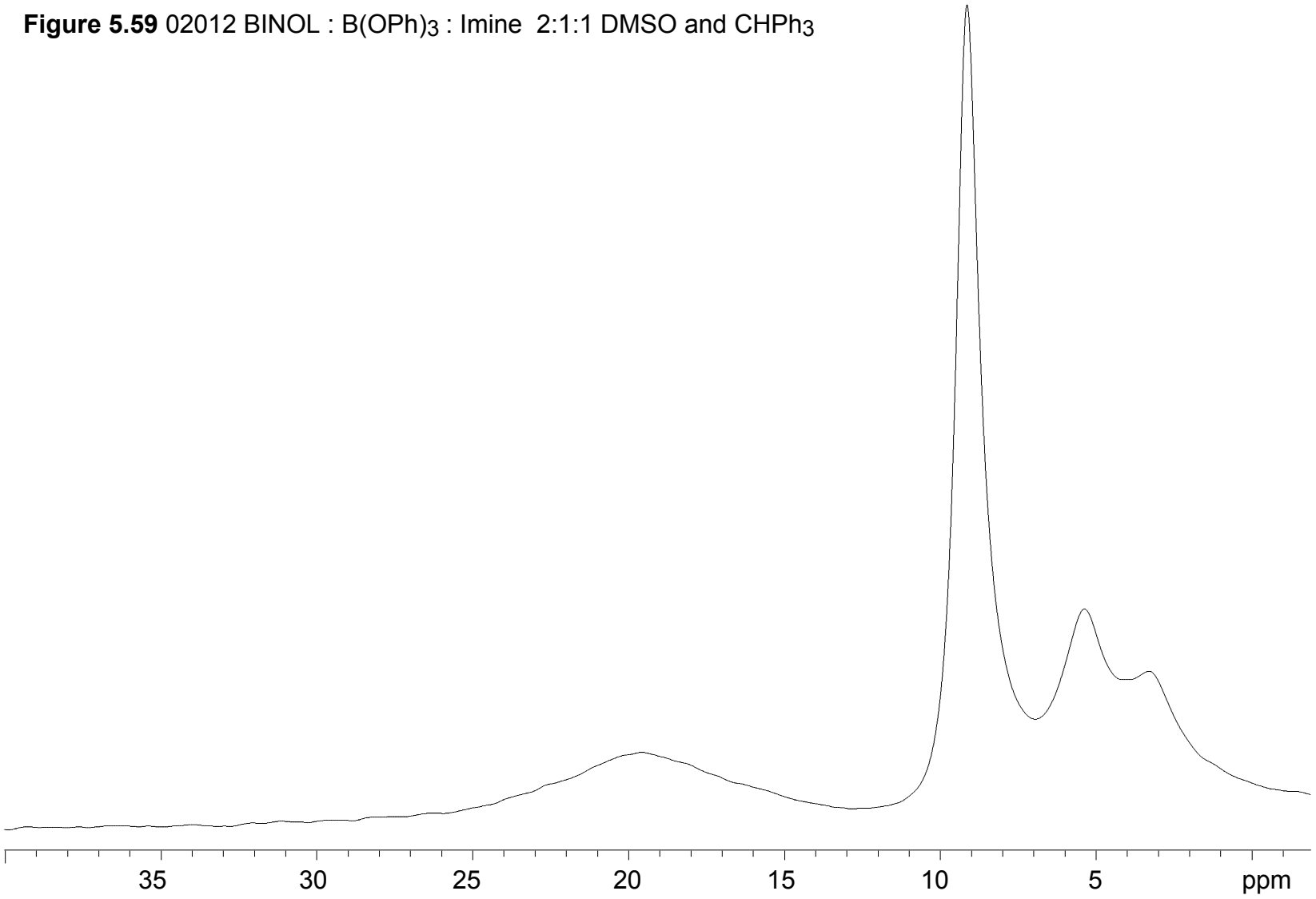

5.3.4 Synthesis of VANOL and *t*-butyl VANOL monomer via the CAEC reaction

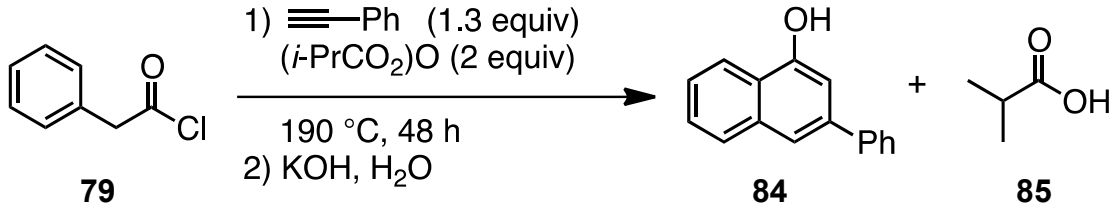

79 **84** **85**

*Preparation of 3-phenylnaphthalen-1-ol (**84**)[55]:* To a flame-dried single neck 2 L flask equipped with a magnetic stir bar was added 2-phenylacetyl chloride (50.5 mL, 59.0 g, 374 mmol), phenyl acetylene (55 mL, 501 mmol), and isobutyric anhydride (125 mL, 731 mmol). The flask was fitted with a condenser flushed with nitrogen with a Teflon sleeve in the joint and Teflon tape wrapped around the joint to secure a tight seal. The mixture was stirred at 190 °C for 48 h with a gentle nitrogen flow over the top of the condenser. In order to minimize the loss of phenyl acetylene through evaporation, two condensers were used on top of the reaction flask. The reaction was cooled to room temperature, and aq KOH (125 g, 2.23 mol in 500 mL of H_2O) was added. The reaction mixture was stirred at 100 °C overnight (13-15 h). The solution was cooled to 0 °C and acidified with 6 N HCl to pH ~6 (100-110 mL). The mixture was then transferred to a separatory funnel using 400 mL of ether. The organic layer was separated, and the aqueous layer was washed with ether (3 x 100 mL). The combined organic layers were washed with sat Na_2CO_3 (3 x 100 mL) and brine (100mL) and dried over $MgSO_4$. After filtration through Celite, the solvent was removed by a rotary evaporator to give a dark brown oil. Hexanes (3 x 50 mL) were added and then removed by a rotary evaporator to give a dark brown solid (92 g) with a mp of 84–89 °C (begins to soften at 71-73 °C). The crude product was taken up in 900 mL of refluxing hexanes/CH_2Cl_2 (4:1), and the hot

solution was poured into a 1 L Erlenmeyer flask leaving some white solid behind (1-2 g) which was taken up in a small amount of hot dichloromethane. Both solutions were covered and allowed to cool to room temperature overnight, and then the solids from each were collected together in a 5 in. Buchner funnel and rinsed with cold hexanes (0 °C, 2 x 200 mL) to give the first crop of **84** as a white fluffy solid in 43% yield (34.9 g, 159 mmol) with a mp of 98.5-99.5 °C. The mother liquor was concentrated to dryness, and the product was crystallized again using hexanes/CH_2Cl_2 (3:1, 400mL) to give a second crop of **84** as a white fluffy solid in 13% yield (10.37 g, 47 mmol) with a mp of 98.5-99.5 °C. Collection of a third crop gave material that was not sufficiently pure by ^1H NMR. Therefore, the third crop and mother liquor residue were combined (~35 g) and purified via column chromatography on silica gel. This mixture was dissolved in CH_2Cl_2 and added to 40 mL of silica gel. After removal of volatiles, the silica gel mixture was loaded onto a silica gel column (5 x 25 cm) that was wet loaded with hexanes. Elution with hexanes/CH_2Cl_2 (2:1) and combining the fractions containing the product gave 18 g of an off-white solid that was shown to contain small amounts of impurities by ^1H NMR. This material was crystallized from 80 mL of a 3:1 mixture of hexanes and CH_2Cl_2 to give the pure product **84** as a white solid (mp = 97.5-98 °C) in 11% yield (9.41 g, 43 mmol).

Spectral data for **84**: R_f = 0.48 (1:3 EtOAc/hexane). ^1H NMR ($CDCl_3$, 300 MHz) δ 5.32 (s, 1H), 7.06 (s, 1H), 7.34 (t, 1H, J = 9 Hz), 7.41-7.50 (m, 4H), 7.62-7.64 (m, 3H), 7.82 (d, 1H, J = 10 Hz), 8.13 (d, 1H, J = 9 Hz); ^{13}C NMR ($CDCl_3$, 75 MHz) δ 108.41, 118.73,

121.39, 123.47, 125.34, 126.86, 127.20, 127.37, 127.99, 128.75, 134.85, 138.73, 140.67, 151.47; mass spectrum, m/z (% rel intensity) 220 M+ (100), 191.0 (45), 189.0 (30), 165.0 (23), 95 (23), 55 (21), 43 (25).

General scheme for the synthesis of t-butyl VANOL monomer **89**:

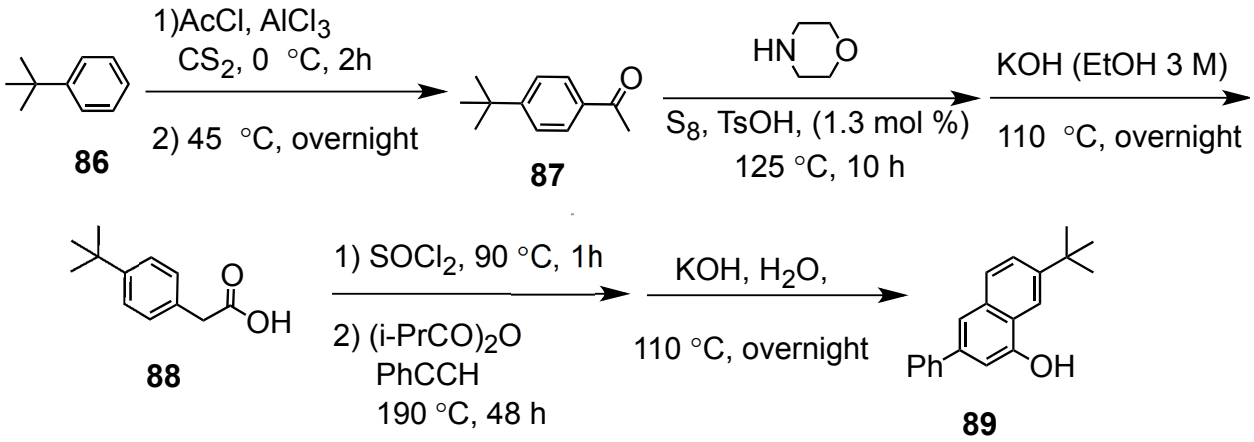

Overall safety: Most compounds in this synthesis are toxic, corrosive, odorous, flammable and deadly. Therefore, everything should be kept in the hood at all times and safety glasses, coat, and often times a mask are required.

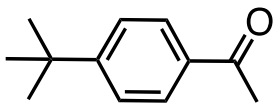

87

*Preparation of 4-tert-butylacetophenone **(87)**[56]:* To a flame-dried 500 mL round bottom flask purged with nitrogen was added $AlCl_3$ (29.3 g, 220 mmol) and CS_2 (100 mL). The solution was taken to 0 °C then through an addition funnel was added a solution of t-butylbenzene (26.8 g, 31 mL, 200 mmol), acetyl chloride (15.7 g, 14.3 mL, 200 mmol) in

CS_2 (50 mL) drop wise (vigorous bubbling occurred after the addition was finished). After stirring at 0 C for 2 hours, the reaction mixture was equipped with a reflux condenser and a N_2 balloon in a septum and refluxed overnight. The resulting mixture was allowed to cool and the CS_2 was removed. The resulting dark brown solution was poured over a slurry of ice (300 g) and H_2SO_4 (30 mL). CH_2Cl_2 (200 mL) was added and the organic layer was separated. The aqueous layer was extracted with CH_2Cl_2 (100 mL X 2). The combined organic layers were dried over $MgSO_4$, filtered, and concentrated. The pure product **87** was obtained as a nearly colorless liquid in 81% isolated yield (28.6 g, 163 mmol) by vacuum distillation (90 °C @ 1 mm Hg).

Spectral data for **87**: ^{1}H NMR ($CDCl_3$, 500 MHz) δ 1.32 (s, 9H), 2.57 (s, 3H), 7.44-7.48 (m, 2H), 7.86-7.90 (m, 2H) ppm; ^{13}C NMR (CDCl3, 125 MHz) δ 26.52, 31.06, 35.07, 125.48, 128.26, 134.60, 156.80, 197.84 ppm; IR (thin film) 2965s, 1684s, 1406s, 1360s, 1271s, 1113s cm-1.

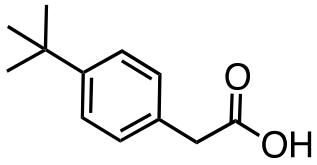

88

*Preparation of 4-tert-butylphenylacetic acid **(88)**[57, 58]:* To a flame-dried 500 mL round bottom flask was added ketone **87** (26.4 g, 150 mmol), morpholine (45 mL, 0.5 mol), sulfur (sublimed, 9.6 g, 0.3 mmol) and *p*-toluene sulfonic acid monohydrate (0.4 g, 2 mmol). The flask was equipped with a reflux condenser, nitrogen balloon and septum.

The mixture was stirred at 125 °C for 10 h. After cooling to room temperature, alcoholic KOH (3 M, 250 mL) (Note 1) was added and the mixture was stirred at 90 °C overnight (Note 2). Once cooled, H_2O (200 mL) was added to the mixture and the solution was transferred to a large Erlenmeyer flask. The reaction mixture was acidified with 6 N HCl to pH 2. CH_2Cl_2 (300 mL) was added and the organic layer was separated. The aqueous layer was extracted with CH_2Cl_2 (100 mL x 2). The organic layers were combined and dried over $MgSO_4$, filtered, and concentrated. The product was purified by silica gel column chromatography (50 mm x 250 mm column, 1:3 CH_2Cl_2/hexanes followed by pure CH_2Cl_2) gave acid **88** as a yellow solid (mp 77-79 °C) in 81 % isolated yield (23.4 g, 122 mmol).

Notes: 1) EtOH/KOH solution takes over an hour to dissolve at room temperature. 2) The procedure called for 110 °C reflux with EtOH/ KOH solution. However, fumes were above the condenser so the reaction was cooled to 90 °C and remained at this temperature for the remainder of the reaction.

Spectral data for **88**: R_f = 0.20 (CH_2Cl_2); ^{1}H NMR ($CDCl_3$, 500 MHz) δ 1.30 (s, 9H), 3.61 (s, 2H), 7.19-7.22 (m, 2H), 7.33-7.36 (m, 2H) ppm; ^{13}C NMR (CDCl3, 125 MHz) δ 31.31, 34.47, 40.50, 125.59, 129.01, 130.19, 150.24, 177.88 ppm; IR (thin film) 2957s, 1715s, 1520s, 1458s, 1402s cm^{-1}.

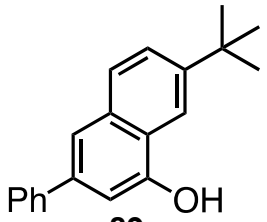

89

Preparation of 7-(tert-butyl)-3-phenylnapthalen-1-ol ***(89)***[37]*:* To a flame-dried 500 mL round bottom flask was added **88** (23.04 g, 120 mmol) and thionyl chloride (32 mL, 439 mmol). The flask was equipped with a reflux condenser and nitrogen balloon through a septum. The mixture was stirred at 90 °C for 1 h (yellow color changed to dark amber). After cooling to room temperature, the volatiles were carefully removed by vacuum (a 2nd liquid nitrogen trap was used to protect the vacuum pump). The flask was then charged with nitrogen gas. Phenylacetylene (17.6 mL, 160 mmol) and isobutyric anhydride (40 mL, 242 mmol) were added to the mixture under a nitrogen atmosphere. The resulting mixture was stirred at 190 °C for 48 h. The mixture was cooled to room temperature followed by the addition of KOH solution (40 g, 714 mmol in 160 mL water). The mixture was stirred at 110 °C overnight. Once the solution cooled to room temperature, EtOAc (300 mL) was added. The organic layer was separated (Note 1). The aqueous layer was extracted with EtOAc (150 mL x 4). The organic layers were combined and washed with brine (300 mL), dried over $MgSO_4$, filtered, and concentrated by rotary evaporation. The product was purified twice by silica gel column chromatography (50 mm x 250 mm column, 1:2 DCM/hexanes then 2:1 DCM/hexanes as eluent) to give t-butyl VANOL monomer **89** as an off-white solid (mp 134-137 °C) in 25% yield (8.3 g, 30 mmol).

Notes: 1) When solution was transferred to a separatory funnel, a huge chunk of brown solid was inside the 500 mL round bottom flask. This solid dissolved with the first two washings of EtOAc.

Spectral data for **89**: R_f = 0.40 (CH_2Cl_2); ^{1}H NMR ($CDCl_3$, 500 MHz) δ 1.43 (s, 9H), 5.25 (s, 1H), 7.06 (d, 1H, *J* = 2.0 Hz), 7.32-7.37 (m, 1H), 7.42 7.47 (m, 2H), 7.59-7.62 (m, 2H), 7.64-7.67 (m, 2H), 7.80 (d, 1H, *J* = 8.5 Hz), 8.08-8.10 (m, 1H) ppm; ^{13}C NMR ($CDCl_3$, 125 MHz) δ 31.31, 35.10, 108.41, 116.25, 118.40, 123.31, 125.80, 127.24, 127.29, 127.81, 128.78, 133.22, 138.19, 141.06, 148.30, 151.66 ppm; IR (thin film) 3505br s, 2961s, 1601s, 1559s, 1458s, 1408s, 1273s cm^{-1}.

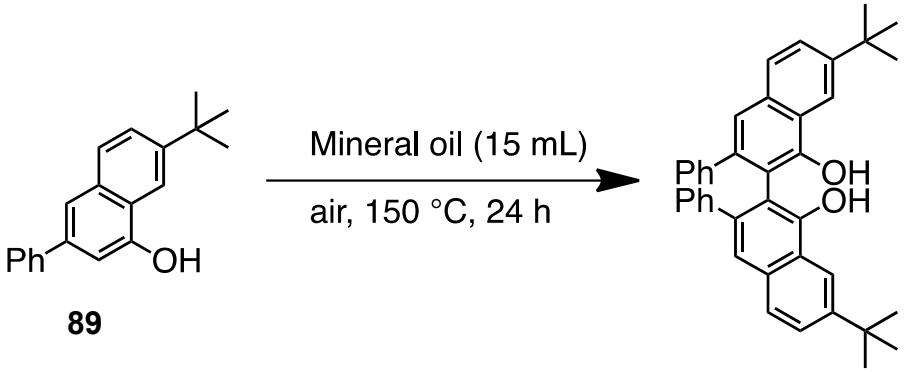

89 **90**

*Preparation of 7,7'-di-tert-butyl-3,3'-diphenyl-[2,2'-binaphthalene]-1,1'-diol (racemic **90**)*[37]*:* To a flame-dried 50 mL 3-neck round bottom flask equipped with a stir bar and cooling condenser was added naphthol **89** (3.17 g, 13.4 mmol) and mineral oil white (15 mL). Oxygen was introduced just above the reaction mixture through a long metal needle via an air outlet located in the reaction hood at a rate of 2-3 bubbles per second.

The reaction was stirred under this slow flow of air at 150 °C for 24 h. All solids melted at this temperature and the solution became homogeneous. Once cooled, the product was loaded onto a silica gel column (50 mm x 250 mm, 1:3 DCM/hexanes) and purified give ligand **90** as a yellow solid in 65% yield (2.39 g, 4.34 mmol). Further purification was done by precipitation. The yellow solid after column chromatography, DCM was added to the yellow solid until no more solid appeared to dissolve. Hexanes were added and the reaction was stirred at 0 C for 10 minutes followed by filtration. The first crop was isolated as a light yellow solid and was subjected to the precipitation procedure once again to give ligand **90** as a white solid in 25% yield (0.93 g, mmol).

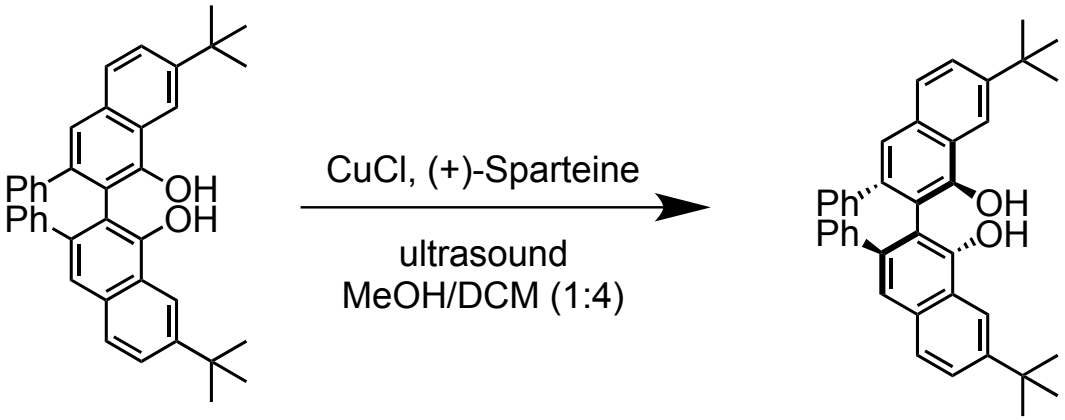

90
Racemic

90

*Deracemization of 7,7'-di-tert-butyl-3,3'-diphenyl-[2,2'-binaphthalene]-1,1'-diol (**90**)*[37]*:* To a flame-dried 50 mL round bottom flask equipped with a stir bar was added CuCl (188 mg, 1.9 mmol), freshly distilled (+)-Sparteine (917 mg, 3.92 mmol) and methanol (33 mL). The neck of the round bottom flask was sealed using a rubber septum. A disposable needle was placed through the rubber septum to allow air inside of the flask. The reaction was sonicated at room temperature for 30 minutes to give a green Cu(II)

Sparteine mixture. The disposable needle was then attached to a bubbler and a long metal needle was placed below the surface of the liquid. A slow nitrogen flow was applied below the surface and the reaction was purged in this manner for 60 minutes. The long metal needle was removed from the liquid and placed just above the surface of the solution. Nitrogen flow was applied in this manner for an additional 30 minutes to complete the purging process. Meanwhile, a 250 mL round bottom flask equipped with a stir bar was flame-dried and charged with racemic *t*-butyl VANOL ligand **90** (615 mg, 1.12 mmol) and CH_2Cl_2 (130 mL). The solution was purged via a nitrogen flow under the solution for 60 minutes (same procedure as the Sparteine solution discussed above). Racemic ligand **90** was then transferred to the Cu(II)-Sparteine solution via a cannula. The combined mixture was sonicated for 15 minutes followed by covering the flask in aluminum and stirring the reaction mixture at room temperature overnight under a nitrogen balloon. $NaHCO_3$ (aq. sat. 14 mL) was slowly added. The volatiles were removed by rotary evaporation and the resulting slurry was extracted with CH_2Cl_2 (3 x 60 mL), dried over $MgSO_4$, and concentrated to give a solid. The crude solid was filtered through a pad of Celite using CH_2Cl_2 in order to remove any inorganic materials. The product was purified twice by silica gel column chromatography (20 mm x 250 mm, 1:3 CH_2Cl_2/hexanes (500 mL) followed by 1:2 CH_2Cl_2/hexanes) to give pure ligand **90** as a white solid (mp = 154-156 °C) in 67% yield (414 mg, mmol). The optical purity was determined to be >99% *ee* by HPLC analysis (Pirkle D Phenylglycine column, 99:1

hexane/*i*PrOH at 254 nm, flow-rate: 1.0 mL/min). Retention times: t_R = 8.32 min for *(R)*-**90** (major) and t_R = 10.19 min for *(S)*-**90** (minor).

Spectral data for **90**: R_f = 0.23 (1:2 CH_2Cl_2/hexanes); ^{1}H NMR ($CDCl_3$, 500 MHz) δ 1.48 (s, 18H), 5.81 (s, 2H), 6.61 (dd, 4H, *J* = 8.0, 1.0 Hz), 6.95 (t, 4H, *J* = 8.0 Hz), 7.03-7.07 (m, 2H), 7.28 (s, 2H), 7.66 (dd, 2H, *J* = 8.5, 2.0 Hz), 7.73 (d, 2H, *J* = 8.5 Hz), 8.29-8.30 (m, 2H) ppm ppm; ^{13}C NMR ($CDCl_3$, 125 MHz) δ 31.33, 35.19, 112.72, 117.71, 121.63, 122.65, 126.39, 127.43, 127.45, 128.90, 132.83, 140.01, 140.40, 148.58, 150.24 (1 sp^2 C not located) ppm.

5.3.5 Long-term stability tests of the VANOL and VAPOL ligands monitored by the AZ reaction

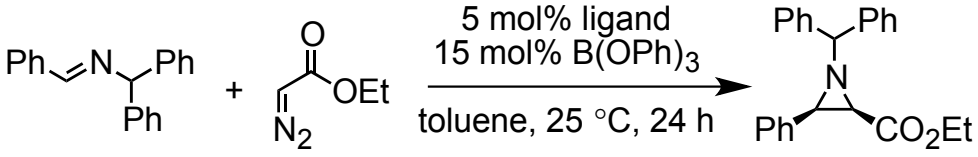

8a **9** **10a**

*General aziridination procedure followed when testing ligand stability (**10a**)[55]:* A 50 mL Schlenk flask equipped with a magnetic stir bar and Teflon cap was flame-dried and cooled under vacuum followed by being flushed with nitrogen. To this flask was added the VANOL or VAPOL ligand (0.05 mmol, VAPOL: 27 mg, VANOL: 22 mg), triphenyl borate (58 mg, 0.20 mmol), and toluene (2 mL). To the stirred reaction was added water (0.9 μL). The flask was sealed under nitrogen and heated to 80 °C for 1 h. At 80 °C, the flask was slowly opened to vacuum (0.1 mm Hg) and remained open for 0.5 h to remove all volatiles. The flask was then cooled to room temperature while still under

vacuum followed by being flushed with nitrogen. Benzhydrylphenyl imine (271 mg, 1.00 mmol) was added to the catalyst solid followed by toluene (2.0 mL). The reaction stirred while the EDA was being measured. EDA (124 μL, 1.20 mmol) was then added to the orange solution and the flask was sealed under nitrogen and allowed to stir at room temperature for 24 h. The reaction mixture was diluted with hexanes (6 mL) and transferred to a pre-weighed 50 mL round bottom flask. The Schlenk flask was rinsed with DCM (3 x 5 mL) and the fractions were added to the 50 mL round bottom flask. The volatiles were removed by rotary evaporation followed by being placed on vacuum (0.1 mm Hg) for 4-6 hours to give the crude aziridine **10a**. The crude product was dissolved in DCM and silica gel was added (2.0 g). The volatiles were removed from the slurry to give a powder that was loaded onto a silica gel column (35 mm x 400 mm, 1:12 EtOAc/hexanes). After purification via silica gel column chromatography, the pure aziridine **10a** was obtained as a white solid. See chapter two experimental for aziridine characterization.

APPENDIX

Crystallographic Data of Selected Compounds

Figure A.1 ORTEP drawing of aziridine **60**

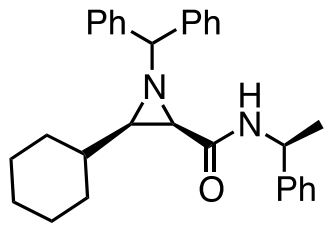

60

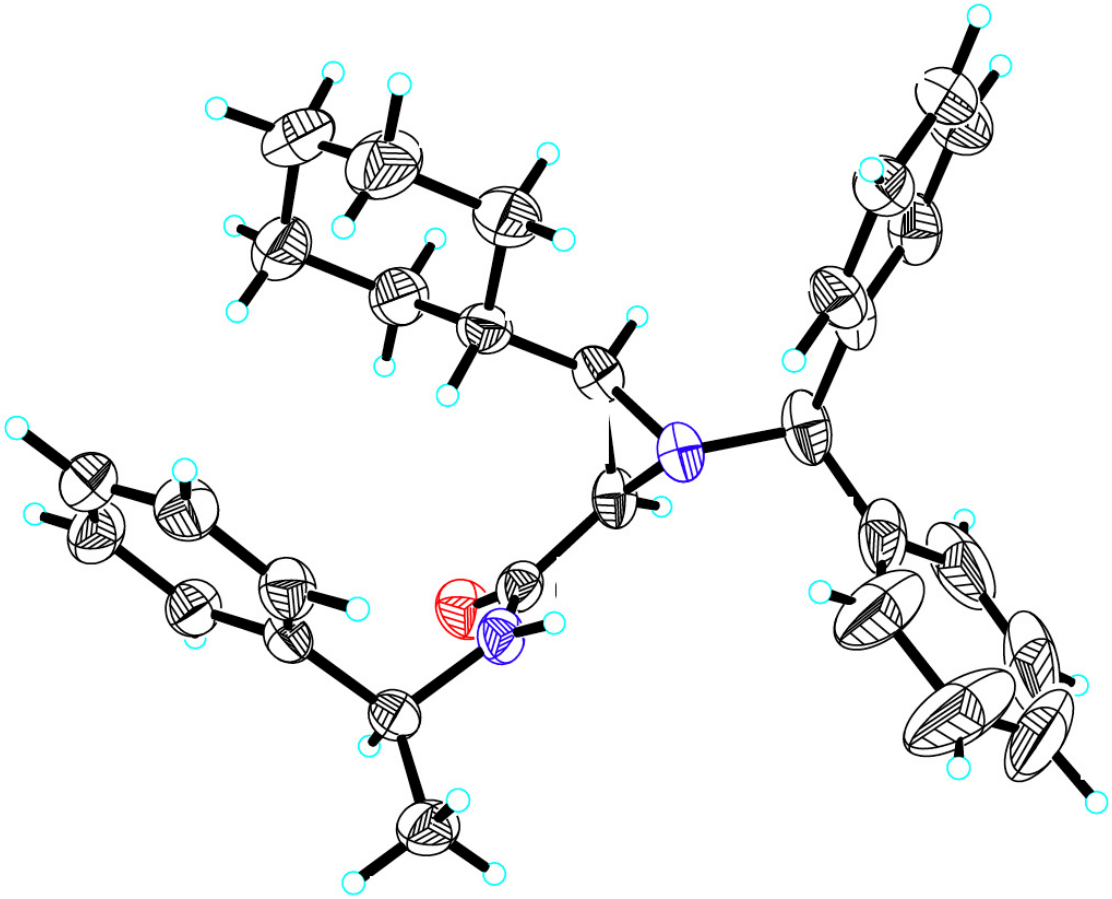

Figure A.1.1. Drawing of the packing along the a-axis of aziridine **60**

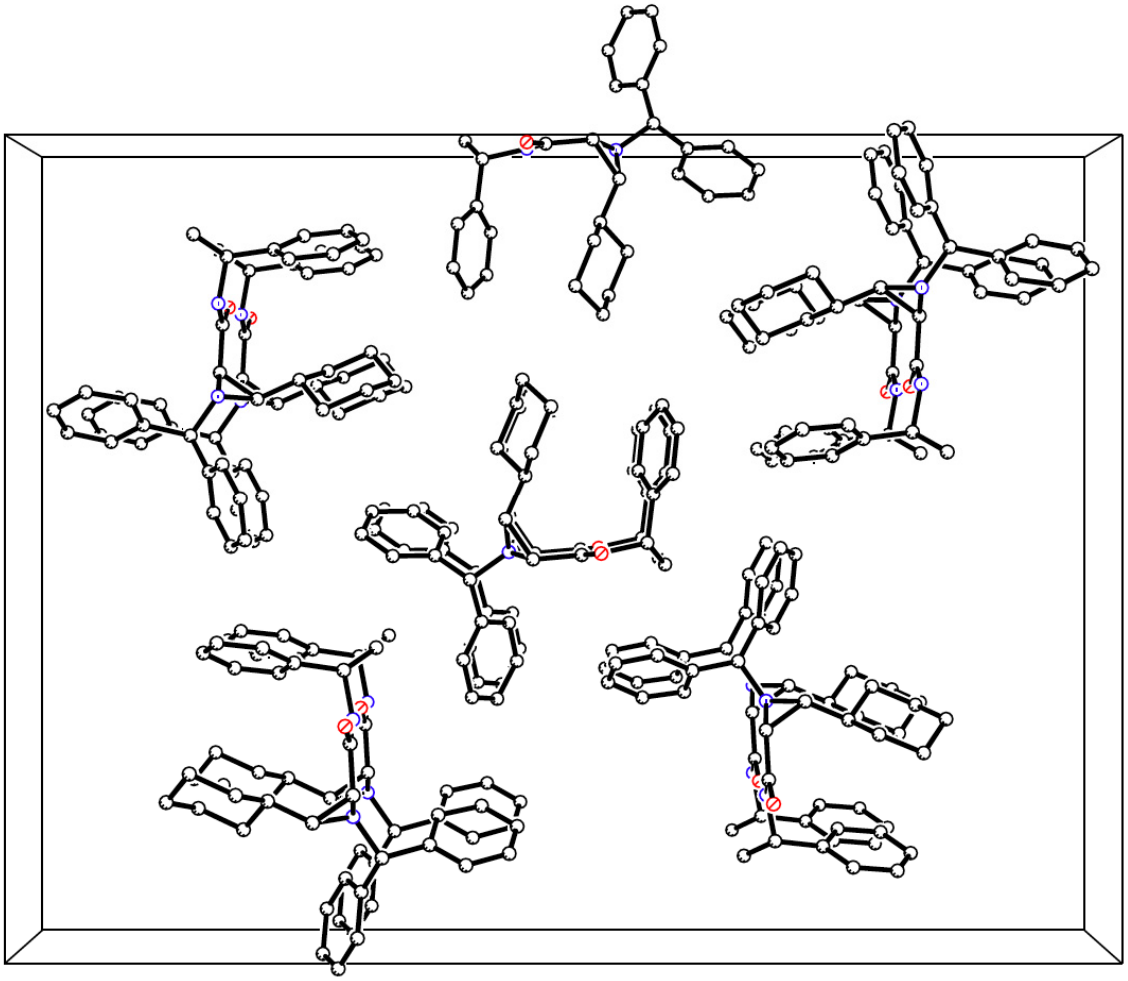

Table A.1.1. Crystal data and structure refinement for the aziridine **60**

Identification code	ww22
Empirical formula	C30 H34 N2 O
Formula weight	438.59
Temperature	172(2) K
Wavelength	1.54178 Å
Crystal system	Orthorhombic
Space group	P 21 21 21
Unit cell dimensions	a = 6.09190(10) Å □= 90°.
	b = 24.9451(2) Å □= 90°.
	c = 33.6623(3) Å □ = 90°.
Volume	5115.43(10) $Å^3$
Z	8
Density (calculated)	1.139 Mg/m^3
Absorption coefficient	0.527 mm^{-1}
F(000)	1888
Crystal size	0.38 x 0.29 x 0.17 mm^3
Theta range for data collection	2.20 to 67.88°.
Index ranges	-7<=h<=7, -29<=k<=29, -39<=l<=40
Reflections collected	33702
Independent reflections	9133 [R(int) = 0.0235]
Completeness to theta = 67.88°	99.3 %
Absorption correction	Semi-empirical from equivalents
Max. and min. transmission	0.9167 and 0.8241
Refinement method	Full-matrix least-squares on F^2
Data / restraints / parameters	9133 / 0 / 598
Goodness-of-fit on F^2	0.983
Final R indices [I>2sigma(I)]	R1 = 0.0527, wR2 = 0.1427
R indices (all data)	R1 = 0.0544, wR2 = 0.1448
Absolute structure parameter	-0.1(3)
Largest diff. peak and hole	0.430 and -0.353 e.$Å^{-3}$

Table A.1.2. Atomic coordinates (x 10^4) and equivalent isotropic displacement parameters ($Å^2$ x 10^3) for aziridine **60**. U(eq) is defined as one third of the trace of the orthogonalized U^{ij} tensor. Aziridine **60** crystallizes as a chiral crystal (results A and B).

	x	y	z	U(eq)
O(1A)	-1970(3)	3017(1)	8147(1)	47(1)
N(1A)	1790(3)	1870(1)	8163(1)	35(1)
N(2A)	1750(3)	3014(1)	8161(1)	36(1)
C(1A)	-254(4)	2179(1)	8190(1)	36(1)
C(2A)	228(4)	1845(1)	7834(1)	37(1)
C(3A)	-217(4)	2778(1)	8165(1)	36(1)
C(4A)	2015(4)	3589(1)	8078(1)	35(1)
C(5A)	3787(4)	3828(1)	8340(1)	45(1)
C(6A)	2450(4)	3667(1)	7636(1)	34(1)
C(7A)	4434(4)	3514(1)	7467(1)	40(1)
C(8A)	4786(4)	3566(1)	7063(1)	43(1)
C(9A)	3180(5)	3774(1)	6821(1)	46(1)
C(10A)	1186(4)	3921(1)	6985(1)	46(1)
C(11A)	826(4)	3868(1)	7391(1)	40(1)
C(12A)	804(4)	2080(1)	7434(1)	38(1)
C(13A)	2281(5)	1702(1)	7195(1)	53(1)
C(14A)	2798(6)	1938(1)	6787(1)	66(1)
C(15A)	725(6)	2068(1)	6558(1)	67(1)
C(16A)	-765(5)	2441(1)	6794(1)	56(1)
C(17A)	-1278(4)	2208(1)	7201(1)	49(1)
C(18A)	1749(4)	1385(1)	8415(1)	46(1)
C(19A)	3019(4)	938(1)	8217(1)	38(1)
C(20A)	5074(4)	1025(1)	8050(1)	40(1)
C(21A)	6198(4)	616(1)	7866(1)	41(1)
C(22A)	5304(5)	108(1)	7844(1)	50(1)
C(23A)	3271(5)	15(1)	8011(1)	59(1)
C(24A)	2134(4)	424(1)	8195(1)	48(1)
C(25A)	2556(5)	1513(1)	8824(1)	60(1)
C(26A)	1445(11)	1309(1)	9151(1)	119(2)
C(27A)	2240(20)	1422(2)	9525(1)	195(6)
C(28A)	4084(17)	1684(3)	9589(2)	182(5)

Table A.1.2 (Cont'd)

C(29A)	5199(10)	1896(3)	9266(2)	151(3)
C(30A)	4407(6)	1809(2)	8885(1)	89(1)
O(1B)	4904(3)	-57(1)	4661(1)	63(1)
N(1B)	1099(3)	-67(1)	5501(1)	36(1)
N(2B)	1184(4)	-79(1)	4652(1)	41(1)
C(1B)	3130(4)	-142(1)	5276(1)	41(1)
C(2B)	2798(4)	347(1)	5526(1)	38(1)
C(3B)	3133(4)	-90(1)	4834(1)	44(1)
C(4B)	967(4)	46(1)	4227(1)	42(1)
C(5B)	-984(5)	-240(1)	4051(1)	53(1)
C(6B)	918(4)	652(1)	4172(1)	40(1)
C(7B)	-896(5)	950(1)	4299(1)	45(1)
C(8B)	-912(5)	1501(1)	4258(1)	52(1)
C(9B)	854(6)	1763(1)	4088(1)	58(1)
C(10B)	2656(5)	1469(1)	3962(1)	53(1)
C(11B)	2673(4)	916(1)	4004(1)	46(1)
C(12B)	2408(4)	890(1)	5349(1)	39(1)
C(13B)	4609(5)	1166(1)	5286(1)	57(1)
C(14B)	4308(6)	1729(1)	5111(1)	70(1)
C(15B)	2800(7)	2065(1)	5373(1)	72(1)
C(16B)	625(6)	1793(1)	5433(1)	60(1)
C(17B)	920(5)	1232(1)	5610(1)	48(1)
C(18B)	1018(4)	-410(1)	5860(1)	44(1)
C(19B)	-179(4)	-121(1)	6192(1)	40(1)
C(20B)	655(5)	-121(1)	6575(1)	53(1)
C(21B)	-430(6)	147(1)	6877(1)	66(1)
C(22B)	-2339(6)	420(1)	6802(1)	60(1)
C(23B)	-3180(5)	423(1)	6421(1)	53(1)
C(24B)	-2119(4)	155(1)	6120(1)	46(1)
C(25B)	42(5)	-945(1)	5759(1)	54(1)
C(26B)	-1747(6)	-984(1)	5511(1)	76(1)
C(27B)	-2673(9)	-1483(2)	5439(2)	125(2)
C(28B)	-1696(12)	-1943(2)	5621(2)	117(2)
C(29B)	73(16)	-1888(2)	5847(1)	135(3)
C(30B)	942(9)	-1406(1)	5922(1)	94(2)

Table A.1.3. Bond lengths [Å] and angles [°] for aziridine **60**

O(1A)-C(3A)	1.225(3)	C(13A)-H(13C)	0.9900
N(1A)-C(2A)	1.463(3)	C(13A)-H(13D)	0.9900
N(1A)-C(1A)	1.467(3)	C(14A)-C(15A)	1.514(5)
N(1A)-C(18A)	1.479(3)	C(14A)-H(14C)	0.9900
N(2A)-C(3A)	1.335(3)	C(14A)-H(14D)	0.9900
N(2A)-C(4A)	1.469(3)	C(15A)-C(16A)	1.523(4)
N(2A)-H(2AA)	0.8800	C(15A)-H(15C)	0.9900
C(1A)-C(2A)	1.492(3)	C(15A)-H(15D)	0.9900
C(1A)-C(3A)	1.497(3)	C(16A)-C(17A)	1.522(4)
C(1A)-H(1A)	1.0000	C(16A)-H(16C)	0.9900
C(2A)-C(12A)	1.509(3)	C(16A)-H(16D)	0.9900
C(2A)-H(2A)	1.0000	C(17A)-H(17C)	0.9900
C(4A)-C(5A)	1.517(3)	C(17A)-H(17D)	0.9900
C(4A)-C(6A)	1.524(3)	C(18A)-C(25A)	1.497(4)
C(4A)-H(4A)	1.0000	C(18A)-C(19A)	1.513(3)
C(5A)-H(5A1)	0.9800	C(18A)-H(18A)	1.0000
C(5A)-H(5A2)	0.9800	C(19A)-C(20A)	1.388(3)
C(5A)-H(5A3)	0.9800	C(19A)-C(24A)	1.393(3)
C(6A)-C(11A)	1.381(3)	C(20A)-C(21A)	1.377(3)
C(6A)-C(7A)	1.387(3)	C(20A)-H(20A)	0.9500
C(7A)-C(8A)	1.383(3)	C(21A)-C(22A)	1.381(3)
C(7A)-H(7A)	0.9500	C(21A)-H(21A)	0.9500
C(8A)-C(9A)	1.375(4)	C(22A)-C(23A)	1.380(4)
C(8A)-H(8A)	0.9500	C(22A)-H(22A)	0.9500
C(9A)-C(10A)	1.384(4)	C(23A)-C(24A)	1.379(4)
C(9A)-H(9A)	0.9500	C(23A)-H(23A)	0.9500
C(10A)-C(11A)	1.390(3)	C(24A)-H(24A)	0.9500
C(10A)-H(10A)	0.9500	C(25A)-C(30A)	1.363(6)
C(11A)-H(11A)	0.9500	C(25A)-C(26A)	1.387(5)
C(12A)-C(17A)	1.525(3)	C(26A)-C(27A)	1.379(9)
C(12A)-C(13A)	1.532(3)	C(26A)-H(26A)	0.9500
C(12A)-H(12A)	1.0000	C(27A)-C(28A)	1.316(15)
C(13A)-C(14A)	1.526(4)	C(27A)-H(27A)	0.9500

Table A.1.3 (Cont'd)

C(28A)-C(29A)	1.386(12)	C(12B)-C(17B)	1.524(3)
C(28A)-H(28C)	0.9500	C(12B)-H(12B)	1.0000
C(29A)-C(30A)	1.388(5)	C(13B)-C(14B)	1.534(4)
C(29A)-H(29A)	0.9500	C(13B)-H(13A)	0.9900
C(30A)-H(30A)	0.9500	C(13B)-H(13B)	0.9900
O(1B)-C(3B)	1.228(3)	C(14B)-C(15B)	1.524(5)
N(1B)-C(1B)	1.463(3)	C(14B)-H(14A)	0.9900
N(1B)-C(2B)	1.466(3)	C(14B)-H(14B)	0.9900
N(1B)-C(18B)	1.480(3)	C(15B)-C(16B)	1.502(5)
N(2B)-C(3B)	1.336(4)	C(15B)-H(15A)	0.9900
N(2B)-C(4B)	1.469(3)	C(15B)-H(15B)	0.9900
N(2B)-H(2BA)	0.8800	C(16B)-C(17B)	1.531(4)
C(1B)-C(3B)	1.494(3)	C(16B)-H(16A)	0.9900
C(1B)-C(2B)	1.498(3)	C(16B)-H(16B)	0.9900
C(1B)-H(1B)	1.0000	C(17B)-H(17A)	0.9900
C(2B)-C(12B)	1.499(3)	C(17B)-H(17B)	0.9900
C(2B)-H(2B)	1.0000	C(18B)-C(25B)	1.498(4)
C(4B)-C(5B)	1.507(4)	C(18B)-C(19B)	1.517(3)
C(4B)-C(6B)	1.525(3)	C(18B)-H(18B)	1.0000
C(4B)-H(4B)	1.0000	C(19B)-C(20B)	1.387(3)
C(5B)-H(5B1)	0.9800	C(19B)-C(24B)	1.389(3)
C(5B)-H(5B2)	0.9800	C(20B)-C(21B)	1.384(4)
C(5B)-H(5B3)	0.9800	C(20B)-H(20B)	0.9500
C(6B)-C(11B)	1.376(4)	C(21B)-C(22B)	1.371(5)
C(6B)-C(7B)	1.399(4)	C(21B)-H(21B)	0.9500
C(7B)-C(8B)	1.383(4)	C(22B)-C(23B)	1.382(4)
C(7B)-H(7B)	0.9500	C(22B)-H(22B)	0.9500
C(8B)-C(9B)	1.382(4)	C(23B)-C(24B)	1.377(4)
C(8B)-H(8B)	0.9500	C(23B)-H(23B)	0.9500
C(9B)-C(10B)	1.386(4)	C(24B)-H(24B)	0.9500
C(9B)-H(9B)	0.9500	C(25B)-C(26B)	1.377(5)
C(10B)-C(11B)	1.388(4)	C(25B)-C(30B)	1.388(4)
C(10B)-H(10B)	0.9500	C(26B)-C(27B)	1.387(5)
C(11B)-H(11B)	0.9500	C(26B)-H(26B)	0.9500

Table A.1.3 (Cont'd)

C(27B)-C(28B)	1.432(9)	C(4A)-C(5A)-H(5A2)	109.5
C(28B)-C(29B)	1.327(9)	C(3B)-N(2B)-H(2BA)	119.0
C(28B)-H(28B)	0.9500	H(5A1)-C(5A)-H(5A2)	109.5
C(29B)-C(30B)	1.337(7)	C(4A)-C(5A)-H(5A3)	109.5
C(29B)-H(29B)	0.9500	H(5A1)-C(5A)-H(5A3)	109.5
C(30B)-H(30B)	0.9500	H(5A2)-C(5A)-H(5A3)	109.5
C(2A)-N(1A)-C(1A)	61.21(14)	C(11A)-C(6A)-C(7A)	118.7(2)
C(2A)-N(1A)-C(18A)	112.88(18)	C(11A)-C(6A)-C(4A)	120.3(2)
C(1A)-N(1A)-C(18A)	112.30(17)	C(7A)-C(6A)-C(4A)	120.97(19)
C(3A)-N(2A)-C(4A)	122.11(18)	C(8A)-C(7A)-C(6A)	120.7(2)
C(3A)-N(2A)-H(2AA)	118.9	C(8A)-C(7A)-H(7A)	119.6
C(4A)-N(2A)-H(2AA)	118.9	C(6A)-C(7A)-H(7A)	119.6
N(1A)-C(1A)-C(2A)	59.25(14)	C(9A)-C(8A)-C(7A)	120.6(2)
N(1A)-C(1A)-C(3A)	120.51(19)	C(9A)-C(8A)-H(8A)	119.7
C(2A)-C(1A)-C(3A)	120.60(18)	C(7A)-C(8A)-H(8A)	119.7
N(1A)-C(1A)-H(1A)	115.1	C(8A)-C(9A)-C(10A)	119.1(2)
C(2A)-C(1A)-H(1A)	115.1	C(8A)-C(9A)-H(9A)	120.4
C(3A)-C(1A)-H(1A)	115.1	C(10A)-C(9A)-H(9A)	120.4
N(1A)-C(2A)-C(1A)	59.54(14)	C(9A)-C(10A)-C(11A)	120.4(2)
N(1A)-C(2A)-C(12A)	120.49(18)	C(9A)-C(10A)-H(10A)	119.8
C(1A)-C(2A)-C(12A)	123.10(18)	C(11A)-C(10A)-H(10A)	119.8
N(1A)-C(2A)-H(2A)	114.3	C(6A)-C(11A)-C(10A)	120.5(2)
C(1A)-C(2A)-H(2A)	114.3	C(6A)-C(11A)-H(11A)	119.8
C(12A)-C(2A)-H(2A)	114.3	C(10A)-C(11A)-H(11A)	119.8
O(1A)-C(3A)-N(2A)	124.5(2)	C(2A)-C(12A)-C(17A)	110.21(19)
O(1A)-C(3A)-C(1A)	118.4(2)	C(2A)-C(12A)-C(13A)	111.46(19)
N(2A)-C(3A)-C(1A)	117.07(18)	C(17A)-C(12A)-C(13A)	110.3(2)
N(2A)-C(4A)-C(5A)	110.52(18)	C(2A)-C(12A)-H(12A)	108.3
N(2A)-C(4A)-C(6A)	109.29(16)	C(17A)-C(12A)-H(12A)	108.3
C(5A)-C(4A)-C(6A)	113.24(19)	C(13A)-C(12A)-H(12A)	108.3
N(2A)-C(4A)-H(4A)	107.9	C(14A)-C(13A)-C(12A)	110.9(2)
C(5A)-C(4A)-H(4A)	107.9	C(14A)-C(13A)-H(13C)	109.5
C(6A)-C(4A)-H(4A)	107.9	C(12A)-C(13A)-H(13C)	109.5
C(4A)-C(5A)-H(5A1)	109.5	C(14A)-C(13A)-H(13D)	109.5

Table A.1.3 (Cont'd)

C(12A)-C(13A)-H(13D)	109.5	C(24A)-C(19A)-C(18A)	120.2(2)
H(13C)-C(13A)-H(13D)	108.1	C(21A)-C(20A)-C(19A)	121.0(2)
C(15A)-C(14A)-C(13A)	111.6(3)	C(21A)-C(20A)-H(20A)	119.5
C(15A)-C(14A)-H(14C)	109.3	C(20A)-C(21A)-C(22A)	120.5(2)
C(13A)-C(14A)-H(14C)	109.3	C(20A)-C(21A)-H(21A)	119.7
C(15A)-C(14A)-H(14D)	109.3	C(22A)-C(21A)-H(21A)	119.7
C(13A)-C(14A)-H(14D)	109.3	C(23A)-C(22A)-C(21A)	119.1(2)
H(14C)-C(14A)-H(14D)	108.0	C(23A)-C(22A)-H(22A)	120.5
C(14A)-C(15A)-C(16A)	111.3(2)	C(21A)-C(22A)-H(22A)	120.5
C(14A)-C(15A)-H(15C)	109.4	C(24A)-C(23A)-C(22A)	120.7(2)
C(16A)-C(15A)-H(15C)	109.4	C(24A)-C(23A)-H(23A)	119.7
C(14A)-C(15A)-H(15D)	109.4	C(22A)-C(23A)-H(23A)	119.7
C(16A)-C(15A)-H(15D)	109.4	C(23A)-C(24A)-C(19A)	120.6(2)
H(15C)-C(15A)-H(15D)	108.0	C(23A)-C(24A)-H(24A)	119.7
C(17A)-C(16A)-C(15A)	111.0(2)	C(19A)-C(24A)-H(24A)	119.7
C(17A)-C(16A)-H(16C)	109.4	C(30A)-C(25A)-C(26A)	119.0(4)
C(15A)-C(16A)-H(16C)	109.4	C(30A)-C(25A)-C(18A)	121.7(3)
C(17A)-C(16A)-H(16D)	109.4	C(26A)-C(25A)-C(18A)	119.3(4)
C(15A)-C(16A)-H(16D)	109.4	C(27A)-C(26A)-C(25A)	118.4(7)
H(16C)-C(16A)-H(16D)	108.0	C(27A)-C(26A)-H(26A)	120.8
C(16A)-C(17A)-C(12A)	111.8(2)	C(25A)-C(26A)-H(26A)	120.8
C(16A)-C(17A)-H(17C)	109.3	C(28A)-C(27A)-C(26A)	123.5(7)
C(12A)-C(17A)-H(17C)	109.3	C(28A)-C(27A)-H(27A)	118.2
C(16A)-C(17A)-H(17D)	109.3	C(26A)-C(27A)-H(27A)	118.2
C(12A)-C(17A)-H(17D)	109.3	C(27A)-C(28A)-C(29A)	118.6(5)
H(17C)-C(17A)-H(17D)	107.9	C(27A)-C(28A)-H(28C)	120.7
N(1A)-C(18A)-C(25A)	110.3(2)	C(29A)-C(28A)-H(28C)	120.7
N(1A)-C(18A)-C(19A)	109.97(18)	C(28A)-C(29A)-C(30A)	119.6(7)
C(25A)-C(18A)-C(19A)	113.31(19)	C(28A)-C(29A)-H(29A)	120.2
N(1A)-C(18A)-H(18A)	107.7	C(30A)-C(29A)-H(29A)	120.2
C(25A)-C(18A)-H(18A)	107.7	C(25A)-C(30A)-C(29A)	120.7(5)
C(19A)-C(18A)-H(18A)	107.7	C(25A)-C(30A)-H(30A)	119.6
C(20A)-C(19A)-C(24A)	118.1(2)	C(29A)-C(30A)-H(30A)	119.6
C(20A)-C(19A)-C(18A)	121.6(2)	C(1B)-N(1B)-C(2B)	61.50(15)

Table A.1.3 (Cont'd)

C(1B)-N(1B)-C(18B)	112.13(17)	C(8B)-C(7B)-C(6B)	120.2(3)
C(2B)-N(1B)-C(18B)	112.66(18)	C(8B)-C(7B)-H(7B)	119.9
C(3B)-N(2B)-C(4B)	122.01(19)	C(6B)-C(7B)-H(7B)	119.9
C(3B)-N(2B)-H(2BA)	119.0	C(9B)-C(8B)-C(7B)	120.3(3)
C(4B)-N(2B)-H(2BA)	119.0	C(9B)-C(8B)-H(8B)	119.8
N(1B)-C(1B)-C(3B)	120.4(2)	C(7B)-C(8B)-H(8B)	119.8
N(1B)-C(1B)-C(2B)	59.32(14)	C(8B)-C(9B)-C(10B)	119.6(2)
C(3B)-C(1B)-C(2B)	119.23(19)	C(8B)-C(9B)-H(9B)	120.2
N(1B)-C(1B)-H(1B)	115.4	C(10B)-C(9B)-H(9B)	120.2
C(3B)-C(1B)-H(1B)	115.4	C(9B)-C(10B)-C(11B)	120.0(3)
C(2B)-C(1B)-H(1B)	115.4	C(9B)-C(10B)-H(10B)	120.0
N(1B)-C(2B)-C(1B)	59.18(15)	C(11B)-C(10B)-H(10B)	120.0
N(1B)-C(2B)-C(12B)	120.21(19)	C(6B)-C(11B)-C(10B)	120.8(3)
C(1B)-C(2B)-C(12B)	122.32(19)	C(6B)-C(11B)-H(11B)	119.6
N(1B)-C(2B)-H(2B)	114.7	C(10B)-C(11B)-H(11B)	119.6
C(1B)-C(2B)-H(2B)	114.7	C(2B)-C(12B)-C(13B)	108.9(2)
C(12B)-C(2B)-H(2B)	114.7	C(2B)-C(12B)-C(17B)	111.75(19)
O(1B)-C(3B)-N(2B)	124.3(2)	C(13B)-C(12B)-C(17B)	110.6(2)
O(1B)-C(3B)-C(1B)	118.5(2)	C(2B)-C(12B)-H(12B)	108.5
N(2B)-C(3B)-C(1B)	117.2(2)	C(13B)-C(12B)-H(12B)	108.5
N(2B)-C(4B)-C(5B)	110.7(2)	C(17B)-C(12B)-H(12B)	108.5
N(2B)-C(4B)-C(6B)	109.30(18)	C(12B)-C(13B)-C(14B)	111.2(2)
C(5B)-C(4B)-C(6B)	113.9(2)	C(12B)-C(13B)-H(13A)	109.4
N(2B)-C(4B)-H(4B)	107.5	C(14B)-C(13B)-H(13A)	109.4
C(5B)-C(4B)-H(4B)	107.5	C(12B)-C(13B)-H(13B)	109.4
C(6B)-C(4B)-H(4B)	107.5	C(14B)-C(13B)-H(13B)	109.4
C(4B)-C(5B)-H(5B1)	109.5	H(13A)-C(13B)-H(13B)	108.0
C(4B)-C(5B)-H(5B2)	109.5	C(15B)-C(14B)-C(13B)	110.8(3)
H(5B1)-C(5B)-H(5B2)	109.5	C(15B)-C(14B)-H(14A)	109.5
C(4B)-C(5B)-H(5B3)	109.5	C(13B)-C(14B)-H(14A)	109.5
H(5B1)-C(5B)-H(5B3)	109.5	C(15B)-C(14B)-H(14B)	109.5
H(5B2)-C(5B)-H(5B3)	109.5	C(13B)-C(14B)-H(14B)	109.5
C(11B)-C(6B)-C(7B)	119.1(2)	H(14A)-C(14B)-H(14B)	108.1
C(11B)-C(6B)-C(4B)	120.6(2)	C(16B)-C(15B)-C(14B)	111.2(2)
C(7B)-C(6B)-C(4B)	120.3(2)	C(16B)-C(15B)-H(15A)	109.4

Table A.1.3 (Cont'd)

C(14B)-C(15B)-H(15A)	109.4
C(16B)-C(15B)-H(15B)	109.4
C(14B)-C(15B)-H(15B)	109.4
H(15A)-C(15B)-H(15B)	108.0
C(15B)-C(16B)-C(17B)	111.2(2)
C(15B)-C(16B)-H(16A)	109.4
C(17B)-C(16B)-H(16A)	109.4
C(15B)-C(16B)-H(16B)	109.4
C(17B)-C(16B)-H(16B)	109.4
H(16A)-C(16B)-H(16B)	108.0
C(12B)-C(17B)-C(16B)	110.9(2)
C(12B)-C(17B)-H(17A)	109.5
C(16B)-C(17B)-H(17A)	109.5
C(12B)-C(17B)-H(17B)	109.5
C(16B)-C(17B)-H(17B)	109.5
H(17A)-C(17B)-H(17B)	108.0
N(1B)-C(18B)-C(25B)	110.1(2)
N(1B)-C(18B)-C(19B)	109.95(19)
C(25B)-C(18B)-C(19B)	113.5(2)
N(1B)-C(18B)-H(18B)	107.7
C(25B)-C(18B)-H(18B)	107.7
C(19B)-C(18B)-H(18B)	107.7
C(20B)-C(19B)-C(24B)	118.3(2)
C(20B)-C(19B)-C(18B)	120.6(2)
C(24B)-C(19B)-C(18B)	121.1(2)
C(21B)-C(20B)-C(19B)	120.5(3)
C(21B)-C(20B)-H(20B)	119.7
C(19B)-C(20B)-H(20B)	119.7
C(22B)-C(21B)-C(20B)	120.6(2)
C(22B)-C(21B)-H(21B)	119.7
C(20B)-C(21B)-H(21B)	119.7
C(21B)-C(22B)-C(23B)	119.3(3)
C(21B)-C(22B)-H(22B)	120.4
C(23B)-C(24B)-C(19B)	120.8(2)
C(23B)-C(22B)-H(22B)	120.4
C(24B)-C(23B)-C(22B)	120.5(3)
C(24B)-C(23B)-H(23B)	119.8
C(22B)-C(23B)-H(23B)	119.8
C(23B)-C(24B)-C(19B)	120.8(2)
C(23B)-C(24B)-H(24B)	119.6
C(19B)-C(24B)-H(24B)	119.6
C(26B)-C(25B)-C(30B)	119.6(3)
C(26B)-C(25B)-C(18B)	121.0(2)
C(30B)-C(25B)-C(18B)	119.4(3)
C(25B)-C(26B)-C(27B)	119.4(4)
C(25B)-C(26B)-H(26B)	120.3
C(27B)-C(26B)-H(26B)	120.3
C(26B)-C(27B)-C(28B)	118.5(5)
C(26B)-C(27B)-H(27B)	120.8
C(28B)-C(27B)-H(27B)	120.8
C(29B)-C(28B)-C(27B)	120.0(4)
C(29B)-C(28B)-H(28B)	120.0
C(27B)-C(28B)-H(28B)	120.0
C(28B)-C(29B)-C(30B)	121.5(5)
C(28B)-C(29B)-H(29B)	119.2
C(30B)-C(29B)-H(29B)	119.2
C(29B)-C(30B)-C(25B)	120.9(5)
C(29B)-C(30B)-H(30B)	119.5
C(25B)-C(30B)-H(30B)	119.5

Symmetry transformations used to generate equivalent atoms:

Table A.1.4. Anisotropic displacement parameters ($Å^2 x\ 10^3$) for aziridine **60**. The anisotropic displacement factor exponent takes the form: $-2\pi^2[h^2 a^{*2} U^{11} + ... + 2 h k a^* b^* U^{12}]$

	U^{11}	U^{22}	U^{33}	U^{23}	U^{13}	U^{12}
O(1A)	41(1)	44(1)	56(1)	0(1)	2(1)	14(1)
N(1A)	31(1)	33(1)	40(1)	9(1)	4(1)	3(1)
N(2A)	40(1)	34(1)	34(1)	3(1)	1(1)	13(1)
C(1A)	31(1)	39(1)	38(1)	11(1)	5(1)	4(1)
C(2A)	31(1)	32(1)	48(1)	3(1)	-1(1)	0(1)
C(3A)	42(1)	40(1)	26(1)	1(1)	3(1)	10(1)
C(4A)	40(1)	30(1)	35(1)	-3(1)	2(1)	8(1)
C(5A)	50(1)	43(1)	41(1)	-8(1)	-4(1)	11(1)
C(6A)	39(1)	25(1)	36(1)	0(1)	-4(1)	2(1)
C(7A)	38(1)	38(1)	43(1)	3(1)	0(1)	6(1)
C(8A)	42(1)	43(1)	46(1)	-1(1)	9(1)	4(1)
C(9A)	61(2)	43(1)	33(1)	0(1)	5(1)	1(1)
C(10A)	48(1)	52(1)	38(1)	3(1)	-10(1)	8(1)
C(11A)	38(1)	41(1)	39(1)	0(1)	-2(1)	9(1)
C(12A)	41(1)	34(1)	39(1)	-4(1)	0(1)	-3(1)
C(13A)	56(2)	51(1)	53(1)	-7(1)	5(1)	10(1)
C(14A)	70(2)	79(2)	50(2)	-7(1)	13(1)	15(2)
C(15A)	91(2)	74(2)	37(1)	-13(1)	-2(2)	5(2)
C(16A)	64(2)	62(2)	42(1)	3(1)	-9(1)	5(1)
C(17A)	48(1)	50(1)	48(1)	-2(1)	-4(1)	8(1)
C(18A)	34(1)	44(1)	58(1)	22(1)	13(1)	6(1)
C(19A)	36(1)	35(1)	44(1)	16(1)	-4(1)	1(1)
C(20A)	36(1)	30(1)	54(1)	3(1)	-2(1)	-3(1)
C(21A)	40(1)	38(1)	46(1)	-1(1)	-2(1)	1(1)
C(22A)	68(2)	34(1)	48(1)	-4(1)	-5(1)	3(1)
C(23A)	75(2)	34(1)	66(2)	1(1)	-8(2)	-13(1)
C(24A)	41(1)	48(1)	57(1)	16(1)	-7(1)	-8(1)
C(25A)	74(2)	63(2)	42(1)	16(1)	16(1)	43(2)
C(26A)	239(6)	51(2)	68(2)	25(2)	74(3)	50(3)
C(27A)	436(16)	111(4)	37(2)	34(2)	59(5)	152(7)
C(28A)	321(12)	173(7)	50(3)	-40(3)	-74(5)	175(8)

Table A.1.4 (Cont'd)

C(29A)	141(4)	223(7)	87(3)	-85(4)	-64(3)	130(5)
C(30A)	69(2)	147(4)	52(2)	-31(2)	-16(2)	51(2)
O(1B)	53(1)	80(1)	56(1)	3(1)	25(1)	11(1)
N(1B)	36(1)	36(1)	35(1)	8(1)	5(1)	2(1)
N(2B)	50(1)	34(1)	40(1)	1(1)	18(1)	3(1)
C(1B)	38(1)	38(1)	46(1)	9(1)	6(1)	7(1)
C(2B)	30(1)	48(1)	36(1)	3(1)	2(1)	3(1)
C(3B)	52(1)	34(1)	45(1)	1(1)	18(1)	7(1)
C(4B)	50(1)	39(1)	38(1)	-6(1)	17(1)	3(1)
C(5B)	63(2)	50(1)	46(1)	-12(1)	17(1)	-3(1)
C(6B)	49(1)	44(1)	26(1)	-1(1)	4(1)	0(1)
C(7B)	53(1)	46(1)	35(1)	-2(1)	6(1)	2(1)
C(8B)	65(2)	50(1)	42(1)	-5(1)	2(1)	15(1)
C(9B)	90(2)	38(1)	45(1)	3(1)	-8(1)	4(1)
C(10B)	66(2)	50(1)	43(1)	9(1)	1(1)	-10(1)
C(11B)	50(1)	52(1)	36(1)	5(1)	8(1)	3(1)
C(12B)	41(1)	39(1)	38(1)	-1(1)	-1(1)	-3(1)
C(13B)	49(2)	50(1)	71(2)	9(1)	6(1)	-7(1)
C(14B)	71(2)	54(2)	84(2)	20(2)	-6(2)	-20(2)
C(15B)	100(3)	39(1)	76(2)	-1(1)	-32(2)	-4(2)
C(16B)	75(2)	50(1)	55(2)	-9(1)	-13(1)	16(1)
C(17B)	50(1)	49(1)	45(1)	-6(1)	-1(1)	4(1)
C(18B)	38(1)	51(1)	44(1)	19(1)	2(1)	8(1)
C(19B)	39(1)	45(1)	37(1)	12(1)	0(1)	-6(1)
C(20B)	61(2)	51(1)	48(1)	14(1)	-13(1)	-7(1)
C(21B)	99(2)	63(2)	36(1)	0(1)	-18(2)	-7(2)
C(22B)	82(2)	60(2)	38(1)	-5(1)	7(1)	-6(2)
C(23B)	54(2)	63(2)	43(1)	-4(1)	7(1)	3(1)
C(24B)	42(1)	64(2)	32(1)	2(1)	0(1)	1(1)
C(25B)	64(2)	40(1)	58(2)	10(1)	30(1)	7(1)
C(26B)	56(2)	52(2)	119(3)	-19(2)	24(2)	-8(1)
C(27B)	111(4)	94(3)	170(5)	-61(3)	65(4)	-46(3)
C(28B)	201(6)	44(2)	107(3)	-20(2)	83(4)	-49(3)
C(29B)	286(9)	46(2)	71(2)	1(2)	52(4)	2(4)
C(30B)	182(5)	48(2)	51(2)	14(1)	26(2)	36(2)

Table A.1.5. Hydrogen coordinates (x 10^4) and isotropic displacement parameters ($Å^2$x 10^3) for aziridine **60**.

	x	y	z	U(eq)
H(2AA)	2924	2820	8209	43
H(1A)	-1382	2027	8375	43
H(2A)	-628	1503	7820	45
H(4A)	599	3771	8143	42
H(5A1)	5189	3649	8286	67
H(5A2)	3392	3776	8620	67
H(5A3)	3925	4212	8284	67
H(7A)	5562	3373	7632	48
H(8A)	6149	3458	6952	52
H(9A)	3436	3816	6544	55
H(10A)	57	4059	6819	55
H(11A)	-548	3970	7501	47
H(12A)	1621	2423	7479	45
H(13C)	3666	1641	7341	64
H(13D)	1537	1352	7161	64
H(14C)	3677	2269	6820	79
H(14D)	3687	1679	6633	79
H(15C)	-72	1732	6498	81
H(15D)	1119	2240	6303	81
H(16C)	-38	2793	6826	67
H(16D)	-2150	2498	6646	67
H(17C)	-2152	1876	7168	58
H(17D)	-2175	2467	7353	58
H(18A)	186	1266	8439	55
H(20A)	5714	1372	8064	48
H(21A)	7600	683	7753	50
H(22A)	6077	-174	7716	60
H(23A)	2647	-334	8000	70
H(24A)	733	354	8308	58
H(26A)	164	1097	9117	143
H(27A)	1421	1304	9748	233
H(28C)	4636	1727	9851	218

Table A.1.5 (Cont'd)

H(29A)	6498	2100	9306	181
H(30A)	5162	1958	8664	107
H(2BA)	-6	-149	4791	50
H(1B)	4170	-414	5386	49
H(2B)	3644	350	5780	46
H(4B)	2309	-93	4090	51
H(5B1)	-2327	-120	4185	79
H(5B2)	-813	-627	4087	79
H(5B3)	-1081	-158	3767	79
H(7B)	-2122	772	4414	54
H(8B)	-2143	1702	4347	63
H(9B)	834	2141	4058	69
H(10B)	3879	1647	3846	63
H(11B)	3910	716	3916	55
H(12B)	1685	843	5084	47
H(13A)	5519	948	5103	68
H(13B)	5391	1192	5543	68
H(14A)	5755	1907	5089	84
H(14B)	3673	1701	4841	84
H(15A)	3508	2124	5634	86
H(15B)	2563	2419	5248	86
H(16A)	-146	1765	5175	72
H(16B)	-293	2012	5614	72
H(17A)	1566	1262	5879	58
H(17B)	-531	1057	5635	58
H(18B)	2563	-473	5949	53
H(20B)	1981	-307	6631	64
H(21B)	154	141	7139	79
H(22B)	-3075	604	7010	72
H(23B)	-4500	612	6367	64
H(24B)	-2721	158	5859	55
H(26B)	-2342	-672	5390	91
H(27B)	-3926	-1518	5273	150
H(28B)	-2315	-2289	5580	141
H(29B)	739	-2198	5959	162

Table A.1.5 (Cont'd)

H(30B)	2193	-1379	6090	113

Table A.1.6. Torsion angles [°] for aziridine **60**

C(18A)-N(1A)-C(1A)-C(2A)	-104.7(2)
C(2A)-N(1A)-C(1A)-C(3A)	-109.7(2)
C(18A)-N(1A)-C(1A)-C(3A)	145.6(2)
C(18A)-N(1A)-C(2A)-C(1A)	103.77(19)
C(1A)-N(1A)-C(2A)-C(12A)	112.9(2)
C(18A)-N(1A)-C(2A)-C(12A)	-143.3(2)
C(3A)-C(1A)-C(2A)-N(1A)	109.5(2)
N(1A)-C(1A)-C(2A)-C(12A)	-108.6(2)
C(3A)-C(1A)-C(2A)-C(12A)	0.9(3)
C(4A)-N(2A)-C(3A)-O(1A)	-8.7(3)
C(4A)-N(2A)-C(3A)-C(1A)	170.76(18)
N(1A)-C(1A)-C(3A)-O(1A)	172.4(2)
C(2A)-C(1A)-C(3A)-O(1A)	102.3(3)
N(1A)-C(1A)-C(3A)-N(2A)	-7.1(3)
C(2A)-C(1A)-C(3A)-N(2A)	-77.2(3)
C(3A)-N(2A)-C(4A)-C(5A)	141.3(2)
C(3A)-N(2A)-C(4A)-C(6A)	-93.4(2)
N(2A)-C(4A)-C(6A)-C(11A)	105.8(2)
C(5A)-C(4A)-C(6A)-C(11A)	-130.5(2)
N(2A)-C(4A)-C(6A)-C(7A)	-71.0(3)
C(5A)-C(4A)-C(6A)-C(7A)	52.7(3)
C(11A)-C(6A)-C(7A)-C(8A)	0.5(3)
C(4A)-C(6A)-C(7A)-C(8A)	177.4(2)
C(6A)-C(7A)-C(8A)-C(9A)	0.4(4)
C(7A)-C(8A)-C(9A)-C(10A)	-1.2(4)
C(8A)-C(9A)-C(10A)-C(11A)	1.1(4)
C(7A)-C(6A)-C(11A)-C(10A)	-0.7(3)
C(4A)-C(6A)-C(11A)-C(10A)	-177.5(2)
C(9A)-C(10A)-C(11A)-C(6A)	-0.1(4)
N(1A)-C(2A)-C(12A)-C(17A)	-157.39(19)
C(1A)-C(2A)-C(12A)-C(17A)	-86.0(3)

Table A.1.6 (Cont'd)

N(1A)-C(2A)-C(12A)-C(13A)	79.8(3)
C(1A)-C(2A)-C(12A)-C(13A)	151.2(2)
C(2A)-C(12A)-C(13A)-C(14A)	178.4(2)
C(17A)-C(12A)-C(13A)-C(14A)	55.6(3)
C(12A)-C(13A)-C(14A)-C(15A)	-56.0(3)
C(13A)-C(14A)-C(15A)-C(16A)	55.6(4)
C(14A)-C(15A)-C(16A)-C(17A)	-55.0(4)
C(15A)-C(16A)-C(17A)-C(12A)	55.7(3)
C(2A)-C(12A)-C(17A)-C(16A)	-179.4(2)
C(13A)-C(12A)-C(17A)-C(16A)	-55.9(3)
C(2A)-N(1A)-C(18A)-C(25A)	-155.4(2)
C(1A)-N(1A)-C(18A)-C(25A)	-88.5(2)
C(2A)-N(1A)-C(18A)-C(19A)	78.9(2)
C(1A)-N(1A)-C(18A)-C(19A)	145.83(19)
N(1A)-C(18A)-C(19A)-C(20A)	46.2(3)
C(25A)-C(18A)-C(19A)-C(20A)	-77.8(3)
N(1A)-C(18A)-C(19A)-C(24A)	-133.4(2)
C(25A)-C(18A)-C(19A)-C(24A)	102.6(3)
C(24A)-C(19A)-C(20A)-C(21A)	0.5(3)
C(18A)-C(19A)-C(20A)-C(21A)	-179.1(2)
C(19A)-C(20A)-C(21A)-C(22A)	-0.2(4)
C(20A)-C(21A)-C(22A)-C(23A)	-0.3(4)
C(21A)-C(22A)-C(23A)-C(24A)	0.5(4)
C(22A)-C(23A)-C(24A)-C(19A)	-0.2(4)
C(20A)-C(19A)-C(24A)-C(23A)	-0.3(3)
C(18A)-C(19A)-C(24A)-C(23A)	179.3(2)
N(1A)-C(18A)-C(25A)-C(30A)	-46.0(3)
C(19A)-C(18A)-C(25A)-C(30A)	77.8(3)
N(1A)-C(18A)-C(25A)-C(26A)	136.5(3)
C(19A)-C(18A)-C(25A)-C(26A)	-99.7(3)
C(30A)-C(25A)-C(26A)-C(27A)	1.0(5)
C(18A)-C(25A)-C(26A)-C(27A)	178.5(4)
C(25A)-C(26A)-C(27A)-C(28A)	-4.5(8)
C(26A)-C(27A)-C(28A)-C(29A)	5.3(10)
C(27A)-C(28A)-C(29A)-C(30A)	-2.6(9)

Table A.1.6 (Cont'd)

C(26A)-C(25A)-C(30A)-C(29A)	1.4(5)
C(18A)-C(25A)-C(30A)-C(29A)	-176.1(3)
C(28A)-C(29A)-C(30A)-C(25A)	-0.6(6)
C(2B)-N(1B)-C(1B)-C(3B)	-108.1(2)
C(18B)-N(1B)-C(1B)-C(3B)	147.3(2)
C(18B)-N(1B)-C(1B)-C(2B)	-104.6(2)
C(18B)-N(1B)-C(2B)-C(1B)	103.8(2)
C(1B)-N(1B)-C(2B)-C(12B)	111.9(2)
C(18B)-N(1B)-C(2B)-C(12B)	-144.3(2)
C(3B)-C(1B)-C(2B)-N(1B)	110.0(2)
N(1B)-C(1B)-C(2B)-C(12B)	-108.4(2)
C(3B)-C(1B)-C(2B)-C(12B)	1.6(3)
C(4B)-N(2B)-C(3B)-O(1B)	-8.5(4)
C(4B)-N(2B)-C(3B)-C(1B)	171.37(19)
N(1B)-C(1B)-C(3B)-O(1B)	166.9(2)
C(2B)-C(1B)-C(3B)-O(1B)	97.4(3)
N(1B)-C(1B)-C(3B)-N(2B)	-13.0(3)
C(2B)-C(1B)-C(3B)-N(2B)	-82.5(3)
C(3B)-N(2B)-C(4B)-C(5B)	149.7(2)
C(3B)-N(2B)-C(4B)-C(6B)	-84.0(3)
N(2B)-C(4B)-C(6B)-C(11B)	108.9(2)
C(5B)-C(4B)-C(6B)-C(11B)	-126.7(2)
N(2B)-C(4B)-C(6B)-C(7B)	-69.8(3)
C(5B)-C(4B)-C(6B)-C(7B)	54.6(3)
C(11B)-C(6B)-C(7B)-C(8B)	-0.4(3)
C(4B)-C(6B)-C(7B)-C(8B)	178.3(2)
C(6B)-C(7B)-C(8B)-C(9B)	0.6(4)
C(7B)-C(8B)-C(9B)-C(10B)	-0.6(4)
C(8B)-C(9B)-C(10B)-C(11B)	0.4(4)
C(7B)-C(6B)-C(11B)-C(10B)	0.2(4)
C(4B)-C(6B)-C(11B)-C(10B)	-178.5(2)
C(9B)-C(10B)-C(11B)-C(6B)	-0.2(4)
N(1B)-C(2B)-C(12B)-C(13B)	-160.4(2)
C(1B)-C(2B)-C(12B)-C(13B)	-89.8(3)
N(1B)-C(2B)-C(12B)-C(17B)	77.1(3)

Table A.1.6 (Cont'd)

C(1B)-C(2B)-C(12B)-C(17B)	147.7(2)
C(2B)-C(12B)-C(13B)-C(14B)	-179.0(2)
C(17B)-C(12B)-C(13B)-C(14B)	-55.8(3)
C(12B)-C(13B)-C(14B)-C(15B)	55.7(4)
C(13B)-C(14B)-C(15B)-C(16B)	-56.0(4)
C(14B)-C(15B)-C(16B)-C(17B)	56.5(3)
C(2B)-C(12B)-C(17B)-C(16B)	177.5(2)
C(13B)-C(12B)-C(17B)-C(16B)	56.0(3)
C(15B)-C(16B)-C(17B)-C(12B)	-56.6(3)
C(1B)-N(1B)-C(18B)-C(25B)	-88.4(2)
C(2B)-N(1B)-C(18B)-C(25B)	-155.52(19)
C(1B)-N(1B)-C(18B)-C(19B)	145.9(2)
C(2B)-N(1B)-C(18B)-C(19B)	78.7(2)
N(1B)-C(18B)-C(19B)-C(20B)	-135.1(2)
C(25B)-C(18B)-C(19B)-C(20B)	101.1(3)
N(1B)-C(18B)-C(19B)-C(24B)	44.2(3)
C(25B)-C(18B)-C(19B)-C(24B)	-79.6(3)
C(24B)-C(19B)-C(20B)-C(21B)	0.1(4)
C(18B)-C(19B)-C(20B)-C(21B)	179.5(3)
C(19B)-C(20B)-C(21B)-C(22B)	-0.4(4)
C(20B)-C(21B)-C(22B)-C(23B)	0.2(5)
C(21B)-C(22B)-C(23B)-C(24B)	0.2(4)
C(22B)-C(23B)-C(24B)-C(19B)	-0.5(4)
C(20B)-C(19B)-C(24B)-C(23B)	0.3(4)
C(18B)-C(19B)-C(24B)-C(23B)	-179.0(2)
N(1B)-C(18B)-C(25B)-C(26B)	-41.4(3)
C(19B)-C(18B)-C(25B)-C(26B)	82.3(3)
N(1B)-C(18B)-C(25B)-C(30B)	139.3(3)
C(19B)-C(18B)-C(25B)-C(30B)	-97.0(3)
C(30B)-C(25B)-C(26B)-C(27B)	2.4(5)
C(18B)-C(25B)-C(26B)-C(27B)	-176.9(3)
C(25B)-C(26B)-C(27B)-C(28B)	-1.3(6)
C(26B)-C(27B)-C(28B)-C(29B)	-1.0(7)
C(27B)-C(28B)-C(29B)-C(30B)	2.3(8)
C(28B)-C(29B)-C(30B)-C(25B)	-1.2(7)

Table A.1.6 (Cont'd)

C(26B)-C(25B)-C(30B)-C(29B)	-1.2(5)
C(18B)-C(25B)-C(30B)-C(29B)	178.2(4)

Symmetry transformations used to generate equivalent atoms:

Figure A.2 ORTEP drawing of compound **73**

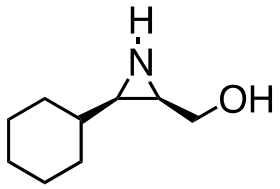

73

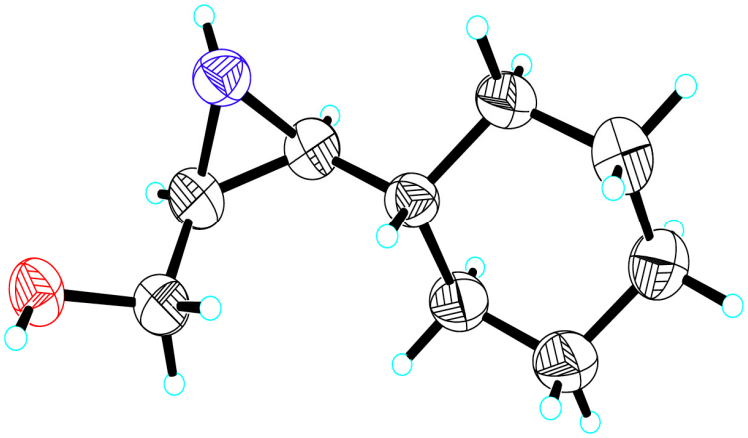

Figure A.2 (Cont'd)

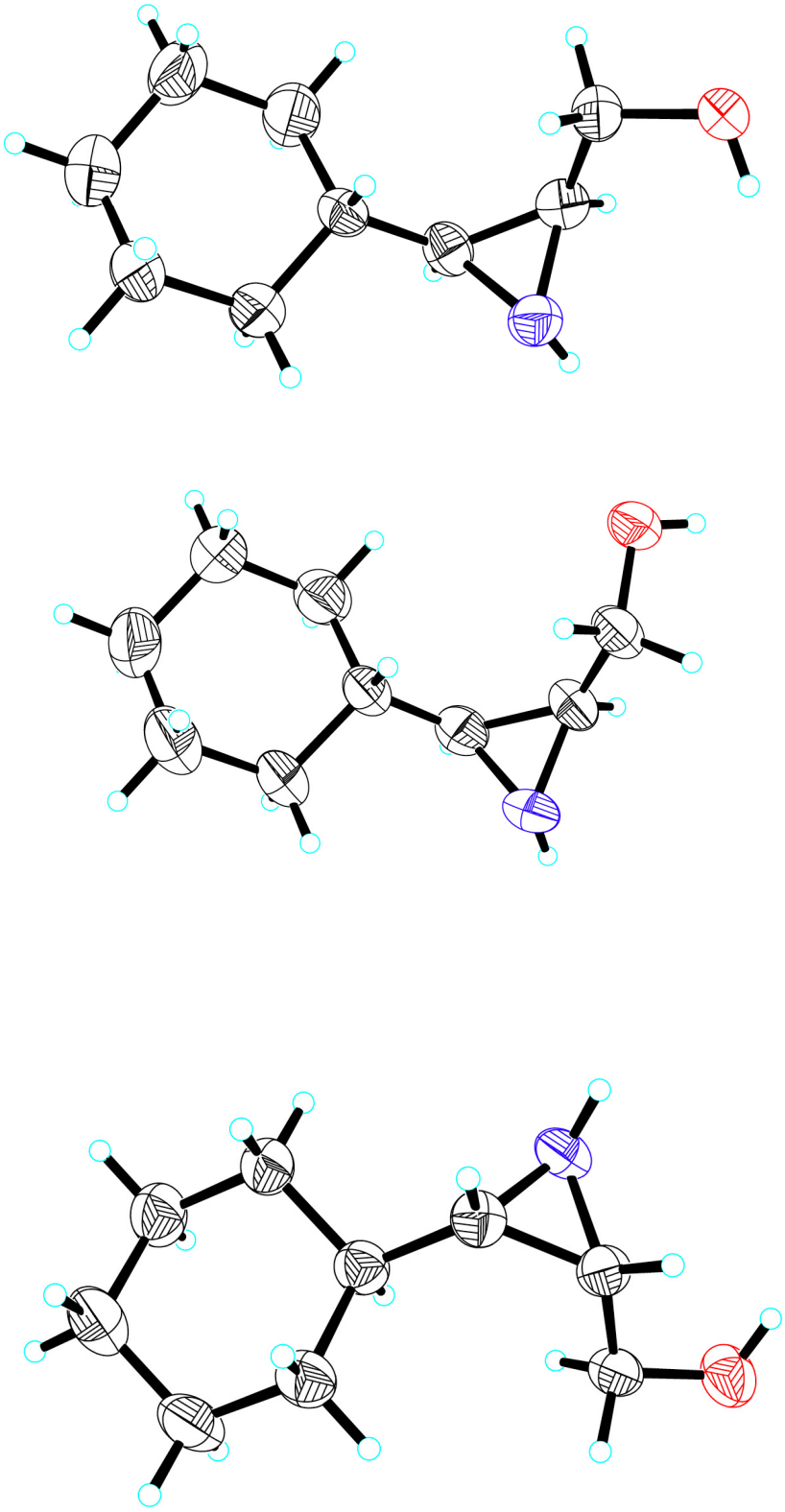

Figure A.2.1 Packing of crystals created by aziridine **73**

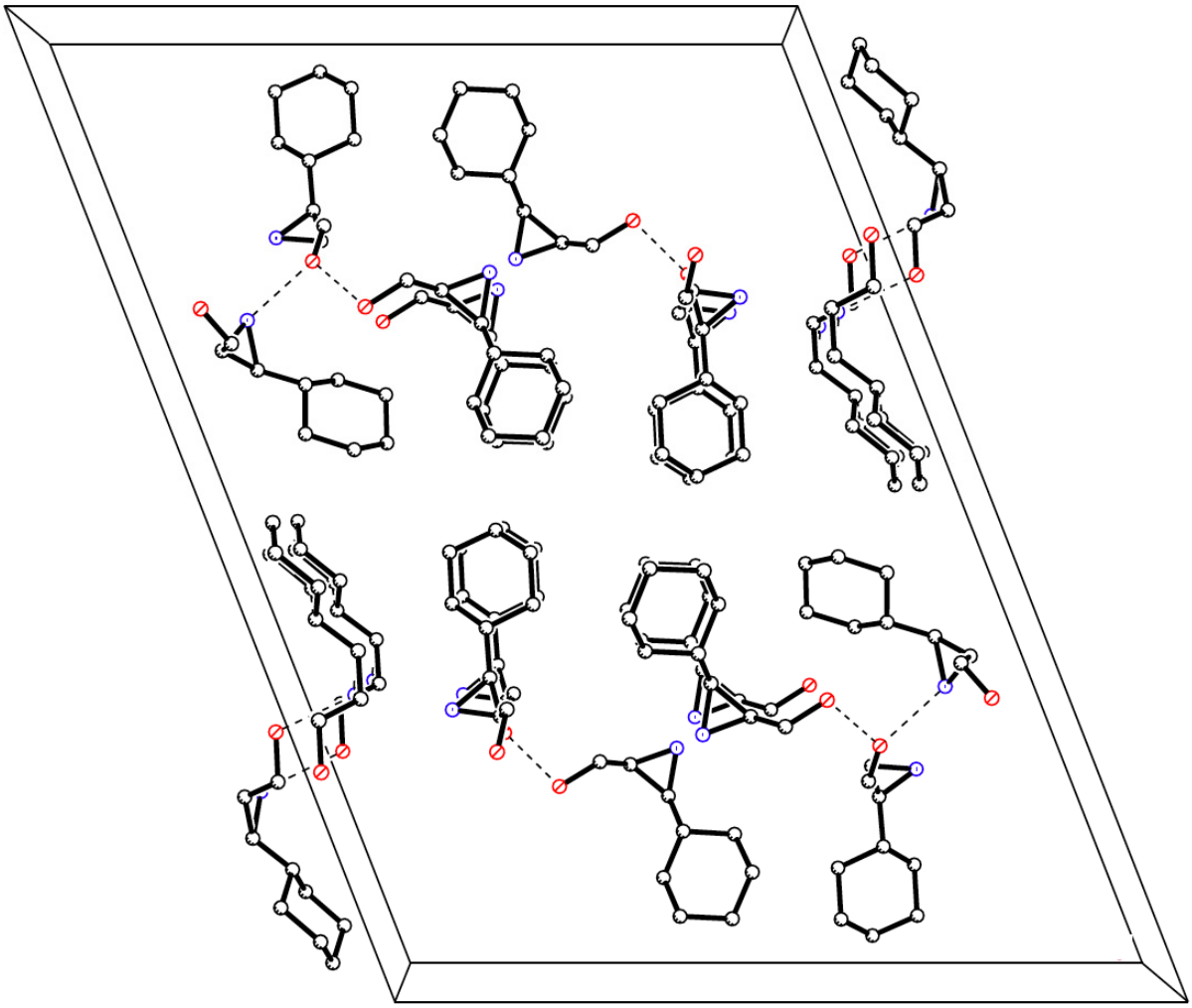

This is a drawing of the packing along the b-axis where the dotted lines represent potential hydrogen bonding.

Table A.2.1. Crystal data and structure refinement for aziridine **73**

Identification code	ww23	
Empirical formula	C9 H17 N O	
Formula weight	155.24	
Temperature	173(2) K	
Wavelength	0.71073 Å	
Crystal system	Monoclinic	
Space group	C 2	
Unit cell dimensions	a = 29.969(4) Å	□= 90°.
	b = 6.1294(8) Å	□= 111.410(2)°.
	c = 22.217(3) Å	□ = 90°.
Volume	3799.5(9) $Å^3$	
Z	16	
Density (calculated)	1.086 Mg/m^3	
Absorption coefficient	0.070 mm^{-1}	
F(000)	1376	
Crystal size	0.48 x 0.12 x 0.05 mm^3	
Theta range for data collection	1.97 to 25.33°.	
Index ranges	-36<=h<=36, -7<=k<=7, -26<=l<=26	
Reflections collected	28903	
Independent reflections	6953 [R(int) = 0.1006]	
Completeness to theta = 25.33°	99.8 %	
Absorption correction	Semi-empirical from equivalents	
Max. and min. transmission	0.9966 and 0.9672	
Refinement method	Full-matrix least-squares on F^2	
Data / restraints / parameters	6953 / 5 / 419	
Goodness-of-fit on F^2	0.964	
Final R indices [I>2sigma(I)]	R1 = 0.0522, wR2 = 0.0968	
R indices (all data)	R1 = 0.1323, wR2 = 0.1246	
Absolute structure parameter	-1(5)	
Extinction coefficient	0.0018(7)	
Largest diff. peak and hole	0.170 and -0.181 e.$Å^{-3}$	

Table A.2.2. Atomic coordinates (x 10^4) and equivalent isotropic displacement parameters ($Å^2$x 10^3) for aziridine **73**. U(eq) is defined as one third of the trace of the orthogonalized U^{ij} tensor.

	x	y	z	U(eq)
O(1A)	7651(2)	2179(12)	9710(3)	44(2)
N(1A)	6949(3)	-1557(17)	9039(4)	43(2)
C(1A)	7139(3)	2216(18)	9485(5)	45(3)
C(2A)	6949(4)	796(19)	8909(5)	43(3)
C(3A)	6487(4)	-405(19)	8745(5)	43(3)
C(4A)	6165(3)	-192(17)	9118(5)	40(3)
C(5A)	5868(4)	-2245(17)	9081(5)	48(3)
C(6A)	5516(4)	-1980(20)	9433(5)	56(3)
C(7A)	5196(4)	-20(20)	9174(6)	60(3)
C(8A)	5489(4)	2020(20)	9218(7)	75(4)
C(9A)	5831(4)	1725(19)	8863(6)	63(4)
O(1B)	7480(2)	10734(11)	7463(3)	48(2)
N(1B)	7137(3)	6215(15)	7922(4)	42(2)
C(1B)	7080(4)	9347(18)	7158(5)	45(3)
C(2B)	7188(3)	7001(18)	7317(4)	38(3)
C(3B)	6819(3)	5365(17)	7288(5)	39(3)
C(4B)	6293(3)	5828(18)	7072(4)	40(3)
C(5B)	6053(3)	4410(20)	7420(5)	61(4)
C(6B)	5512(4)	4820(30)	7181(6)	84(5)
C(7B)	5283(4)	4500(20)	6465(6)	79(4)
C(8B)	5512(4)	5950(30)	6111(5)	81(5)
C(9B)	6053(4)	5550(20)	6346(5)	68(4)
O(1C)	7002(2)	8386(13)	3035(3)	51(2)
N(1C)	7379(3)	6978(18)	4793(4)	51(3)
C(1C)	7268(4)	8601(19)	3705(4)	46(3)
C(2C)	7199(3)	6704(19)	4081(4)	46(3)
C(3C)	6859(4)	6625(18)	4428(4)	47(3)
C(4C)	6529(4)	8430(20)	4447(4)	44(3)
C(5C)	6029(4)	8100(20)	3942(5)	60(3)
C(6C)	5678(4)	9840(30)	3974(5)	78(4)

Table A.2.2 (Cont'd)

C(7C)	5657(5)	9980(30)	4647(6)	88(5)
C(8C)	6155(5)	10350(20)	5150(6)	81(4)
C(9C)	6502(4)	8590(20)	5115(5)	60(3)
O(1D)	8040(3)	4595(12)	9039(3)	50(2)
N(1D)	8077(3)	-543(15)	8657(4)	39(2)
C(1D)	8374(3)	3340(17)	8863(5)	38(3)
C(2D)	8416(3)	1033(16)	9092(4)	35(2)
C(3D)	8598(3)	-714(16)	8783(4)	36(3)
C(4D)	8754(3)	-357(18)	8216(4)	38(2)
C(5D)	9276(3)	351(18)	8451(5)	44(3)
C(6D)	9443(4)	660(20)	7887(5)	54(3)
C(7D)	9362(4)	-1360(20)	7465(5)	56(3)
C(8D)	8845(4)	-2090(20)	7242(5)	52(3)
C(9D)	8683(4)	-2430(18)	7813(5)	45(3)

Table A.2.3. Bond lengths [Å] and angles [°] for aziridine **73**

O(1A)-C(1A)	1.428(10)	C(5A)-H(5A2)	0.9900
O(1A)-H(1A)	0.8400	C(6A)-C(7A)	1.514(15)
N(1A)-C(2A)	1.471(13)	C(6A)-H(6A1)	0.9900
N(1A)-C(3A)	1.478(13)	C(6A)-H(6A2)	0.9900
N(1A)-H(1AB)	0.84(10)	C(7A)-C(8A)	1.509(17)
C(1A)-C(2A)	1.480(14)	C(7A)-H(7A1)	0.9900
C(1A)-H(1A1)	0.9900	C(7A)-H(7A2)	0.9900
C(1A)-H(1A2)	0.9900	C(8A)-C(9A)	1.514(15)
C(2A)-C(3A)	1.491(14)	C(8A)-H(8A1)	0.9900
C(2A)-H(2A)	1.0000	C(8A)-H(8A2)	0.9900
C(3A)-C(4A)	1.488(13)	C(9A)-H(9A1)	0.9900
C(3A)-H(3A)	1.0000	C(9A)-H(9A2)	0.9900
C(4A)-C(9A)	1.514(14)	O(1B)-C(1B)	1.423(11)
C(4A)-C(5A)	1.526(14)	O(1B)-H(1B)	0.8400
C(4A)-H(4A)	1.0000	N(1B)-C(3B)	1.478(12)
C(5A)-C(6A)	1.533(13)	N(1B)-C(2B)	1.486(12)
C(5A)-H(5A1)	0.9900	N(1B)-H(1BB)	0.87(6)

Table A.2.3 (Cont'd)

C(1B)-C(2B)	1.488(14)	C(3C)-C(4C)	1.494(14)
C(1B)-H(1B1)	0.9900	C(3C)-H(3C)	1.0000
C(1B)-H(1B2)	0.9900	C(4C)-C(9C)	1.518(12)
C(2B)-C(3B)	1.478(13)	C(4C)-C(5C)	1.524(13)
C(2B)-H(2B)	1.0000	C(4C)-H(4C)	1.0000
C(3B)-C(4B)	1.498(12)	C(5C)-C(6C)	1.516(16)
C(3B)-H(3B)	1.0000	C(5C)-H(5C1)	0.9900
C(4B)-C(5B)	1.509(13)	C(5C)-H(5C2)	0.9900
C(4B)-C(9B)	1.516(12)	C(6C)-C(7C)	1.521(15)
C(4B)-H(4B)	1.0000	C(6C)-H(6C1)	0.9900
C(5B)-C(6B)	1.534(14)	C(6C)-H(6C2)	0.9900
C(5B)-H(5B1)	0.9900	C(7C)-C(8C)	1.521(18)
C(5B)-H(5B2)	0.9900	C(7C)-H(7C1)	0.9900
C(6B)-C(7B)	1.497(15)	C(7C)-H(7C2)	0.9900
C(6B)-H(6B1)	0.9900	C(8C)-C(9C)	1.520(16)
C(6B)-H(6B2)	0.9900	C(8C)-H(8C1)	0.9900
C(7B)-C(8B)	1.509(15)	C(8C)-H(8C2)	0.9900
C(7B)-H(7B1)	0.9900	C(9C)-H(9C1)	0.9900
C(7B)-H(7B2)	0.9900	C(9C)-H(9C2)	0.9900
C(8B)-C(9B)	1.532(14)	O(1D)-C(1D)	1.427(11)
C(8B)-H(8B1)	0.9900	O(1D)-H(1D)	0.8400
C(8B)-H(8B2)	0.9900	N(1D)-C(2D)	1.478(12)
C(9B)-H(9B1)	0.9900	N(1D)-C(3D)	1.484(11)
C(9B)-H(9B2)	0.9900	N(1D)-H(1DB)	0.88(5)
O(1C)-C(1C)	1.415(10)	C(1D)-C(2D)	1.493(13)
O(1C)-H(1C)	0.8400	C(1D)-H(1D1)	0.9900
N(1C)-C(2C)	1.482(12)	C(1D)-H(1D2)	0.9900
N(1C)-C(3C)	1.487(13)	C(2D)-C(3D)	1.479(12)
N(1C)-H(1CB)	0.88(6)	C(2D)-H(2D)	1.0000
C(1C)-C(2C)	1.490(14)	C(3D)-C(4D)	1.510(12)
C(1C)-H(1C1)	0.9900	C(3D)-H(3D)	1.0000
C(1C)-H(1C2)	0.9900	C(4D)-C(5D)	1.522(12)
C(2C)-C(3C)	1.485(13)	C(4D)-C(9D)	1.525(13)
C(2C)-H(2C)	1.0000	C(4D)-H(4D)	1.0000

Table A.2.3 (Cont'd)

C(5D)-C(6D)	1.521(12)	N(1A)-C(3A)-H(3A)	114.5
C(5D)-H(5D1)	0.9900	C(4A)-C(3A)-H(3A)	114.5
C(5D)-H(5D2)	0.9900	C(2A)-C(3A)-H(3A)	114.5
C(6D)-C(7D)	1.521(15)	C(3A)-C(4A)-C(9A)	109.5(9)
C(6D)-H(6D1)	0.9900	C(3A)-C(4A)-C(5A)	112.4(9)
C(6D)-H(6D2)	0.9900	C(9A)-C(4A)-C(5A)	109.1(8)
C(7D)-C(8D)	1.512(13)	C(3A)-C(4A)-H(4A)	108.6
C(7D)-H(7D1)	0.9900	C(9A)-C(4A)-H(4A)	108.6
C(7D)-H(7D2)	0.9900	C(5A)-C(4A)-H(4A)	108.6
C(8D)-C(9D)	1.527(13)	C(4A)-C(5A)-C(6A)	112.4(9)
C(8D)-H(8D1)	0.9900	C(4A)-C(5A)-H(5A1)	109.1
C(8D)-H(8D2)	0.9900	C(6A)-C(5A)-H(5A1)	109.1
C(9D)-H(9D1)	0.9900	C(4A)-C(5A)-H(5A2)	109.1
C(9D)-H(9D2)	0.9900	C(6A)-C(5A)-H(5A2)	109.1
		H(5A1)-C(5A)-H(5A2)	107.9
C(1A)-O(1A)-H(1A)	109.5	C(7A)-C(6A)-C(5A)	110.5(9)
C(2A)-N(1A)-C(3A)	60.8(7)	C(7A)-C(6A)-H(6A1)	109.5
C(2A)-N(1A)-H(1AB)	115(8)	C(5A)-C(6A)-H(6A1)	109.5
C(3A)-N(1A)-H(1AB)	110(7)	C(7A)-C(6A)-H(6A2)	109.5
O(1A)-C(1A)-C(2A)	108.6(8)	C(5A)-C(6A)-H(6A2)	109.5
O(1A)-C(1A)-H(1A1)	110.0	H(6A1)-C(6A)-H(6A2)	108.1
C(2A)-C(1A)-H(1A1)	110.0	C(8A)-C(7A)-C(6A)	110.9(9)
O(1A)-C(1A)-H(1A2)	110.0	C(8A)-C(7A)-H(7A1)	109.5
C(2A)-C(1A)-H(1A2)	110.0	C(6A)-C(7A)-H(7A1)	109.5
H(1A1)-C(1A)-H(1A2)	108.4	C(8A)-C(7A)-H(7A2)	109.5
N(1A)-C(2A)-C(1A)	115.8(9)	C(6A)-C(7A)-H(7A2)	109.5
N(1A)-C(2A)-C(3A)	59.9(7)	H(7A1)-C(7A)-H(7A2)	108.0
C(1A)-C(2A)-C(3A)	122.2(9)	C(7A)-C(8A)-C(9A)	110.9(11)
N(1A)-C(2A)-H(2A)	115.7	C(7A)-C(8A)-H(8A1)	109.5
C(1A)-C(2A)-H(2A)	115.7	C(9A)-C(8A)-H(8A1)	109.5
C(3A)-C(2A)-H(2A)	115.7	C(7A)-C(8A)-H(8A2)	109.5
N(1A)-C(3A)-C(4A)	119.3(9)	C(9A)-C(8A)-H(8A2)	109.5
N(1A)-C(3A)-C(2A)	59.4(6)	H(8A1)-C(8A)-H(8A2)	108.0
C(4A)-C(3A)-C(2A)	123.6(9)	C(8A)-C(9A)-C(4A)	112.1(10)

Table A.2.3 (Cont'd)

C(8A)-C(9A)-H(9A1)	109.2
C(4A)-C(9A)-H(9A1)	109.2
C(8A)-C(9A)-H(9A2)	109.2
C(4A)-C(9A)-H(9A2)	109.2
H(9A1)-C(9A)-H(9A2)	107.9
C(1B)-O(1B)-H(1B)	109.5
C(3B)-N(1B)-C(2B)	59.8(6)
C(3B)-N(1B)-H(1BB)	111(10)
C(2B)-N(1B)-H(1BB)	103(9)
O(1B)-C(1B)-C(2B)	113.0(9)
O(1B)-C(1B)-H(1B1)	109.0
C(2B)-C(1B)-H(1B1)	109.0
O(1B)-C(1B)-H(1B2)	109.0
C(2B)-C(1B)-H(1B2)	109.0
H(1B1)-C(1B)-H(1B2)	107.8
C(3B)-C(2B)-N(1B)	59.8(6)
C(3B)-C(2B)-C(1B)	123.4(9)
N(1B)-C(2B)-C(1B)	116.3(9)
C(3B)-C(2B)-H(2B)	115.2
N(1B)-C(2B)-H(2B)	115.2
C(1B)-C(2B)-H(2B)	115.2
N(1B)-C(3B)-C(2B)	60.4(6)
N(1B)-C(3B)-C(4B)	118.4(8)
C(2B)-C(3B)-C(4B)	124.7(10)
N(1B)-C(3B)-H(3B)	114.2
C(2B)-C(3B)-H(3B)	114.2
C(4B)-C(3B)-H(3B)	114.2
C(3B)-C(4B)-C(5B)	111.6(8)
C(3B)-C(4B)-C(9B)	110.7(8)
C(5B)-C(4B)-C(9B)	110.5(9)
C(3B)-C(4B)-H(4B)	107.9
C(5B)-C(4B)-H(4B)	107.9
C(9B)-C(4B)-H(4B)	107.9
C(4B)-C(5B)-C(6B)	111.6(9)
C(4B)-C(5B)-H(5B1)	109.3
C(6B)-C(5B)-H(5B1)	109.3
C(4B)-C(5B)-H(5B2)	109.3
C(6B)-C(5B)-H(5B2)	109.3
H(5B1)-C(5B)-H(5B2)	108.0
C(7B)-C(6B)-C(5B)	111.3(10)
C(7B)-C(6B)-H(6B1)	109.4
C(5B)-C(6B)-H(6B1)	109.4
C(7B)-C(6B)-H(6B2)	109.4
C(5B)-C(6B)-H(6B2)	109.4
H(6B1)-C(6B)-H(6B2)	108.0
C(6B)-C(7B)-C(8B)	111.1(10)
C(6B)-C(7B)-H(7B1)	109.4
C(8B)-C(7B)-H(7B1)	109.4
C(6B)-C(7B)-H(7B2)	109.4
C(8B)-C(7B)-H(7B2)	109.4
H(7B1)-C(7B)-H(7B2)	108.0
C(7B)-C(8B)-C(9B)	110.6(11)
C(7B)-C(8B)-H(8B1)	109.5
C(9B)-C(8B)-H(8B1)	109.5
C(7B)-C(8B)-H(8B2)	109.5
C(9B)-C(8B)-H(8B2)	109.5
H(8B1)-C(8B)-H(8B2)	108.1
C(4B)-C(9B)-C(8B)	112.2(9)
C(4B)-C(9B)-H(9B1)	109.2
C(8B)-C(9B)-H(9B1)	109.2
C(4B)-C(9B)-H(9B2)	109.2
C(8B)-C(9B)-H(9B2)	109.2
H(9B1)-C(9B)-H(9B2)	107.9
C(1C)-O(1C)-H(1C)	109.5
C(2C)-N(1C)-C(3C)	60.0(6)
C(2C)-N(1C)-H(1CB)	110(10)
C(3C)-N(1C)-H(1CB)	107(10)
O(1C)-C(1C)-C(2C)	112.1(9)
O(1C)-C(1C)-H(1C1)	109.2

Table A.2.3 (Cont'd)

C(2C)-C(1C)-H(1C1)	109.2	H(6C1)-C(6C)-H(6C2)	108.0
O(1C)-C(1C)-H(1C2)	109.2	C(8C)-C(7C)-C(6C)	110.3(10)
C(2C)-C(1C)-H(1C2)	109.2	C(8C)-C(7C)-H(7C1)	109.6
H(1C1)-C(1C)-H(1C2)	107.9	C(6C)-C(7C)-H(7C1)	109.6
N(1C)-C(2C)-C(3C)	60.2(6)	C(8C)-C(7C)-H(7C2)	109.6
N(1C)-C(2C)-C(1C)	116.0(9)	C(6C)-C(7C)-H(7C2)	109.6
C(3C)-C(2C)-C(1C)	125.4(10)	H(7C1)-C(7C)-H(7C2)	108.1
N(1C)-C(2C)-H(2C)	114.6	C(9C)-C(8C)-C(7C)	111.2(11)
C(3C)-C(2C)-H(2C)	114.6	C(9C)-C(8C)-H(8C1)	109.4
C(1C)-C(2C)-H(2C)	114.6	C(7C)-C(8C)-H(8C1)	109.4
C(2C)-C(3C)-N(1C)	59.8(6)	C(9C)-C(8C)-H(8C2)	109.4
C(2C)-C(3C)-C(4C)	125.3(10)	C(7C)-C(8C)-H(8C2)	109.4
N(1C)-C(3C)-C(4C)	116.7(9)	H(8C1)-C(8C)-H(8C2)	108.0
C(2C)-C(3C)-H(3C)	114.5	C(4C)-C(9C)-C(8C)	112.2(9)
N(1C)-C(3C)-H(3C)	114.5	C(4C)-C(9C)-H(9C1)	109.2
C(4C)-C(3C)-H(3C)	114.5	C(8C)-C(9C)-H(9C1)	109.2
C(3C)-C(4C)-C(9C)	110.5(9)	C(4C)-C(9C)-H(9C2)	109.2
C(3C)-C(4C)-C(5C)	111.5(9)	C(8C)-C(9C)-H(9C2)	109.2
C(9C)-C(4C)-C(5C)	109.8(8)	H(9C1)-C(9C)-H(9C2)	107.9
C(3C)-C(4C)-H(4C)	108.4	C(1D)-O(1D)-H(1D)	109.5
C(9C)-C(4C)-H(4C)	108.4	C(2D)-N(1D)-C(3D)	59.9(6)
C(5C)-C(4C)-H(4C)	108.4	C(2D)-N(1D)-H(1DB)	109(6)
C(6C)-C(5C)-C(4C)	112.7(10)	C(3D)-N(1D)-H(1DB)	109(6)
C(6C)-C(5C)-H(5C1)	109.0	O(1D)-C(1D)-C(2D)	113.4(8)
C(4C)-C(5C)-H(5C1)	109.0	O(1D)-C(1D)-H(1D1)	108.9
C(6C)-C(5C)-H(5C2)	109.0	C(2D)-C(1D)-H(1D1)	108.9
C(4C)-C(5C)-H(5C2)	109.0	O(1D)-C(1D)-H(1D2)	108.9
H(5C1)-C(5C)-H(5C2)	107.8	C(2D)-C(1D)-H(1D2)	108.9
C(5C)-C(6C)-C(7C)	111.3(11)	H(1D1)-C(1D)-H(1D2)	107.7
C(5C)-C(6C)-H(6C1)	109.4	N(1D)-C(2D)-C(3D)	60.3(6)
C(7C)-C(6C)-H(6C1)	109.4	N(1D)-C(2D)-C(1D)	116.3(8)
C(5C)-C(6C)-H(6C2)	109.4	C(3D)-C(2D)-C(1D)	121.8(8)
C(7C)-C(6C)-H(6C2)	109.4	N(1D)-C(2D)-H(2D)	115.6

Table A.2.3 (Cont'd)

C(3D)-C(2D)-H(2D)	115.6
C(1D)-C(2D)-H(2D)	115.6
C(2D)-C(3D)-N(1D)	59.8(6)
C(2D)-C(3D)-C(4D)	124.1(9)
N(1D)-C(3D)-C(4D)	117.1(8)
C(2D)-C(3D)-H(3D)	114.8
N(1D)-C(3D)-H(3D)	114.8
C(4D)-C(3D)-H(3D)	114.8
C(3D)-C(4D)-C(5D)	110.4(8)
C(3D)-C(4D)-C(9D)	110.5(9)
C(5D)-C(4D)-C(9D)	110.1(8)
C(3D)-C(4D)-H(4D)	108.6
C(5D)-C(4D)-H(4D)	108.6
C(9D)-C(4D)-H(4D)	108.6
C(6D)-C(5D)-C(4D)	111.1(8)
C(6D)-C(5D)-H(5D1)	109.4
C(4D)-C(5D)-H(5D1)	109.4
C(6D)-C(5D)-H(5D2)	109.4
C(4D)-C(5D)-H(5D2)	109.4
H(5D1)-C(5D)-H(5D2)	108.0
C(5D)-C(6D)-C(7D)	112.2(9)
C(5D)-C(6D)-H(6D1)	109.2
C(7D)-C(6D)-H(6D1)	109.2
C(5D)-C(6D)-H(6D2)	109.2
C(7D)-C(6D)-H(6D2)	109.2
H(6D1)-C(6D)-H(6D2)	107.9
C(8D)-C(7D)-C(6D)	110.9(9)
C(8D)-C(7D)-H(7D1)	109.4
C(6D)-C(7D)-H(7D1)	109.4
C(8D)-C(7D)-H(7D2)	109.4
C(6D)-C(7D)-H(7D2)	109.4
H(7D1)-C(7D)-H(7D2)	108.0
C(8D)-C(9D)-H(9D1)	109.5
C(7D)-C(8D)-C(9D)	111.5(8)
C(7D)-C(8D)-H(8D1)	109.3
C(9D)-C(8D)-H(8D1)	109.3
C(7D)-C(8D)-H(8D2)	109.3
C(9D)-C(8D)-H(8D2)	109.3
H(8D1)-C(8D)-H(8D2)	108.0
C(4D)-C(9D)-C(8D)	110.9(9)
C(4D)-C(9D)-H(9D1)	109.5
C(4D)-C(9D)-H(9D2)	109.5
C(8D)-C(9D)-H(9D2)	109.5
H(9D1)-C(9D)-H(9D2)	108.0

Symmetry transformations used to generate equivalent atoms:

Table A.2.4. Anisotropic displacement parameters ($Å^2 x\ 10^3$) for ww23. The anisotropic displacement factor exponent takes the form: $-2\pi^2[h^2 a^{*2} U^{11} + ... + 2 h k a^* b^* U^{12}]$

	U^{11}	U^{22}	U^{33}	U^{23}	U^{13}	U^{12}
O(1A)	44(4)	52(5)	40(4)	-3(4)	19(3)	-8(4)
N(1A)	51(6)	42(6)	40(5)	-8(5)	23(5)	-2(5)
C(1A)	45(7)	43(7)	47(7)	-3(6)	17(5)	-3(6)
C(2A)	48(7)	44(8)	38(6)	4(6)	15(5)	-5(6)
C(3A)	43(6)	48(7)	33(6)	0(6)	9(5)	1(6)
C(4A)	39(6)	37(7)	39(6)	-4(5)	10(5)	0(6)
C(5A)	52(7)	35(7)	58(7)	1(6)	20(6)	0(6)
C(6A)	51(7)	60(9)	55(7)	4(7)	18(6)	-6(7)
C(7A)	47(7)	61(9)	70(8)	-3(7)	20(6)	2(7)
C(8A)	56(8)	46(8)	122(12)	-13(8)	31(8)	3(7)
C(9A)	51(7)	34(7)	104(10)	8(7)	27(7)	8(6)
O(1B)	44(4)	47(5)	45(4)	12(4)	7(4)	-12(4)
N(1B)	38(5)	50(6)	38(5)	4(5)	14(4)	1(5)
C(1B)	40(6)	53(8)	40(6)	1(6)	12(5)	-9(6)
C(2B)	41(6)	38(7)	37(6)	-2(5)	17(5)	3(6)
C(3B)	42(6)	39(7)	44(7)	-4(5)	22(5)	-3(5)
C(4B)	42(6)	46(7)	36(6)	3(5)	17(5)	-7(6)
C(5B)	44(7)	85(10)	52(7)	21(7)	17(6)	-4(7)
C(6B)	41(7)	149(14)	64(9)	40(9)	21(7)	-11(9)
C(7B)	48(8)	105(12)	76(10)	12(9)	11(7)	-17(8)
C(8B)	46(8)	146(14)	43(7)	17(8)	7(6)	-10(9)
C(9B)	52(8)	113(12)	41(7)	2(7)	19(6)	-14(8)
O(1C)	57(5)	64(6)	34(4)	5(4)	19(4)	15(4)
N(1C)	54(6)	67(8)	29(5)	7(5)	12(4)	2(6)
C(1C)	54(7)	55(8)	35(6)	1(6)	22(5)	-3(6)
C(2C)	55(7)	50(8)	37(6)	0(6)	24(6)	0(6)
C(3C)	56(7)	47(8)	41(6)	5(6)	20(6)	-1(6)
C(4C)	51(7)	51(7)	36(6)	1(6)	22(5)	2(6)
C(5C)	61(8)	70(9)	51(7)	4(7)	23(6)	-3(7)
C(6C)	66(9)	109(12)	62(9)	20(8)	28(7)	32(9)

Table A.2.4 (Cont'd)

C(7C)	88(10)	112(13)	85(10)	28(9)	58(9)	40(10)
C(8C)	97(11)	102(12)	60(9)	10(8)	49(9)	25(9)
C(9C)	68(8)	79(9)	42(7)	2(7)	30(6)	10(7)
O(1D)	61(5)	42(4)	60(5)	10(4)	36(4)	7(4)
N(1D)	37(5)	44(6)	39(5)	4(5)	17(4)	-8(5)
C(1D)	36(6)	37(7)	43(6)	1(5)	16(5)	-6(5)
C(2D)	41(6)	33(6)	29(5)	0(5)	13(5)	-4(5)
C(3D)	38(6)	37(7)	32(6)	3(5)	12(5)	1(5)
C(4D)	35(6)	40(7)	38(6)	-1(6)	13(5)	-2(6)
C(5D)	34(6)	51(8)	46(7)	-6(6)	14(5)	-7(5)
C(6D)	46(7)	68(9)	53(7)	-4(7)	24(6)	-20(6)
C(7D)	42(7)	77(9)	52(7)	-3(7)	23(6)	-5(6)
C(8D)	52(7)	60(8)	46(6)	-9(6)	21(6)	-3(6)
C(9D)	46(6)	49(8)	46(6)	-13(6)	23(5)	-9(6)

Table A.2.5. Hydrogen coordinates (x 10^4) and isotropic displacement parameters ($Å^2$x 10^3) for aziridine **73**

	x	y	z	U(eq)
H(1A)	7764	2545	10101	66
H(1AB)	7000(30)	-2360(180)	8760(50)	60(40)
H(1A1)	7022	3727	9372	54
H(1A2)	7030	1685	9829	54
H(2A)	7040	1214	8534	52
H(3A)	6317	-692	8273	51
H(4A)	6366	91	9581	47
H(5A1)	6086	-3480	9275	58
H(5A2)	5687	-2601	8622	58
H(6A1)	5317	-3309	9372	67
H(6A2)	5697	-1791	9902	67
H(7A1)	4989	-282	8718	72
H(7A2)	4986	187	9426	72

Table A.2.5 (Cont'd)

H(8A1)	5674	2355	9678	90
H(8A2)	5273	3261	9029	90
H(9A1)	6023	3071	8907	76
H(9A2)	5643	1500	8397	76
H(1B)	7646	10219	7827	72
H(1BB)	7390(40)	5400(200)	8090(60)	120(60)
H(1B1)	6973	9538	6683	54
H(1B2)	6813	9793	7292	54
H(2B)	7473	6422	7235	46
H(3B)	6897	3849	7192	47
H(4B)	6253	7384	7179	48
H(5B1)	6196	4708	7890	73
H(5B2)	6113	2855	7352	73
H(6B1)	5365	3805	7402	101
H(6B2)	5452	6327	7292	101
H(7B1)	4937	4842	6323	95
H(7B2)	5316	2959	6358	95
H(8B1)	5451	7501	6183	97
H(8B2)	5366	5659	5641	97
H(9B1)	6111	4050	6227	82
H(9B2)	6198	6580	6127	82
H(1C)	7161	7666	2862	77
H(1CB)	7500(50)	5740(150)	4980(70)	110(60)
H(1C1)	7168	9953	3865	56
H(1C2)	7612	8737	3774	56
H(2C)	7271	5254	3932	55
H(3C)	6742	5129	4473	57
H(4C)	6660	9831	4352	53
H(5C1)	6047	8118	3507	72
H(5C2)	5907	6653	4007	72
H(6C1)	5355	9501	3656	93
H(6C2)	5777	11272	3858	93
H(7C1)	5443	11189	4663	105
H(7C2)	5523	8603	4745	105
H(8C1)	6275	11795	5077	97

Table A.2.5 (Cont'd)

H(8C2)	6138	10353	5587	97
H(9C1)	6825	8915	5435	72
H(9C2)	6399	7167	5230	72
H(1D)	7901	3785	9221	75
H(1DB)	8000(30)	-1520(130)	8890(40)	40(30)
H(1D1)	8693	4042	9045	45
H(1D2)	8274	3345	8386	45
H(2D)	8483	835	9564	41
H(3D)	8766	-1933	9078	43
H(4D)	8552	826	7938	46
H(5D1)	9315	1736	8694	53
H(5D2)	9478	-769	8748	53
H(6D1)	9789	1029	8056	65
H(6D2)	9268	1907	7620	65
H(7D1)	9447	-1042	7083	67
H(7D2)	9573	-2552	7712	67
H(8D1)	8807	-3476	6999	62
H(8D2)	8638	-981	6948	62
H(9D1)	8340	-2848	7650	54
H(9D2)	8870	-3634	8087	54

Table A.2.6. Torsion angles [°] for aziridine **73**

C(3A)-N(1A)-C(2A)-C(1A)	113.8(10)
O(1A)-C(1A)-C(2A)-N(1A)	80.1(11)
O(1A)-C(1A)-C(2A)-C(3A)	149.4(9)
C(2A)-N(1A)-C(3A)-C(4A)	-113.9(11)
C(1A)-C(2A)-C(3A)-N(1A)	-103.3(11)
N(1A)-C(2A)-C(3A)-C(4A)	106.8(11)
C(1A)-C(2A)-C(3A)-C(4A)	3.6(17)
N(1A)-C(3A)-C(4A)-C(9A)	157.4(10)
C(2A)-C(3A)-C(4A)-C(9A)	86.5(12)
N(1A)-C(3A)-C(4A)-C(5A)	-81.2(12)
C(2A)-C(3A)-C(4A)-C(5A)	-152.1(10)

Table A.2.6 (Cont'd)

C(3A)-C(4A)-C(5A)-C(6A)	-176.7(9)
C(9A)-C(4A)-C(5A)-C(6A)	-55.1(11)
C(4A)-C(5A)-C(6A)-C(7A)	55.5(12)
C(5A)-C(6A)-C(7A)-C(8A)	-55.4(13)
C(6A)-C(7A)-C(8A)-C(9A)	56.7(14)
C(7A)-C(8A)-C(9A)-C(4A)	-57.7(14)
C(3A)-C(4A)-C(9A)-C(8A)	179.4(10)
C(5A)-C(4A)-C(9A)-C(8A)	56.0(12)
C(3B)-N(1B)-C(2B)-C(1B)	115.1(10)
O(1B)-C(1B)-C(2B)-C(3B)	155.3(8)
O(1B)-C(1B)-C(2B)-N(1B)	85.5(11)
C(2B)-N(1B)-C(3B)-C(4B)	-115.9(11)
C(1B)-C(2B)-C(3B)-N(1B)	-103.3(10)
N(1B)-C(2B)-C(3B)-C(4B)	105.8(10)
C(1B)-C(2B)-C(3B)-C(4B)	2.4(15)
N(1B)-C(3B)-C(4B)-C(5B)	-76.0(12)
C(2B)-C(3B)-C(4B)-C(5B)	-148.0(10)
N(1B)-C(3B)-C(4B)-C(9B)	160.5(9)
C(2B)-C(3B)-C(4B)-C(9B)	88.5(12)
C(3B)-C(4B)-C(5B)-C(6B)	-177.8(11)
C(9B)-C(4B)-C(5B)-C(6B)	-54.1(14)
C(4B)-C(5B)-C(6B)-C(7B)	55.9(16)
C(5B)-C(6B)-C(7B)-C(8B)	-56.6(16)
C(6B)-C(7B)-C(8B)-C(9B)	56.2(16)
C(3B)-C(4B)-C(9B)-C(8B)	178.5(11)
C(5B)-C(4B)-C(9B)-C(8B)	54.3(14)
C(7B)-C(8B)-C(9B)-C(4B)	-55.4(15)
C(3C)-N(1C)-C(2C)-C(1C)	117.5(11)
O(1C)-C(1C)-C(2C)-N(1C)	-167.7(8)
O(1C)-C(1C)-C(2C)-C(3C)	-97.1(11)
C(1C)-C(2C)-C(3C)-N(1C)	-102.3(12)
N(1C)-C(2C)-C(3C)-C(4C)	103.0(12)
C(1C)-C(2C)-C(3C)-C(4C)	0.7(16)
C(2C)-N(1C)-C(3C)-C(4C)	-117.1(10)
C(2C)-C(3C)-C(4C)-C(9C)	-141.0(10)

Table A.2.6 (Cont'd)

N(1C)-C(3C)-C(4C)-C(9C)	-70.4(12)
C(2C)-C(3C)-C(4C)-C(5C)	96.7(12)
N(1C)-C(3C)-C(4C)-C(5C)	167.2(8)
C(3C)-C(4C)-C(5C)-C(6C)	176.9(10)
C(9C)-C(4C)-C(5C)-C(6C)	54.2(13)
C(4C)-C(5C)-C(6C)-C(7C)	-55.5(15)
C(5C)-C(6C)-C(7C)-C(8C)	55.4(16)
C(6C)-C(7C)-C(8C)-C(9C)	-55.9(15)
C(3C)-C(4C)-C(9C)-C(8C)	-177.8(11)
C(5C)-C(4C)-C(9C)-C(8C)	-54.5(14)
C(7C)-C(8C)-C(9C)-C(4C)	56.5(14)
C(3D)-N(1D)-C(2D)-C(1D)	113.2(9)
O(1D)-C(1D)-C(2D)-N(1D)	88.0(10)
O(1D)-C(1D)-C(2D)-C(3D)	157.9(8)
C(1D)-C(2D)-C(3D)-N(1D)	-104.3(10)
N(1D)-C(2D)-C(3D)-C(4D)	104.1(10)
C(1D)-C(2D)-C(3D)-C(4D)	-0.2(14)
C(2D)-N(1D)-C(3D)-C(4D)	-115.5(10)
C(2D)-C(3D)-C(4D)-C(5D)	86.0(11)
N(1D)-C(3D)-C(4D)-C(5D)	156.4(9)
C(2D)-C(3D)-C(4D)-C(9D)	-152.0(9)
N(1D)-C(3D)-C(4D)-C(9D)	-81.5(11)
C(3D)-C(4D)-C(5D)-C(6D)	178.6(9)
C(9D)-C(4D)-C(5D)-C(6D)	56.3(12)
C(4D)-C(5D)-C(6D)-C(7D)	-55.2(13)
C(5D)-C(6D)-C(7D)-C(8D)	53.9(12)
C(6D)-C(7D)-C(8D)-C(9D)	-54.5(13)
C(3D)-C(4D)-C(9D)-C(8D)	-179.4(8)
C(5D)-C(4D)-C(9D)-C(8D)	-57.2(11)
C(7D)-C(8D)-C(9D)-C(4D)	56.8(12)

Symmetry transformations used to generate equivalent atoms:

Table A.2.7. Hydrogen bonds for aziridine **73** [Å and °]

D-H...A	d(D-H)	d(H...A)	d(D...A)	<(DHA)
O(1A)-H(1A)...N(1A)#1	0.84	1.87	2.709(11)	176.1
N(1A)-H(1AB)...N(1B)#2	0.84(10)	2.24(10)	3.060(12)	167(10)
O(1B)-H(1B)...N(1D)#3	0.84	1.88	2.718(10)	171.0
N(1B)-H(1BB)...O(1D)	0.87(6)	2.34(9)	3.092(12)	145(12)
O(1D)-H(1D)...O(1A)	0.84	1.82	2.653(9)	172.9
N(1C)-H(1CB)...N(1C)#4	0.88(6)	2.36(7)	3.206(5)	162(14)
O(1C)-H(1C)...O(1B)#4	0.84	1.91	2.745(9)	172.8
N(1D)-H(1DB)...O(1D)#2	0.88(5)	2.40(8)	3.112(11)	138(8)

Symmetry transformations used to generate equivalent atoms:
#1 -x+3/2,y+1/2,-z+2 #2 x,y-1,z #3 x,y+1,z #4 -x+3/2,y-1/2,-z+1

REFERENCES

1. Osborn, H. M. I.; Sweeney, J. *Tetrahedron: Asymmetry* **1997**, *8*, 1693.

2. Büchold, C.; Hemberger, Y.; Heindl, C.; Welker, A.; Degel, B.; Pfruffer, T.; Staib, P.; Schneider, S.; Rosenthal, P. J.; Gut, J.; Morschhäusauser, J.; Bringmann, G.; Schirmeister, T. *Chem Med Chem* **2011**, *6*, 141.

3. Wang, Z.; Li, F.; Zhao, L.; He, Q.; Chen, F.; Zheng, C. *Tetrahedron* **2011**, *67*, 9199.

4. Lu, P. *Terahedron* **2010**, *66*, 2549.

5. Von Richter, V. *Chem. Ber.* **1873**, *6*, 1252.

6. R. Pummerer, E. Prell, A. Rieche *Chem. Ber.* **1926**, *59*, 2159.

7. For reviews on BINOL catalysis see (a) Brunel, J. M.* *Chem. Rev*. **2005,** *105*, 857. (b) Chen, Y.; Yekta, S.; Yudin, A. K.* *Chem. Rev*. **2003**, *103*, 3155□

8. Bao, J.; Wulff, W. D.; Rheingold, A. L. *J. Am. Chem. Soc.* **1993**, *115*, 3814.

9. Newman, C. A.; Antilla, J. C.; Chen, P.; Predeus, A. V.; Fielding, L.; Wulff, W. D. *J. Am. Chem. Soc.* **2007**, *129*, 7216.

10. Ren, H.; Wulff, W. D. *J. Am. Chem. Soc.* **2011**, *133*, 5656.

11. Gupta, A.; Wulff, W. D. Unpublished results.

12. Xue, S.; Yu, S.; Deng, Y.; Wulff, W. D. *Angew. Chem. Int. Ed.* **2001**, *40*, 2271.

13. Bolm, C.; Frison, J.-C.; Zhang, Y.; Wulff, W. D. *Synlett* **2004**, 1619.

14. Lou, S.; Schaus, S. E. *J. Am. Chem. Soc.* **2008**, *130*, 6922.

15. Huang, L.; Zhao, W.; Wulff, W. D. Unpublished results.

16. (a) Antilla, J. C.; Wulff, W. D. *J. Am. Chem. Soc.* **1999**, *121*, 5099. (b) Antilla, J. C.; Wulff, W. D. *Angew. Chem. Int. Ed.* **2000**, *39*, 4518. (c) Loncaric, C.; Wulff, W. D. *Org. Lett.* **2001**, *3*, 3675. (d) Patwardhan, A. P.; Lu, Z.; Pulgam, V. R.; Wulff, W. D. *Org. Lett.* **2005**, *7*, 2201. (e) Patwardhan, A. P.; Pulgam, V. R.; Zhang, Y.; Wulff, W. D. *Angew. Chem. Int. Ed.* **2005**, *44*, 6169. (f) Deng, Y.; Lee, Y. R.; Newman, C. A.; Wulff, W. D. *Eur. J. Org. Chem.* **2007**, 2068. (g) Lu, Z.; Zhang, Y.; Wulff, W. D. *J. Am. Chem. Soc.* **2007**, *129*, 7185. (h) Zhang, Y.; Desai, A.; Lu, Z.; Hu, G.; Ding, Z.; Wulff, W. D. *Chem. Eur. J.* **2008**, *14*, 3785. (i) Zhang, Y.; Lu, Z.; Desai, A.; Wulff, W. D. *Org. Lett.* **2008**, *8*, 5429. (j) Hu, G.; Huang, L.; Huang, R. H.; Wulff, W. D. *J. Am. Chem. Soc.* **2009**, *131*, 15615. (k) Zhang, Y.; Lu, Z.;

Wulff, W. D. *Synlett*, **2009**, 2715.

17. Wipf*, P.; Lyon, M. A. *ARKIVOC, **2007**, xii,* 91.

18. Dixon, D. J.*, Tillman, A. L. *Synlett*, **2005**, *17*, 2635.

19. Matsui, K.; Takizawa, S.; Sasai, H.* *J. Am. Chem. Soc.*, **2005**, 127, 3680.

20. Hashimoto, T.; Maruoka, K.* *J. Am. Chem. Soc.* **2007**, *129*, 10054.

21. Hashimoto, T.; Uchiyama, N.; Maruoka, K. *J. Am. Chem. Soc.* **2008**, *130*, 14380.

22. For reviews on chiral phosphoric acid catalysis see: (a) Connon, S. J. *Angew. Chem., Int. Ed.* **2006**, *45*, 3909. (b) Akiyama, T. *Chem. Rev.* **2007**, *107*, 5744. (c) Adair, G.; Mukherjee, S.; List, B. *Aldrichim. Acta* **2008**, *41*, 31.

23. For selected examples of the phosphoric acid catalyzed reactions, see: (a) Akiyama, T.; Itoh, J.; Yokota, K.; Fuchibe, K. *Angew. Chem., Int. Ed.* **2004**, *43*, 1566. (b) Uraguchi, D.; Terada, M. *J. Am. Chem. Soc.* **2004**, *126*, 5356.

24. Akiyama, T.*; Suzuki, T.; Mori, K. *Org. Syn.* **2009**, *11*, 2445.

25. Zeng, X.; Zeng, X.; Xu, Z.; Lu, M.; Zhong, G.* *Org. Lett*. **2009**, *11*, 3036.

26. Chai, Z.; Bouillon, J.-P.; Cahard, D.* *Chem. Comm.* **2012**, *48*, 9471.

27. Hashimoto, T.; Nakatsu, H.; Yamamoto, K.; Maruoka, K.* *J. Am. Chem. Soc.* **2011**, *133*, 9730.

28. Rampalakos, C.; Wulff, W. D.* *Adv. Synth. Catal.* **2008**, *350*, 1785.

29. Desai, A. A.; Wulff, W. D. *Synthesis* **2010**, 3670.

30. Desai, A. A.; Wulff, W. D. *J. Am. Chem. Soc.* **2010**, *132*, 13100.

31. Hu, G.; Gupta, A. K.; Huang, R. H.; Mukherjee, M.; Wulff, W. D. * *J. Am. Chem. Soc.* **2010**, *132*, 14669.

32. (a) Vetticatt, M.; Desai, A.; Wulff, W. D. *J. Am. Chem. Soc.* **2010**, *132*, 13104. (b) Vetticatt, M.; Desai, A. A.; Wulff, W. D. *J. Org. Chem.* **2013**, accepted for publication.

33. Hodges, J. A.; Raines, R. T. *Org. Lett.* **2006**, *21*, 4695-4697.

34. Gupta, A. K.; Mukherjee, M.; Hu, G.; Wulff, W. D. *J. Org. Chem.* **2012**, *77*, 7932.

35. Yakabe, S.; Hirano, M.; Morimoto, T. *Syn. Comm.* **1999**, *29 (2)*, 295.

36. Hansch, C.; Leo, A.; Taft, R. W. *Chem. Rev.* **1991**, *91*, 165.

37. Guan, Y. PhD Dissertation, Department of Chemistry, Michigan State University, **2012**.

38. Mukherjee, M.; Gupta, A. K.; Lu, Z.; Zhang, Y.; Wulff, W. D. *J. Org. Chem*. **2010**, *75*, 5643.

39. Hu, G. PhD Dissertation, Department of Chemistry, Michigan State University, **2007**.

40. Potyen, M.; Josyula, K. V. B.; Schuck, M.; Lu, S.; Gao, P.; Hevitt, C. *Org. Process Res. Dev.* **2007**, *11*, 210.

41. Gupta, A. K.; Mukherjee, M.; Wulff, W. D. *Org. Lett.* **2011**, *13*, 5866.

42. (a) de Graaff, C.; Ruijter, E.; Orru, R. V. A. *Chem. Soc. Rev.* **2012**, *41*, 3969. (b) Guillena, G.; Ramon, D. J.; Yus, M. *Tetrahedron: Asymmetry* **2007**, *18*, 693. (c) Ramon, D. J.; Yus, M. *Angew. Chem., Int. Ed.* **2005**, *44*, 1602. (d) *Multicomponent Reactions*; Zhu, J.; Bienayme, H., Eds.; Wiley-VCH: Weinheim, **2005**.

43. Kelly, T. R.; Whiting, A.; Chandrakumar, N. S. *J. Am. Chem. Soc.* **1986**, *108*, 3510.

44. Brown, H. C.; Heim, P.; Yoon, N. M. *J. Am. Chem. Soc.* **1970**, *92*, 1637.

45. (a) Pearlman, W. M. *Tetrahedron Lett.,* **1967**, 1663. (b) Bacque, E.; Paris, J-M.; Le Bitoux, S. *Synth. Commun.* **1995**, *25*, 803. (c) Bernotas, R. C.; Cube, R.V. *Synthe. Commun.* **1990**, *20*, 1209.

46. Lu, Z. PhD Dissertation, Department of Chemistry, Michigan State University, **2008**.

47. Nimmagadda, R.D.; McRae, C. *Tetrahedron Lett.* **2006**, *47*, 5755.

48. Hattori, K.; Yamamoto, H. *J. Org. Chem.* **1992**, *57*, 3264.

49. Ishihara, K.; Yamamoto, H. *J. Am. Chem. Soc.* **1994**, *116*, 1561.

50. Ishihara, K.; Miyata, M.; Hattori, K.; Tada, T.; Yamamoto, H. *J. Am. Chem. Soc.* **1994**, *116*, 10520.

51. Kaufmann, D.; Boese, R. *Angew. Chem. Int. Ed.* **1990**, *29*, 545.

52. Brown, H. C.; Stocky, T. P. *J. Am. Chem. Soc.* **1977**, *99*, 8218.

53. Bao, J.; Wulff, W. D.; Dominy, J. B.; Fumo, M. J.; Grant, E. B.; Rob, A. C.; Whitcomb, M. C.; Yeung, S.-M.; Ostrander, R. L.; Rheingold, A. L. J. Am. Chem. Soc. **1996**, *118*, 3392–3405.

54. Ding, Z.; Xue, S.; Wulff, W. D. *Chem. Asian J.* **2011**, *6*, 2130.

55. Ding, Z.; Osminski, W. E. G.; Ren, H.; Wulff, W. D. *Org. Process Res. Dev.* **2011**, *15*, 1089.

56. Tanaka, H.; Kubota, J.; Miyahara, S.; Kuroboshi, M. *Bull. Chem. Soc. Jpn*. **2005**, *78*, 1677.

57. Szyma'ska, E.; Frydenvang, K.; Contreras-Sanz, A.; Pickering, D. S.; Frola, E.; Serafimoska, Z.; Nielsen, B.; Kastrup, J. S.; Johansen, T. N. *J. Med. Chem*. **2011**, *54*, 7289.

58. Yousefi, B. H.; Jordis, U. 10th Electronic Conference on Synthetic Organic Chemistry.

59. (a) Wolfe, J. P.; Wagaw, S.; Marcoux, J.-F.; Buchwald, S. L. *Acc. Chem. Res.* **1998**, *31*, 805. (b) Hartwig, J. F. *Acc. Chem. Res.* **1998**, *31*, 852.

60. Ding, Z. PhD Dissertation, Department of Chemistry, Michigan State University, **2008**.

61. Schwab, J. M. *J. Org. Chem.* **1983**, *48*, 2105.